

Investigation of the Synthesis, Reactivity and Biological Properties of  
Various 6-Substituted D-Fructose Derivatives

by

Thomas Wayne Scully

A thesis submitted in partial fulfillment of the requirements for the degree of

Doctor of Philosophy

Department of Chemistry  
University of Alberta

© Thomas Wayne Scully, 2017

## Abstract

The detection of small tumors growing in complex organs, including breast tissue, is a challenge in modern medical imaging. The use of positron emission tomography (PET) and tracer molecules containing radionuclei such as  $^{18}\text{F}$  have been of significant value to detect small tumors. The commonly used PET tracer [ $^{18}\text{F}$ ]-2-fluoro-2-deoxy-D-glucose ([ $^{18}\text{F}$ ]-FDG) is widely used but it suffers from several important limitations. [ $^{18}\text{F}$ ]-FDG provides false positives in PET scans and has a very short half-life resulting from the rapid decay of the  $^{18}\text{F}$  nucleus. This short half-life requires that the  $^{18}\text{F}$  is produced immediately before it is incorporated into the tracer molecule and that the tracer is used very soon after it is produced. The specialized facilities needed to produce  $^{18}\text{F}$  for medical purposes limits the number of scans that can be performed as only a small number of these facilities exist.

Tissue specific transport of tracer molecules is dictated by what type of biomolecule they are intended to mimic, and how well they are recognized by the transport machinery of the cell. [ $^{18}\text{F}$ ]-FDG is transported through the hexose transporter (GLUT) pathway as it is a D-glucose mimic. There are 14 known members of the GLUT family each with a different substrate specificity and/or tissue distribution. For example, GLUT1 is a ubiquitously expressed D-glucose transporter while GLUT5 is a D-fructose transporter which is only expressed in a small number of tissues, including breast tumor tissue. To date no GLUT5 specific tracer molecule that can be used for medical imaging exists. Creation of a tracer molecule with the desired properties must begin with the creation of a scaffold that is recognized as D-fructose by GLUT5 but can carry with it an observable moiety. To

circumvent the limitations of the PET imaging modality a fluorescent tag could be appended to a D-fructose scaffold allowing for real time imaging without the short half-life of  $^{18}\text{F}$ .

Chapter 1 on this thesis outlines a broad introduction to the body of knowledge around the GLUT transporters, their structure, substrate binding, tissue distribution, and mechanism of transport. Further, an overview of small molecules which have been shown to be transported by the GLUT transporters is included. Chapter 2 outlines the initial studies towards the selective functionalization of D-fructose at the C6 position in order to attach a fluorescent dye to D-fructose via this carbon. Chapter 3 outlines a second strategy employed to functionalize the C6 position of D-fructose by incorporation of an iodine atom to C6. This intermediate was used as a precursor for many metal mediated transformations. Further, Chapter 3 outlines the use of the alkyl iodide as a radical precursor for intramolecular cyclization reactions as well as reduction to produce the natural product 6-deoxy-D-fructose. In Chapter 4, a set of four 6-amino-6-deoxy-hexose derivatives which are attached to the NBD fluorophore were evaluated for their biological properties with EMT6 and MCF7 breast cancer cell lines. The ability of these compounds to be taken up by these cell lines, the pathway by which the compounds were transported, and their efflux profiles were evaluated by flow cytometry.

## Preface

The synthesis and biological evaluation, via methods not covered in this thesis, of 6NBDF, 6NBDP, 6NBDT, and 6NBDS were published as O-M. Soueidan, T. W. Scully, J. Kaur, R. Panigrhi, A. Belovodskiy, V. Do, C. D. Matier, M. J. Lemieux, F. Wuest, C. Cheeseman, and F. G. West. *ACS Chem. Bio.* **2017**, 12, 1087-1094.

6NBDF, 6NBDP, 6NBDT, and 6NBDS were produced by Dr. O. Soueidan while in the West group. They were supplied as yellow/green solids that were dissolved in sterile buffer solution.

## **Dedication**

If all of this was easy

It wouldn't matter how it ends

-Dan Mangan

Nobody cares

Work harder

-Cameron Hanes

## Acknowledgements

I would like to thank Dr. F.G. West for the years of supervision, training, and education. Without his support I would never have been able to develop as a scientist and as a human being in the ways I have. I would also like to extend thanks to the members of my supervisory and thesis committee for their valuable input through my research the development of this document.

The many members of the West Group and the greater UofA community who have been influenced me in my time here are wide reaching and almost too numerous to mention. Senior group members such as Dr. V. Lofstrand, Dr. O. Scadeng, Dr. R. Fradette, Dr. N. Hosseini are only a few of the valued coworkers I was privileged to share the lab with.

Dr. C. Cheeseman and the members of his research group were welcoming and extremely helpful in teaching me the biological techniques and methods required to generate viable cell cultures and flow cytometry data.

The highly skilled members of the UofA analytical and NMR facilities were extremely skilled and able to resolve any issue that arose. Their consistently excellent work day in and day out allowed for so much of my research to carry on smoothly.

I must also acknowledge the support of my family, friends, and loved ones who helped me maintain my sanity and commitment through long days, dark nights, and times that tested me past what I thought my limits were. I have a new found appreciation for the importance of the community one builds around themselves and the strength that can give you.

My time at the UofA and living in Edmonton has changed me in many ways. Some are apparent and others are much harder to quantify. I like to think that every interaction I've

had and every person here has influenced my life in some way. There have been far too many to mention each one here but if you knew me well enough to be reading these words...

Your influence was felt, and I thank you for it.

## Table of Contents:

Abstract.....	ii
Preface .....	iv
Dedication.....	v
Acknowledgements .....	vi
Table of Contents: .....	viii
List of Figures: .....	x
List of Tables:.....	xii
List of Schemes: .....	xiii
List of Symbols and Abbreviations .....	xv
Chapter 1: Introduction.....	1
1.1: GLUT Transporters: A Brief History .....	1
1.2: The Structure of the GLUT Substrate Binding Site .....	7
1.3: The ICH Domain and Its Role in Substrate Transport .....	8
1.4: GLUT5: Expression and Its Role in Breast Cancer .....	11
1.5: A Brief Introduction to Molecular Imaging Techniques and Tracer Compounds .....	16
1.6: Small Molecule Substrates of GLUT1: Synthesis and Evaluation.....	19
1.7: Small Molecules as Structural Probes of the GLUT5 Binding Site .....	24
1.8: Small Molecule Imaging Agents: The Utilization of the GLUT5 Pathway .....	28
1.9: GLUT5 Substrates: In vivo Evaluation and Imaging .....	36
1.10: Retention of Small Molecule Probes Inside Target Cells .....	41
1.11: Goal of this Research.....	43
1.12: References: .....	46
Chapter 2: Attempts Towards Using the C6 Position of D-Fructose as an Electrophile Through Selective Oxidation. ....	52
2.1: Synthetic Rational to a C6 Functionalized D-Fructose Derivative. ....	52
2.2: Production of a Suitable Substrate for Oxidation Reactions.....	54
2.3: Initial Attempts to Afford D-Fructose Aldehyde Derivative 58 via Selective Oxidation. 58	58
2.4: Attempts to Use TEMPO Mediated Oxidations to Produce Compound 58.....	62
2.5: Attempted Oxidation of Partially Protected D-Fructose Derivatives 25, 51, and 54 with Hypervalent Iodine Oxidants.....	65
2.6: Attempted Transition Metal Mediated Oxidation of Partially Protected D-Fructose 25 .	69
2.7: Attempted One-Pot Oxidation/Trapping of D-Fructose Derivative 58.....	73
2.8: Attempted Oxidation of Iodo-Fructose derivative via the Kornblum Oxidation .....	75
2.9: Summary .....	76
2.10: Experimental: .....	77
2.11: References: .....	87

Chapter 3: Attempted Derivatization of 6-Deoxy-6-Iodo-D-Fructose in Efforts Towards a Fluorescently Tagged Molecular Imaging Agent .....	90
3.1: Rationale for Experimental Plan .....	90
3.2: Attempted Metal-Halogen Exchange .....	91
3.2: Attempts to Generate a Grignard Reagent from the Corresponding Alkyl Iodide Derived From D-Fructose .....	92
3.3: Attempts to Generate an Alkyl lithium Reagent from the Corresponding Iodo-D-Fructose Derivative. ....	96
3.4: Attempts to Generate a Grignard Reagent Under Barbier-Type Conditions From a Iodo-D-Fructose Derivative. ....	98
3.5: Attempts to Create a New C-C Bond at C6 of D-Fructose via a Radical Cyclization Reaction .....	105
3.6 Reduction of the C6 Iodide Via Nucleophilic Hydride or Radical Mediated Reactions..	110
3.7: Summary .....	114
3.8: Future Directions: .....	115
3.9: Experimental: .....	115
3.10: References .....	122
Chapter 4: Evaluation of 6-NBD-Hexose Derivatives by Flow Cytometry .....	126
4.1: A Brief Introduction to Flow Cytometry .....	126
4.2: The use of Flow Cytometry to Investigate the Transport of NBD Labelled Compounds	129
4.3: Determination of the Appropriate Cell Lines for the Evaluation of New Compounds...	131
4.4: Evaluation of 6NBDF as a GLUT Substrate Through Flow Cytometry .....	133
4.5: Evaluation of 6NBDF as a GLUT Substrate Through Flow Cytometry .....	141
4.6: Evaluation of 6NBDS as a GLUT Substrate Through Flow Cytometry .....	143
4.7: Evaluation of 6NBDF as a GLUT Substrate Through Flow Cytometry .....	144
4.8: Evaluation of 1NBDF as a GLUT Substrate Through Flow Cytometry .....	147
4.9: Conclusion: .....	152
4.10: Experimental: .....	154
4.11: References: .....	158
Chapter 5: Conclusions and Future Directions .....	160
5.1: Conclusions .....	160
5.2: Future Directions .....	161
5.3: References: .....	164
Bibliography: .....	165
Appendix I: Selected NMR Spectra .....	177
Appendix II: Selected Flow Cytometry Raw Data .....	188

## List of Figures:

Figure 1.1: Crystal structure of GLUT1 coloured by secondary structure succession. Left. Side on view. Right: Top down view through central pore.....	1
Figure 1.2 Sequence homology map of the GLUT family of transport proteins.....	2
Figure 1.3 The crystal structure of GLUT1 with the 6 helices nearest the N-terminal coloured green and the 6 helices nearest the C-terminal end coloured blue. The ICH domain has been coloured red to differentiate it from the helices which span the membrane.....	4
Figure 1.4: A diagram of a transporter going through a cycle of the Simple Carrier Model commencing with the transporter in the outward-open, substrate free conformation and continuing clockwise to complete one cycle of transport.....	6
Figure 1.5: A side on view of the ICH domain held below the intramembrane helical bundles.....	9
Figure 1.6: A diagram showing the potential for the overestimation of a tumors size by FDG PET imaging. Left: Tumor tissue (black) is surrounded by inflamed immune tissue (yellow). Both of these tissues can contain a large amount of GLUT5 which transports FDG. Right: the resulting estimation of the tumor disuse derived from FDG imaging which highlights both the tumor and inflamed tissue (red).....	22
Figure 1.7: A selection of modified hexose compounds produced and tested by the Holman group and their reported affinities for GLUT5.....	25
Figure 1.8: A selection of ring fused compounds produced by the Holman group and their reported affinities to GLUT5.....	26
Figure 1.9: Two examples of anhydromanitol derivates bearing a photoaffinity labels produced and used by the Holman group.....	27
Figure 1.10: High affinity GLUT5 substrates produced by the Holman group and their reported affinities for GLUT5.....	28
Figure 1.11: The structure of 6NBDP, 6NBDT, and 6NBDS which were produced by West and co-workers.....	34
Figure 1.12: The phosphorylation of D-fructose by fructokinase (left) or hexokinase (right) ..	42
Figure 1.13: A representative goal compound to be synthesized in this research project.....	44
Figure 4.1: A general overview of a flow cytometer.....	128
Figure 4.2: The structure of 6NBDG.....	130
Figure 4.3: The structure of 6NBDF, 6NBDP, 6NBDT, and 6NBDS. <sup>21</sup> .....	132
Figure 4.4: Observed uptake of 6NBDF (250 $\mu$ M) in EMT6 cells.....	134
Figure 4.5: Inhibition of 6NBDF (250 $\mu$ M) with varying concentrations of extracellular D-fructose in EMT6 cells.....	135
Figure 4.6: Uptake of 6NBDF (250 $\mu$ M) with varying, high concentrations of extracellular D-fructose in EMT6 cells.....	136
Figure 4.7: Uptake of 6NBDF (250 $\mu$ M) with varying concentrations of extracellular D-glucose in EMT6 cells.....	137
Figure 4.9: Uptake of 6NBDF (250 $\mu$ M) with cytochalasin B (250 $\mu$ M) in EMT6 cells.....	138
Figure 4.10: Uptake of 6NBDF (250 $\mu$ M) in EMT6 cells over a 4 hour time course.....	139
Figure 4.11: Uptake of 6NBDF (500 $\mu$ M) in MCF7 cells.....	140
Figure 4.12: Uptake of 6NBDP at 750 $\mu$ M or 2 mM in MCF7 cells.....	142
Figure 4.13: Uptake of 6NBDS (500 $\mu$ M) in EMT6 cells.....	144

Figure 4.14: Uptake of 6NBDP (750 $\mu$ M) in MCF7 cells.....	144
Figure 4.15: Uptake of 6NBDT (375 $\mu$ M) in EMT6 cells. ....	145
Figure 4.16: Uptake of 6NBDT (375 $\mu$ M) with varying concentrations of extracellular D-glucose in EMT6 .....	146
Figure 4.17: Uptake of 6NBDT at 375 $\mu$ M or 500 $\mu$ M in MCF7 cells. ....	147
Figure 4.18: The structure of 1NBDF. ....	148
Figure 4.19: Uptake of 1NBDF (250 $\mu$ M) in EMT6 cells.....	148
Figure 4.20: Uptake of 1NBDF (500 $\mu$ M) in MCF7 cells.....	150
Figure 4.21: Uptake of 1NBDF (500 $\mu$ M) and the effect of co-incubation with extracellular D-fructose (250 $\mu$ M) in MCF7 cells. ....	150
Figure 4.22: Uptake of 1NBDF (500 $\mu$ M) and the effect of co-incubation with extracellular D-glucose (50 or 100 $\mu$ M) in MCF7 cells. ....	151

## List of Tables:

Table 1.1: The preferred substrate, affinity, and tissue distribution of a select set of the GLUT transporter family. ....	3
Table 2.1: Optimization of the selective removal of the 4,4'-DMT group from the C6 position of 57. ....	58
Table 2.2: Screening of conditions to selectively oxidize the C6 hydroxyl of 25, 51, or 54 to produce the desired aldehyde 58, 59, or 60. ....	60
Table 2.3: Investigation of Tempo mediated oxidations of 25, 51, and 54 to afford the desired aldehyde 58, 59, or 60. ....	64
Table 2.4: Investigation of hypervalent iodide based oxidants for the conversion of 25, 51, or 54 to the desired aldehyde 58, 59, or 60. ....	68
Table 2.5: Investigation of copper-molecular oxygen co-oxidants for TEMPO mediated oxidation of 25 or 51 to afford the desired aldehyde 58 or 59. ....	72
Table 3.1: Attempted formation and trapping of a Grignard-type reagent from iodo-fructose derivative 83. <sup>a</sup> ....	94
Table 3.2: Investigation of the formation of an alkyllithium reagent from 83 and the resulting products observed. <sup>a</sup> ....	98
Table 3.3: Investigation of the formation of a Barbier reagent from 78. <sup>a</sup> ....	104

## List of Schemes:

Scheme 1.1: The two general methods for the production of 2FDG along with the structure of Kryptofix 222. ....	21
Scheme 1.2: The coupling of the NBD moiety to the relevant amino hexose to generate 6NBDG or 2NBDG. ....	23
Scheme 1.3: The route of Gambhir and co-workers to produce 1NBDF and 1Cy5DF from D-glucose via the Amadori rearrangement. ....	29
Scheme 1.4: The route of the McQuade group to produce 1NBDM from D-glucosamine. ....	31
Scheme 1.5: The route of West and co-workers to produce 6NBDF from the known intermediate 25. ....	33
Scheme 1.6: The synthesis of 6FDF from D-fructose as published by West, Cheeseman, Wuest and co-workers. ....	37
Scheme 1.7: The synthesis of [ <sup>18</sup> F]6FDF from the tosylated precursor. ....	38
Scheme 1.8: The synthesis of [ <sup>18</sup> F]1FDAM as carried out by Sun and co-workers. ....	39
Scheme 1.9: The synthesis of 3FDF as carried out by West, Cheeseman, Wuest and co-workers. ....	40
Scheme 1.10: The proposed route from D-fructose to a goal compound bearing the desired functionality including an NBD dye moiety, a short tether chain, and a secondary hydroxyl at the C6 position of the D-fructose skeleton. ....	45
Scheme 2.1: Protection of D-fructose via the method of Hong and co-workers <sup>4</sup> to yield intermediate 25. ....	54
Scheme 2.2: Production of the key, selectively protected compound 51 via protection/deprotection of the C6 tosylate through Na-naphthalide reduction. ....	55
Scheme 2.3: Production of the partially protected compound 54 via tritylation/detrylation at the C6 position. ....	56
Scheme 2.4: Production of the partially protected compound 54 through a protection/deprotection strategy utilizing the 4,4'-dimethoxytrityl group. ....	57
Scheme 2.5: The disproportionation of TEMPO from a free radical and hydroxylamine for to the active oxoammonium salt. ....	63
Scheme 2.6: Reduced nucleophilicity of 25, 51, or 54 as the result of intramolecular hydrogen bonding disfavors the attack on the oxoammonium salt 62 which prevents the irreversible deprotonation step from occurring. ....	65
Scheme 2.7: A generalized mechanism of DMP oxidation of a primary alcohol 71 to the corresponding aldehyde 72. ....	66
Scheme 2.8: The oxidation of the D-ribose derivative 73 to the corresponding aldehyde 74 as carried out by Finney and More. <sup>34</sup> ....	67
Scheme 2.9: An abbreviated mechanistic cycle of the Cu/O <sub>2</sub> /TEMPO system used for the oxidation of a primary alcohol to an aldehyde as described by Stahl and co-workers. (L) <sub>3</sub> =2,2'-bipyridine (bpy), N-methyl-indole (NMI). <sup>47</sup> ....	70
Scheme 2.10: Oxidation of a sterically demanding primary alcohol to the corresponding aldehyde under the conditions of Stahl and co-workers. <sup>43</sup> ....	71

Scheme 2.11: General reaction of attempts to intercept a C6 aldehyde of 51 created in the reaction mixture by the addition of an excess of allyl magnesium bromide to give 77. ....	74
Scheme 2.12: The use of the Appel reaction to create the C6 iodide 78 which was subjected to Kornblum oxidation.....	76
Scheme 3.1: Proposed route from 78 to 82 via an alkyl metal mediated C-C bond formation at the C6 position of 78 and further manipulations. ....	92
Scheme 3.2: The route of Madsen and Lauritsen in their formal synthesis of the naturally occurring iminosugar australine. <sup>8,9</sup> .....	95
Scheme 3.3: The Barbier type reactions carried out by Malvestiti and co-workers (top) <sup>17</sup> and Ma and co-workers (bottom) <sup>42</sup> utilizing low valent metals to carry out the nucleophilic addition of an allyl unit into an aldehyde. ....	101
Scheme 3.4: The work of Whitesides and co-workers (top) and Lee and Chan (bottom) utilizing indium mediated Barbier reactions to alkylate carbohydrate scaffolds at the anomeric position. <sup>46,47</sup> .....	103
Scheme 3.5: Test reactions using benzaldehyde and allyl bromide were carried out using each of the conditions listed in Table 3.3 All reaction gave the desired product 101 as determined by crude <sup>1</sup> H-NMR.....	105
Scheme 3.6: Mechanism of the release of methoxyl radical 103 arising from iodine radical abstraction from the C6 position of 78. ....	105
Scheme 3.7: Production of cyclized intermediates via a radical cyclization derived from D-xylose or D-glucose as prepared by Alves and co-workers. <sup>57</sup> .....	106
Scheme 3.8: Proposed route from 78 to 113 via a radical cyclization and reductive ring opening to afford the desired C-C bond formation from C6 to the β-carbon on crotonic acid. ....	107
Scheme 3.9: Proposed mechanism of the radical reduction of 109 which prevents the capture of cyclized product 117 because of the low stability or short lifetime of radical intermediate 115. ....	109
Scheme 3.10: Reduction of 78 to 121 via lithium aluminum hydride.....	111
Scheme 3.11: Reduction of 78 to 121 via the radical reduction utilizing Bu <sub>3</sub> SnH and AIBN. ....	112
Scheme 3.12: Deprotection of 121 to give 6-deoxy-D-fructose. ....	113
Scheme 3.13: Route from 2,5-anhydro-manitol to the deoxygenated derivative 123 .....	115
Scheme 5.2: Approach to a D-fructose derivative modified at the C3 hydroxyl through a protection/deprotection strategy. ....	163
Scheme 5.3: A possible route to produce 133, which could be used for photo cross linking to GLUT5. ....	163

## List of Symbols and Abbreviations

Ac	acetyl
Ac <sub>2</sub> O	acetic anhydride
AIBN	azobisisobutyronitrile
app	apparent (spectral)
APT	attached proton test (a NMR technique)
ATP	adenosine triphosphate
Bn	benzyl
br	broad (spectral)
Bz	benzoyl
calcd	calculated
cm <sup>-1</sup>	wavenumber
<sup>13</sup> C-NMR	carbon 13 nuclear magnetic resonance
1Cy5D	1- <i>N</i> -1-amino-deoxyfructose-[(2 <i>E</i> )-1,1-dimethyl-2-[(2 <i>E</i> ,4 <i>E</i> )-5-(1,1,3-trimethylbenzo[ <i>e</i> ]indol-3-ium-2-yl)penta-2,4-dienylidene]benzo[ <i>e</i> ]indol-3-yl]hexanoate
DBU	1,8-diazabicyclo[5.4.0]undec-7-ene
DCM	dichloromethane
DMF	<i>N,N</i> -dimethylformamide
DOG	2-deoxy-D-glucose
δ	chemical shift in part per million downfield from tetramethylsilane
d	doublet (spectral)
dd	doublet of doublets (spectral)
DMAP	4-dimethylaminopyridine
4,4'-DMT	4,4'-dimethoxytrityl
dq	doublet of quartets (spectral)
dr	diastereometric ratio
dt	doublet of triplets (spectral)

ESI	electrospray ionization (mass spectrometry)
Et	ethyl
ee	enantiomeric excess
equiv.	equivalent
$^{18}\text{F}$	an isotope of fluorine (a known PET emitter)
2FDG	2-deoxy-2-fluoro-D-glucose
1FDF	1-deoxy-1-fluoro-D-fructose
3FDF	3-deoxy-3-fluoro-D-fructose
6FDF	6-deoxy-6-fluoro-D-fructose
1FDAM	1-fluoro-1-deoxy-2,5-anhydromannitol
FK	fructokinase (also referred to as ketohexokinase)
GLUT	membrane hexose transporter
HepG2	a human breast tumor cell line
Hex	hexane (mixture of isomers)
HK	hexokinase
$^1\text{H-NMR}$	Proton nuclear magnet resonance
<i>in vivo</i>	referring to studies performed in living organisms
<i>in vitro</i>	referring to studies performed in cell cultures
ICH	intracellular helical domain (protein)
IR780	a near infrared emitting chromophore
$J$	coupling constant (in NMR)
$K_i$	the concentration of 50% inhibition
L	litre(s)
LiHMDS	lithium hexamethyldisilaside
$\mu$	micro
M	metal atom: moles per litre
Me	methyl
MHz	megahertz

m.p.	melting point
m	multiplet (spectral): milli
mol	number of moles
MS	mass spectrometry
NBD	7-nitrobenz-2-oxa-1,3,-diazole
NBDCI	4-chloro-7-nitrobenzofurazan
1NBDF	1-( <i>N</i> -(7-nitrobenz-2-oxa-1,3-diazol-4-yl)amino)-1-deoxyfructose
6NBDF	6-( <i>N</i> -(7-nitrobenz-2-oxa-1,3-diazol-4-yl)amino)-6-deoxyfructose
2NBDF	2-( <i>N</i> -(7-nitrobenz-2-oxa-1,3-diazol-4-yl)amino)-2-deoxyglucose
6NBDF	6-( <i>N</i> -(7-nitrobenz-2-oxa-1,3-diazol-4-yl)amino)-6-deoxyglucose
1NBDM	1-( <i>N</i> -(7-nitrobenz-2-oxa-1,3-diazol-4-yl)amino)-1-amino-2,5-anhydromannitol
6NBDF	6-( <i>N</i> -(7-nitrobenz-2-oxa-1,3-diazol-4-yl)amino)-6-deoxyfructose
6NBDS	6-( <i>N</i> -(7-nitrobenz-2-oxa-1,3-diazol-4-yl)amino)-6-deoxysorbose
6NBDF	6-( <i>N</i> -(7-nitrobenz-2-oxa-1,3-diazol-4-yl)amino)-6-deoxytagotose
NMO	<i>N</i> -methylmorpholine <i>N</i> -oxide
NMR	nuclear magnetic resonance
Nu	nucleophile
OAc	acetate
OEt	ethoxy
OMe	methoxy
PCR	polymerase chain reaction
PET	positron emission tomography
Ph	phenyl
Pg	protecting group
<i>i</i> Pr	isopropyl
Py	pyridine
TsOH	<i>p</i> -toluenesulphonic acid
q	quartet (spectral)

R	generalized alkyl group of substituent
R <sub>f</sub>	retention factor (chromatography)
RT-PCR	real time polymerase chain reaction
r.t.	room temperature
S <sub>N</sub> 1	unimolecular nucleophilic substitution
S <sub>N</sub> 2	bimolecular nucleophilic substitution
s	singlet (spectral)
SLC2A	the gene family of major facilitated transporters
t	triplet (spectral)
T	temperature
<sup>95</sup> Tc	an isotope of technetium (a known PET emitter)
Tol	toluene
TBS	<i>tert</i> -butyldimethylsilyl
TBDPS	<i>tert</i> -butyldiphenylsilyl
TMS	trimethylsilyl
TBAF	tetra- <i>N</i> -butylammonium fluoride
Tr	trityl
TFA	trifluoroacetic acid
Tf	trifluoromethanesulfonyl: triflate
Tf <sub>2</sub> O	trifluoromethanesulfonyl anhydride
TPAP	tetrapropylammonium perruthenate
Ts	<i>p</i> -toluenesulfonyl: tosyl
THF	tetrahydrofuran
TM	transmembrane (protein)
TEA	triethylamine (also referred to as Et <sub>3</sub> N)
TLC	thin layer chromatography
UV	ultra violet
X	generalized heteroatom

## Chapter 1: Introduction

### 1.1: GLUT Transporters: A Brief History

Since its first isolation by Bell and co-workers in 1990 from human skeletal muscle tissue, GLUT5 has been a target of interest by researchers in many disciplines.<sup>1</sup> As a member of the major facilitator superfamily of transporters and belonging to the gene family SLC2A, GLUT5, like all other members of the GLUT family, is a hexose transporter which is found in the cell membrane (Figure 1.1).<sup>2-4</sup> The field of GLUT research has grown over the past three decades and now includes a wide breadth of subtopics.

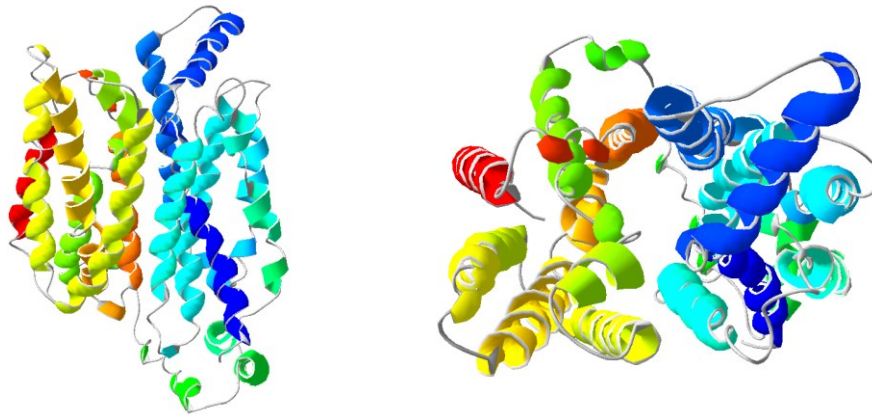


**Figure 1.1: Crystal structure of GLUT1 coloured by secondary structure succession. Left. Side on view. Right: Top down view through central pore.**

GLUT1 was the first GLUT protein that was isolated and cloned by Mueckler and co-workers in 1985.<sup>5-7</sup> Later on, four additional members of the GLUT family were rapidly located.<sup>8-10</sup> Currently 14 members of the GLUT family have been reported, which are grouped into three classes based on sequence homology (Figure 1.2).<sup>3</sup> The most ancient of these members, denoted HMIT1 (GLUT13), is a proton-myoinositol symporter<sup>11</sup> which shows

strong sequence and structural homology to the other members of the GLUT family as well as to hexose transporters found in bacteria and plants.<sup>12-14</sup> Though the crystal structures of several members of the GLUT family, including GLUT1<sup>15</sup> and GLUT5,<sup>16</sup> have recently been determined, a great deal of information had been gained about the mechanism of action and kinetics of these transports prior to the crystal structures being solved.

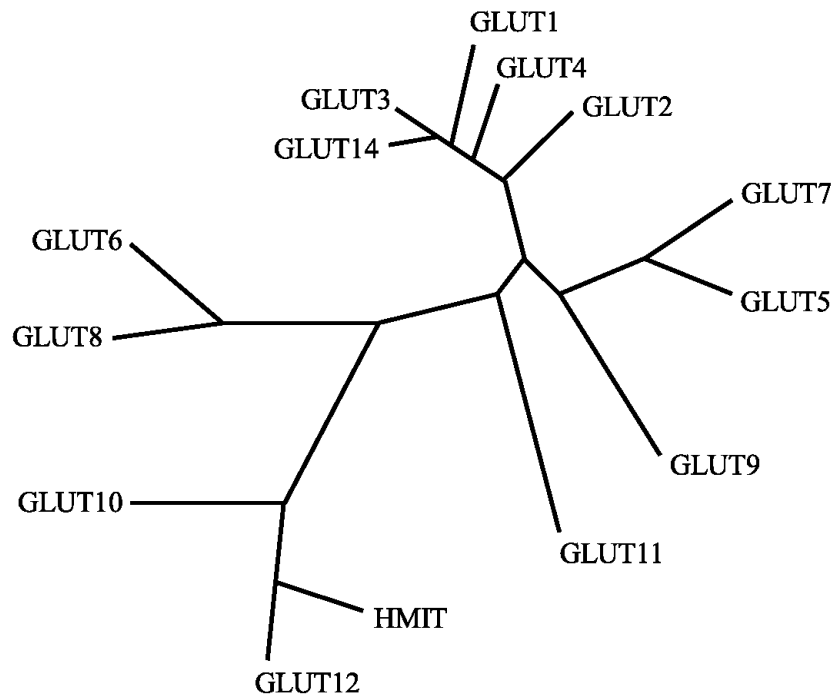


**Figure 1.1** Sequence homology map of the GLUT family of transport proteins.

In their initial report in 1985 report Bell and co-workers identified the gene sequence of GLUT1 and many structural aspects of the protein.<sup>7</sup> From the found 2850 nucleotide sequence Mueckler and co-workers used a hydropathy map as well as other techniques to predict that GLUT1 would have its C and N termini inside the cell, 12 membrane spanning regions, and a large endocellular loop between the 6<sup>th</sup> and 7<sup>th</sup> transmembrane regions. The crystal structure of GLUT1 published 29 years later definitively confirmed these structural

components.<sup>15</sup> In those intervening years the field of GLUT research has been by no means idle. Detailed analysis of the members of the GLUT family positively identified their substrate specificity, kinetics, and tissue distribution (Table 1.1). These findings have been well reviewed by several researchers in the field of GLUT research including Carruthers,<sup>17</sup> Cheeseman,<sup>18</sup> and Mueckler.<sup>19</sup> The knowledge provided by these researchers, and many others, most relevant to the research at hand is presented below.

**Table 1.1: The preferred substrate, affinity, and tissue distribution of a select set of the GLUT transporter family.**

<b>GLUT</b>	<b>Substrate</b>	<b>Affinity (Km)</b>	<b>Tissue Distribution</b>
1	D-glucose / galactose	5 mM (D-glucose)	Ubiquitous
2	D-glucose / D-fructose	11 mM (D-glucose)	Intestine, kidney, liver
3	D-glucose / galactose	1 mM (D-glucose)	Neurons
4	D-glucose	5 mM	Fat, muscle
5	D-fructose	6 mM	Intestine, sperm
8	D-glucose	2.4 mM	Testis, brain, fat, liver, spleen
13 (HMIT)	myoinositol	0.1 mM	Brain

GLUT1 is expressed in nearly all human tissue types including red blood cells which made it an attractive and useful target for study.<sup>20</sup> The GLUT transporters are highly similar in tertiary structure, which was first probed by experimental techniques and molecular modeling, and was correctly identified as 12 helices which form a tight bundle.<sup>21-24</sup> These helices are between 15 and 40 amino acid residues in length and form a barrel like structure with a central aqueous pore containing a binding site for the substrate.<sup>12,25,26</sup> The first-six and second-six transmembrane helices are arranged in an alternating-tipped structure which allows only one face of the protein to be exposed to either the extracellular or intracellular matrix at a time (Figure 1.3).<sup>16,27,28</sup>

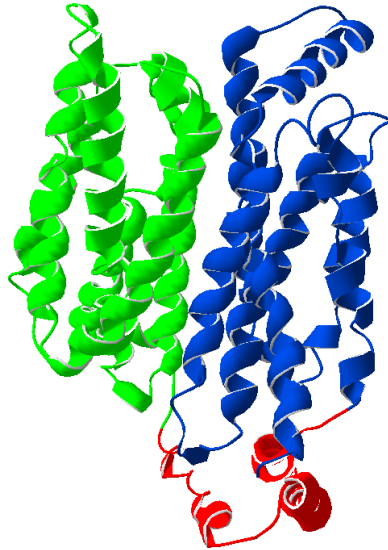


**Figure 1.2** The crystal structure of GLUT1 with the 6 helices nearest the N-terminal coloured green and the 6 helices nearest the C-terminal end coloured blue. The ICH domain has been coloured red to differentiate it from the helices which span the membrane.

The simple allosteric model for membrane pumps proposed by Jardetzky<sup>29</sup> in 1996 lends itself well to this type of transporter structure. Jardetzky proposed that a membrane transporter protein would sit with the central pore exposed to the extracellular matrix until a substrate bound to a recognition site. This binding event would cause a conformational shift which initiates a shift to a conformation where the pore and substrate are exposed to the intracellular environment. At this point the substrate could dissociate from the protein and be released into the cell. Jardetzky also pointed out the rearrangement of the protein between its differing orientations must be very subtle as large conformational changes would require too much energy per cycle to make the cycle efficient. In the case of an ion or ATP coupled pump the energy for conformation change can be obtained through these processes.<sup>30</sup> In the case of facilitated uniporters, such as GLUT proteins, the energetic demand for a shift in orientation must be very small as they lack a clear energy source for this event.

This type of transport is now referred to as the Simple Carrier Model and has been shown to exist in several membrane bound transporters (Figure 1.4).<sup>12,14,31-33</sup> The general mechanism of this type of transport is believed to involve three forms of the transport protein and four steps in the transport mechanism. Initially the transport protein is in an outward-open conformation and the substrate is not in the binding site. Upon binding to the protein a conformational shift is initiated and the protein shifts to its occluded state. In this state the substrate and the substrate-binding site are exposed to neither the extracellular or intracellular matrix. The protein then continues its conformational shift to an inward-open conformation where the substrate is exposed to the intracellular matrix. Here the substrate can dissociate from the protein and leave the protein in an inward-open, substrate free state. The protein then must return to its outward-open state so that another cycle of transport can begin. The transition from inward-open, substrate free to outward-open, substrate free is believed to be the rate limiting step in the cycle.<sup>33</sup>

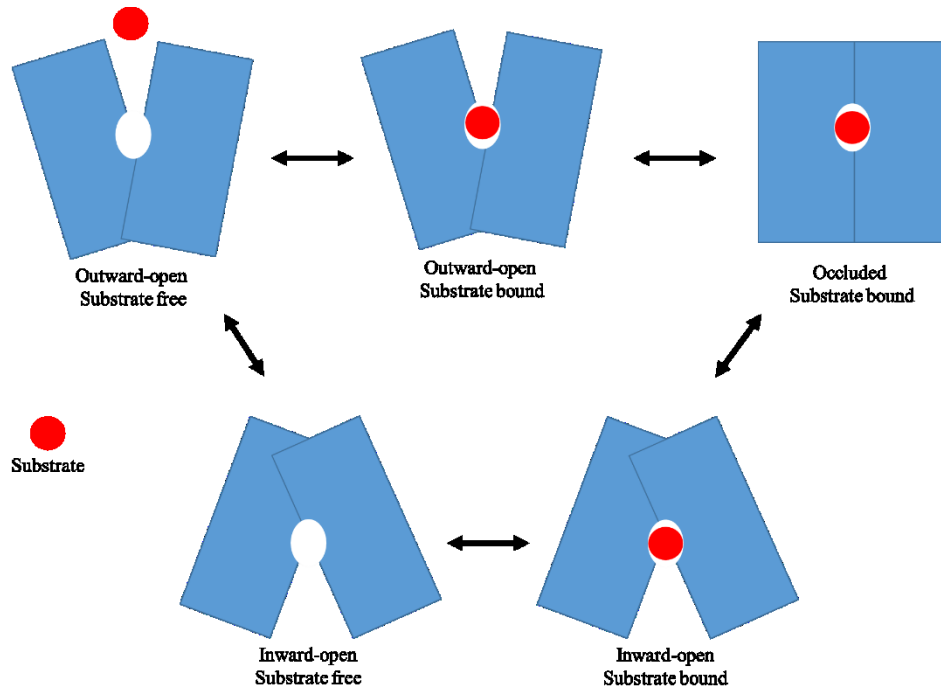


**Figure 1.3: A diagram of a transporter going through a cycle of the Simple Carrier Model commencing with the transporter in the outward-open, substrate free conformation and continuing clockwise to complete one cycle of transport.**

In specific regard to the GLUT transporters the Simple Carrier Model has been employed to describe the transports of hexoses<sup>34</sup> and has been studied computationally by Kaback and co-workers.<sup>35</sup> The binding site inside the central pore of a GLUT protein must be able to recognize a specific hexose and allow the conformational shift required for transport. This binding site must be specific enough to distinguish closely related hexoses such as D-glucose and D-galactose but tolerant enough to allow for recognition of a hexoses in both anomeric forms as well as in furanose and pyranose rings. This tight regulation of substrate specificity is believed to be achieved by a complex series of hydrogen bonding and hydrophobic interactions.<sup>15,16,26,35-37</sup>

## 1.2: The Structure of the GLUT Substrate Binding Site

Previous research into how various hexoses and inhibitors of the GLUTs interacted with these proteins gave valuable insight into the mechanism of transport. The recent crystal structures of GLUT1, GLUT5 and other members of the human GLUT family have resulted in a much more detailed understanding of the hexose binding site than ever before.<sup>10,15,22,26,27,38-41</sup> Using the published crystal structures, a detailed map of the residues that line the pore was established. In addition several techniques including site specific mutation and molecular modeling aided in the elucidation of the key interactions between the substrate hexose and the GLUT in the binding site.<sup>15,16</sup> In the human GLUT5 and GLUT1 structures it was found that Ile169, Ile173, Gln166, and Trp419 among others were conserved in the binding site. The hydrophobic Ile169 and Ile173 residues as well as Trp419 provide evidence for the importance of hydrophobic interactions in the binding site. It is also of note that Trp388 in human GLUT1 is an alanine residue in GLUT5 making the binding pocket slightly deeper. This Trp to Ala mutation also makes GLUT5 insensitive to cytochalasin B, a known inhibitor of GLUT1 but not GLUT5.<sup>8,16,42</sup>

It has also been shown experimentally that several isoleucine and valine residues in the binding site are critical to substrate specificity. Cheeseman and co-workers demonstrated that site directed mutagenesis of valine and isoleucine residues in GLUT1, GLUT2, GLUT5, and GLUT7 resulted in a shift in selectivity or a loss of function.<sup>43,44</sup> The ability of GLUT2 to transport D-fructose was lost with the Ile322Val mutation. The corresponding Ile296Val mutant of GLUT5 also lost the ability to transport D-fructose but maintained the ability to transport D-glucose when expressed in oocytes.<sup>43</sup> Sequence alignment reveals that Ile314 in GLUT7 is equivalent to Ile322 in GLUT2 or Ile296 in GLUT5 respectively and that the

Ile314Val mutation in GLUT7 causes the loss of D-fructose but not D-glucose transport.<sup>44</sup>

These small, yet extremely meaningful changes to the binding pocket are an excellent example and stark reminder of the intricate and delicate balance that exists between a substrate and its binding site in these transport proteins.

The crystal structure of the homolog of GLUT1 in *E. coli*, a D-xylose permease called XylE, was used along with the crystal structure of GLUT1 to model the hexose binding site interactions by Kaback and co-workers in 2014.<sup>35</sup> Several interactions predicted in this publication were supported by previous experimental data while other predicted interactions have yet to be confirmed by other methods. Kaback and co-workers accurately identified the importance of the isoleucine residues which Cheeseman and co-workers identified as well as the significance of Trp388 deep in the pore.<sup>35,44</sup> They also correctly suggested the involvement of His419 and Tyr32 in GLUT5 that were later shown to be involved in binding of D-fructose.<sup>16,35</sup> Kaback and co-workers also predict the involvement of Ser392 in the human GLUT5 binding site, a hypothesized binding interaction that has yet to be suggested by experimental or crystallographic data.<sup>35</sup>

### **1.3: The ICH Domain and Its Role in Substrate Transport**

In the original publication of the GLUT1 structure by Mueckler and co-workers a large, intracellular loop between transmembrane domains 6 and 7 was reported.<sup>7</sup> At the time, the structure and function of this loop was unknown and it had been proposed that this region exists as an unorganized loop.<sup>27</sup> The crystal structure of XylE showed that this region existed

as a series of helical sections that associated when the protein was in the outward-open conformation.<sup>26</sup> It has recently been shown that there are several small helices and they play a key role in the transport mechanism of GLUT proteins and their homologs.<sup>15</sup> This region, referred to as the intracellular helical or ICH domain, appears to act as a lock when the GLUT is in the outward open conformation. This lock is released upon substrate binding and conformation shift to the inward open conformation (Figure 1.5).<sup>15</sup>

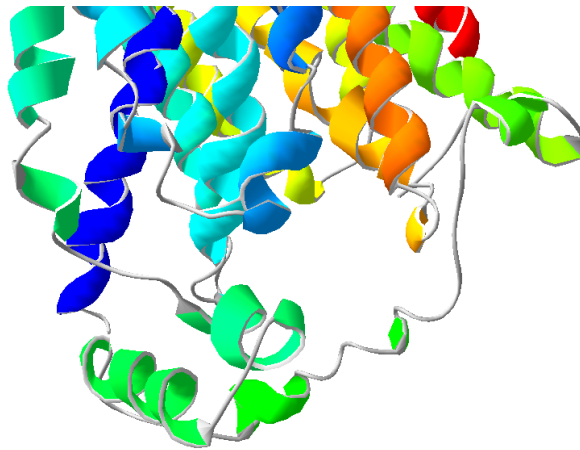


**Figure 1.5: A side on view of the ICH domain held below the intramembrane helical bundles.**

The GLUT1 crystal structure indicates that a series of hydrogen bonds help maintain the protein in its outward-open conformation. Deng and co-workers proposed that the guanidinium group of Arg153 forms two hydrogen bonds with Lys458 and that Arg212 interacts with Glu461 forming further hydrogen bonds which helps hold their respective helices in close proximity. The researchers also noted that Asp329 has a critical role in holding the protein in its outward-open conformation through a strong interaction with the backbone amides of Gly154 and Lys155.<sup>15</sup>

A year after the GLUT1 crystal structure was revealed by Deng and co-workers, Nomura and co-workers published their structure of GLUT5. They observed a series of salt bridges between the transmembrane domains and the ICH domain that appear to further stabilize the outward-open conformation. They also noted that the cytoplasmic ends of transmembrane domains 3, 4, and 5 were linked via these salt bridges to transmembrane regions 9, 10, and 11. Key residues, including Glu151 which is proposed to form a salt bridge with Arg97 and Arg407, link transmembrane domains 4 with 3 and 11 respectively. Glu400 in transmembrane domain 10 is also proposed to link to Arg158 and Arg340 in transmembrane domains 5 and 9 to further stabilize the protein. When the protein shifts to the inward-open conformations these interactions are separated by 7-13 Angstroms, making the relevant residues much too far apart for meaningful interactions to exist. Furthermore, Nomura and co-workers found that mutations of these bridging residues to neutral amino acids resulted in fully folded proteins that were arrested in the inward-open conformation and were non-competent transporters. It is likely that these salt bridges, along with others which exist between the transmembrane helical bundles, act to help maintain the overall tertiary structure of the protein.<sup>16</sup> Many of the human diseases related to impaired GLUT function are caused by gene mutations that map onto the ICH domain or around the sites at which the transmembrane bundles interact further highlighting the importance of these gating interactions.<sup>15,16,45-48</sup>

The energy involved in the outward-open to inward-open conformation interconversion has never been quantitatively calculated or measured. The Simple Carrier Model and modern computational work both indicate that the return of the empty protein to the outward-open conformation after dissociation of the substrate is the rate limiting step in

the cycle. This hypothesis is in agreement with kinetic data collected while studying the GLUT transporters including trans and cis-stimulation experiments.<sup>10,18,35</sup> It must be assumed that the energy required for the conformational shift is quite low and that GLUT proteins exist in a metastable state. Without the energetic impetus provided through a coupled transport mechanism (proton or ion), or transport being an ATP driven process, the barrier to conformational change must be small. If a large energetic barrier existed between the outward-open and inward-open conformations the high level of substrate specificity could not exist as the subtle binding of a hexose would not create an energetic impetus for protein conformational shift.

#### **1.4: GLUT5: Expression and Its Role in Breast Cancer**

Breast cancer is the most common form of cancer diagnosed in women and it is the second leading cause of cancer related deaths in Canada. It is estimated that in 2016 more than 25,000 new cases of breast cancer will be diagnosed in Canada and nearly 5,000 women will die from breast cancer.<sup>49</sup> The earlier a cancerous tumor can be detected the more likely a positive outcome for the patient will be.<sup>50-52</sup> Detection of cancerous masses inside breast tissue is a challenging task, particularly in the important early stages of the disease, due to the nature of breast tissue and the small size of early stage tumors. Breast tissue is rich in adipose tissue, ducts, glands, and other complex structures which can make the interpretation of a mammogram difficult. Mammography and self-exam serve as useful methodologies for the detection of tumors once they reach a sufficient size to be seen on a mammogram or detected manually but smaller tumors are much more challenging to find.<sup>50-52</sup> New methodologies for

the early detection of breast tumors are clearly needed. To differentiate cancerous cells from the various types of healthy tissues that may surround it morphological differences in the cancerous cells must be found and exploited.

From the initial report by Warburg and co-workers in 1927<sup>53</sup> the metabolic role of hexoses including D-glucose, D-fructose and others has been widely studied and comprehensively reviewed on many occasions.<sup>54,55</sup> The so called Warburg effect is a noted trait of cancer cells in which a large increase in the rate of uptake of simple sugars is observed. The rapidly growing and dividing cancer cells have a huge energetic demand and respond by upregulating hexose transport and metabolism to feed that demand. In most cases this is accomplished by an increase in GLUT1 expression which allows for rapid D-glucose transport.<sup>56</sup> Further, cancer cells rely more on glycolysis than the citric acid cycle to produce energy. Warburg proposed that the mitochondria in cancer cells had a decreased or impaired functionality which has recently been confirmed through the analysis of mitochondrial DNA from tumor cells.<sup>53,57</sup> Several other known oncogenes have been linked to dysfunctional hexose metabolism and transport in cancer cells.<sup>58,59</sup> Due to its ubiquitous distribution and specificity for D-glucose GLUT1 has frequently been found to be overexpressed in the human cancers while other members of the GLUT family have not.<sup>56</sup>

Another member of the GLUT family that has been studied in relationship to human cancers is GLUT5. Not only is GLUT5 one of the few GLUTs that can transport D-fructose<sup>60</sup>, it has a narrow tissue distribution in the human body,<sup>18,20</sup> usually found in sperm<sup>8</sup>, the small intestine<sup>61</sup>, the liver<sup>62</sup> and adipose tissue<sup>63</sup> GLUT5 has also been found to be both present, and overexpressed in human breast cancers.<sup>64,65</sup> In their 1996 report Vera and co-workers showed that GLUT5 was present on the membrane of the immortalized human breast cancer cell lines

MCF-7 and MDA-468.<sup>64</sup> Through a combination of immunohistochemical techniques and substrate uptake measurements the presence of a large amount of GLUT5 on the surface of these cell lines was established. Vera and co-workers first showed that [<sup>14</sup>C]-2-deoxy-D-glucose (DOG) entered the cell lines of interest using 2-methoxy-glucose as a standard.<sup>64</sup> 2-deoxy-3-O-D-methoxy-glucose is known to be transported by GLUT1 but not metabolized, though it is phosphorylated in the cell cytosol.<sup>42</sup> After confirming their methodology with DOG they showed that D-fructose also entered the cell lines via the same methodology and that this uptake was inhibited by the addition of Cytochalasin B.<sup>42</sup> Vera and co-workers identified a band corresponding the molecular weight of GLUT5 using a Western Blot technique and an anti-GLUT5 antibody. They also showed the presence of GLUT1 and GLUT2 via this technique with complementary antibodies. Finally, an anti-GLUT5 antibody was linked to fluorescein and a confocal image of cells stained with this antibody adduct were obtained in MCF-7 and MDA-468 cells while no fluorescent image was observed in healthy breast tissue. Through complimentary methodology with anti-GLUT1 and anti-GLUT2 antibodies, Vera and co-workers identified GLUT1 and GLUT2 on both MCF-7 and MDA-468 cells and initially reported that no staining was observed in normal tissue with the GLUT5 antibody. In a correction, published soon after their initial report, they did report some GLUT5 staining in normal breast tissue. The presence of these three GLUT transporters accounts for the observed transport of DOG, 2-deoxy-3-O-methoxy-D-glucose and D-fructose that the authors found. This also accounts for the sensitivity to Cytochalasin B observed when recording D-fructose uptake as GLUT2 would be inhibited by Cytochalasin B.<sup>64</sup>

Antisense oligonucleotides against GLUT5 were constructed by Fung and co-workers in 2004<sup>66</sup> which led to the reduction of GLUT5 expression when applied to MCF-7 and MDA-

MB-231 cell lines. MDA-MB-231 cells are another line of GLUT expressing, human breast cancer cells which the authors used to compare GLUT expression and activity. The application of antisense oligonucleotides resulted in a decrease in GLUT5 mRNA as well as the amount of expressed GLUT5 on the cell surface as probed by RT-PCR and Western Blotting. The result of this decrease in GLUT5 expression was a corresponding decrease in cell proliferation and a decreased amount of D-fructose being taken up into the cells. This study combined with the earlier work of Vera and co-workers shows strong support for the presence of an abundance of GLUT5 on these breast cancer cells and that Western Blotting is a reliable method to determine the presence of these proteins on the cell surface.<sup>64,66</sup>

A counterpoint to the work performed by Vera and co-workers and Fung and co-workers was published in 2011 by Gambhir and co-workers.<sup>67</sup> In this publication the authors used the same cell lines as the Vera and Fung groups, MCF-7 and MDA-468, as well as MCF-10A which is an immortalized breast cancer cell that is often used as a normal breast tissue cell line in *in vitro* experiments due to its expressed morphology.<sup>68</sup> They found that MCF-7 and MCF-10A cells took up similar amounts of [<sup>14</sup>C]-D-glucose and [<sup>14</sup>C]-D-fructose while MDA-468 cells took up more [<sup>14</sup>C]-D-fructose than [<sup>14</sup>C]-D-glucose and more [<sup>14</sup>C]-D-fructose than the other cell lines took up of either hexose. This was in contrast to the amount of GLUT5 mRNA that was found through qPCR analysis. MCF-10A was found to have much more GLUT5 mRNA than either of the other cell lines despite showing low D-fructose uptake. When attempting to reproduce the results of Vera and co-workers, Gambhir's group was unable to find a Western Blot band corresponding to GLUT5 in MDA-468 cells and only a small band from MCF-7 cells. They also found that the uptake of D-fructose in MDA-468 and MCF-7 cells was inhibited by the presence of Cytochalasin B, though this inhibitor is known

to not inhibit the GLUT5 pathway. SiRNA of GLUT5 was produced to carry out knockdown experiments in MCF-7 cells and incubation of the cells with the siRNA resulted in a significant decrease in the relative GLUT5 mRNA level but almost no change in the [<sup>14</sup>C]-D-fructose uptake. Gambhir and co-workers concluded from these results that GLUT5 is not over-expressed in MCF-7 and MDA-468 cell lines and in turn is not over-expressed in human breast cancers.<sup>67</sup>

The conclusions of Gambhir are strongly stated in this 2011 publication. This is despite the opposing observations by the groups of Vera and Fung outlined above. Further, the work of Chinnaiyan and co-workers showed that D-fructose transport was linked strongly to a type of prostate cancer that is believed to express GLUT5.<sup>69</sup> Further, previous work by Gambhir's group showed that labelled derivatives of D-fructose can be transported by GLUT5 expressing cells. The corresponding results will be described in-depth later in this chapter (Section 1.8).<sup>70</sup> The debate concerning the presence and expression levels of GLUT5 in many forms of human breast cancers is ongoing in the literature of this field. Though the exact expression level of GLUT5 in breast cancer cells is debated its presence is widely accepted. Further, it is clear that the relationship between GLUT5 mRNA and GLUT5 present on the cell membrane is not directly correlative as the central dogma of molecular biology would predict.<sup>71</sup> This non-typical expression in breast cancer tissue has been utilized by a handful of research groups in an attempt to produce substrates specific for GLUT5 for several purposes which will be discussed in-depth below.

## 1.5: A Brief Introduction to Molecular Imaging Techniques and Tracer Compounds

The field of molecular imaging includes a wide number of techniques which are all employed to measure biological processes at the molecular and/or cellular levels. Positron emission tomography (PET) and optical imaging both utilize tracer molecules to enable the *in vivo* visualization of specific tissues. Tracer molecules are small molecules that are functionalized in some fashion so that they can be visualized once they have accumulated in a specific tissue or type of cell. The type of functionalization present on the molecule is dependent on the imaging modality being employed. In the case of PET imaging a radionuclide is incorporated into the tracer molecule while in optical imaging a fluorophore is incorporated onto the tracer compound.<sup>72-74</sup>

PET tracers utilize positron emitting radionuclides such as  $^{18}\text{F}$ ,  $^{11}\text{C}$ , or  $^{95}\text{Tc}$  etc.<sup>75</sup> These nuclei decay to emit a positron, the antimatter equivalent of an electron which bears a +1 charge. These high energy particles are emitted from the nucleus and then travel a short distance. While travelling outside the nucleus the positron loses kinetic energy rapidly until it is at a similar energy level to that of an electron surrounding a nearby atom. The interaction of a positron with the suitable kinetic energy and an electron results in the annihilation process which results in the conversion of the positron and electron into 2 gamma rays. The gamma rays escape at a  $180^\circ$  angle relative to the orientation of the collision event and do not interact with the surrounding tissues. The escaping gamma rays can be detected by a gamma ray detector which can be built to encircle the tissue or patient being examined. The detector and associated computer programs can then render an image based on the calculated source of the gamma rays to give a two or three dimensional image of where positrons are being produced

with the tissue. This image can directly be correlated to the amount of PET probe molecule which is in those tissues.<sup>76-78</sup>

PET imaging has several advantages which make it attractive as a medical imaging modality. Firstly, there are no naturally occurring gamma ray emitters inside the human body so there is essentially no background signal in a medical PET scan. Further, the gamma rays resulting from positron annihilation do not interact with the tissues of the body and thus there is no limit to the depth in the body from which a PET image can be obtained.

Unfortunately, PET imaging also has two major drawbacks which limit its application.<sup>72</sup> Positron emitting nuclei can only be produced with a cyclotron particle accelerator. These large, expensive, and extremely complicated facilities are much too large and specialized to be installed in every location where PET imaging could be of use. The PET emitting nuclei produced also have short half-lives;  $^{18}\text{F}$  has a half-life of 109.8 minutes and  $^{11}\text{C}$  has a half-life of only 20 minutes for example.<sup>79,80</sup> PET tracer compounds must be produced and used within a very short period of time and cannot be transported long distances from the production facility and still retain a useful amount of active nuclei.<sup>75</sup>

PET tracers must also be designed so that they accumulate in the desired tissue and that the radionuclei can be incorporated in a late stage of the synthesis. If the production process takes too long from the point of radionuclei incorporation to completion then the tracer molecule will lose much of its positron emitting potential and the tracer will not be able to produce a PET image of sufficient quality. The tracer compounds must also accumulate in the target tissue. This optimization can be a long and labour intensive process. This process can take many years or even decades. The design and optimization of some of the more common PET probes has been elegantly reviewed in the literature several times.<sup>76-78</sup> Optical

imaging stands as an imaging modality that could help alleviate the issues with PET imaging but is not without limitations of its own.

Optical imaging involves tracer compounds, much like PET imaging, but rather than being functionalized with radionuclide optical imaging probes have dye molecules appended to them. These dyes vary widely in chemical structure but their role as part of the optical imaging tracer is the same. The dyes absorb a photon of light at a specific wavelength which promotes an electron from the  $\pi$ -system of the dye to an excited state. From this excited state the electron can then decay back to a ground state concurrent with the release of energy in the form of a photon at a different wavelength than the photon which initially excited the electron. The difference in wavelength between the wavelength of excitation and that of emission is known as the Stokes Shift of the dye. The excitation and emission wavelengths of a dye can be tuned by altering the size (length), and composition (linearity, heteroatoms, etc) of the conjugated  $\pi$ -system in the dye.<sup>77,81,82</sup>

Much like PET tracer compounds, optical imaging tracers must be specifically designed so that they are taken up into only the desired tissue types. This tracer design is further complicated by the presence of the large dye molecule attached to the tracer compound. These dyes commonly possess poly-functionalized and long conjugated  $\pi$ -systems. These are inherently hydrophobic which limits their solubility in aqueous media. Optical imaging agents are desirable as they do not suffer from the rapid radio decay observed with PET radionuclides; optical imaging dyes have stable lifespans of months to years. The detection equipment used with optical probes is also much less expensive than PET detectors.<sup>77</sup> The type and structure of dye as well as the nature of the tracer molecule both

need to be examined during the production of an optical imaging probe so that the final tracer compound will have all the required traits.<sup>83</sup>

In addition to the constraints on the design of optical imaging tracer compounds imposed by the dye, optical imaging also suffers from poor light penetration into tissues. The excitation light must reach the dye in order to excite the dye and it must do so in sufficient intensity so that the resulting emitted light is detectable after it exits the tissue. This limits optical imaging to a few centimeters of tissue depth in most cases.<sup>77</sup> This limitation in light penetration is due to the composition of living tissue. The abundance of complex biomolecules including proteins and nucleic acids acts as a shield to the light attempting to penetrate the tissue. The exact depth a photon of a given wavelength can penetrate into a tissue is dependent on both the wavelength of the photon and the composition of the tissue being irradiated.<sup>82,84-87</sup>

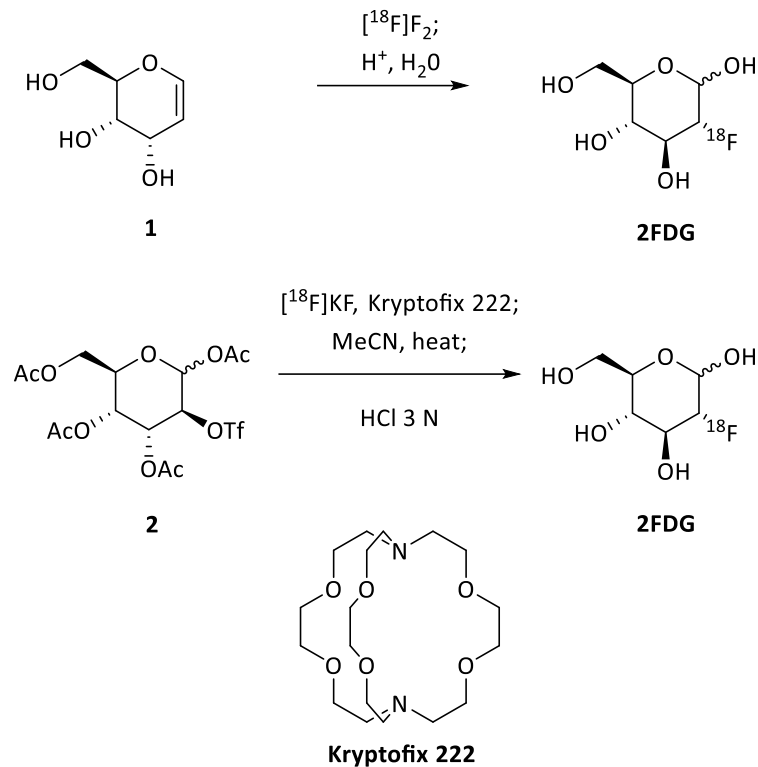
A number of both PET and optical imaging tracers which have been developed in the past and have been used for *in vitro* and *in vivo* imaging utilizing the GLUT transport pathway, are described in more detail below.

## **1.6: Small Molecule Substrates of GLUT1: Synthesis and Evaluation**

After its first appearance in the literature<sup>88</sup> 2-deoxy-2-fluoro-D-glucose (2FDG), more specifically its <sup>18</sup>F analog, has been widely used in medical imaging.<sup>79</sup> The clinical role of 2FDG as a PET imaging agent has been reviewed several times<sup>89-92</sup> and guidelines are in place for its use.<sup>93</sup> 2FDG has also served as one of the first probes into the substrate tolerance

of the GLUT transporters. As GLUT1 has been found to be overexpressed in many human cancers, including breast cancer,<sup>94</sup> a GLUT1 specific imaging agent like 2FDG has proven to be of great clinical use for decades. However, the use of  $^{18}\text{F}$  as a radiotracer has several drawbacks. Though the production of [ $^{18}\text{F}$ ]2FDG is now routine,<sup>95</sup>  $^{18}\text{F}$  can only be produced in a cyclotron facility<sup>96</sup> and has a half-life of 109.7 minutes<sup>97</sup> meaning that its production and application is limited to areas immediately around facilities capable of producing the  $^{18}\text{F}$  isotope.

2FDG was first produced by treatment of D-glucal, **1**, with [ $^{18}\text{F}$ ]- $\text{F}_2$  in an aqueous solution which yields a 4:1 mixture of [ $^{18}\text{F}$ ]2FDG and [ $^{18}\text{F}$ ]-2-fluoro-2-deoxy-D-manopyranose.<sup>88</sup> The currently used preparation for [ $^{18}\text{F}$ ]2FDG involves the displacement of a triflate leaving group from **2** by a fluoride anion in the presence of the potassium chelator Kryptofix 222.<sup>98</sup> Removal of the acetate protecting groups from **2** yields [ $^{18}\text{F}$ ]2FDG (Scheme 1.1).<sup>99</sup>



**Scheme 1.1: The two general methods for the production of 2FDG along with the structure of Kryptofix 222.**

The tissue uptake selectivity of 2FDG is also an issue in many tumor types. Due to the ubiquitous expression of GLUT1 throughout the human body 2FDG PET imaging faces several issues including false positive tests and overestimation of tumor margins. False positives can result when a tissue type which strongly expresses GLUT1, for example adipose tissue or immune cells are found near a suspected tumor site.<sup>100</sup> When the PET image is resolved a dense area of radioactivity will be observed and diagnosed as tumor tissue despite it being healthy tissue which has taken up a large amount of 2FDG due only to its normal expression of GLUT1.<sup>101</sup> This can also cause an overestimation of the size of a tumor and the removal of tissue needlessly during resection. It is also possible that a resection surgery could miss a portion of a real tumor which is buried in tissue that is highlighted by 2FDG PET

imaging (Figure 1.6).<sup>102,103</sup> A probe that is more specific to a particular tumor type is clearly of need to the medical and scientific field as a whole.

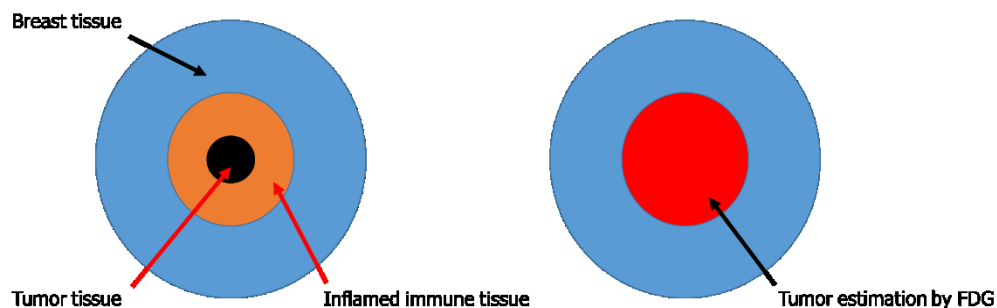
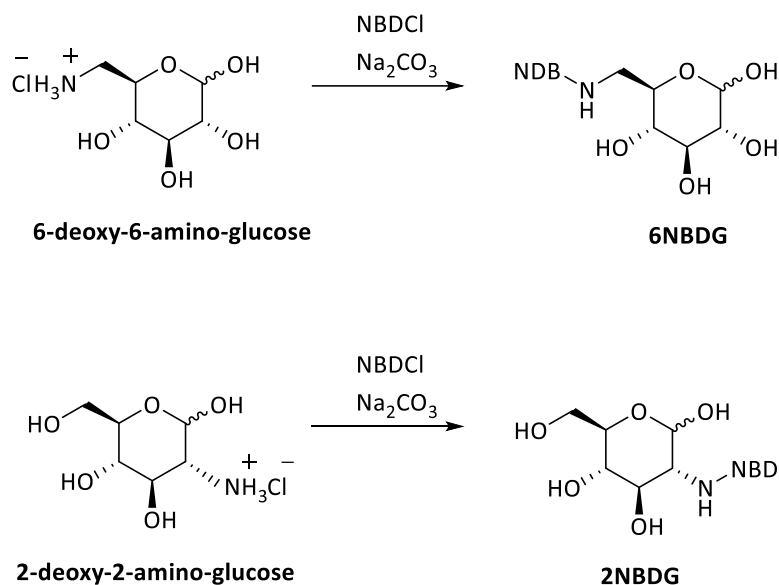


**Figure 1.6: A diagram showing the potential for the overestimation of a tumors size by FDG PET imaging. Left: Tumor tissue (black) is surrounded by inflamed immune tissue (yellow). Both of these tissues can contain a large amount of GLUT5 which transports FDG. Right: the resulting estimation of the tumor disuse derived from FDG imaging which highlights both the tumor and inflamed tissue (red).**

Significant work has been done using hexoses tethered to the small fluorescent dye 7-nitrobenz-2-oxa-1,3,-diazol-4-yl (NBD) namely 6-(*N*-(7-nitrobenz-2-oxa-1,3-diazol-4-yl)amino)-6-deoxyglucose (6NBDG)<sup>104–107</sup> and 2-(*N*-(7-nitrobenz-2-oxa-1,3-diazol-4-yl)amino)-2-deoxyglucose (2NBDG)<sup>108–113</sup> as probes for D-glucose uptake. This work has paved the way for modern work with the GLUT5 pathway.



**Scheme 1.2: The coupling of the NBD moiety to the relevant amino hexose to generate 6NBDG or 2NBDG.**

Since its first synthesis in 1985 by Speizer and co-workers,<sup>104</sup> 6NBDG has been used as a convenient probe to monitor the uptake of D-glucose in several cell types. 2NBDG has been used in similar studies since it was first reported by Yoshioka and co-workers<sup>114</sup> in 1996 (Scheme 1.2). These two compounds are similar in general chemical structure varying only at the position of dye attachment, C6 vs. C2. It has been repeatedly observed that these probes are taken into cells via the D-glucose uptake pathway, primarily via GLUT1. Despite the presence of the large, aromatic, hydrophobic, and moderately functionalized dye appended to the hexose these probes are transported and accumulate inside cells though their transport is slow.<sup>106,108,113,115,116</sup> This result is interesting as the binding site within GLUT1 is very similar to that of GLUT5, which is discussed above, and has stringent recognition elements.<sup>26</sup> With the knowledge that a small dye like NBD can enter via GLUT1 when appended to a D-glucose scaffold extension to an NBD appended another hexose to serve as a probe was inevitable.

## 1.7: Small Molecules as Structural Probes of the GLUT5 Binding Site

The first art in regards to NBD labelled D-fructose probes began long before the crystal structure of GLUT1 or GLUT5 were known. In 2000 Holman and co-workers published a study in which they developed several analogs of simple hexoses and screened them as inhibitors for GLUT5 (3-12, Figure 1.7).<sup>117</sup> This work was followed up by a second publication in 2003 divulging a new set of fused ring analogs of D-fructose that allowed Holman and co-workers to further probe the binding pocket of GLUT5.<sup>39</sup> In these landmark publications Holman and co-workers made several key observations about the substrate tolerance of the GLUT5. Through the systematic alkylation of the C1, C2, C3, C4, and C6 positions of D-fructofuranose they were able to show that only alkylation at the C6 position was well tolerated by GLUT5. Addition of an allyl or bulky alkyl groups at the other free hydroxyls resulted in the compounds not being able to inhibit the transport of [<sup>14</sup>C]-D-fructose, presumably this was because the allylated/alkylated substrate was not binding to GLUT5 as strongly as the C6 modified analogs. The Holman group also found that the epimers of D-fructose, D-psicose (**10**), D-tagotose (**11**) and L-sorbose (**12**), showed weaker binding than the D-fructose analogs. Interestingly they also observed that 2,5-anhydromannitol was a reasonably potent inhibitor of GLUT5.<sup>117</sup>

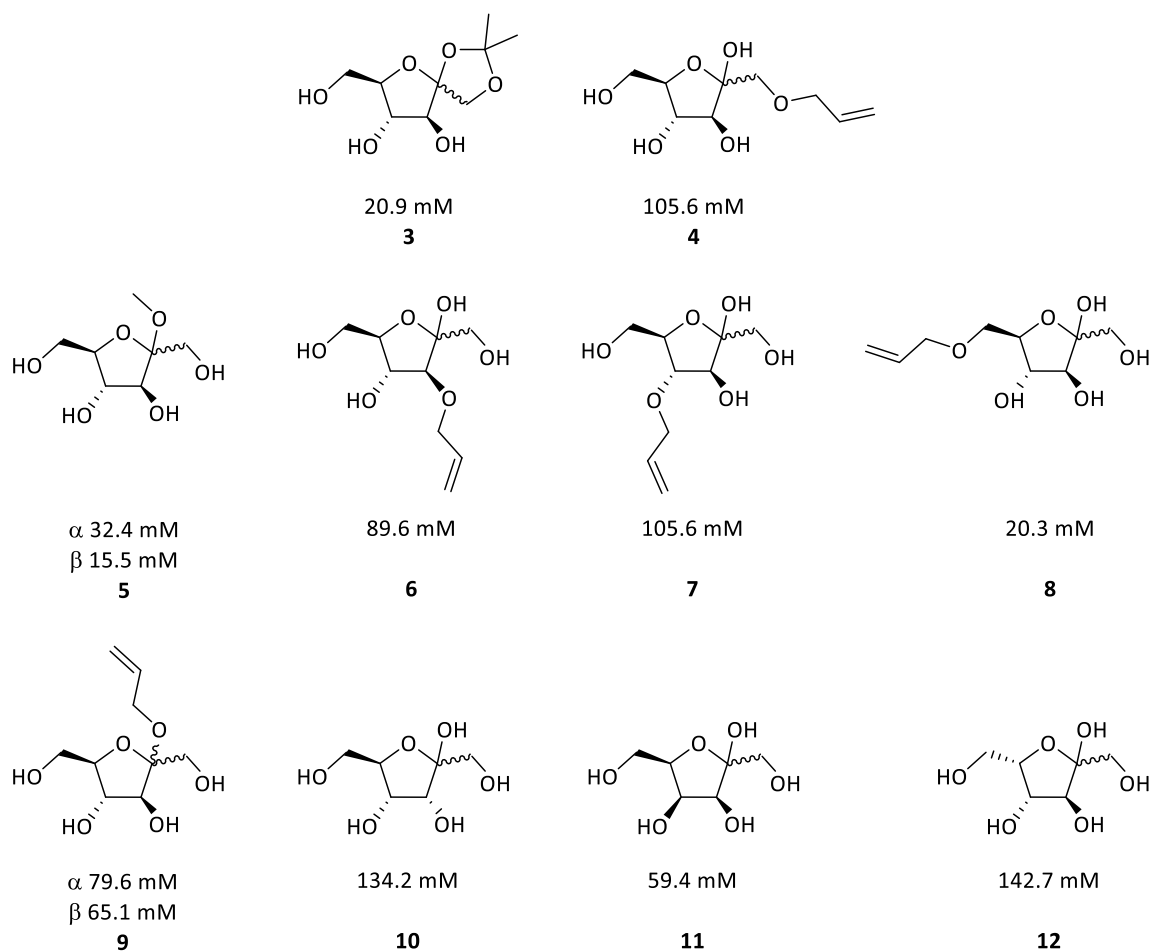


**Figure 1.7: A selection of modified hexose compounds produced and tested by the Holman group and their reported affinities for GLUT5.**

In their second publication Holman's group generated a series of 1,3-oxazolidin-2-thiones and 1,3-oxazolin-2-one compounds (**13-16**, Figure 1.8).<sup>39</sup> These fused ring systems would now present different hydrogen bond partners to the GLUT5 binding pocket which would be shifted slightly in their orientation compared to D-fructose. These families of compounds were compared to D-fructose for their ability to bind to GLUT5 and inhibit the uptake of [<sup>14</sup>C]-D-fructose. Based on their  $K_i$  values these ring fused compounds were comparable, and in many cases even better inhibitors than D-fructose. The most potent inhibitors were the 1,3-oxaxolin-2-one derivatives of L-sorbose with a benzyl group on the C1

oxygen (**15**,  $K_i = 3.1$  mM) and the corresponding non-benzylated derivative (**14**,  $K_i = 7.2$  mM) both of which are better binders than D-fructose itself ( $K_i = 15.5$  mM). The addition of the 1,3-oxazolin-2-thione system to D-fructose had a notable effect increasing the observed  $K_i$  to 24.9 mM as in **13** and larger perturbations were poorly tolerated by GLUT5 exemplified by the 1,3-oxazolin-2-thione derivative of L-arabinose (**16**) which had a  $K_i$  of 122.8 mM. These two structure-activity-relationship (SAR) studies showed that the C1, C2, C3, and C6 positions could be modified and would still act as GLUT5 substrates/binders as long as hydrogen bond capability was maintained at the C1, C2, and C3 positions.<sup>39</sup>

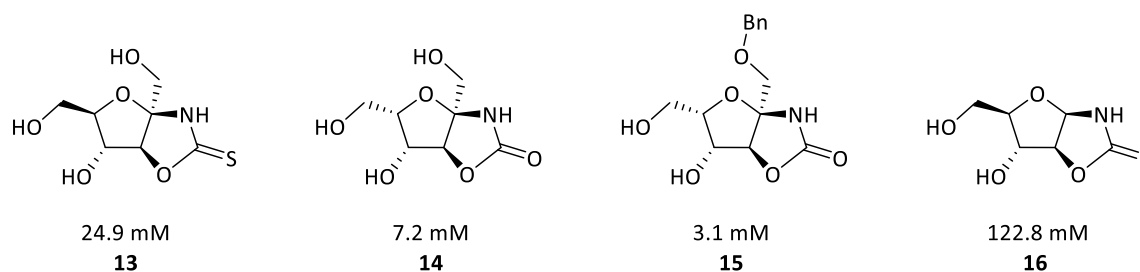


**Figure 1.8: A selection of ring fused compounds produced by the Holman group and their reported affinities to GLUT5.**

While working on the SAR studies presented above Holman and co-workers also produced a small family of photoaffinity labels for GLUT5.<sup>118</sup> In this 2002 publication a family of D-fructose and 2,5-anhydromanitol derivatives were produced with aryl-diazine moieties attached to the 6 position of the hexose (**17,18**, Figure 1.9). These compounds were incubated with GLUT5 expressing CHO cells and irradiated in a photoreactor.<sup>119</sup> The cell membrane material was isolated and probed through Western Blotting with an anti-GLUT5 antibody to reveal a GLUT5 sized band which was tagged by the photoaffinity label.

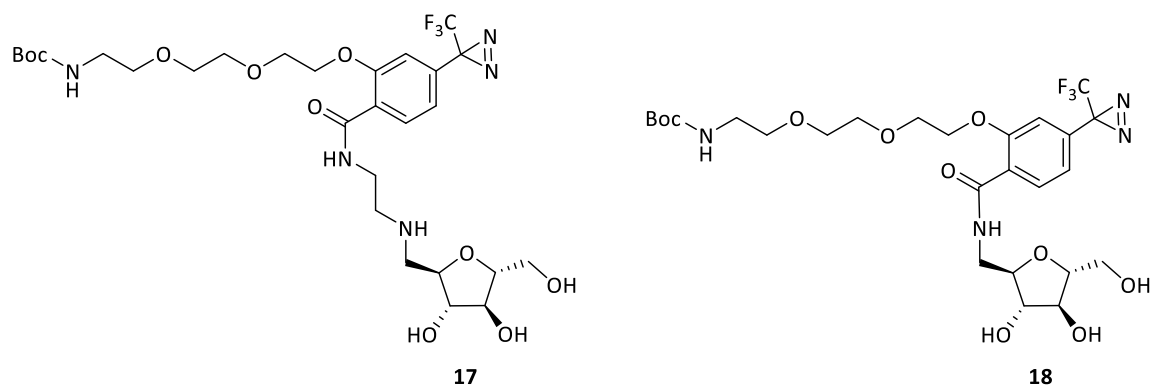


**Figure 1.9: Two examples of anhydromannitol derivatives bearing a photoaffinity labels produced and used by the Holman group.**

The authors also developed a small subset of D-fructose and 2,5-anhydromannitol derivatives based on their earlier results<sup>117</sup> which are appended with allyl or 2,4-dinitrophenyl groups at the C1 or C6 position (Figure 1.10). The highest affinity compound tested was found to be 1,5-bis(1-amino-2,5-anhydromannitol)-2,4-dinitrobenzene (**19**) with a  $K_i$  of 0.52 mM followed closely by N-(2,4-dinitrophenyl)-amino-2,5-anhydromannitol (**20**) with a  $K_i$  of 0.56 nM. Among the smaller molecules, allylated compounds 1-allylamino-2,5-anhydromannitol (**21**) was found to be the strongest binder with a  $K_i$  of 2.66 mM. This work gave further weight to the idea that the 6 position of the sugar could be functionalized to a wide extent and recognition by GLUT5 would be maintained. In the case of many of Holman and co-workers compounds, they found an enhancement in binding strength upon the addition of bulky or hydrophobic moiety to the C6 position.<sup>39,117,118</sup>

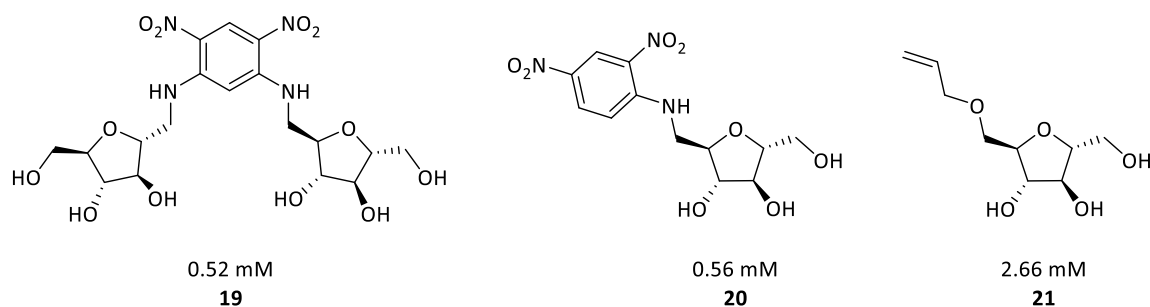
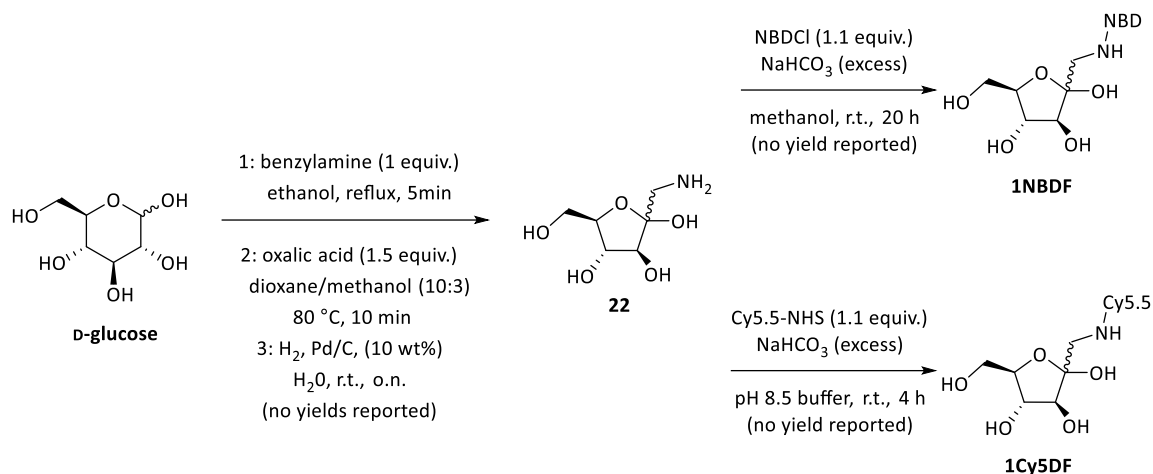


**Figure 1.10: High affinity GLUT5 substrates produced by the Holman group and their reported affinities for GLUT5.**

## 1.8: Small Molecule Imaging Agents: The Utilization of the GLUT5 Pathway

Expanding on the work of Holman and co-workers, Gambhir and co-workers published in 2007 showcasing their new fluorescent D-fructose derivatives 1-(*N*-(7-nitrobenzo-2-oxa-1,3-diazol-4-yl)amino)-1-deoxyfructose (1NBDF) and 1-*N*-1-amino-deoxyfructose-[(2*E*)-1,1-dimethyl-2-[(2*E*,4*E*)-5-(1,1,3-trimethylbenzo[*e*]indol-3-ium-2-yl)penta-2,4-dienylidene]benzo[*e*]indol-3-yl]hexanoate (1Cy5DF).<sup>70</sup> These compounds were produced from the common intermediate 1-amino-1-deoxyfructose (**22**) and the fluorescent dye was appended directly through substitution chemistry with the commercially available 4-chloro-7-nitrobenzofurazan (NBDCI) or the succinamide ester of the Cy5 dye (Cy5.5-NHS) (Scheme 1.3).



**Scheme 1.3: The route of Gambhir and co-workers to produce 1NBDF and 1Cy5DF from D-glucose via the Amadori rearrangement.**

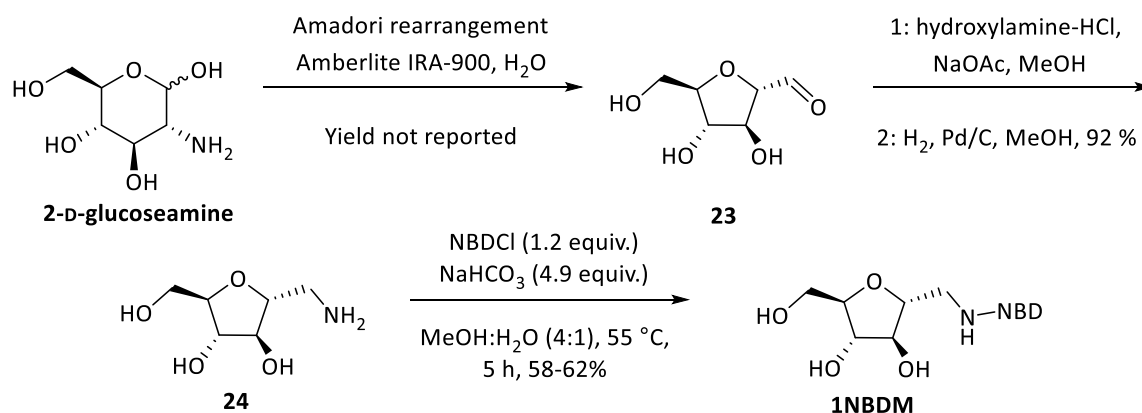
To demonstrate the utility of these compounds Gambhir and co-workers used confocal microscopy and flow cytometry to show that these compounds could be internalized by three human breast cancer lines which express GLUT5 and not by the HepG2 cell line which does not express GLUT5 as a negative control. They found that 1NBDF was taken into the MCF-7, MBA-MB-231, and MDA-MB-435 breast cancer cells as demonstrated by a clear confocal image which was obtained after incubation with a 10  $\mu$ M solution of their probe compound for 15 minutes. 1Cy5DF was taken into the cells but resulted in a much lower fluorescent intensity in all of the studied cancer cell lines. It was also observed that the location of 1Cy5DF inside the cell appeared to be different than that of 1NBDF. The larger 1Cy5DF did not accumulate throughout the cytoplasm of the cell, rather it was localized to several small sub-regions inside the cell. Conversely, the smaller 1NBDF appeared to be distributed evenly throughout the cytoplasm. At low temperature the authors found essentially no transport of any of their probes hinting that the mechanism of uptake was transporter mediated and not the result of passive diffusion which would have been observed even at low temperature. The

authors briefly discussed the results of their flow cytometry work but did not display it in the main body of this publication nor any supporting information. They commented that the results of flow cytometry matched with those of confocal microscopy but did not elaborate further or provide experimental results. The HepG2 cell line did show a weak fluorescent image when incubated with 1NBDF, a strong fluorescent image with 1Cy5DF, and a very strong fluorescent image when 2NBDG was used. This was unsurprising since these cells were not believed to express GLUT5 at a meaningful level and were known to express GLUT1, the transporter which would handle the uptake of 2NBDG. It is of note that 1Cy5DF gave a good image in these cells as it appeared to be easily entering cells that lack GLUT5.

In an attempt to determine the exact pathway these probes were being transported, Gambhir and co-workers ran inhibition experiments using D-fructose or D-glucose as the uptake inhibitor in 50 mM concentrations. They observed that 1NBDF uptake was inhibited by D-fructose and by D-glucose both using confocal microscopy and flow cytometry, though the flow cytometry data were not presented in the publication. The uptake of 1Cy5DF was not affected by either of the unlabelled hexoses leading the authors to conclude that 1Cy5DF was not transported via a GLUT mediated pathway. They do conclude that 1NBDF is being transported primarily by GLUT5 despite the apparent inhibition by D-glucose, which should not affect the GLUT5 pathway. A partial explanation is given in that while performing flow cytometry experiments the authors were unable to find a direct, concentration based relationship between the level of 1NBDF transport inhibition and the amount of either D-fructose or D-glucose used as the inhibitor. They proposed that this is due to the large excess of unlabelled hexose present in the extracellular solution causing unpredictable effects on the cells at a global level rather than on the GLUT transporters alone. Without the flow cytometry

data being presented this proposal is impossible to discuss further. With these results Gambhir and co-workers concluded that 1NBDF was transported primarily through the GLUT5 pathway acting as a D-fructose mimic while 1Cy5DF was being taken up through a different, non-GLUT mediated mechanism.<sup>70</sup>

From the work of Holman and co-workers probing the substrate requirements of GLUT5 the group of McQuade noticed that 2,5-anhydromannitol, the 2-deoxy C<sub>2</sub> symmetric derivative of D-fructose, was a substrate for GLUT5.<sup>39,117</sup> They utilized the commercially available 2-D-glucosamine to produce 1-amino-2,5-anhydromannitol (**24**) through a short sequence of steps via the Amadori rearrangement to afford **23**. Then 1-amino-2,5-anhydromannitol could then be directly coupled to NBDCI to produce 1-(*N*-(7-nitrobenz-2-oxa-1,3-diazol-4-yl)amino)-1-amino-2,5-anhydromannitol (1NBDM) (Scheme 1.4).<sup>120</sup>



**Scheme 1.4: The route of the McQuade group to produce 1NBDM from D-glucosamine.**

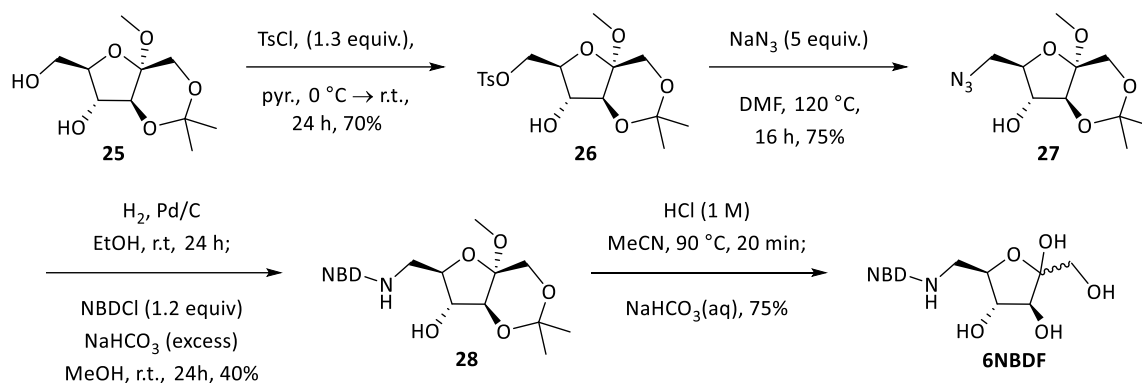
In their 2013 publication, McQuade and co-workers demonstrated through several methods that 1NBDM was taken into MCF7 cells via GLUT5. Initially they utilized a confocal microscope capable of measuring gained fluorescence quantitatively while recording a fluorescent image. When MCF7 cells were incubated with a 10  $\mu$ M solution of 1NBDM a time dependent increase in fluorescence was observed as well as a clear fluorescent image

after 15 minutes. They also undertook inhibition experiments using D-fructose or D-glucose to determine their effect on 1NBDM uptake. Low concentrations of either hexose did not affect the uptake of their compound while increasing concentrations of D-fructose did inhibit 1NBDM uptake. The same concentrations of D-glucose had no effect on the uptake of 1NBDM. In contrast they did find that the uptake of 1NBDF and 2NBDG were both affected by increasing concentrations of either D-fructose or D-glucose.

McQuade and co-workers also addressed the presence of GLUT2 in MCF7 cells. GLUT2 is capable of transporting D-fructose and D-glucose as well as 2-D-glucosamine.<sup>18,121</sup> To evaluate if 1NBDM was being transported by GLUT2 they challenged their uptake experiments with increasing concentrations of 2-D-glucosamine from 0.01 mM to 50 mM. They observed no statistical change in the amount of 1NBDM transport however they did find a strong inhibition of 1NBDF transport.

McQuade and co-workers further demonstrated that the normal breast cancer cell line 184B5 is able to take up some 1NBDG and very little 1NBDM. The relative uptake amount for both compounds is much lower in the 184B5 cells than in MCF7 cells, presumably owing to the lower overall level of transporter expression and global cell metabolism in these non-cancerous cells. With their results McQuade and co-workers concluded that 1NBDM is a GLUT5 substrate and shows a high level of specificity for this pathway over other GLUTs. The authors further challenge the conclusions of Gambhir and co-workers in that 1NBDF does not appear to be a good GLUT5 substrate. Rather it appears that 1NBDF is a GLUT2 substrate as demonstrated by sensitivity to both D-fructose and D-glucose in uptake studies as found by Gambhir<sup>70</sup> and McQuade plus the inhibitory effect of co-incubation with 2-D-glucoseamine found by McQuade.<sup>120</sup>

In a recent publication by the West, Cheeseman and Wuest<sup>122</sup> groups the NBD moiety was directly attached to D-fructose at the C6 position (Scheme 1.5). This was accomplished via a selective protection/deprotection strategy which started by protection of the C1, C2, and C3 hydroxyls to produce **25** in a single step from D-fructose. Tosylation of **25** gives **26** which can react with sodium azide to yield **27** in high overall yield. From the azide **27**, reduction afforded the amine **28** which could be coupled with NBD-Cl followed by deprotection to give the final compound 6NBDF.



**Scheme 1.5:** The route of West and co-workers to produce 6NBDF from the known intermediate **25**.

This type of strategy was repeated with D-psicose, D-tagatose, and L-sorbose, representing the C3, C4, and C5 epimers of D-fructose respectively, allowing the authors to produce 6NBDF, 6NBDF, and 6NBDF (Figure 1.11). These compounds were incubated with MCF7 and EMT6 cell lines so that their transport characteristics could be determined and measured. The authors used inhibition assays, confocal microscopy, and a fluorescent plate reader to determine how their compounds entered the cells. They also utilized *in silico* molecular docking to help explain the observed results.

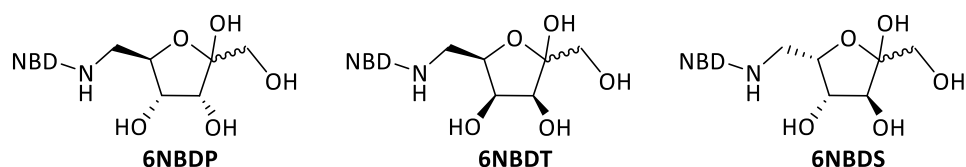


**Figure 1.11: The structure of 6NBDP, 6NBDT, and 6NBDS which were produced by West and co-workers.**

Utilizing [ $^{14}\text{C}$ ]-D-fructose or [ $^{14}\text{C}$ ]-D-glucose as the indicator molecules all 4 NBD labelled hexoses were examined for their ability to act as inhibitors to the uptake of the radiolabelled hexoses. The authors found that 6NBDF was able to inhibit the [ $^{14}\text{C}$ ]-D-fructose uptake in both cell lines while the other NBD labelled compounds inhibited [ $^{14}\text{C}$ ]-D-glucose with IC<sub>50</sub> values below 3 mM in all cases. There was no inhibition of [ $^{14}\text{C}$ ]-D-glucose observed by 6NBDF and no inhibition of [ $^{14}\text{C}$ ]-D-fructose by 6NBDP, 6NBDT, or 6NBDS indicating that these compounds were being handled by different transport pathways, 6NBDF via a D-fructose transport pathway and the other compounds by a D-glucose transport pathway.

The fluorescent plate reader technique was employed to directly measure the uptake of these fluorescent hexoses and all four produced a time dependent uptake curve over a 2 hour time course. The uptake of 6NBDF was inhibited by the addition of D-fructose to the solution but not by the addition of D-glucose. The other fluorescently labelled hexoses were not inhibited by D-fructose addition though they were by the addition of D-glucose. Furthermore, it was indicated that 6NBDF was being transported by a different pathway than the other compounds. Confocal microscopy was carried out using these fluorescent compounds to produce a fluorescent image. The generated images clearly showed that the compounds entered into both the MCF7 and EMT6 cells. Inhibition experiments complimentary to those used with radiolabelled hexoses and the fluorescent plate reader technique showed that D-fructose was again able to inhibit 6NBDF uptake and D-glucose inhibited 6NBDP, 6NBDT,

and 6NBDS. 6NBDF was again insensitive to the presence of D-glucose and the other hexoses were insensitive to D-fructose. These experimental results indicated that 6NBDF was being transported by the GLUT5 pathway while the other fluorescently labelled compounds were being handled by a different transport pathway, likely GLUT1 and/or GLUT2 based on the authors observations and previous knowledge of which GLUTs are expressed by these cells. The sensitivity of 6NBDP, 6NBDT, and 6NBDS to the addition of D-glucose in the uptake studies also supports the hypothesis that GLUT1/GLUT2 are responsible for their transport. Control experiments varying incubation temperature or a GLUT5 negative cell line transfected with GLUT5 mRNA clearly showed that the observed uptake is due to a GLUT mediated pathway.

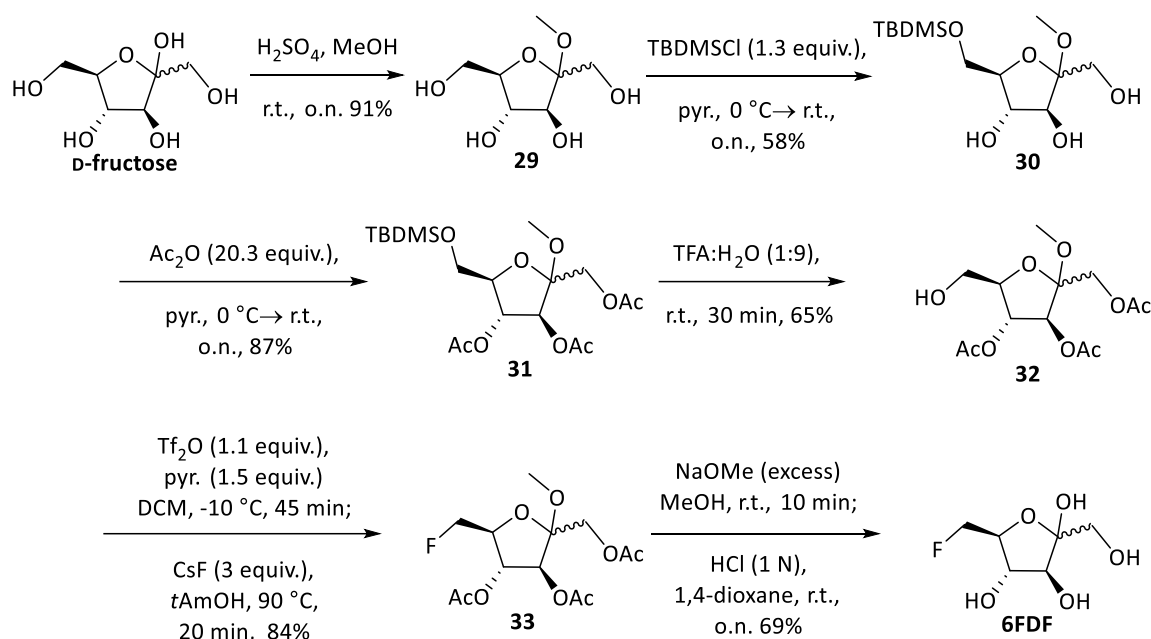
Computational docking studies carried out by the authors using the AutoDock program predicted that 6NBDF would bind to the GLUT5 binding site in the same orientation as D-fructose, with the C6 portion of the hexose oriented towards the extracellular matrix and the C1, C2 end of the hexose deep in the binding site. In contrast, 6NBDP, 6NBDT, and 6NBDS are predicted to orient with the C6 end of the hexose and the NBD moiety oriented into the binding site in their lowest energy conformations. This difference in orientation would account for the observed inability of 6NBDP, 6NBDT, and 6NBDS to enter into cells via the GLUT5 pathway. The computational results also predicted that the binding site of GLUT1/GLUT2 was more permissive to modifications at the C3, C4, and C5 positions. Experimentally this prediction was validated by the long history of modified D-glucose analogs that have been employed as imaging agents including 2NBDG and 2FDG. The authors concluded that this experimental and computational work further demonstrates that the C6 end of D-fructose oriented away from the binding site of GLUT5. The relatively large

NBD group also appeared to be freely transported through the GLUT pore once the hexose moiety makes the appropriate binding interactions. These attributes of the C6 position made it a viable target for modification in future generations of GLUT5 substrates including imaging agents or drug delivery vehicles.<sup>122</sup>

## 1.9: GLUT5 Substrates: In vivo Evaluation and Imaging

The groups of Cheeseman and West took inspiration from the work of Holman and the 2FDG field which resulted in them synthesizing 6-deoxy-6-fluoro-D-fructose (6FDF) (Scheme 1.6).<sup>121</sup> This compound was produced in a six step procedure from D-fructose and was isolated in only the furanose ring form. First D-fructose was methylated in acidified methanol to give **29** in 91 % yield. Silyl protection of the C6 position was achieved using the bulky, *t*-butyl-dimethyl-silyl chloride giving **30** which was globally acylated to afford **31**. Removal of the silyl ether was accomplished using TFA producing **32** in moderate yield. The free hydroxyl at C6 of **32** was then activated as the triflate which was displaced by fluoride using CsF to give **33**. Simple deprotection of **33** gave 6FDF. Evaluation of 6FDF in MCF7 and MDA-MB-231 human breast cancer cells revealed that the presence of 6FDF in solution strongly inhibited the uptake of [<sup>14</sup>C]-D-fructose. Through a complimentary study the authors observed that 6FDF was a much weaker inhibitor of [<sup>14</sup>C]-D-glucose uptake with an apparent  $K_i$  of 916  $\mu\text{M}$  in MCF7 cells and 2860  $\mu\text{M}$  in MDA-MB-231 cells compared to 154  $\mu\text{M}$  and 330  $\mu\text{M}$  for inhibition of [<sup>14</sup>C]-D-fructose in those cell lines respectively. Confocal microscopy using fluorescently labelled anti-GLUT1, anti-GLUT2 and anti-GLUT5 antibodies along with Western Blotting revealed that the MCF7 and MDA-MB-231 cells

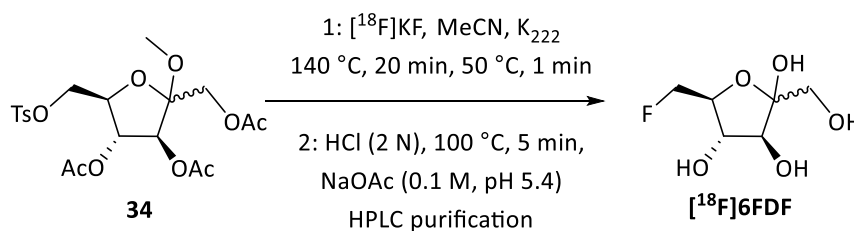
expressed all three of these GLUT transporters. To rule out the involvement of GLUT1 and GLUT2 in the transport of 6FDF, Cytochalasin B was used to inhibit the action of GLUT1 and GLUT2 but no significant effect on the results of studies using 6FDF as a [<sup>14</sup>C]-D-fructose inhibitor were observed.



**Scheme 1.6: The synthesis of 6FDF from D-fructose as published by West, Cheeseman, Wuest and co-workers.**

Two years later the radiopharmacological evaluation of [<sup>18</sup>F]6FDF was published using [<sup>18</sup>F]6FDF prepared from [<sup>18</sup>F]KF and the tosylated precursor **34** which was synthesized via a similar route as used by West, Cheeseman, Wuest and co-workers. (Scheme 1.7).<sup>123</sup> In this publication the authors show through the use of whole body imaging of BALB/c mice bearing either a murine breast cancer (EMT6 cell line) or a xenograft human breast cancer (MCF7 cell line), that [<sup>18</sup>F]6FDF is taken into these tumors. The authors also found that the uptake of [<sup>18</sup>F]6FDF with a sufficient bias over normal tissue as to make a clear PET image of the tumor. It was also observed that when [<sup>18</sup>F]6FDF uptake in the mice was compared to that

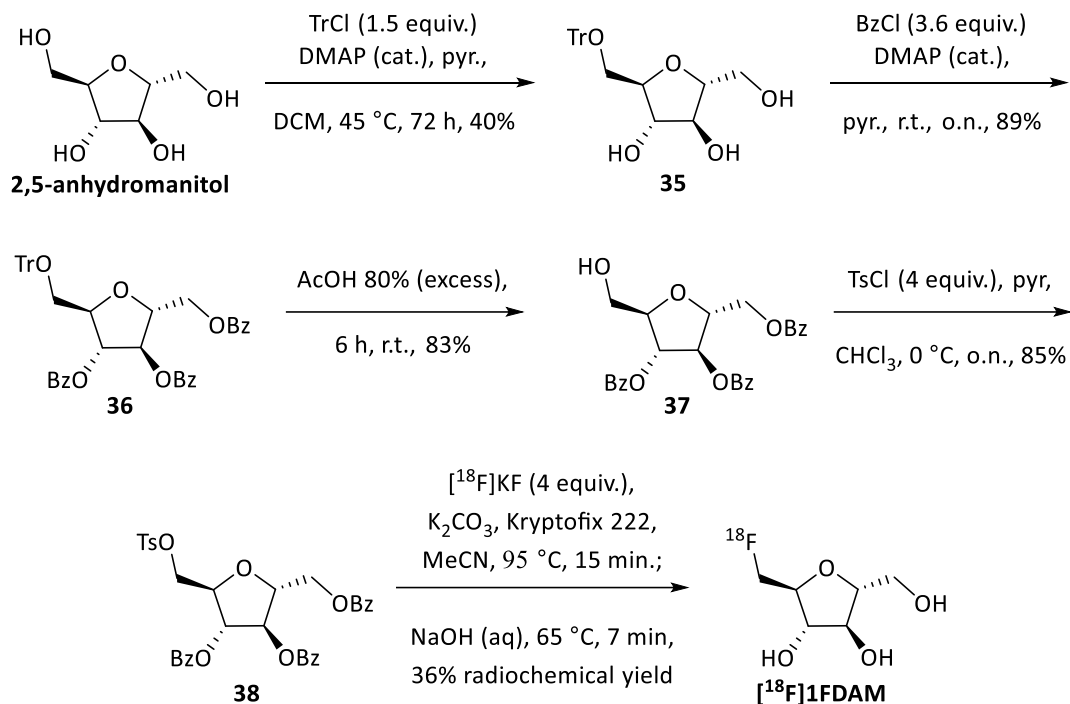
to [ $^{18}\text{F}$ ]2FDG, the [ $^{18}\text{F}$ ]6FDF accumulated in the tumor much faster than did [ $^{18}\text{F}$ ]2FDG. Accumulation took only 15 minutes for [ $^{18}\text{F}$ ]6FDF as compared to 2 hours for [ $^{18}\text{F}$ ]2FDG. Further, the [ $^{18}\text{F}$ ]6FDF was observed to wash out of the tumor in approximately 2 hours while [ $^{18}\text{F}$ ]2FDG was retained in the tumor for a length of time so long that the natural isotopic decay was the limiting factor in imaging the mouse.<sup>123</sup>



**Scheme 1.7: The synthesis of [ $^{18}\text{F}$ ]6FDF from the tosylated precursor.**

Fluorination of the C1 position of 2,5-anhydromannitol was probed by Sun and co-workers in 2013 when they published the synthesis and evaluation of 1- [ $^{18}\text{F}$ ]fluoro-1-deoxy-2,5-anhydromannitol (1FDAM/[ $^{18}\text{F}$ ]1FDAM) (Scheme 1.8).<sup>124</sup> Sun and co-workers used a multi-step procedure to create an advanced, perbenzoylated intermediate bearing a C1 tosylate (**38**) which was replaced by [ $^{18}\text{F}$ ]KF under strong heating conditions before the benzoyl groups were removed to reveal [ $^{18}\text{F}$ ]1FDAM. This intermediate was produced through a selective protection at the C6 hydroxyl of 2,5-anhydromannitol with a triphenylmethyl (trityl) group (**35**) before the remaining hydroxyl groups were benzoylated (**36**). De-tritylation using acetic acid gave **37** which was tosylated to give **38**. [ $^{18}\text{F}$ ]1FDAM was then rapidly purified and injected into a rabbit with a MCF7 tumor growing inside it. The tumor-bearing rabbit was imaged in a whole body PET imaging scanner and a PET image was generated showing accumulation of [ $^{18}\text{F}$ ]1FDAM in the tumor. It was also observed that a large portion of the [ $^{18}\text{F}$ ]1FDAM was observed to be in the liver and kidneys. The authors

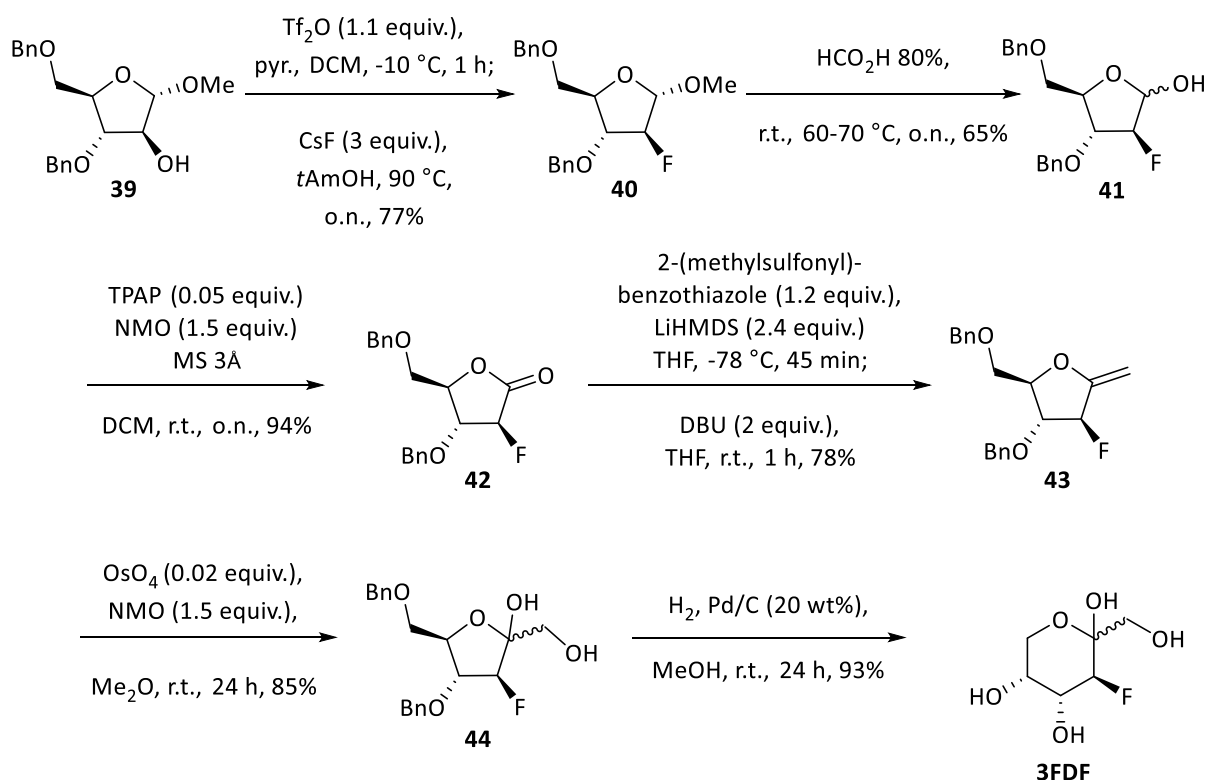
noted this is not a surprising result as a great deal of the probe molecule may be undergoing metabolism in the liver through the natural 2,5-anhydromannitol metabolism pathway.<sup>125</sup>



**Scheme 1.8:** The synthesis of [<sup>18</sup>F]1FDAM as carried out by Sun and co-workers.

Most recently the groups of Cheeseman, West, and Wuest collaborated further for their report of 3-deoxy-3-fluoro-D-fructose (3FDF).<sup>126</sup> This compound was synthesized in a short sequence, and on sufficient scale to allow for evaluation of the properties in regards to transport by GLUTs (Scheme 1.9). From the selectively protected intermediate **39** fluorine was introduced via the displacement of a triflate with fluoride from CsF to give **40**. The anomeric position was then demethylated to give **41** which was oxidized to **42** before Julia olefination was used to introduce a new methylene yielding **43**. Upjohn dihydroxylation of **43** gives **44** as a mixture of anomers, which is debenzylated to give 3FDF. They also compared this compound to 1FDAM as well as 2,5-anhydromannitol to evaluate the relative properties of 3FDF. Utilizing the MCF7 and EMT6 cell lines they were able to show that both 3FDF

and 1FDAM were potent inhibitors of the uptake of [ $^{14}\text{C}$ ]D-fructose. In the murine EMT6 cells 1FDAM was able to inhibit [ $^{14}\text{C}$ ]D-fructose with an  $\text{IC}_{50}$  of 6.82  $\mu\text{M}$  and in MCF7 cells with an  $\text{IC}_{50}$  of 3.98  $\mu\text{M}$ . 3FDF was also able to inhibit the uptake of [ $^{14}\text{C}$ ]D-fructose in EMT6 and MCF7 cells with  $\text{IC}_{50}$  values of 1.16 and 0.67  $\mu\text{M}$  respectively. These inhibition values are quite comparable, yet higher than those of unlabelled 2,5-anhydromannitol which inhibits [ $^{14}\text{C}$ ]D-fructose uptake in EMT6 and MCF7 cells with  $\text{IC}_{50}$  values of 0.58 and 0.09  $\mu\text{M}$  respectively.



**Scheme 1.9: The synthesis of 3FDF as carried out by West, Cheeseman, Wuest and co-workers.**

The uptake of 3FDF and 1FDAM was also monitored directly through the synthesis and use of a  $^{14}\text{C}$  labelled version of each compound. A time- and dose-dependent uptake curve was found for both compounds in MCF7 and EMT6 cell lines as well as in *Xenopus laevis* oocytes which had been injected with GLUT5 mRNA. As with previous work in the

field the role of GLUT1 and GLUT2 had to be addressed before the authors could conclusively argue that 3FDF was a GLUT5 substrate. Inhibition of GLUT1 and GLUT2 was done by the addition of Cytocholasin B to the incubation medium and no significant response was found in 3FDF or 1FDAM uptake. These combined results showed that 3FDF and 1FDAM were most likely GLUT5 substrates and entered these cell lines through that pathway.<sup>126</sup>

## **1.10: Retention of Small Molecule Probes Inside Target Cells**

In the previous section a number of small molecule probes, both GLUT substrate binding or medical imaging probes, were introduced and their biological and/or radiopharmacological evaluations were reviewed. One commonality amongst all of these small molecules is that they do not accumulate over a long period of time inside the cells of interest. In the case of the <sup>18</sup>F labelled compounds the naturally short half-life of <sup>18</sup>F means that the compounds will only be visible to a PET detector while enough radioactive decay is occurring. This is acceptable from an imaging standpoint as the probes currently being used are taken into the target cells on a time scale amenable to imaging these short lived probes.<sup>91</sup> In the case of fluorescently labelled imagine probes the lifetime of the fluorophore is much longer than the <sup>18</sup>F life time. The fluorophores functionally do not degrade until they are incubated with a cell line and even then there is no definitive evidence that they are rapidly broken down.<sup>114</sup>

In the known metabolic pathways for D-fructose and 2,5-anhydromannitol the first critical step is phosphorylation by hexokinase or fructokinase which transforms the neutral hexoses into charged hexophosphates which are unable to leave the cell through passive diffusion or via a GLUT mediated pathway (Figure 1.12).<sup>18,70,127–131</sup> Hexokinase is able to phosphorylate several hexoses at C6 position while fructokinase is able to do so on the C1 positions of hexoses in the furanose form. Previous research into the substrate specificity of these two important kinase enzymes showed that the replacement of the hydroxyl at either the C1 or C6 position will prevent the action of these enzymes.<sup>132,133</sup>

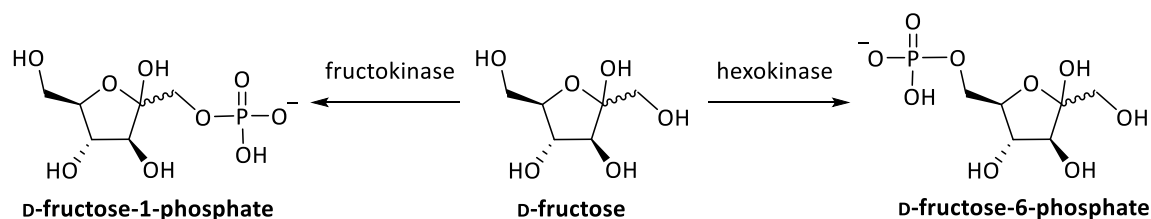


**Figure 1.12: The phosphorylation of D-fructose by fructokinase (left) or hexokinase (right)**

Gambhir and co-workers did work on this issue of phosphorylation in their 2007 publication in which they examined the levels of fructokinase and hexokinase expressed in the cell lines being studied.<sup>70</sup> They found through Western blot analysis that hexokinase was expressed at high levels in MCF7 cells and at moderate levels by MDA-MB-231 and MDA-MB-435 cell lines and that fructokinase was expressed at very low levels in all of these cell lines. This finding is, in part, what steered this research group towards their work with 1NBDF and 1Cy5DF, both retaining a free C6 hydroxyl that could be phosphorylated by hexokinase provided that those compounds were able to fit into the phosphorylation site of hexokinase.

In more recent work by the groups of Sun, McQuade and West, Cheeseman and Wuest the C1 position of D-fructose and 2,5-anhydromannitol are functionalized with various fluorine or fluorophore groups which allow for both GLUT5 selectivity and the possibility of C6 phosphorylation by hexokinase. As these groups also worked with the MCF7 and related cell lines it was somewhat surprising to see that none of these reports include signs of the compounds being phosphorylated and retained in the cells.<sup>120,121,123,124,126</sup> The exception of this is the whole animal imaging done by Sun and co-workers which shows accumulations of 1FDAM in the liver though there was no investigation done to determine if this is a result of phosphorylation and metabolism in the liver or simply a result of 1FDAM being in blood circulation and a large amount of the total blood volume being in the liver.<sup>124</sup>

## **1.11: Goal of this Research**

A thorough review of the available literature regarding the binding site of GLUT5, its substrate tolerance, and the numerous substrates that have been generated to target GLUT5 and other members of the GLUT family have indicated many key aspects of what a new generation of GLUT5 substrates should look like. The base of a new GLUT5 substrate should stem from D-fructose and maintain as much of that structure and its natural stereochemistry as possible. The fructofuranose ring should maintain the C1, C3, and C4 hydroxyl groups so that they can engage in binding with the appropriate residues inside the GLUT5 binding site and their stereochemistry should not be modified. The C1 position, if left unmodified could be phosphorylated inside the cell by fructokinase to trap the probe within the cell. The C6 position seems to offer the greatest tolerance for functionalization. As demonstrated by West,

Cheeseman, and Wuest in their 2016 publication, 6NBDF was transported by GLUT5 but not phosphorylated and trapped. 6NBDF lacks a C6 hydroxyl that could be phosphorylated by hexokinase. If a hydroxyl were present at that position it could, in theory, be phosphorylated so long as the compound could fit into the hexokinase active site. To that end, the goal of this research project was to produce a derivative of D-fructose which was attached to the NBD dye via the C6 carbon leaving the hydroxyl functionality in place (Figure 1.13). Our hypothesis is that this should allow for the NBD labelled compound to enter a cell via GLUT5, as observed with 6NBDF, and leave a free C6 and C1 hydroxyl for possible phosphorylation and thus, metabolic trapping in the cell.

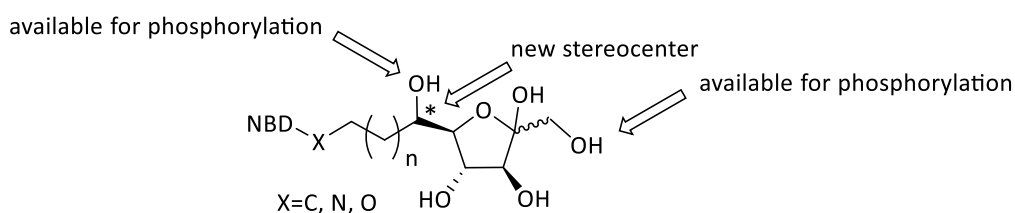
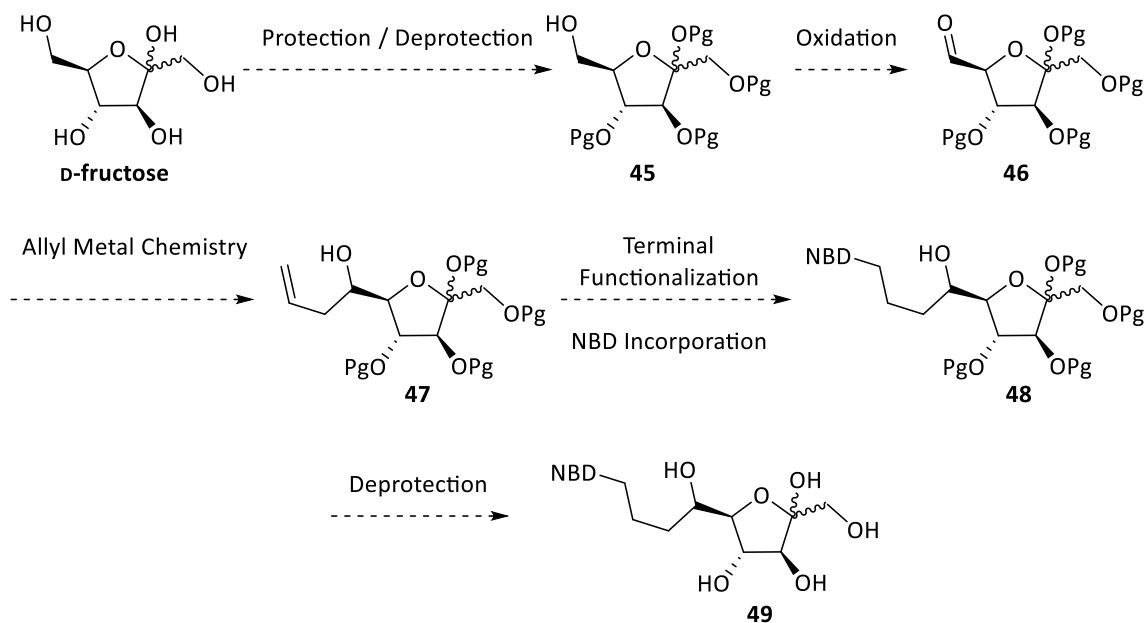


**Figure 1.13: A representative goal compound to be synthesized in this research project.**

This compound is envisioned to arise from several modifications to the inexpensive and easily available starting material D-fructose (Scheme 1.10). Initially selective protection/deprotection chemistry will be used to protect the hydroxyls at C1, C2, C3, and C4 while leaving the C6 hydroxyl open for functionalization (**45**). Next, the C6 hydroxyl could be oxidized to the aldehyde (**46**) so that an alkyl metal, or other appropriate nucleophile, could be utilized to add a linker chain to carbon 6 and return the attached oxygen to the hydroxyl form (**47**). The allyl group would be a convenient initial linker as the terminal olefin is a good handle for further modification and it is a relatively small group. An addition reaction using an allyl nucleophile will create a new stereocenter at the C6 position (**48**) which is not present

in D-fructose. The diastereomers at C6, particularly while the compound is partially protected, should be separable allowing for investigation of the effect of absolute configuration at C6. If one diastereomer is found to be a superior substrate for GLUT5 the synthesis could be modified to include asymmetric addition of the nucleophile to produce the desired isomer in greater yield and efficiency. The terminal end of the linker chain would then be modified so that the NBD unit could be attached either via an amine or through a metal catalysed coupling reaction utilizing a terminal alkyl halide (**49**).



**Scheme 1.10:** The proposed route from D-fructose to a goal compound bearing the desired functionality including an NBD dye moiety, a short tether chain, and a secondary hydroxyl at the C6 position of the D-fructose skeleton.

The linker unit between the C6 carbon of the D-fructose ring and the NBD moiety could vary in length, atomic composition, and functionalization depending on the aspects of the final compounds physical characteristics which may need to be altered. These could include incorporation of hydrophobic or hydrophilic units to affect lipophilicity and steric bulk of the final compound. Incorporation of one, or several, PEG units to the chain should increase the

solubility of the final compound in aqueous media if required and increase the distance between the hexose and the NBD moiety. Further, incorporation of other functionalities to the linker chain, including branch points or heteroatoms, will help develop our general understanding of the tolerances of the GLUT5 binding site so that future generations of probe compounds can be more intelligently designed.

## 1.12: References:

- (1) Kayano, T.; Burant, C. F.; Fukumoto, H.; Gould, G. W.; Fan, Y. S.; Eddy, R. L.; Byers, M. G.; Shows, T. B.; Seino, S.; Bell, G. I. *J. Biol. Chem.* **1990**, *265* (22), 13276–13282.
- (2) Marger, M. D.; Saier, M. H. *Trends Biochem. Sci.* **1993**, *18* (1), 13–20.
- (3) Joost, H.-G.; Bell, G. I.; Best, J. D.; Birnbaum, M. J.; Charron, M. J.; Chen, Y. T.; Doege, H.; James, D. E.; Lodish, H. F.; Moley, K. H.; Moley, J. F.; Mueckler, M.; Rogers, S.; Schürmann, A.; Seino, S.; Thorens, B. *Am. J. Physiol. - Endocrinol. Metab.* **2002**, *282* (4), E974–E976.
- (4) Uldry, M.; Thorens, B. *Pflüg. Arch.* **2003**, *447* (5), 480–489.
- (5) Sogin, D. C.; Hinkle, P. C. *J. Supramol. Struct.* **1978**, *8* (4), 447–453.
- (6) Micihiro Kashahara; Peter, C. Hinkle. *J Biol Chem* **1977**, *252* (20), 7384–7390.
- (7) Mueckler, M.; Caruso, C.; Baldwin, S. A.; Panico, M.; Blench, I.; Morris, H. R.; Allard, W. J.; Lienhard, G. E.; Lodish, H. F. *Science* **1985**, *229* (4717), 941–945.
- (8) Burant, C. F.; Takeda, J.; Brot-Laroche, E.; Bell, G. I.; Davidson, N. O. *J. Biol. Chem.* **1992**, *267* (21), 14523–14526.
- (9) Colville, C. A.; Seatter, M. J.; Gould, G. W. *Biochem. J.* **1993**, *294* (Pt 3), 753–760.
- (10) Colville, C. A.; Seatter, M. J.; Jess, T. J.; Gould, G. W.; Thomas, H. M. *Biochem. J.* **1993**, *290* (3), 701–706.
- (11) Uldry, M.; Ibberson, M.; Horisberger, J.-D.; Chatton, J.-Y.; Riederer, B. M.; Thorens, B. *EMBO J.* **2001**, *20* (16), 4467–4477.
- (12) Abramson, J.; Smirnova, I.; Kasho, V.; Verner, G.; Kaback, H. R.; Iwata, S. *Science* **2003**, *301* (5633), 610–615.
- (13) Chen, L.-Q.; Hou, B.-H.; Lalonde, S.; Takanaga, H.; Hartung, M. L.; Qu, X.-Q.; Guo, W.-J.; Kim, J.-G.; Underwood, W.; Chaudhuri, B.; Chermak, D.; Antony, G.; White, F. F.; Somerville, S. C.; Mudgett, M. B.; Frommer, W. B. *Nature* **2010**, *468* (7323), 527–532.
- (14) Tao, Y.; Cheung, L. S.; Li, S.; Eom, J.-S.; Chen, L.-Q.; Xu, Y.; Perry, K.; Frommer, W. B.; Feng, L. *Nature* **2015**, *527* (7577), 259–263.
- (15) Deng, D.; Xu, C.; Sun, P.; Wu, J.; Yan, C.; Hu, M.; Yan, N. *Nature* **2014**, *510* (7503), 121–125.

- (16) Nomura, N.; Verdon, G.; Kang, H. J.; Shimamura, T.; Nomura, Y.; Sonoda, Y.; Hussien, S. A.; Qureshi, A. A.; Coincon, M.; Sato, Y.; Abe, H.; Nakada-Nakura, Y.; Hino, T.; Arakawa, T.; Kusano-Arai, O.; Iwanari, H.; Murata, T.; Kobayashi, T.; Hamakubo, T.; Kasahara, M.; Iwata, S.; Drew, D. *Nature* **2015**, *526* (7573), 397–401.
- (17) Carruthers, A.; DeZutter, J.; Ganguly, A.; Devaskar, S. U. *Am. J. Physiol. - Endocrinol. Metab.* **2009**, *297* (4), E836–E848.
- (18) Manolescu, A. R.; Witkowska, K.; Kinnaird, A.; Cessford, T.; Cheeseman, C. *Physiology* **2007**, *22* (4), 234–240.
- (19) Mueckler, M. *Eur. J. Biochem.* **1994**, *219* (3), 713–725.
- (20) Zhao, F.-Q.; Keating, A. F. *Curr. Genomics* **2007**, *8* (2), 113–128.
- (21) Davies, A.; Ciardelli, T. L.; Lienhard, G. E.; Boyle, J. M.; Whetton, A. D.; Baldwin, S. A. *Biochem. J.* **1990**, *266* (3), 799–808.
- (22) Zuniga, F. A.; Shi, G.; Haller, J. F.; Rubashkin, A.; Flynn, D. R.; Iserovich, P.; Fischbarg, J. *J. Biol. Chem.* **2001**, *276* (48), 44970–44975.
- (23) Lachaal, M.; Rampal, A. L.; Lee, W.; Shi, Y.; Jung, C. Y. *J. Biol. Chem.* **1996**, *271* (9), 5225–5230.
- (24) Mueckler, M.; Makepeace, C. *J. Biol. Chem.* **2006**, *281* (48), 36993–36998.
- (25) Ibberson, M.; Uldry, M.; Thorens, B. *J. Biol. Chem.* **2000**, *275* (7), 4607–4612.
- (26) Sun, L.; Zeng, X.; Yan, C.; Sun, X.; Gong, X.; Rao, Y.; Yan, N. *Nature* **2012**, *490* (7420), 361–366.
- (27) Salas-Burgos, A.; Iserovich, P.; Zuniga, F.; Vera, J. C.; Fischbarg, J. *Biophys. J.* **2004**, *87* (5), 2990–2999.
- (28) Barnett, J. E.; Holman, G. D.; Chalkley, R. A.; Munday, K. A. *Biochem. J.* **1975**, *145* (3), 417–429.
- (29) Oleg Jardetzky. *Nature* **1966**, *211*, 969–970.
- (30) Anandakrishnan, R.; Zuckerman, D. M. *PLOS ONE* **2017**, *12* (3), e0173500.
- (31) Hoare, D. G. *Biochem. J.* **1972**, *127* (3), 62P.
- (32) Hernández, J. A. *J. Membr. Biol.* **1998**, *165* (3), 235–242.
- (33) Stein, W. D. *Ann. N. Y. Acad. Sci.* **1972**, *195* (1), 412–428.
- (34) Deng, D.; Sun, P.; Yan, C.; Ke, M.; Jiang, X.; Xiong, L.; Ren, W.; Hirata, K.; Yamamoto, M.; Fan, S.; Yan, N. *Nature* **2015**, *526* (7573), 391–396.
- (35) Madej, M. G.; Sun, L.; Yan, N.; Kaback, H. R. *Proc. Natl. Acad. Sci. U. S. A.* **2014**, *111* (7), E719–E727.
- (36) Madej, M. G.; Kaback, H. R. *Proc. Natl. Acad. Sci. U. S. A.* **2013**, *110* (50), E4831–E4838.
- (37) Madej, M. G.; Dang, S.; Yan, N.; Kaback, H. R. *Proc. Natl. Acad. Sci.* **2013**, *110* (15), 5870–5874.
- (38) Dimitriadis, G.; Maratou, E.; Boutati, E.; Psarra, K.; Papasteriades, C.; Raptis, S. A. *Cytometry A* **2005**, *64A* (1), 27–33.
- (39) Girniene, J.; Tatibouët, A.; Sackus, A.; Yang, J.; Holman, G. D.; Rollin, P. *Carbohydr. Res.* **2003**, *338* (8), 711–719.
- (40) Gould, G. W.; Holman, G. D. *Biochem. J.* **1993**, *295* (Pt 2), 329.
- (41) Carruthers, A.; Helgerson, A. L. *Biochemistry (Mosc.)* **1991**, *30* (16), 3907–3915.
- (42) Carruthers, A. *Physiol. Rev.* **1990**, *70* (4), 1135–1176.
- (43) Manolescu, A.; Salas-Burgos, A. M.; Fischbarg, J.; Cheeseman, C. I. *J. Biol. Chem.* **2005**, *280* (52), 42978–42983.

- (44) Manolescu, A. R.; Augustin, R.; Moley, K.; Cheeseman, C. *Mol. Membr. Biol.* **2007**, *24* (5–6), 455–463.
- (45) De Giorgis, V.; Veggiotti, P. *Seizure* **2013**, *22* (10), 803–811.
- (46) Brockmann, K. *Brain Dev.* **2009**, *31* (7), 545–552.
- (47) Wang, D.; Pascual, J. M.; De Vivo, D. In *GeneReviews*(®); Pagon, R. A., Adam, M. P., Ardinger, H. H., Wallace, S. E., Amemiya, A., Bean, L. J., Bird, T. D., Fong, C.-T., Mefford, H. C., Smith, R. J., Stephens, K., Eds.; University of Washington, Seattle: Seattle (WA), 1993.
- (48) Klepper, J. *Epilepsia* **2008**, *49*, 46–49.
- (49) Breast cancer statistics - Canadian Cancer Society <http://www.cancer.ca/en/cancer-information/cancer-type/breast/statistics/?region=bc> (accessed Dec 14, 2016).
- (50) Autier, P.; Boniol, M.; Smans, M.; Sullivan, R.; Boyle, P. *PLOS ONE* **2016**, *11* (4), e0154113.
- (51) Franklin D. Gaylis; Jae Choi; A. Karim Kader; Peter R. Eby; Tamer M. Fouad; H. Gilbert Welch; David H. Gorski; Peter C. Albertsen. *N. Engl. J. Med.* **2016**, *374* (6), 594–596.
- (52) Berry, D. A.; Cronin, K. A.; Plevritis, S. K.; Fryback, D. G.; Clarke, L.; Zelen, M.; Mandelblatt, J. S.; Yakovlev, A. Y.; Habbema, J. D. F.; Feuer, E. J. *N. Engl. J. Med.* **2005**, *353* (17), 1784–1792.
- (53) Warburg, O.; Wind, F.; Negelein, E. *J. Gen. Physiol.* **1927**, *8* (6), 519–530.
- (54) Koppenol, W. H.; Bounds, P. L.; Dang, C. V. *Nat. Rev. Cancer* **2011**, *11* (5), 325–337.
- (55) Kim, J.; Dang, C. V. *Cancer Res.* **2006**, *66* (18), 8927–8930.
- (56) Chan, D. A.; Sutphin, P. D.; Nguyen, P.; Turcotte, S.; Lai, E. W.; Banh, A.; Reynolds, G. E.; Chi, J.-T.; Wu, J.; Solow-Cordero, D. E.; Bonnet, M.; Flanagan, J. U.; Bouley, D. M.; Graves, E. E.; Denny, W. A.; Hay, M. P.; Giaccia, A. J. *Sci. Transl. Med.* **2011**, *3* (94), 94ra70-94ra70.
- (57) Gottlieb, E.; Tomlinson, I. P. M. *Nat. Rev. Cancer* **2005**, *5* (11), 857–866.
- (58) Elstrom, R. L.; Bauer, D. E.; Buzzai, M.; Karnauskas, R.; Harris, M. H.; Plas, D. R.; Zhuang, H.; Cinalli, R. M.; Alavi, A.; Rudin, C. M.; Thompson, C. B. *Cancer Res.* **2004**, *64* (11), 3892–3899.
- (59) Kim, J.; Dang, C. V. *Trends Biochem. Sci.* **2005**, *30* (3), 142–150.
- (60) Buchs, A. E.; Sasson, S.; Joost, H. G.; Cerasi, E. *Endocrinology* **1998**, *139* (3), 827–831.
- (61) Blakemore, S. J.; Aledo, J. C.; James, J.; Campbell, F. C.; Lucocq, J. M.; Hundal, H. S. *Biochem. J.* **1995**, *309* (Pt 1), 7–12.
- (62) Thorens, B.; Cheng, Z. Q.; Brown, D.; Lodish, H. F. *Am. J. Physiol.-Cell Physiol.* **1990**, *259* (2), C279–C285.
- (63) Wardzzala, L.J., Cushman, S.W., Salans, L.B. Mechanism of insulin action on glucose transport in the isolated rat adipose cell.8002.full.pdf <http://www.jbc.org/content/253/22/8002.full.pdf?sid=6037dd77-9afd-4b06-9d95-9bdfc30bda8f> (accessed Sep 29, 2016).
- (64) Zamora-León, S. P.; Golde, D. W.; Concha, I. I.; Rivas, C. I.; Delgado-López, F.; Baselga, J.; Nualart, F.; Vera, J. C. *Proc. Natl. Acad. Sci.* **1996**, *93* (5), 1847–1852.
- (65) Godoy, A.; Ulloa, V.; Rodríguez, F.; Reinicke, K.; Yañez, A. J.; García, M. de los A.; Medina, R. A.; Carrasco, M.; Barberis, S.; Castro, T.; Martínez, F.; Koch, X.; Vera, J.

- C.; Poblete, M. T.; Figueroa, C. D.; Peruzzo, B.; Pérez, F.; Nualart, F. *J. Cell. Physiol.* **2006**, *207* (3), 614–627.
- (66) Chan, K. k.; Chan, J. Y. W.; Chung, K. K. W.; Fung, K.-P. *J. Cell. Biochem.* **2004**, *93* (6), 1134–1142.
- (67) Gowrishankar, G.; Zitzmann-Kolbe, S.; Junutula, A.; Reeves, R.; Levi, J.; Srinivasan, A.; Bruus-Jensen, K.; Cyr, J.; Dinkelborg, L.; Gambhir, S. S. *PLoS ONE* **2011**, *6* (11), e26902.
- (68) Soule, H. D.; Maloney, T. M.; Wolman, S. R.; Peterson, W. D.; Brenz, R.; McGrath, C. M.; Russo, J.; Pauley, R. J.; Jones, R. F.; Brooks, S. C. *Cancer Res.* **1990**, *50* (18), 6075–6086.
- (69) Sreekumar, A.; Poisson, L. M.; Rajendiran, T. M.; Khan, A. P.; Cao, Q.; Yu, J.; Laxman, B.; Mehra, R.; Lonigro, R. J.; Li, Y.; Nyati, M. K.; Ahsan, A.; Kalyana-Sundaram, S.; Han, B.; Cao, X.; Byun, J.; Omenn, G. S.; Ghosh, D.; Pennathur, S.; Alexander, D. C.; Berger, A.; Shuster, J. R.; Wei, J. T.; Varambally, S.; Beecher, C.; Chinnaiyan, A. M. *Nature* **2009**, *457* (7231), 910–914.
- (70) Levi, J.; Cheng, Z.; Gheysens, O.; Patel, M.; Chan, C. T.; Wang, Y.; Namavari, M.; Gambhir, S. S. *Bioconjug. Chem.* **2007**, *18* (3), 628–634.
- (71) Crick, F. *Nature* **1970**, *227* (5258), 561–563.
- (72) James, M. L.; Gambhir, S. S. *Physiol. Rev.* **2012**, *92* (2), 897–965.
- (73) Wang, D. S.; Dake, M. D.; Park, J. M.; Kuo, M. D. *J. Vasc. Interv. Radiol.* **2006**, *17* (9), 1405–1423.
- (74) Nolting, D. D.; Nickels, M. L.; Guo, N.; Pham, W. *Am. J. Nucl. Med. Mol. Imaging* **2012**, *2* (3), 273–306.
- (75) Maschauer, S.; Prante, O. *BioMed Res. Int.* **2014**, *2014*, e214748.
- (76) Imam, S. K. *Cancer Biother. Radiopharm.* **2010**, *25* (3), 365–374.
- (77) Ntziachristos, V. *Nat. Methods* **2010**, *7* (8), 603–614.
- (78) Couturier, O.; Luxen, A.; Chatal, J.-F.; Vuillez, J.-P.; Rigo, P.; Hustinx, R. *Eur. J. Nucl. Med. Mol. Imaging* **2004**, *31* (8), 1182–1206.
- (79) Cox, B. L.; Mackie, T. R.; Eliceiri, K. W. *Am. J. Nucl. Med. Mol. Imaging* **2014**, *5* (1), 1–13.
- (80) Tu, Z.; Mach, R. H. *Curr. Top. Med. Chem.* **2010**, *10* (11), 1060–1095.
- (81) Lee, E. S.; Kim, T. S.; Kim, S.-K. *Korean J. Radiol.* **2015**, *16* (1), 21–31.
- (82) Fernández-Suárez, M.; Ting, A. Y. *Nat. Rev. Mol. Cell Biol.* **2008**, *9* (12), 929–943.
- (83) Fei, X.; Gu, Y. *Prog. Nat. Sci.* **2009**, *19* (1), 1–7.
- (84) Hayashi-Takanaka, Y.; Stasevich, T. J.; Kurumizaka, H.; Nozaki, N.; Kimura, H. *PLOS ONE* **2014**, *9* (9), e106271.
- (85) Fass, L. *Mol. Oncol.* **2008**, *2* (2), 115–152.
- (86) Frangioni, J. *Curr. Opin. Chem. Biol.* **2003**, *7* (5), 626–634.
- (87) Burdette, J. E. *J. Mol. Endocrinol.* **2008**, *40* (6), 253.
- (88) Pacák, J.; Točík, Z.; Černý, M. *J. Chem. Soc. Chem. Commun.* **1969**, No. 2, 77–77.
- (89) Nasim Khan; Noboru Oriuchi; Tetsuya Higuchi; Keigo Endo. *Cancer Control* **2005**, *12* (4), 254–260.
- (90) Surasi, D. S.; Bhambhani, P.; Baldwin, J. A.; Almodovar, S. E.; O'Malley, J. P. *J. Nucl. Med. Technol.* **2014**, *42* (1), 5–13.

- (91) Tse, N. Y.; Hoh, C. K.; Hawkins, R. A.; Zinner, M. J.; Dahlbom, M.; Choi, Y.; Maddahi, J.; Brunicardi, F. C.; Phelps, M. E.; Glaspy, J. A. *Ann. Surg.* **1992**, *216* (1), 27–34.
- (92) Krivokapich, J.; Barrio, J. R.; Huang, S.-C.; Schelbert, H. R. *J. Am. Coll. Cardiol.* **1990**, *16* (5), 1158–1167.
- (93) Boellaard, R.; O’Doherty, M. J.; Weber, W. A.; Mottaghy, F. M.; Lonsdale, M. N.; Stroobants, S. G.; Oyen, W. J. G.; Kotzerke, J.; Hoekstra, O. S.; Pruim, J.; Marsden, P. K.; Tatsch, K.; Hoekstra, C. J.; Visser, E. P.; Arends, B.; Verzijlbergen, F. J.; Zijlstra, J. M.; Comans, E. F. I.; Lammertsma, A. A.; Paans, A. M.; Willemsen, A. T.; Beyer, T.; Bockisch, A.; Schaefer-Prokop, C.; Delbeke, D.; Baum, R. P.; Chiti, A.; Krause, B. *J. Eur. J. Nucl. Med. Mol. Imaging* **2010**, *37* (1), 181–200.
- (94) Brown, R. S.; Wahl, R. L. *Cancer* **1993**, *72* (10), 2979–2985.
- (95) Jr, B.; Ns, M.; Jr, R. G.; A, N.; Js, C.; De, K. *J. Nucl. Med. Off. Publ. Soc. Nucl. Med.* **1981**, *22* (4), 372–375.
- (96) Kiselev, M. Y.; Lai, D. Process and apparatus for production of F-18 fluoride. US6567492 B2, May 20, 2003.
- (97) Carlson, C. H.; Singer, L.; Service, D. H.; Armstrong, W. D. *Int. J. Appl. Radiat. Isot.* **1959**, *4* (3), 210–213.
- (98) Tahiri, M.; Doppelt, P.; Fischer, J.; Weiss, R. *ResearchGate* **1987**, *127* (1), L1–L3.
- (99) Lee, C.-C.; Sui, G.; Elizarov, A.; Shu, C. J.; Shin, Y.-S.; Dooley, A. N.; Huang, J.; Daridon, A.; Wyatt, P.; Stout, D.; Kolb, H. C.; Witte, O. N.; Satyamurthy, N.; Heath, J. R.; Phelps, M. E.; Quake, S. R.; Tseng, H.-R. *Science* **2005**, *310* (5755), 1793–1796.
- (100) Yeung, H. W. D.; Grewal, R. K.; Gonen, M.; Schöder, H.; Larson, S. M. *J. Nucl. Med.* **2003**, *44* (11), 1789–1796.
- (101) Cohade, C.; Osman, M.; Leal, J.; Wahl, R. L. *J. Nucl. Med.* **2003**, *44* (11), 1797–1803.
- (102) Chang, J. M.; Lee, H. J.; Goo, J. M.; Lee, H.-Y.; Lee, J. J.; Chung, J.-K.; Im, J.-G. *Korean J. Radiol.* **2006**, *7* (1), 57.
- (103) Rosenbaum, S. J.; Lind, T.; Antoch, G.; Bockisch, A. *Eur. Radiol.* **2005**, *16* (5), 1054–1065.
- (104) Speizer, L.; Haugland, R.; Kutchai, H. *Biochim. Biophys. Acta BBA - Biomembr.* **1985**, *815* (1), 75–84.
- (105) Aller, C. B.; Ehmann, S.; Gilman-Sachs, A.; Snyder, A. K. *Cytometry* **1997**, *27* (3), 262–268.
- (106) Barros, L. F.; Bittner, C. X.; Loaiza, A.; Ruminot, I.; Larenas, V.; Moldenhauer, H.; Oyarzún, C.; Alvarez, M. *J. Neurochem.* **2009**, *109*, 94–100.
- (107) DiNuzzo, M.; Giove, F.; Maraviglia, B.; Mangia, S. *J. Neurochem.* **2013**, *125* (2), 236–246.
- (108) Chen, Y.; Zhang, J.; Zhang, X. *J. Mol. Neurosci.* **2015**, *55* (1), 126–130.
- (109) Raeisi, E.; Mir, L. M. *J. Membr. Biol.* **2012**, *245* (10), 633–642.
- (110) Yamamoto, T.; Tanaka, S.; Suga, S.; Watanabe, S.; Nagatomo, K.; Sasaki, A.; Nishiuchi, Y.; Teshima, T.; Yamada, K. *Bioorg. Med. Chem. Lett.* **2011**, *21* (13), 4088–4096.
- (111) Zou, C.; Wang, Y.; Shen, Z. *J. Biochem. Biophys. Methods* **2005**, *64* (3), 207–215.
- (112) Nitin, N.; Carlson, A. L.; Muldoon, T.; El-Naggar, A. K.; Gillenwater, A.; Richards-Kortum, R. *Int. J. Cancer* **2009**, *124* (11), 2634–2642.

- (113) Tao, J.; Diaz, R. K.; Teixeira, C. R. V.; Hackmann, T. J. *Biochemistry (Mosc.)* **2016**, *55* (18), 2578–2589.
- (114) Yoshioka, K.; Saito, M.; Oh, K.-B.; Nemoto, Y.; Matsuoka, H.; Natsume, M.; Abe, H. *Biosci. Biotechnol. Biochem.* **1996**, *60* (11), 1899–1901.
- (115) Zou, C.; Wang, Y.; Shen, Z. *J. Biochem. Biophys. Methods* **2005**, *64* (3), 207–215.
- (116) DiNuzzo, M.; Giove, F.; Maraviglia, B.; Mangia, S. *J. Neurochem.* **2013**, *125* (2), 236–246.
- (117) Tatibouët, A.; Yang, J.; Morin, C.; Holman, G. D. *Bioorg. Med. Chem.* **2000**, *8* (7), 1825–1833.
- (118) Jing, Y.; Dowden, J.; Tatibouët, A.; Hatanaka, Y.; Holman, G. D. *Biochem. J.* **2002**, *367* (2), 533–539.
- (119) Inukai, K.; Katagiri, H.; Takata, K.; Asano, T.; Anai, M.; Ishihara, H.; Nakazaki, M.; Kikuchi, M.; Yazaki, Y.; Oka, Y. *Endocrinology* **1995**, *136* (11), 4850–4857.
- (120) Tanasova, M.; Plutschack, M.; Muroski, M. E.; Sturla, S. J.; Strouse, G. F.; McQuade, D. T. *ChemBioChem* **2013**, *14* (10), 1263–1270.
- (121) Trayner, B. J.; Grant, T. N.; West, F. G.; Cheeseman, C. I. *Bioorg. Med. Chem.* **2009**, *17* (15), 5488–5495.
- (122) Soueidan, O.-M.; Scully, T. W.; Kaur, J.; Panigrahi, R.; Belovodskiy, A.; Do, V.; Matier, C. D.; Lemieux, M. J.; Wuest, F.; Cheeseman, C.; West, F. G. *ACS Chem. Biol.* **2017**, *12* (4), 1087–1094.
- (123) Wuest, M.; Trayner, B. J.; Grant, T. N.; Jans, H.-S.; Mercer, J. R.; Murray, D.; West, F. G.; McEwan, A. J. B.; Wuest, F.; Cheeseman, C. I. *Nucl. Med. Biol.* **2011**, *38* (4), 461–475.
- (124) Niu, B.; Wen, X.; Jia, Z.; Wu, X.; Guo, W.; Sun, H. *Chin. J. Chem.* **2013**, *31* (9), 1159–1163.
- (125) Padgett, H. C.; Schmidt, D. G.; Luxen, A.; Bida, G. T.; Satyamurthy, N.; Barrio, J. R. *Int. J. Rad. Appl. Instrum. [A]* **1989**, *40* (5), 433–445.
- (126) Soueidan, O.-M.; Trayner, B. J.; Grant, T. N.; Henderson, J. R.; Wuest, F.; West, F. G.; Cheeseman, C. I. *Org. Biomol. Chem.* **2015**, *13* (23), 6511–6521.
- (127) Banhegyi, G.; Csala, M.; Benedetti, A. *J. Mol. Endocrinol.* **2008**, *42* (4), 283–289.
- (128) Mulukutla, B. C.; Khan, S.; Lange, A.; Hu, W.-S. *Trends Biotechnol.* **2010**, *28* (9), 476–484.
- (129) Akram, M.; Hamid, A. *Obes. Res. Clin. Pract.* **2013**, *7* (2), e89–e94.
- (130) Malaisse, W.J., et al. *Int J Biochem* **1991**, *23* (12), 1471–1481.
- (131) Malaisse, W.J., et al. *Diabetes Res* **1991**, *16* (1), 19–24.
- (132) Raushel, F. M.; Cleland, W. W. *J. Biol. Chem.* **1973**, *248* (23), 8174–8177.
- (133) Bais, R.; James, H. M.; Rofe, A. M.; Conyers, R. A. *Biochem. J.* **1985**, *230* (1), 53–60.

## **Chapter 2: Attempts Towards Using the C6 Position of D-Fructose as an Electrophile Through Selective Oxidation.**

### **2.1: Synthetic Rational to a C6 Functionalized D-Fructose Derivative.**

The polyol nature of carbohydrates commonly requires a protection/deprotection strategy to be employed so that only one of the nearly chemically equivalent hydroxyl groups can be functionalized. Carbohydrates do not generally tolerate selective nucleophilic or electrophilic reactions at one carbon centre, therefore protection of the other hydroxyl groups is necessary.<sup>1</sup> Carbohydrates also exist in a mixture of anomers in both the furanose (5-membered rings) and pyranose (6-membered rings) ring forms. This constant flux between configurations further complicates selective reactions and purifications.<sup>2</sup> D-Fructose is particularly challenging because it contains two nearly identical primary hydroxyl groups and two secondary hydroxyl groups when in its furanose ring form.<sup>2</sup> D-fructose is an inexpensive, commercially available starting material. Therefore, regardless of the synthetic challenges associated with its derivatization, it is an attractive point to start the synthesis of D-fructose-derived molecular probes. To overcome the inherent complications related to the structure and reactivity of D-fructose, selective, partial protection was envisioned as the first step in a synthetic route to a viable imagine probe.

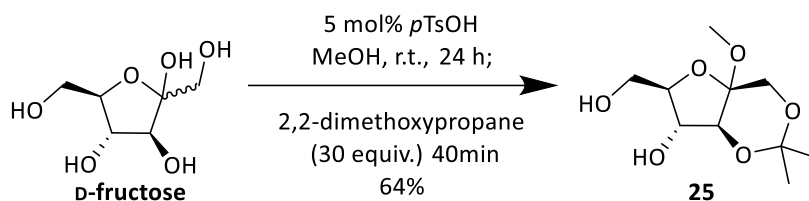
As outlined in Section 1.11, the formation of a new C-C bond at C-6 of D-fructose is crucial to creating the desired product in this research project as described in Section 1.11. This new C-C bond would link the D-fructose backbone to a dye molecule. Initially, the most straightforward method to produce the new C-C bond to C6 of D-fructose appeared to be

selective oxidation of the C6 hydroxyl to the corresponding aldehyde. This species could then react with any number of carbon based nucleophiles to produce the desired bond. This oxidation was attempted via a large suite of conditions ranging from classical reactions, including chromium based reagents, to much more modern reactions, such as copper catalysed oxidations utilizing O<sub>2</sub> as the oxidant. Keeping in line with the long-term goals of this project any methodology used in synthesis should be scalable and be cost effective so that an appreciable amount of final product can be isolated and carried into *in vitro* or *in vivo* studies.

In order to produce the key aldehyde intermediate desired, several transformations had to be carried out on D-fructose. Firstly, the hydroxyl groups that are not intended to be oxidized had to be protected. Then the C6 hydroxyl had to be oxidized to the corresponding aldehyde to provide a convenient handle for functionalization at C6. Selective protection methodologies for carbohydrates are well established in the literature<sup>3</sup> while selective oxidation of primary alcohols to aldehydes in functionality-dense compounds such as carbohydrates appeared to be the more challenging task. To this end, many different methodologies were employed utilizing a diverse set of reaction conditions. An incomplete list of these methodologies is presented below grouped by category of reaction or family of reagents used. Relevant examples in for each type of oxidation attempted are referred to directly here while many other reaction conditions that were attempted are not presented in this document. A brief introduction to the immediately relevant literature is presented in each subsection of this chapter along with the results of the associated reactions.

## 2.2: Production of a Suitable Substrate for Oxidation Reactions

Hong and co-workers in 2013 demonstrated the quick, simple, and efficient conversion of D-fructose to 2-methoxy-1,3-O-isopropylidene-fructofuranoside (**25**) in a one pot reaction (Scheme 2.1).<sup>4</sup> The reported reaction proved to be scalable and was instrumental to the progress of the synthetic work discussed herein. Previously published methods to generate this intermediate from sucrose or D-fructose were also carried out but the methodology of Hong and co-workers proved to be most scalable.<sup>5</sup> Purification of **25** was accomplished using standard column chromatography and yielded the  $\alpha$ -anomer as the major product without significant deviation in overall yield from the published conditions (64% vs. 70%).<sup>4</sup>

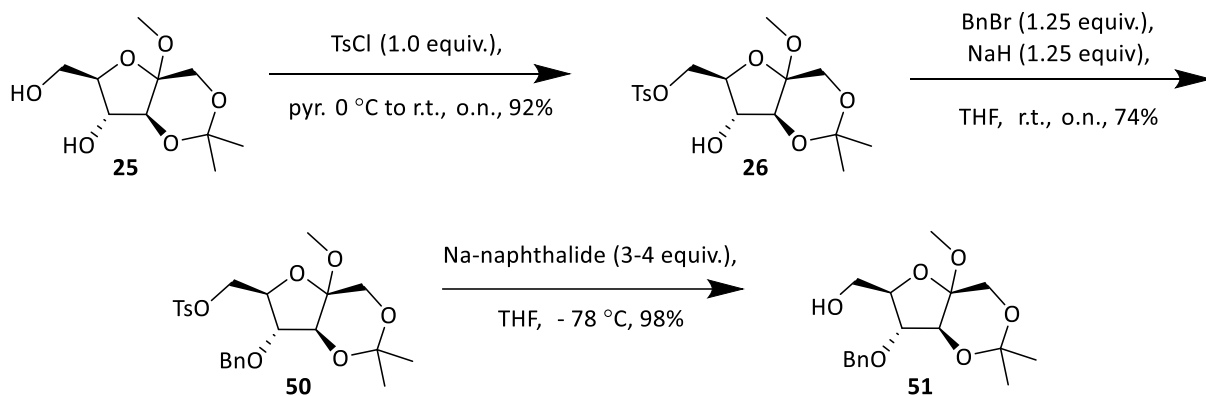


Scheme 2.1 Protection of D-fructose via the method of Hong and co-workers<sup>4</sup> to yield intermediate **25**.

Compound **25** contains a single primary hydroxyl and a single secondary hydroxyl functional group which, according to reports in the literature, should be chemically distinct enough for a selective oxidation of the primary hydroxyl with or without the protection of the C4 secondary hydroxyl.

With **25** in hand, synthetic efforts initially focused on using an orthogonal protection/deprotection strategy to protect the C4 hydroxyl functional group and have the C6 hydroxyl free for oxidation to the corresponding aldehyde. To this end protection of the C6 hydroxyl was carried out using para-toluene-sulfonyl chloride (*p*TsCl) in pyridine to give **26** with a high degree of selectivity. The C4 secondary hydroxyl was then protected as the benzyl

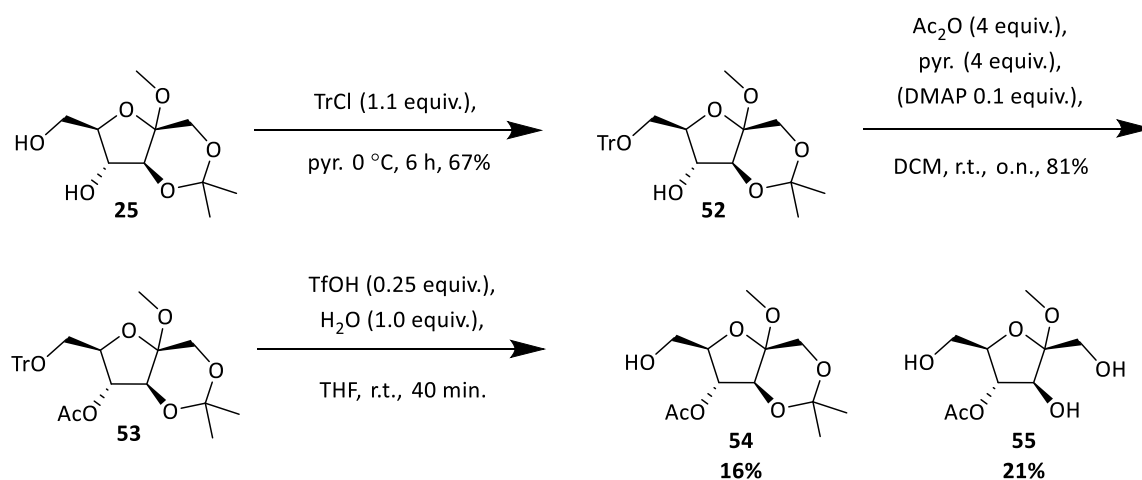
ether to give fully protected intermediate **50** (Scheme 2.2). Using the methodology of Robins and co-workers, treatment of **50** with a previously prepared solution of sodium naphthalide efficiently and cleanly removed the tosyl group to give **51** as the primary alcohol,<sup>6</sup> setting the stage for the synthesis of the desired fructose aldehyde derivative (Scheme 2.2).



**Scheme 2.2: Production of the key, selectively protected compound **51** via protection/deprotection of the C6 tosylate through Na-naphthalide reduction.**

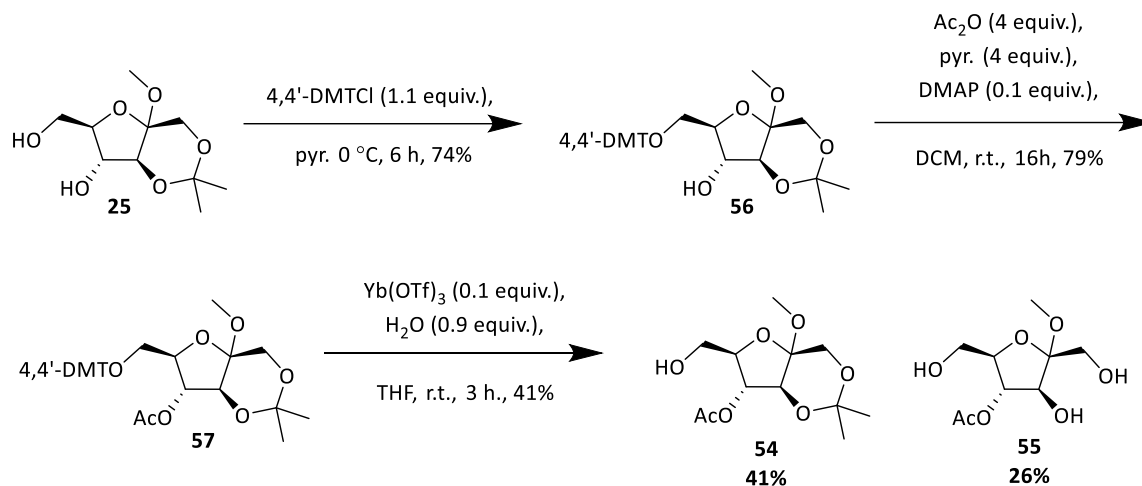
While optimizing the above tosylation/detosylation pathway to **51** several other pathways were also explored. An analogous route utilizing triphenylmethyl chloride (trityl chloride, TrCl) as the protecting group for the C6 hydroxyl group was also attempted concurrently with the tosylation approach (Scheme 2.3). Addition of a trityl group to the C6 hydroxyl proceeded smoothly to give **52** in good yield and with complete selectivity for the C6 hydroxyl. This selectivity is likely due to the large size of the reactive trityl cation which reacts with the less sterically encumbered primary hydroxyl more readily than the secondary hydroxyl.<sup>7</sup> The subsequent protection of the C4 hydroxyl however was found to be inhibited in many cases by the large size of the trityl group. Benzoylation, for example, was found to proceed with very low yields while acetylation of the C4 hydroxyl proceeded much better (presumably due to the smaller size of the acetyl group) providing fully protected sugar **53**. Application of

Lewis or Brønsted acids to remove the trityl protecting group was found to also effect the removal of the acetal protecting group furnishing a mixture of **54** and **55** favouring the undesired **55** in low overall yield. Harsher reactions conditions employing larger stoichiometric equivalents of reagents, higher temperatures or reaction times provided worse selectivity between the two protecting groups producing **55** almost exclusively.



**Scheme 2.3: Production of the partially protected compound 54 via tritylation/detritylation at the C6 position.**

Employing the more reactive 4,4'-dimethoxy-trityl (4,4'-DMT) group gave **56** and **57** following similar conditions to route in Scheme 2.3. The deprotection of **57** gave more of the desired **54** rather than the doubly deprotected **55** albeit still in low yields and poor selectivity (Scheme 2.4). Attempted optimization of the removal of the trityl or 4,4'-DMT group is further outlined in Table 2.1.



**Scheme 2.4: Production of the partially protected compound 54 through a protection/deprotection strategy utilizing the 4,4'-dimethoxytrityl group.**

The use of strong protic acids resulted in full consumption of the starting material (Table 2.1 entries 1, 2); however isolation of the products of these reactions revealed that the undesired, double deprotection product was produced in high yield. Other protic acids (entries 3, 4, 5) also gave the undesired product exclusively, although the exact yield of these test reactions was not determined. Investigation of Lewis acids to afford this transformation began with FeCl<sub>3</sub> and In(OTf)<sub>3</sub>, both of which failed to consume the starting material (entries 6, 7). Changing the Lewis acid to ZnCl<sub>2</sub> consumed much of the starting material and produced a small amount of the desired product while the double deprotection product was the major product of the reaction (entry 8). The conditions of Giese and co-workers using ytterbium triflate were found to be the most efficient means to the selective mono-deprotection (entry 9).<sup>8</sup>

**Table 2.2: Optimization of the selective removal of the 4,4'-DMT group from the C6 position of 57.**

Entry	Reagent <sup>a</sup>	Temperature (°C)	Solvent	Conversion (%) <sup>b</sup>	<b>54</b> (%) <sup>c</sup>	<b>55</b> (%) <sup>c</sup>
1	HCl	22	THF	100	0	92
2	H <sub>2</sub> SO <sub>4</sub>	22	THF	100	0	87
3	H <sub>3</sub> PO <sub>4</sub>	22	THF	100	0	n.d.
4	NaH <sub>2</sub> PO <sub>4</sub>	22	THF	100	0	n.d.
5	<i>p</i> TsOH	22	THF	100	0	n.d.
6	FeCl <sub>3</sub>	22	THF	0	0	0
7	In(OTf) <sub>3</sub> <sup>d</sup>	22	THF	0	0	0
8	ZnCl <sub>2</sub>	22	THF	83	< 5	45
9	Yb(OTf) <sub>3</sub> <sup>e</sup>	22	THF	84	41	26

a: used in 0.25 equivalent unless otherwise noted. b: conversion based on recovered S.M. c: n.d (not determined). d: 0.3 equivalent of In(OTf)<sub>3</sub> and 1 equivalent of H<sub>2</sub>O. e: 0.1 equivalent Yb(OTf)<sub>3</sub> and 0.9 equivalents of H<sub>2</sub>O.

Neither of these routes was optimized to give **54** in greater yield, nor was found to provide **51** or **54** in as high of purity as the tosylation/detosylation route. The greater expense of TrCl or 4,4'-DMT compared to *p*TsCl further contributed to the undesirability of these routes leading the abandonment of further reaction optimization.

### 2.3: Initial Attempts to Afford D-Fructose Aldehyde Derivative **58** via Selective Oxidation

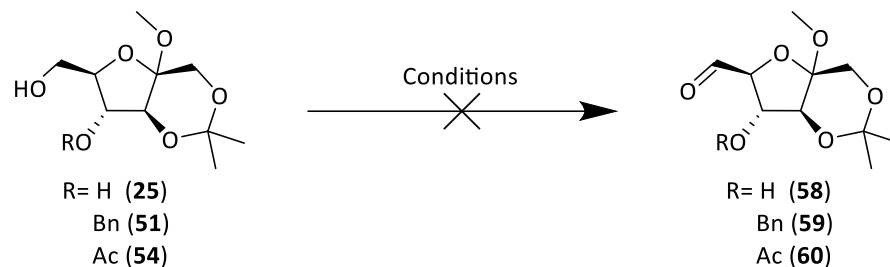
The oxidation of alcohols to aldehydes, ketones, and other products is a staple of modern organic chemistry and a multitude of reactions have been developed to afford this transformation. Some of the earliest reagents utilized for this purpose applied chromium,<sup>9</sup> manganese,<sup>10</sup> or activated dimethyl sulfoxide (DMSO) species.<sup>11</sup> Though these oxidations have significant literature precedent in a variety of synthetic endeavors,<sup>12</sup> the oxygen-dense scaffold of D-fructose brought with it the potential for many unwanted side reactions. The conditions of many reactions, for example sulfuric acid employed in Jones' conditions, would likely not be amenable to use with a carbohydrate.<sup>13</sup> Nonetheless these classical conditions were initially

employed to determine if oxidation would be faster than any potentially unwanted side reactions.

Table 2.2 summarizes some of the conditions attempted and the resulting products. Chromium based oxidation conditions were initially employed (Table 2.2 entries 1-4) and it was found that the Jones' conditions led to decomposition of the starting material while PCC, PDC, and  $\text{NaCrO}_4$  failed to consume the starting material.  $\text{KMnO}_4$  was able to consume the starting material but led only to decomposition and none of the expected product (entry 5).  $\text{MnO}_2$  did not consume the starting material, even when 5 equivalents of the oxidant was used (entries 6, 7).

When these reactions were repeated under more forcing conditions (e.g. increased equivalents of oxidization agent, higher temperature, longer reaction times) decomposition was observed with no signs of the desired product by crude  $^1\text{H-NMR}$  (not shown).

**Table 3.2: Screening of conditions to selectively oxidize the C6 hydroxyl of 25, 51, or 54 to produce the desired aldehyde 58, 59, or 60.**



Entry	Reagent	Equivalents	Solvent	Temperature (°C) <sup>a</sup>	Conversion (%) <sup>b</sup>	Product (%)
1	Jones	1.25	Acetone	22	100	0
2	PCC	2	THF	22 → 66	0	0
3	PDC	2	THF	22 → 66	0	0
4	Na <sub>2</sub> CrO <sub>4</sub>	2	THF	22 → 66	0	0
5	KMnO <sub>4</sub>	1.1	THF	22	100	0
6	MnO <sub>2</sub>	1.25	THF	22	0	0
7	MnO <sub>2</sub>	5	THF	66	0	0
8	DMSO/C <sub>2</sub> O <sub>2</sub> Cl <sub>2</sub> /Et <sub>3</sub> N	1.1	THF	-78	100	0
9	DMSO/C <sub>2</sub> O <sub>2</sub> Cl <sub>2</sub> /Et <sub>3</sub> N	1.1	DCM	-78	100	0
10	DMSO/Tf <sub>2</sub> O/Et <sub>3</sub> N	1.1	THF	-78	100	0
11	DMSO/DCC/ TfOH/Pyridine	1.1	THF	-78	0	0
12	DMSO/DCC/ TfOH/Pyridine	1.1	THF	-41 → 22	0	0
13	DMSO/DCC/ TfOH/Pyridine	1.1	DCM	22 → 39	0	0
14	DMSO/DCC/ TfOH/Pyridine	5	THF	22 → 66	0	0
15	DMSO/SO <sub>3</sub> Py/Et <sub>3</sub> N	1.5	THF	22 → 66	0	0
16	DMSO/SO <sub>3</sub> Py/Et <sub>3</sub> N	5	THF	22 → 66	15	0

a: Reactions started at room temperature were held there for 6 hours before being heated for a further 24 hours b: Determined by recovered starting material

The oxidation conditions published by Swern and co-workers<sup>14</sup> and the modification utilizing trifluoroacetic anhydride<sup>11</sup> to replace oxalyl chloride have been shown to be more amenable to functionally dense substrates. Though the literature precedent indicated that these conditions would cleanly oxidize **25**, **51**, or **54** to the corresponding aldehydes, only

decomposition of the starting materials was observed (Table 2.2 entries 8 and 9). Using Tf<sub>2</sub>O in place of oxalyl chloride also led to the decomposition of the starting material without any sign of the desired aldehyde being formed (entry 10). Further disappointment was found using the Pfitzner-Moffatt oxidation,<sup>15</sup> which is similar to the Swern oxidation in that DMSO is employed as the oxidizing agent but differs in that N,N'-dicyclohexylcarbodiimide (DCC) is used to activate the DMSO rather than oxalyl chloride or trifluoroacetic anhydride. Despite numerous attempts to push these oxidations by changing solvent or temperature, only unreacted starting material, or decomposed/non-characterizable material was recovered in all cases (entries 11-14). Parikh-Doering oxidation was also unsuccessful with 1.5 equivalents of the oxidizing agent (entry 15) though a small amount of conversion to an unidentifiable black solid was observed when 5 equivalents of oxidizing agent was used in THF heated to reflux (entry 16).<sup>16</sup> There was no difference in product distribution found between the use of **25** or any of its protected analogs including **51** and **54** when submitted to the reaction conditions listed in Table 2.2.

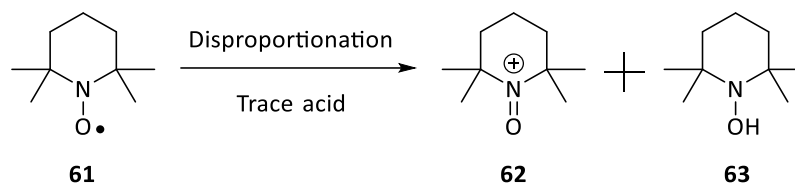
After observing the above results a theory was proposed that **25**, bearing a free hydroxyl at C4, could assist directing an oxidizing agent to the C6 position through hydrogen bonding. This does not appear to be the case as there was no difference in the observed products (decomposition or non-consumption) between **25** or its protected derivatives. It is also of note that the Swern oxidation conditions led to rapid consumption of the starting material from which no isolable product could be recovered. It is possible that in the unprotected case of **25** the C4 hydroxyl is oxidized to the ketone which contributes to the decomposition of the material. In the case of **51** or **54** this oxidation is impossible though decomposition is still observed. As the recovered material from these reactions was a complex mixture of many compounds which

could not be individually isolated and characterized the route through which these materials decomposed is unknown.

## 2.4: Attempts to Use TEMPO Mediated Oxidations to Produce Compound 58.

Organocatalytic methods using (2,2,6,6-tetramethyl-piperidin-1-yl)oxyl (TEMPO) with a variety of co-oxidants were also explored. These oxidations all rely upon the active oxoammonium salt of TEMPO which must be regenerated *in situ* through the use of a co-oxidant. The oxoammonium salt was first reported by Golubev, Voronina, and Rozantsev<sup>17</sup> and the use of this reagent as an oxidant for alcohols was later shown by Cella and co-workers.<sup>18</sup> The conditions of Anelli and co-workers<sup>19</sup> have long been the standard for TEMPO-mediated oxidations of alcohols and this reaction now carries Anelli's name in the chemical vernacular. This, along with the later modifications by Zhao and co-workers<sup>20</sup> have been reported to cleanly oxidize primary alcohols to aldehydes across a wide range of substrates. Unfortunately, these conditions, using a variety of solvents, did not yield an isolable amount of the desired aldehyde as shown in Table 2.3.

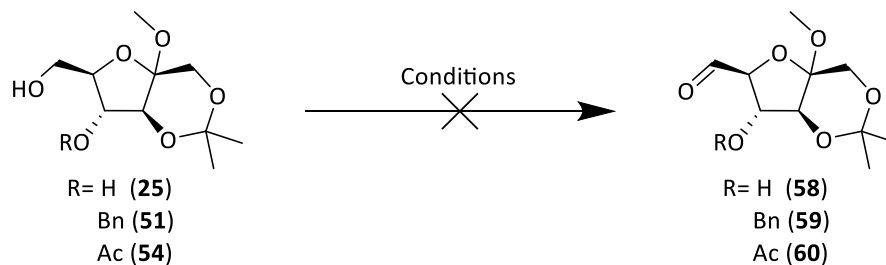
TEMPO, in its commercially available free radical form **61**, will disproportionate to the oxoammonium salt **62** and the corresponding hydroxylamine **63** in the presence of trace acid (Scheme 2.5).<sup>21-23</sup> The oxoammonium salt is reduced to the hydroxylamine after the oxidation reaction and thus the co-oxidant must be able to oxidize the hydroxylamine **63** to the oxoammonium salt to complete the catalytic cycle.



**Scheme 2.5: The disproportionation of TEMPO from a free radical and hydroxylamine for to the active oxoammonium salt.**

The use of the sodium chlorite/sodium hypochlorite (Table 2.3 entries 1, 2) or the sodium hypochlorite/potassium bromide co-oxidant systems (entry 3, 4), which have been reported extensively, did not produce the desired product **58**, **59**, or **60**.<sup>20</sup> A number of other co-oxidants were used, with little success. Literature precedent indicated that **25**, **51**, or **54** should have been viable substrates for all of these oxidation conditions but no desired aldehyde could be isolated.<sup>24,25</sup> Additional aliquots of catalyst or co-oxidant only provided further decomposition of the starting material or no further observable reaction of the starting material. Changing the co-oxidant to (diacetoxyiodo)benzene (DAIB) (entries 5, 6) or [bis(trifluoroacetoxy)iodo]benzene (BTIB) (entry 7, 8) also failed to produce any aldehyde product.<sup>26,27</sup> Calcium hypochlorite and iron (III) nitrate also gave no conversion of any of the starting materials employed (entries 9-12) despite a reasonable literature precedent that these should be appropriate conditions for the desired oxidation.<sup>28-30</sup> All of the attempted conditions were screened in several solvents (not all results shown) with TEMPO-catalyst loading ranging from 10 mol% to 125 mol% and temperatures ranging from -10 °C to 82 °C in acetonitrile heated to reflux. In all cases only unreacted starting material or decomposed material was recovered from the reaction mixtures.

**Table 2.4: Investigation of Tempo mediated oxidations of 25, 51, and 54 to afford the desired aldehyde 58, 59, or 60.**



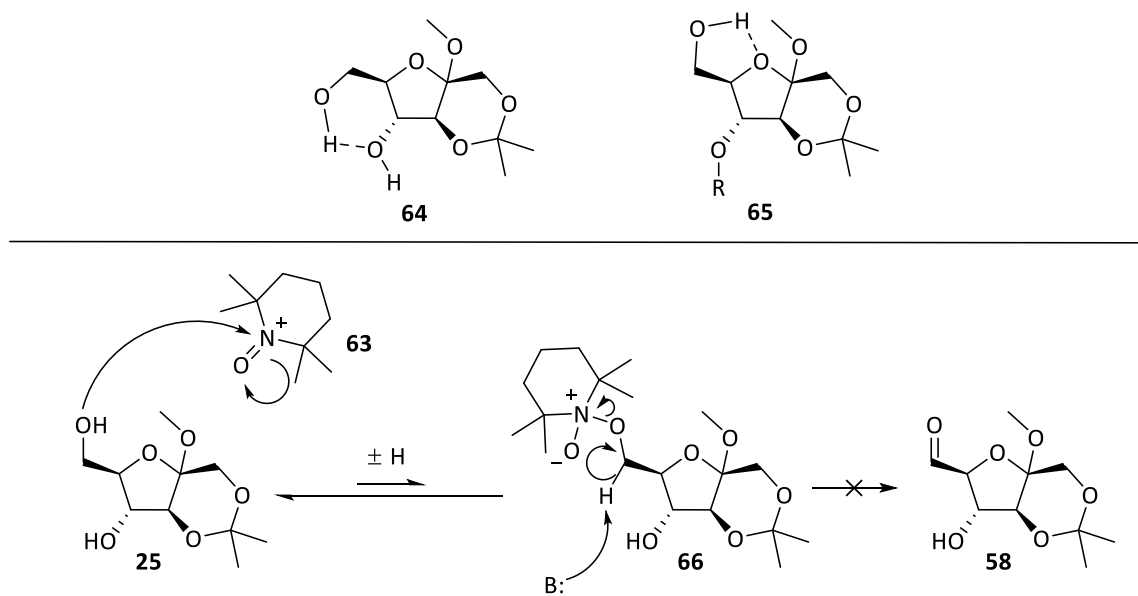
Entry	Co-oxidant (equiv)	TEMPO (equiv) <sup>a</sup>	Solvent	Temperature ( °C) <sup>b</sup>
1	NaClO (1.5)	0.1 / 1.25	THF	22 → 66 <sup>c</sup>
2	NaClO (1.5)	0.1 / 1.25	MeCN	22 → 82 <sup>c</sup>
3	KBr (1.5) / NaOCl (0.5)	0.1 / 1.25	THF	22 → 66
4	KBr (1.5) / NaOCl (0.5)	0.1 / 1.25	MeCN	22 → 82
5	DAIB (1.5)	0.1 / 1.25	THF	22 → 66
6	DAIB (1.5)	0.1 / 1.25	MeCN	22 → 82 <sup>c</sup>
7	BTIB (1.5)	0.1 / 1.25	THF	22 → 66
8	BTIB (1.5)	0.1 / 1.25	MeCN	22 → 82
9	Ca(OCl) <sub>2</sub> (1.5)	0.1 / 1.25	THF	22 → 66 <sup>c</sup>
10	Ca(OCl) <sub>2</sub> (1.5)	0.1 / 1.25	MeCN	22 → 82 <sup>c</sup>
11	Fe(NO <sub>2</sub> ) <sub>3</sub> (0.1)	0.1 / 1.25	THF	22 → 66
12	Fe(NO <sub>2</sub> ) <sub>3</sub> (1.5)	0.1 / 1.25	MeCN	22 → 82

a: reactions were run simultaneously with either 0.1 or 1.25 equivalents of TEMPO in separate vessels.

b: reactions were run at 22 °C for 48 h and then heated for 48 h. c: a separate reaction with the described conditions was stirred at 22 °C for 15 days.

The quality of the TEMPO and co-oxidants being used were examined by <sup>1</sup>H-NMR, <sup>13</sup>C-NMR and HRMS and they were found to be of high purity. Test reactions using the conditions described in Table 2.3 on benzyl alcohol gave benzaldehyde in high yields in all cases, most frequently at room temperature with 10 mol% TEMPO and 1.25 equivalents of the co-oxidant. These reactions took a comparable time to the published conditions from the relevant literature. Considering the successful oxidation of other alcohols under identical conditions, the partially protected fructose substrate **25** appears to be incompatible with the desired oxidation state change.

The inactivity of **25**, **51**, and **54** in reactions involving TEMPO could be due to reduced nucleophilicity of these materials towards the active oxoammonium salt. Intramolecular hydrogen bonding between either the C4 hydroxyl, in the case of **25**, or with the ring oxygen, in the cases of **51** and **54**, would result in the C6 hydroxyl being less nucleophilic as shown by the elaborated structures **64** and **65**. The addition of the C6 hydroxyl to the oxoammonium species **63** is a reversible reaction and a poor nucleophile may release from the TEMPO species before the non-reversible deprotonation from **66** can occur (Scheme 2.6).

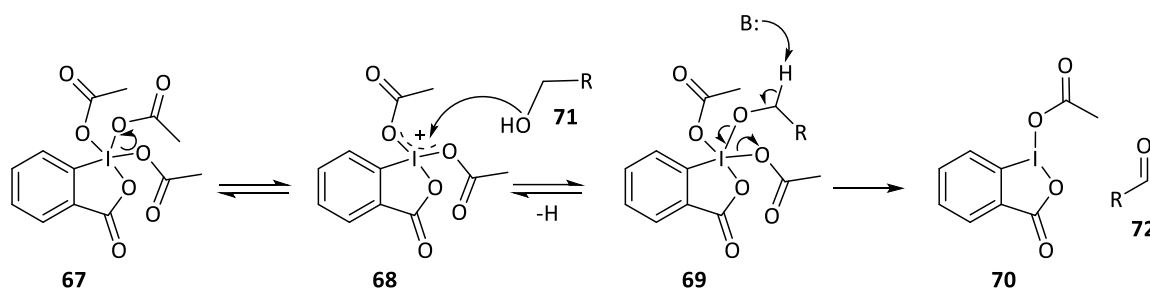


**Scheme 2.6:** Reduced nucleophilicity of **25**, **51**, or **54** as the result of intramolecular hydrogen bonding disfavours the attack on the oxoammonium salt **62** which prevents the irreversible deprotonation step from occurring.

## 2.5: Attempted Oxidation of Partially Protected D-Fructose Derivatives **25**, **51**, and **54** with Hypervalent Iodine Oxidants.

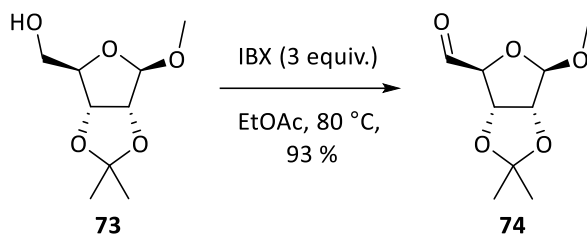
A number of the modern hypervalent iodine reagents were then employed in attempts to oxidize the C6 hydroxyl compounds **25**, **51**, and **54**. The most widely known of these is the

Dess-Martin periodinane (DMP, **67**) which has been shown to oxidize primary and secondary alcohols to the corresponding aldehyde or ketone.<sup>31,32</sup> DMP oxidation, and other hypervalent iodine reagents, operate through similar mechanisms. Ligand exchange around iodine replaces one of the acetate or other I-O bonds on the reagent with a new I-O bond (**67** to **69** via **68**); the new oxygen being from the substrate alcohol **71**. The released anionic ligand can then deprotonate the carbon the alcohol oxygen is attached to, generating the newly reduced iodine species **70**, the desired aldehyde **72**, and a second equivalent of ligand from the iodine centre (Scheme 2.7). The activity of these iodine based reagents can be mediated by the choice of ligands on the iodine center and the oxidation state of iodine in the reagent thus significant room for the screening of conditions exists with these reagents.<sup>33</sup>



**Scheme 2.7:** A generalized mechanism of DMP oxidation of a primary alcohol **71** to the corresponding aldehyde **72**.

In a publication from Finney and More in 2002 a substrate arising from D-ribose, **73**, was oxidized cleanly to **74** in 93% yield using IBX (Scheme 2.8). This substrate has a furanose ring structure that is quite similar to that of **25**, though the stereochemistry at C2 is inverted. Further, the substrate used by Finney and More does not have a linked ring fusing the C3 and C1 hydroxyl groups.<sup>34</sup> This example, and other similar examples in the literature, prompted a screening of DMP, IBX, and other hypervalent iodine oxidants to afford the desired conversion of the C6 hydroxyl compound **25** to the corresponding aldehyde **58**.



**Scheme 2.8: The oxidation of the D-ribose derivative 73 to the corresponding aldehyde 74 as carried out by Finney and More.<sup>34</sup>**

DMP (Table 2.4 entries 1,2), 2-iodoxbenzoic acid (IBX) (Table 2.4 entries 3, 4), (diacetoxyiodo)benzene (DIAB) (entry 5), [bis(trifluoroacetoxy)iodo]benzene (BTIB) (entry 6), and iodobenzene (entry 7) are all mechanistically related insofar as they rely on hypervalent iodine to oxidize alcohols, and the published substrate scope of these reactions suggested the reagents should cleanly and efficiently perform the desired oxidation.<sup>24,31,32,35–38</sup> Generally the reactions gave unreacted starting material or decomposition when more forcing conditions were employed (longer reaction times, addition of greater stoichiometric equivalents of oxidizing agent, or increasing the reaction temperature).

**Table 2.5: Investigation of hypervalent iodide based oxidants for the conversion of 25, 51, or 54 to the desired aldehyde 58, 59, or 60.**



Entry	Reagent	Equivalents	Temperature (° C) <sup>a</sup>	Solvent	Conversion (%) <sup>b</sup>	Yield (%)
1	DMP	1.1	22 <sup>c</sup>	DCM	8	0
2	DMP	2.25	22 <sup>d</sup>	DCM	34	11
						R=Bn ( <b>59</b> )
3	IBX	1.5	22 → 66	THF	0	0
4	IBX	3	22 → 39	THF	0	0
5	DIAB	3	22 → 66	THF	0	0
6	BTIB	3	22 → 66	THF	0	0
7	PhIO	3	22 → 66	THF	0	0

a: reactions were run at 22 °C for 48 h and then heated for 48 h b: Determined by recovered starting material c: reaction was stopped after 24 h d: reaction was stopped between 48 and 54 h; extending reaction time did not improve yield

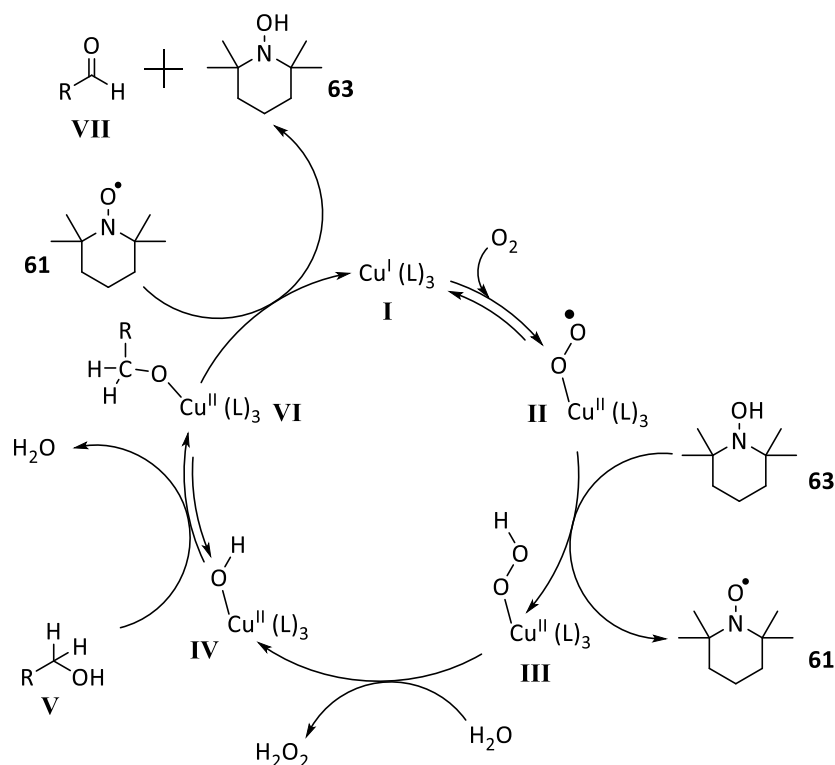
The sole exception to all of the failed reactions was found to be via the use of Dess-Martin periodinane (entry 2, Table 2.4) to produce fructose aldehyde derivative **58**. Optimization of this reaction failed to achieve more than a trace yield of **58**, and unfortunately scaling up the partially competent reaction conditions failed to provide sufficient quantities of fructose aldehyde derivative **58** for further study. The multiple iterations of this reaction gave only a few milligrams of product combined yet compound **58** was capable of being isolated as a colourless oil and fully characterized. A useful amount of this compound could not be collected from a single reaction or by combining the product of several reactions as **58** was prone to decomposition being left at ambient conditions. Further methodologies were applied in order to increase the amount of **58** that could be obtained.

DMP and IBX are known to give lower yields with sterically demanding substrates due to the steric bulk around the iodine (V) center encumbering the approach of sterically demanding alcohols.<sup>39,40</sup> The relative nucleophilicity of the incoming alcohol is also of importance as the first step in the reaction is fully reversible and the active complex **69** must exist long enough for the deprotonation to occur as with TEMPO mediated oxidations described above. The reactivity of the iodine (V) center in DMP appears to be at a suitable level to allow for the reaction to proceed, though in low yield. The less reactive iodine (III) species such as DIAB do not appear to be reactive enough to allow for the desired oxidation to proceed.

## 2.6: Attempted Transition Metal Mediated Oxidation of Partially Protected D-Fructose **25**

Both ruthenium and copper are well precedented to effect the oxidation of primary and secondary alcohols to aldehydes and ketones respectively. The copper-oxygen oxidation system has been published on several groups, notably by Stahl and co-workers and by Lumb and co-workers.<sup>41-46</sup> As deduced by Stahl and co-workers, the mechanism of copper-oxo mediated chemistry involves a copper(I)/copper(II) cycle using molecular oxygen as the terminal oxidant and the [Cu(bpy)NMI] complex as the active oxidizing agent (Scheme 2.9).<sup>47</sup> In this catalyst system molecular oxygen adds to the initial copper(I) species **I** to produce radical species **II**. TEMPO, in its hydroxylamine form **63**, can then take part in a single electron transfer with **II** to generate the peroxy intermediate **III** and the TEMPO free radical **61**. Water in the reaction mixture will then react with **III** to generate hydrogen peroxide and the key oxygenated copper(II) species **IV**. Intermediate **IV** will undergo ligand exchange with the alcohol substrate

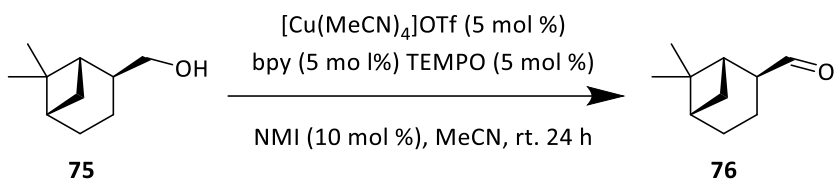
V to give VI which is primed for an oxidation reaction mediated by the TEMPO free radical 61. The oxidation reaction regenerates the catalyst I and releases the aldehyde product VII as well as the reduced TEMPO derivative 63.<sup>48</sup>



**Scheme 2.9:** An abbreviated mechanistic cycle of the Cu/O<sub>2</sub>/TEMPO system used for the oxidation of a primary alcohol to an aldehyde as described by Stahl and co-workers. (L)<sub>3</sub>=2,2'-bipyridine (bpy), N-methyl-indole (NMI).<sup>47</sup>

Stahl and co-workers demonstrated that their system could efficiently oxidize a sterically hindered alcohol **75** in high yields under their optimized conditions to give **76** (Scheme 2.10). This mild system allows for TEMPO to be used in a reaction and not have a high concentration of co-oxidants in solution which may affect the substrate or product of the reaction in an unwanted fashion. Lumb and co-workers later adopted the copper-oxo system to act without the need of a co-catalyst such as TEMPO. Initially they used this system to oxidize phenols to ortho-quinones and other functionalized aromatic products.<sup>46,49</sup> They then moved on

and developed a system which was capable of oxidizing aliphatic alcohols under mild conditions using molecular oxygen as the oxidant.<sup>45</sup> With the published success of these two groups affording similar products to the one desired in this research project, a series of test reactions was carried out.



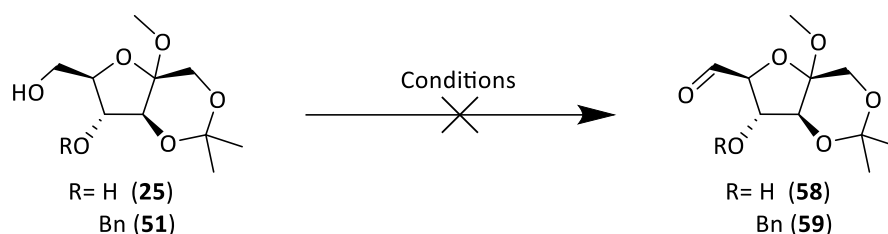
**Scheme 2.10: Oxidation of a sterically demanding primary alcohol to the corresponding aldehyde under the conditions of Stahl and co-workers.<sup>43</sup>**

Following the procedure optimized by Stahl and co-workers<sup>43</sup> the use of 0.1 or 0.5 equivalents of copper (I) and (II) salts including CuBr (Table 2.5 entries 1-3), CuBr<sub>2</sub> (entries 4, 5), Cu(OTf)<sub>2</sub> (entries 6, 7), Cu(OTf) (entries 8, 9), CuCl (entries 10, 11) and CuCl<sub>2</sub> (entries 12, 13) failed to give the desired product at room temperature or when heated to reflux. These conditions gave either decomposition or failed to consume the starting material. The majority of cases showed no consumption of the starting material while the use of copper (I) or copper (II) triflates gave decomposition of the starting material when 0.5 equivalents of the copper triflates were used. This is likely the result of triflic acid in solution reacting with the starting material and effecting the deprotection of the acetal protecting group followed by possible dehydration of the free hydroxyl functional groups.

Further screening of oxidation conditions was carried out including the use of tetrapropylammonium perruthenate (TPAP) in both the classic Ley-Griffith oxidation and later modifications of that reaction.<sup>50-53</sup> TPAP mediated oxidation using various N-oxides as

stoichiometric co-oxidants for the ruthenium catalyst are well known to cleanly produce aldehydes from primary alcohols.<sup>54,55</sup> As with the copper mediated oxidations, TPAP catalysed reactions gave no signs of starting material consumption despite the large excess of TRAP and co-oxidant used in these screening reactions or heating in MeCN or DCM (Table 2.5 entries 14-17).

**Table 2.6: Investigation of copper-molecular oxygen co-oxidants for TEMPO mediated oxidation of 25 or 51 to afford the desired aldehyde 58 or 59.**



Entry	Conditions (equivalents) <sup>a</sup>	Solvent	Temperature (°C) <sup>b</sup>
1	CuBr (0.1) 1-Me-Imid (0.1) BPY (0.1) TEMPO (0.05) O <sub>2</sub>	MeCN	22 → 82 <sup>c</sup>
2	CuBr (0.1) 1-Me-Imid (0.1) BPY (0.1) TEMPO (0.05) O <sub>2</sub>	DCM	22 → 39
3	CuBr (0.5) 1-Me-Imid (0.5) BPY (0.5) TEMPO (0.25) O <sub>2</sub>	MeCN	22 → 82
4	CuBr <sub>2</sub> (0.1) 1-Me-Imid (0.1) BPY (0.1) TEMPO (0.05) O <sub>2</sub>	MeCN	22 → 82
5	CuBr <sub>2</sub> (0.5) 1-Me-Imid (0.5) BPY (0.5) TEMPO (0.25) O <sub>2</sub>	MeCN	22 → 82
6	Cu(OTf) <sub>2</sub> (0.1) 1-Me-Imid (0.1) BPY (0.1) TEMPO (0.05) O <sub>2</sub>	MeCN	22 → 82
7	Cu(OTf) <sub>2</sub> (0.5) 1-Me-Imid (0.5) BPY (0.5) TEMPO (0.25) O <sub>2</sub>	MeCN	22 → 82
8	CuOTf (0.1) 1-Me-Imid (0.1) BPY (0.1) TEMPO (0.05) O <sub>2</sub>	MeCN	22 → 82
9	CuOTf (0.5) 1-Me-Imid (0.5) BPY (0.5) TEMPO (0.25) O <sub>2</sub>	MeCN	22 → 82
10	CuCl (0.1) 1-Me-Imid (0.1) BPY (0.1) TEMPO (0.05) O <sub>2</sub>	MeCN	22 → 82
11	CuCl (0.5) 1-Me-Imid (0.5) BPY (0.5) TEMPO (0.25) O <sub>2</sub>	MeCN	22 → 82
12	CuCl <sub>2</sub> (0.1) 1-Me-Imid (0.1) BPY (0.1) TEMPO (0.05) O <sub>2</sub>	MeCN	22 → 82
13	CuCl <sub>2</sub> (0.5) 1-Me-Imid (0.5) BPY (0.5) TEMPO (0.25) O <sub>2</sub>	MeCN	22 → 82
14	TPAP (0.1) NMO (1.25) H <sub>2</sub> O (1.25)	DCM	22 → 39
15	TPAP (0.5) NMO (2.5) H <sub>2</sub> O (3)	DCM	22 → 82
16	TPAP (0.1) NMO (1.25) H <sub>2</sub> O (1.25)	MeCN	22 → 82
17	TPAP (0.5) NMO (2.5) H <sub>2</sub> O (3)	MeCN	22 → 82

a: O<sub>2</sub> was bubbled through the solution from a balloon of pure O<sub>2</sub>. b: reactions were run at 22 °C for 48 h and then heated for 48 h. c: a separate reaction with the described conditions was stirred at 22 °C for 10 days.

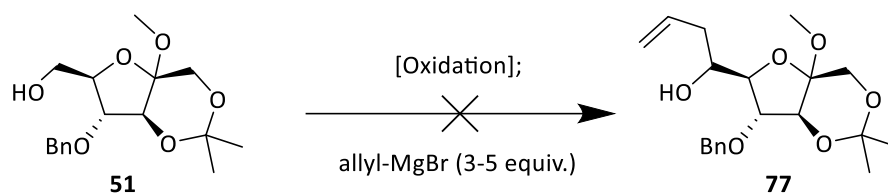
The key step in the mechanism of this oxidation involves the reversible addition of the substrate hydroxyl to the copper center, **IV** in Scheme 2.9, and the release of water. As

mentioned above the C6 hydroxyl of **25** appears to be a poor nucleophile and its protected derivative **51** seems to be too sterically encumbered to approach the oxidizing agents be that DMP, TEMPO or the [Cu(bpy)NMI] complex. After screening the above conditions it is apparent that the complexation of the C6 hydroxyl compound **25** or its protected derivative **54** to an active oxidation center is fleeting with the equilibrium favouring the disassociated forms. If the intermediate corresponding to **IV** in Scheme 2.9 does not exist long enough in solution for the deprotonation to occur the desired transformation will never occur on a viable scale unless the equilibrium can be shifted in a meaningful way which does not appear to be a feasible option in the case of this reaction.

## **2.7: Attempted One-Pot Oxidation/Trapping of D-Fructose Derivative 58**

Although isolation of any significant amount of fructose aldehyde **58** proved to be intangible up to this point, we hypothesized that the aldehyde may be being formed in the reaction mixture, then undergoing polymerization or other decomposition pathways upon work-up or attempted isolation. <sup>1</sup>H-NMR spectra of several crude reaction mixtures did not show any diagnostic signals of an aldehyde being present. The carbonyl compounds may have been formed in too low a concentration to be observed. To determine if this was the case several of the above reactions were repeated but rather than undergoing a standard quench and work-up procedure, the reaction mixtures were instead quenched with a large excess of allylmagnesium bromide. The allyl Grignard reagent was chosen as it is highly reactive, is a small, hard nucleophile and, the product of reaction would have diagnostic peaks in the <sup>1</sup>H-NMR spectrum

which would be well separated from the signals of the starting material, other reagents, or solvents. These interception attempts were quenched after the addition of allylmagnesium bromide with the minimal amount of water and concentrated by rotary evaporation in a warm water bath under high vacuum to remove solvent, water, and the allyl alcohol produced (Scheme 2.11). None of the diagnostic peaks expected for an allyl addition product **77** were found in the crude  $^1\text{H-NMR}$  spectra of any of these attempts and no spots on TLC were observed to indicate that the aldehyde had been produced *in situ* and had been intercepted by allylmagnesium bromide.

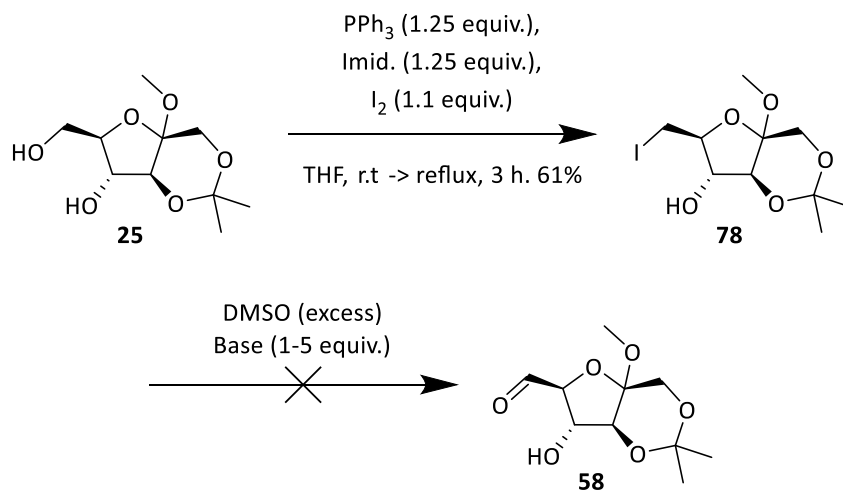


**Scheme 2.11: General reaction of attempts to intercept a C6 aldehyde of **51** created in the reaction mixture by the addition of an excess of allyl magnesium bromide to give **77**.**

In order to test the viability of performing both the oxidation of partially protected fructose **51** and the trapping of fructose aldehyde derivative in one-pot, substrate **51** was subjected to a given set of oxidizing conditions from Table 2.3 or Table 2.4 for 24 hours at room temperature (Scheme 2.11). Directly following the 24 hour period 3-5 equivalents of allyl magnesium bromide (0.5 M in THF) was added to the solution. After 5 minutes the reaction was quenched by the dropwise addition of water until bubbling ceased. The reaction mixture was then concentrated to dryness, dissolved in  $\text{CDCl}_3$  and filtered through a celite plug before a crude  $^1\text{H-NMR}$  spectrum was collected. Crude  $^1\text{H-NMR}$  spectra were very complex; however, the region between 4.5 ppm and 6.5 ppm lacked the diagnostic signals of an allyl group, implying the reactions failed to give significant amounts of any allylated compounds.

## 2.8: Attempted Oxidation of Iodo-Fructose derivative via the Kornblum Oxidation

The observed robustness of partially protected fructose alcohol **25** to forcing temperatures and super stoichiometric equivalents of metal and organic oxidizing reagents provided some anecdotal evidence that the primary alcohol may be much less reactive than originally expected. With this in mind **25** was transformed into the corresponding alkyl iodide **78** via the Appel reaction<sup>56</sup> using conditions similar to those used by Madsen and co-workers (Scheme 2.12).<sup>57</sup> We hypothesized alkyl iodide **78** should be more reactive than the primary alcohol in **25** and may be amenable to the Kornblum oxidation conditions.<sup>58</sup> The Kornblum oxidation involves displacing an alkyl halide, usually an iodide or bromide, with DMSO under high heat. With iodide **78** in hand Kornblum oxidation was attempted at temperatures ranging from 22 °C to 200 °C but no consumption of the starting material was observed in all cases. The two step preparation of iodide **78** from D-fructose gave rapid access to large quantities of this C6 functionalized compound and attention was turned to using **78** as a C6 nucleophilic species rather than trying to make a C6 electrophilic species and these studies are outlined in Chapter 3.



**Scheme 2.12:** The use of the Appel reaction to create the C6 iodide **78** which was subjected to Kornblum oxidation.

Though the C6 hydroxyl compound **25** was found to be unreactive to nearly all the oxidations conditions attempted as described previously, it was found to be a competent substrate in the Appel reaction to afford iodide **78**. This is likely due to the strong thermodynamic driving force of the Appel reaction, phosphorus-oxygen bond formation. The P-O single bond and subsequent P=O double bond formed are highly stable unlike the intermediates formed in the oxygenation reactions described above, accounting for the success of the Appel reaction on the same substrate that failed to react under oxidation conditions.

## 2.9: Summary

After committing significant time into the oxidation of **25** it became apparent that this strategy was not going to result in the desired compounds. The apparent low nucleophilicity of the C6 hydroxyl compound **25** impedes its reactivity with electrophilic oxidizing agents such as IBX, TEMPO, or the  $[\text{Cu}(\text{bpy})\text{NMI}]$  complex. Only a very small amount of the desired

aldehyde **58** could be obtained from a reaction with DMP that failed upon scale up and could not be optimized despite an exhaustive effort. Rather than abandoning this line of experimentation entirely the focus was shifted to using **78** as a C6 nucleophile. With the C6 iodide **78** in hand attention was turned to the creation of an alkyl metal species which could be used to afford the needed C-C bond formation from C6. These efforts are outlined in Chapter 3.

## **2.10: Experimental:**

All reactions were carried out in oven-dried glassware sealed with a rubber septa and vented to room air unless otherwise stated. Transfer of anhydrous solvents and reagents was accomplished with oven-dried syringes or via cannula transfer. The following solvents when used in reactions were purified using a solvent purification system manufactured by LC Technology Solutions Inc. and operated according to the manufactures specifications before use: dichloromethane (DCM), diethyl ether (Et<sub>2</sub>O), tetrahydrofuran (THF), acetonitrile (MeCN). Toluene (PhMe) was distilled before use from sodium metal under a positive nitrogen atmosphere. Pyridine was dried over solid KOH for a minimum of 24 hours before use. All other commercially available solvents and reagents were used without additional purification and were purchased from the Sigma-Aldrich company. Thin layer chromatography was carried out on glass plates coated with 0.25 mm silica gel produced by the SiliCycle Company. Visualization of spots on the TLC plates was achieved via UV light or treatment with 2.5% *p*-anisaldehyde in AcOH: H<sub>2</sub>SO<sub>4</sub>: EtOH in a 1:3:38 ratio and heated to give colour development. Flash chromatography columns were packed with 230-400 mesh silica gel produced by the Silicycle Company with the specified solvent system. Proton nuclear magnetic resonance spectra (<sup>1</sup>H-NMR) were recorded at 400 MHz or 500 MHz in the

indicated solvents. Chemical shifts were reported in ppm using the solvent peak as the internal standard. The reported coupling constants were reported in hertz (Hz) and standard notation was used to describe the multiplicity of each of the signals observed: singlet (s), doublet (d), triplet (t), broad (br), multiplet (m), etc. Carbon nuclear magnetic resonance spectra ( $^{13}\text{C}$ -NMR) were recorded at 100 MHz or 125 MHz in the indicated solvents. The solvent peaks were reported in ppm and the solvent peaks were used as the internal standard. Infrared spectra (IR) were measured with a Nic-Plan FTIR Microscope instrument. IR spectra were reported in  $\text{cm}^{-1}$  from neat samples as recorded using a Mattson Galaxy Series FT-IR 3000 spectrometer. Mass spectra were determined on a Kratos MS50 high-resolution electrospray instrument recording in positive ion mode. Optical rotations were recorded on a Perkin Elmer 241 Polarimeter using the D line of sodium (589 nm).

#### **Synthesis of methyl 1,3-*O*-isopropylidene- $\alpha$ -D-fructofuranoside (25):**

The synthesis of 1,3-*O*-isopropylidene- $\alpha$ -D-fructofuranoside was adapted from the work of Hong and co-workers. *p*TsOH (30 mg, 0.17 mmol) was added to 50 mL methanol and stirred for 15 min. To this solution D-fructose (5 g, 27.8 mmol) was added and stirred for 24 h at room temperature. 2,2-Dimethoxypropane (35 mL, 285.7 mmol) was added and stirred for 45 min before solid, powdered sodium hydrogen carbonate (5 g, 60.0 mmol) was added to the solution. The mixture was immediately filtered and the solvent was removed under reduced pressure. The yellow syrup was purified through a silica gel column using 10 % MeOH:DCM affording a pale yellow syrup (4.17 g, 17.8 mmol, 64%).  $R_f$  0.45 (6 % MeOH:DCM)  $^1\text{H}$ -NMR and  $^{13}\text{C}$ -NMR were consistent with the published data of Hong and co-workers.<sup>4</sup>

**Synthesis of methyl 1,3-O-isopropylidene-6-O-(*p*-tolylsulfonyl)- $\alpha$ -D-fructofuranoside (26):**

The synthesis of methyl 1,3-O-isopropylidene-6-O-(*p*-tolylsulfonyl)- $\alpha$ -D-fructofuranoside was adapted from the procedure of Jung and Co-workers. Compound **25** (0.758 g, 3.2 mmol) was dissolved in DMC (25 mL) and pyridine (10 mL) was added before the solution was cooled to 0 °C. To this solution *p*TsCl (0.608 g, 3.2 mmol) was added and stirred for 24 h while being allowed to warm to room temperature. The reaction mixture was neutralized with HCl (10 % w/v) and extracted with DCM (3 x 20 mL). The organic layers were combined, washed with brine (10 mL) and dried over anhydrous MgSO<sub>4</sub> before the solvent was removed under reduced pressure. The yellow-orange oil was purified through a silica gel column using 50 % EtOAc:Hex to afford an off yellow oil (1.21 g, 2.9 mmol, 92 %). R<sub>f</sub> 0.4 (50 % EtOAc:Hex). <sup>1</sup>H-NMR and <sup>13</sup>C-NMR were consistent with the published data of Jung and co-workers.

**Synthesis of methyl 1,3-O-isopropylidene-4-O-benzyl-6-O-(*p*-tolylsulfonyl)- $\alpha$ -D-fructofuranoside (50):**

Compound **26** (0.748 g, 1.8 mmol) was dissolved in THF (35 mL) before benzyl bromide (0.462 g, 2.7 mmol) was added in one portion. NaH (0.110 g, 60 % dispersed in mineral oil, 2.7 mmol) was then added in 3 portions over 3 minutes. The reaction was stirred for 24 h at room temperature before water (20 mL), and HCl (5 mL, 10 % w/v) were added. The reaction mixture was extracted with DCM (3 x 15 mL). The organic layers were combined and washed with brine (10 mL), before being dried over MgSO<sub>4</sub> and the solvent was removed under reduced pressure. The clear oil was purified through a silica gel column using 25 % EtOAc:Hex to afford a white crystalline solid (0.621 g, 1.3 mmol, 74 %); R<sub>f</sub> 0.68 (50 % EtOAc:Hex); [ $\alpha$ ]<sub>D</sub><sup>20</sup> +49.96 (*c* 1.33, DCM); MP 86.2-87.8 °C; IR: 3088, 3064, 3032, 2989, 2938, 2876, 2836, 1921, 1812, 1718, 1654, 1589, 1496, 1454, 1367, 1294, 1268, 1220, 1190,

1177, 1151, 1097, 1028, 979, 939, 976, 939, 911, 891, 859, 815, 791, 738, 699, 666; HRMS Expected 478.56 Observed M+Na 501.16 °C; <sup>1</sup>H NMR (498 MHz, CDCl<sub>3</sub>) δ 7.85 – 7.77 (m, 2H), 7.43 – 7.26 (m, 7H), 4.66 (dd, J = 4.8, 1.1 Hz, 1H), 4.61 – 4.51 (m, 2H), 4.21 (q, J = 5.0 Hz, 1H), 3.98 (d, J = 1.0 Hz, 1H), 3.92 – 3.77 (m, 2H), 3.62 (d, J = 5.1 Hz, 2H), 3.27 (s, 3H), 2.43 (d, J = 0.7 Hz, 3H), 1.29 (d, J = 0.7 Hz, 3H), 1.25 (d, J = 0.7 Hz, 3H); <sup>13</sup>C NMR (126 MHz, CDCl<sub>3</sub>) δ 144.83, 137.33, 132.90, 129.80, 128.49, 128.10, 127.94, 127.90, 103.24, 99.20, 84.81, 80.08, 79.23, 77.29, 77.04, 76.78, 72.35, 69.31, 61.86, 60.40, 48.62, 26.67, 21.65, 20.88.

**Synthesis of methyl 1,3-*O*-isopropylidene-4-*O*-benzyl- $\alpha$ -D-fructofuranoside (51):**

Compound **50** (0.517 g, 1.01 mmol) was dissolved in THF (50 mL) under a positive nitrogen atmosphere and cooled to -78 °C. Via cannula a solution of sodium naphthalenide (0.8 M in THF, prepared as per Robins and co-workers) at -78 °C was transferred to the solution of ## dropwise until the dark green/black colour persisted in the reaction vessel. The reaction was stirred at -78 °C for 30 min before water (15 mL) was added in one portion causing the solution to solidify. The reaction was warmed to room temperature and stirred for 30 minutes. The reaction mixture was concentrated under reduced pressure. The white, crystalline solid was purified through a silica gel column using 30 % EtOAc:Hex to afford an off yellow oil (0.507 g, 0.98 mmol 98 %); R<sub>f</sub> 0.28 (30% EtOAc:Hex); [ $\alpha$ ]<sub>D</sub><sup>20</sup> +67.36 (*c* 1.17, DCM); IR: 3464, 3062, 3031, 2989, 2939, 2834, 1723, 1603, 1497, 1454, 1375, 1298, 1267, 1220, 1168, 1150, 1100, 1060, 1028, 999, 940, 897, 859, 745, 700; HRMS Expected: 324.16 Observed: M+Na 347.15; <sup>1</sup>H NMR (498 MHz, CDCl<sub>3</sub>) δ 7.41 – 7.26 (m, 5H), 4.72 (ABq, J=4.72, 4.5Hz, 1H), 4.50 (ABq, J=4.72, 4.5Hz, 1H), 4.17 – 4.12 (m, 2H), 3.94 (d, J = 12.2 Hz, 1H), 3.92 – 3.82 (m, 2H), 3.67 (dd, J = 11.9, 4.4 Hz, 1H), 3.33 (s, 3H), 1.44 (d, J = 0.7 Hz, 3H), 1.38 (d, J

= 0.7 Hz, 3H);  $^{13}\text{C}$  NMR (126 MHz,  $\text{CDCl}_3$ )  $\delta$  137.64, 128.47, 127.91, 127.89, 102.33, 99.12, 84.71, 83.36, 79.26, 77.27, 77.02, 76.77, 72.57, 62.61, 62.17, 48.51, 31.25, 29.72, 27.10, 20.54, 14.14.

**Synthesis of methyl 1,3-*O*-isopropylidene-6-*O*-triphenylmethyl- $\alpha$ -D-fructofuranoside (52):**

Compound **25** (1.34 g, 5.1 mmol) was dissolved in pyridine (15 mL) and cooled to 0 °C. Triphenylmethyl chloride (1.55 g, 5.59 mmol) was added in 5 portions over 1 hour and the solution was stirred for 6h. The reaction mixture was diluted with water (10 mL) and then neutralized with HCl (30 % w/v). The mixture was extracted with DCM (3 x 15 mL), the organic fractions were combined, washed with brine (10 mL) and dried over  $\text{MgSO}_4$  before the solvent was removed under reduced pressure. The yellow oil was purified through a silica gel column using 30 % EtOAc:Hex to afford a pale yellow oil (1.626 g, 3.42 mmol, 67%). Rf 0.44 (50 % EtOAc:Hex);  $[\alpha]_{\text{D}}^{20} +3.04$  ( $c$  1.02, DCM); IR: 3462, 3086, 3058, 3023, 2990, 2938, 2876, 2834, 1964, 1818, 1723, 1596, 1491, 1448, 1407, 1375, 1303, 1266, 1169, 1151, 1096, 1074, 1032, 986, 938, 899, 856, 765, 746, 737, 706; HRMS Expected: 476.22  
Observed: M+Na 499.20;  $^1\text{H}$  NMR (500 MHz,  $\text{CDCl}_3$ )  $\delta$  7.55 – 7.46 (m, 7H), 7.37 – 7.28 (m, 8H), 7.28 – 7.21 (m, 4H), 4.23 (td,  $J$  = 6.3, 2.5 Hz, 1H), 4.06 – 4.00 (m, 2H), 3.99 – 3.89 (m, 2H), 3.46 (dd,  $J$  = 9.4, 6.5 Hz, 1H), 3.34 (s, 3H), 3.22 (dd,  $J$  = 9.4, 6.2 Hz, 1H), 2.61 (d,  $J$  = 10.4 Hz, 1H), 1.44 (s, 3H), 1.23 – 1.19 (m, 3H);  $^{13}\text{C}$  NMR (126 MHz,  $\text{CDCl}_3$ )  $\delta$  144.01, 128.80, 128.73, 127.96, 127.93, 127.81, 127.25, 126.93, 101.90, 98.55, 86.61, 86.48, 79.74, 78.28, 64.36, 61.88, 48.72, 27.61, 19.67.

**Synthesis of methyl 1,3-*O*-isopropylidene-4-*O*-acetyl-6-*O*-triphenylmethyl- $\alpha$ -D-fructofuranoside (53):**

Compound **52** (1.07 g, 2.25 mmol) was dissolved in DCM (15 mL) and pyridine (5 mL) and cooled to 0 °C before DMAP (0.0274 g, 0.225 mmol) and acetic anhydride (0.918 g, 9.00 mmol) were added. The reaction was stirred overnight and allowed to warm to room temperature. The reaction was diluted with water (10 mL), and neutralized with HCl (10 % w/v) before being extracted with DCM (3 x 15 mL). The organic layers were combined and washed with brine (10 mL), before being dried over MgSO<sub>4</sub> and the solvent was removed under reduced pressure. The clear oil was purified through a silica gel column using 25 % EtOAc:Hex to afford a clear oil (0.944 g, 1.82 mmol, 81%). R<sub>f</sub> 0.52 (35 % EtOAc:Hex); [ $\alpha$ ]<sub>D</sub><sup>20</sup> +14.93 (*c* 0.71, DCM); IR: 3058, 3022, 2991, 2938, 2871, 2832, 1961, 1825, 1744, 1701, 1633, 1597, 1491, 1449, 1373, 1236, 1173, 1173, 1152, 1109, 1051, 1031, 1002, 952, 941, 919, 899, 856, 765, 707; HRMS Expected 518.61 Observed 541.21 M+Na; <sup>1</sup>H NMR (498 MHz, CDCl<sub>3</sub>)  $\delta$  7.55 – 7.47 (m, 6H), 7.35 – 7.21 (m, 9H), 4.13 (ddd, *J* = 5.9, 4.7, 4.2 Hz, 1H), 4.06 (d, *J* = 0.8 Hz, 1H), 3.99 – 3.87 (m, 2H), 3.48 – 3.34 (m, 2H), 3.33 (s, 3H), 2.08 (s, 3H), 1.45 (d, *J* = 0.7 Hz, 3H), 1.32 (d, *J* = 0.7 Hz, 3H); <sup>13</sup>C NMR (126 MHz, CDCl<sub>3</sub>)  $\delta$  170.07, 144.02, 128.83, 127.76, 126.93, 102.74, 99.33, 86.64, 82.38, 79.65, 79.09, 64.02, 62.39, 48.53, 26.74, 20.99, 20.64.

#### **Synthesis of methyl 1,3-*O*-isopropylidene-4-*O*-acetyl- $\alpha$ -D-fructofuranoside (**54**):**

Compound **53** (0.181 g, 0.349 mmol) was dissolved in THF (20 mL) and water (0.0063 mL, 0.349 mmol) was added. Trifluoroacetic acid (0.001 g, 0.087 mmol) was added and the reaction was stirred for 40 min. Solid, powdered sodium hydrogen carbonate (1 g, 11.9 mmol) was added in one portion and the mixture was diluted with water (40 mL). The mixture was then extracted with DCM (3 x 20 mL) and the organic layers were combined, washed with brine (10 mL) and dried over MgSO<sub>4</sub> before the solvent was removed under

reduced vacuum. The off white solid was purified through a silica gel column using 20 % EtOAc:Hex to afford a clear oil (0.017 g, 0.056 mmol). Rf 0.38 (35 % EtOAc:Hex);  $[\alpha]_D^{20} +4.38$  (*c* 0.90, DCM); IR: 3479, 2991, 2942, 2837, 1743, 1454, 1375, 1333, 1240, 1172, 1151, 1109, 1081, 1051, 1031, 1002, 941, 884, 856, 764, 707; HRMS Expected: 276.29 Observed M+Na: 299.11;  $^1\text{H}$  NMR (400 MHz,  $\text{CDCl}_3$ )  $\delta$  4.92 – 4.87 (m, 1H), 4.13 (d, *J* = 1.7 Hz, 1H), 4.05 (dt, *J* = 4.9, 3.5 Hz, 1H), 4.00 – 3.77 (m, 4H), 3.34 – 3.24 (m, 3H), 2.34 (t, *J* = 6.2 Hz, 1H), 2.18 – 2.03 (m, 3H), 1.44 (s, 3H), 1.38 (s, 3H);  $^{13}\text{C}$  NMR (126 MHz,  $\text{CDCl}_3$ )  $\delta$  170.62, 101.33, 99.07, 84.22, 79.31, 78.98, 62.80, 62.26, 48.59, 27.46, 20.94, 19.77.

**Synthesis of methyl 1,3-*O*-isopropylidene-6-*O*-(4,4'-dimethoxytriphenylmethyl)- $\alpha$ -D-fructofuranoside (56):**

Compound **25** (0.953 g, 3.24 mmol) was dissolved in pyridine (15 mL) and cooled to 0 °C. 4,4'-dimethoxytriphenylmethyl chloride (1.204 g, 3.56 mmol) was added in 5 portions over 1 hour and the solution was stirred for 6h. The reaction mixture was diluted with water (10 mL) and then neutralized with HCl (30 % w/v). The mixture was extracted with DCM (3 x 15 mL), the organic fractions were combined, washed with brine (10 mL) and dried over  $\text{MgSO}_4$  before the solvent was removed under reduced pressure. The yellow oil was purified through a silica gel column using 30 % EtOAc:Hex to afford a pale yellow oil (1.16 g, 2.17 mmol, 67%). Rf (50 % EtOAc:Hex);  $[\alpha]_D^{20} +3.13$  (*c* 1.29, DCM); IR: 3474, 3056, 3035, 2991, 2930, 2873, 2836, 2049, 1898, 1608, 1582, 1509, 1463, 1446, 1414, 1375, 1301, 1251, 1221, 1176, 1153, 1094, 1074, 1034, 986, 938, 901, 755, 736, 727, 703, 675; HRMS Expected 536.62 Observed 559.23 M+Na;  $^1\text{H}$  NMR (500 MHz,  $\text{CDCl}_3$ )  $\delta$  7.53 – 7.47 (m, 2H), 7.41 – 7.34 (m, 4H), 7.33 – 7.25 (m, 3H), 7.24 – 7.19 (m, 1H), 6.87 – 6.80 (m, 4H), 4.20 (td, *J* = 6.4, 2.5 Hz, 1H), 4.05 – 3.98 (m, 2H), 3.98 – 3.88 (m, 2H), 3.79 (s, 6H), 3.42 (dd, *J* = 9.3, 6.4 Hz,

1H), 3.33 (s, 3H), 3.19 (dd, J = 9.4, 6.4 Hz, 1H), 2.55 (d, J = 10.4 Hz, 1H), 1.43 (s, 3H), 1.23 – 1.19 (m, 3H); <sup>13</sup>C NMR (126 MHz, CDCl<sub>3</sub>) δ 158.39, 144.97, 136.31, 136.15, 130.15, 130.12, 128.26, 127.77, 126.63, 113.10, 113.08, 101.86, 98.54, 86.47, 86.01, 79.75, 78.35, 77.29, 77.03, 76.78, 64.17, 61.86, 55.20, 48.70, 27.60, 19.65.

**Synthesis of methyl 1,3-*O*-isopropylidene-4-*O*-acetyl-6-*O*-(4,4'-dimethoxy-triphenylmethyl- $\alpha$ -D-fructofuranoside (57):**

Compound **56** (0.862 g, 1.61 mmol) was dissolved in DCM (15 mL) and pyridine (0.508 g, 6.43 mmol) and cooled to 0 °C before DMAP (0.019 g, 0.161 mmol) and acetic anhydride (0.656 g, 6.43 mmol) were added. The reaction was stirred overnight and allowed to warm to room temperature. The reaction was diluted with water (10 mL), and neutralized with HCl (10 % w/v) before being extracted with DCM (3 x 15 mL). The organic layers were combined and washed with brine (10 mL), before being dried over MgSO<sub>4</sub> and the solvent was removed under reduced pressure. The clear oil was purified through a silica gel column using 25 % EtOAc:Hex to afford a clear oil (0.735 g, 1.27 mmol, 79%). R<sub>f</sub> 0.37 (40 % EtOAc:Hex); [ $\alpha$ ]<sub>D</sub><sup>20</sup> +11.82 (*c* 2.99, DCM); IR: 3498, 3057, 3035, 2992, 2939, 2836, 2044, 1899, 1743, 1608, 1582, 1509, 1463, 1446, 1415, 1374, 1300, 1248, 1176, 1109, 1081, 1035, 953, 941, 888, 856, 830, 790, 755, 736, 703; HRMS: Expected 578.66 Observed M+Na 601.2; <sup>1</sup>H NMR (500 MHz, CDCl<sub>3</sub>) δ 7.55 – 7.45 (m, 3H), 7.44 – 7.33 (m, 5H), 7.33 – 7.24 (m, 4H), 7.24 – 7.16 (m, 3H), 6.87 – 6.80 (m, 6H), 4.18 – 4.09 (m, 2H), 4.06 (d, J = 0.7 Hz, 1H), 3.95 – 3.89 (m, 2H), 3.79 (d, J = 3.7 Hz, 8H), 3.40 (dd, J = 9.8, 5.9 Hz, 1H), 3.35 – 3.33 (m, 1H), 3.32 (s, 3H), 2.07 (s, 3H), 1.44 (s, 3H), 1.33 (s, 3H); <sup>13</sup>C NMR (126 MHz, CDCl<sub>3</sub>) δ 170.06, 158.42, 145.06, 136.25, 136.21, 130.20, 130.17, 129.16, 128.30, 127.83, 127.80, 127.74,

127.70, 126.64, 113.16, 113.07, 113.03, 102.65, 99.29, 86.04, 82.41, 79.66, 79.11, 63.84, 62.80, 62.39, 62.25, 55.23, 55.19, 48.50, 27.45, 26.79, 20.98, 20.93, 20.60, 19.80.

**Synthesis of methyl 1,3-*O*-isopropylidene-4-*O*-acetyl- $\alpha$ -D-fructofuranoside (54) via Removal of the 4,4'-dimethoxy-trityl group:**

Compound **57** (0.447 g, 0.773 mmol) was dissolved in THF (20 mL) and water (0.0012 mL, 0.696 mmol) was added. Ytterbium (III) triflate (0.0479 g, 0.077 mmol) was added in one portion and the reaction was stirred for 3 h. The reaction mixture was diluted with water (20 mL) then extracted with DCM (3 x 20 mL) and the organic layers were combined, washed with brine (10 mL) and dried over MgSO<sub>4</sub> before the solvent was removed under reduced vacuum. The off white solid was purified through a silica gel column using 20 % EtOAc:Hex to afford a colourless oil (0.097 g, 0.317 mmol, 41%). Rf 0.28 (30% EtOAc:Hex)

**Synthesis of methyl 1,3-*O*-isopropylidene-4-*O*-benzyl- $\alpha$ -D-fructofuranoside-6-al (59):**

Compound **51** (0.071 g, 0.22 mmol) was dissolved in DCM (25 mL) at room temperature and DMP (0.212 g, 0.50 mmol) was added in one portion. The reaction mixture was stirred for 48-54 h before water (25 mL) was added. The reaction mixture was extracted with DCM (3 x 20 mL), the organic fractions were combined, washed with brine (10 mL) and dried over MgSO<sub>4</sub> before the solvent was removed under reduced vacuum. The pale-yellow oil was purified through a silica gel column using 6% MeOH:DCM to give a colourless oil (0.0074 g, 0.023 mmol, 11 %) Rf 0.47 (6% MeOH:DCM); [ $\alpha$ ]<sub>D</sub><sup>20</sup> -11.83 (*c* 0.59, DCM); IR: 3436, 2990, 2941, 2838, 1735, 1627, 1453, 1377, 1305, 1269, 1221, 1150, 1102, 1028, 941, 892, 857, 762, 734, 702; Expected 322.36 Observed M+Na (acetal dimer) 667.8; <sup>1</sup>H NMR (498 MHz, CDCl<sub>3</sub>)  $\delta$  9.69 (d, J = 1.4 Hz, 1H), 7.42 – 7.27 (m, 5H), 4.74 – 4.57 (m, 2H), 4.48 (dd, J = 2.8,

1.4 Hz, 1H), 4.19 (d, J = 0.7 Hz, 1H), 4.08 – 3.92 (m, 3H), 3.37 (s, 3H), 1.44 (d, J = 0.7 Hz, 3H), 1.33 (d, J = 0.7 Hz, 3H); <sup>13</sup>C NMR (126 MHz, CDCl<sub>3</sub>) δ 200.66, 137.14, 128.49, 127.97, 127.95, 127.93, 102.91, 98.70, 87.94, 86.41, 72.27, 62.41, 49.09, 27.39, 19.89.

#### **Typical procedure for oxidation reactions:**

To a flask containing starting material (0.5 mmol) dissolved in the indicated solvent (15 mL) held at the indicated temperature under a positive atmosphere of nitrogen or oxygen (via balloon) was added the oxidizing agent with any indicated additives. The reaction was stirred for the designated time before being diluted with water (10 mL). The mixture was extracted with DCM (3 x 10 mL), the organic fractions were combined and washed with brine (10 mL) and dried over MgSO<sub>4</sub> before the solvent was removed under reduced pressure. Workup procedures for reactions involving Jones reagent, iron salts, or copper salts were modified as per the original publications of those conditions. The crude residue that was recovered after the removal of solvent was re-dissolved in CDCl<sub>3</sub>, passed through a Celite plug and analysed by <sup>1</sup>H-NMR and TLC.

#### **Synthesis of methyl 1,3-*O*-isopropylidene-6-deoxy-6-iodo- $\alpha$ -D-fructofuranoside (78):**

Compound **25** (1.17 g, 5.00 mmol) was dissolved in THF (75 mL) and then iodine (2.00 g, 7.9 mmol), and imidazole (0.37 g, 7.9 mmol) were added and allowed to stir for 10 min.

Triphenylphosphine (2.07 g, 7.9 mmol) was added in 4 portions over 20 min and the reaction was heated to reflux for 3 hours. The yellow/brown reaction mixture turned colourless and a white precipitate was observed to form. The reaction was cooled to room temperature and concentrated under reduced pressure. The crude pale yellow solid was purified through a silica gel column using 40 % EtOAc:Hex to afford a colourless oil (1.05 g, 3.05mmol, 61%).

Rf 0.57 (40% EtOAc:Hex) <sup>1</sup>H-NMR, and <sup>13</sup>C-NMR were consistent with those published by Ye and co-workers.<sup>60</sup>

## 2.11: References:

- (1) Litjens, R. E. J. N.; van den Bos, L. J.; Codée, J. D. C.; Overkleeft, H. S.; van der Marel, G. A. *Carbohydr. Res.* **2007**, *342* (3–4), 419–429.
- (2) Angyal, S. J.; Bethell, G. S. *Aust. J. Chem.* **1976**, *29* (6), 1249–1265.
- (3) Pétursson, S. *J. Chem. Educ.* **1997**, *74* (11), 1297.
- (4) Yu, K.; Zhao, X.; Wu, W.; Hong, Z. *Tetrahedron Lett.* **2013**, *54* (22), 2788–2790.
- (5) Hanaya, T.; Sato, N.; Yamamoto, H. *Carbohydr. Res.* **2005**, *340* (16), 2494–2501.
- (6) Lewandowska, E.; Neschadimenko, V.; Wnuk, S. F.; Robins, M. J. *Tetrahedron* **1997**, *53* (18), 6295–6302.
- (7) Helferich, B. In *Advances in Carbohydrate Chemistry*; W.W. Pigman, M. L. W. and S. P., Ed.; Academic Press, 1948; Vol. 3, pp 79–111.
- (8) Lu, R. J.; Liu, D.; Giese, R. W. *Tetrahedron Lett.* **2000**, *41* (16), 2817–2819.
- (9) Bowden, K.; Heilbron, I. M.; Jones, E. R. H.; Weedon, B. C. L. *J. Chem. Soc.* **1946**, No. 0, 39–45.
- (10) Jefford, C. W.; Wang, Y. *J. Chem. Soc., Chem. Commun.* **1988**, No. 10, 634–635.
- (11) Omura, K.; Sharma, A. K.; Swern, D. *J. Org. Chem.* **1976**, *41* (6), 957–962.
- (12) Tojo, G.; Fernandez, M. I. *Oxidation of Alcohols to Aldehydes and Ketones: A Guide to Current Common Practice*; Springer Science & Business Media, 2006.
- (13) Jeong, T. S.; Choi, C. H.; Lee, J. Y.; Oh, K. K. *Bioresour. Technol.* **2012**, *116*, 435–440.
- (14) Omura, K.; Swern, D. *Tetrahedron* **1978**, *34* (11), 1651–1660.
- (15) Pfitzner, K. E.; Moffatt, J. G. *J. Am. Chem. Soc.* **1963**, *85* (19), 3027–3028.
- (16) Parikh, J. R.; Doering, W. v. E. *J. Am. Chem. Soc.* **1967**, *89* (21), 5505–5507.
- (17) Golubev, V. A.; Voronina, G. N.; Rozantsev, E. G. *Bull. Acad. Sci. USSR Div. Chem. Sci.* **1970**, *19* (11), 2449–2451.
- (18) Cella, J. A.; Kelley, J. A.; Kenahan, E. F. *J. Org. Chem.* **1975**, *40* (12), 1860–1862.
- (19) Lucio Anelli, P.; Biffi, C.; Montanari, F.; Quici, S. *J. Org. Chem.* **1987**, *52* (12), 2559–2562.
- (20) Zhao, M.; Li, J.; Mano, E.; Song, Z.; Tschaen, D. M.; Grabowski, E. J. J.; Reider, P. J. *J. Org. Chem.* **1999**, *64* (7), 2564–2566.
- (21) Sen, V. D.; Golubev, V. A. *J. Phys. Org. Chem.* **2009**, *22* (2), 138–143.
- (22) Bobbitt, J. M. *ChemInform* **2011**, *42* (21), 1–10.
- (23) Ma, Y.; Loyns, C.; Price, P.; Chechik, V. *Org. Biomol. Chem.* **2011**, *9* (15), 5573–5578.
- (24) Sheldon, R. A.; Arends, I. W. C. E.; ten Brink, G.-J.; Dijkstra, A. *Acc. Chem. Res.* **2002**, *35* (9), 774–781.
- (25) Angelin, M.; Hermansson, M.; Dong, H.; Ramström, O. *Eur. J. Org. Chem.* **2006**, *2006* (19), 4323–4326.

- (26) Hamada, S.; Wada, Y.; Sasamori, T.; Tokitoh, N.; Furura, T.; Kawabata, T. *Tetrahedron Lett.* **2014**, *55* (11), 1943–1945.
- (27) Zhdankin, V. V. *Arkivoc* **2009**, *1*, 1–62.
- (28) Reddy, S. R.; Stella, S.; Chadha, A. *Synth. Commun.* **2012**, *42* (23), 3493–3503.
- (29) Liu, J.; Ma, S. *Tetrahedron* **2013**, *69* (47), 10161–10167.
- (30) Liu, J.; Ma, S. *Org. Biomol. Chem.* **2013**, *11* (25), 4186–4193.
- (31) Dess, D. B.; Martin, J. C. *J. Org. Chem.* **1983**, *48* (22), 4155–4156.
- (32) Meyer, S. D.; Schreiber, S. L. *J. Org. Chem.* **1994**, *59* (24), 7549–7552.
- (33) Yadav, J. S.; Reddy, B. V. S.; Basak, A. K.; Venkat Narsaiah, A. *Tetrahedron* **2004**, *60* (9), 2131–2135.
- (34) More, J. D.; Finney, N. S. *Org. Lett.* **2002**, *4* (17), 3001–3003.
- (35) Marco Frigerio, Marco Santagostino, Simona Sputore, and Giovanni Palmisano. *J. Org. Chem.* **1995**, *60*, 7272–7276.
- (36) Guérin, C.; Bellosta, V.; Guillamot, G.; Cossy, J. *Org. Lett.* **2011**, *13* (13), 3534–3537.
- (37) Uyanik, M.; Ishihara, K. *Chem. Commun.* **2009**, No. 16, 2086.
- (38) Tohma, H.; Kita, Y. *Adv. Synth. Catal.* **2004**, *346* (23), 111–124.
- (39) Thottumkara, A. P.; Bowsher, M. S.; Vinod, T. K. *Org. Lett.* **2005**, *7* (14), 2933–2936.
- (40) Nicolaou, K. C.; Mathison, C. J. N.; Montagnon, T. *J. Am. Chem. Soc.* **2004**, *126* (16), 5192–5201.
- (41) Piccialli, V.; Zaccaria, S.; Oliviero, G.; D’Errico, S.; D’Atri, V.; Borbone, N. *Eur. J. Org. Chem.* **2012**, *2012* (23), 4293–4305.
- (42) Minkyung Lim,; Seungchan Oh,; and Hakjune Rhee. *Bull Korean Chem Soc* **2011**, *32* (8), 3179–3182.
- (43) Hoover, J. M.; Stahl, S. S. *J. Am. Chem. Soc.* **2011**, *133* (42), 16901–16910.
- (44) Markó, I. E.; Gautier, A.; Dumeunier, R.; Doda, K.; Philippart, F.; Brown, S. M.; Urch, C. J. *Angew. Chem. Int. Ed.* **2004**, *43* (12), 1588–1591.
- (45) Xu, B.; Lumb, J.-P.; Arndtsen, B. A. *Angew. Chem. Int. Ed.* **2015**, *54* (14), 4208–4211.
- (46) Allen, S. E.; Walvoord, R. R.; Padilla-Salinas, R.; Kozlowski, M. C. *Chem. Rev.* **2013**, *113* (8), 6234–6458.
- (47) Hoover, J. M.; Ryland, B. L.; Stahl, S. S. *J. Am. Chem. Soc.* **2013**, *135* (6).
- (48) Hoover, J. M.; Steves, J. E.; Stahl, S. S. *Nat. Protoc.* **2012**, *7* (6), 1161–1166.
- (49) Esguerra, K. V. N.; Fall, Y.; Petitjean, L.; Lumb, J.-P. *J. Am. Chem. Soc.* **2014**, *136* (21), 7662–7668.
- (50) Ley, S. V.; Norman, J.; Griffith, W. P.; Marsden, S. P. *Synthesis* **1994**, *1994* (7), 639–666.
- (51) Griffith, W. P.; Ley, S. V.; Whitcombe, G. P.; White, A. D. *J. Chem. Soc., Chem. Commun.* **1987**, No. 21, 1625–1627.
- (52) Schmidt, A.-K. C.; Stark, C. B. W. *Org. Lett.* **2011**, *13* (16), 4164–4167.
- (53) J. Zerk, T.; W. Moore, P.; M. Williams, C.; V. Bernhardt, P. *Chem. Commun.* **2016**, *52* (67), 10301–10304.
- (54) Read, C. D. G.; Moore, P. W.; Williams, C. M. *Green Chem* **2015**, *17* (9), 4537–4540.
- (55) Moore, P. W.; Mirzayans, P. M.; Williams, C. M. *Chem. – Eur. J.* **2015**, *21* (9), 3567–3571.
- (56) Appel, R. *Angew. Chem. Int. Ed. Engl.* **1975**, *14* (12), 801–811.
- (57) Skaanderup, P. R.; Poulsen, C. S.; Hyltoft, L.; Jørgensen, M. R.; Madsen, R. *Synthesis* **2002**, *2002* (12), 1721–1727.

- (58) Kornblum, N.; Powers, J. W.; Anderson, G. J.; Jones, W. J.; Larson, H. O.; Levand, O.; Weaver, W. M. *J. Am. Chem. Soc.* **1957**, 79 (24), 6562–6562.
- (59) Kwon, H. B.; von Itzstein, M.; Jung, K-Y. *Tetrahedron Lett.* **2009**, 50, 2543-2544
- (60) Wang, G-N.; Yang, L.; Zhang, Li-H.; Ye, X-S. *J. Org. Chem.* **2011** 76, 2001-2009

## Chapter 3: Attempted Derivatization of 6-Deoxy-6-Iodo-D-Fructose in Efforts Towards a Fluorescently Tagged Molecular Imaging Agent

### 3.1: Rationale for Experimental Plan

While investigating the synthesis of the D-fructose aldehyde derivative as described in Chapter 2, the iodinated derivative **78** was synthesized (Scheme 2.12). We hypothesized that once a new carbon-carbon bond had been formed from the 6 positions, the subsequent installation of the desired OH group and the fluorescent dye could be done in short order. As shown previously in Chapter 2, application of the standard Appel reaction conditions enabled a high yielding and scalable approach to this C6 halogenated intermediate. This intermediate provides a synthetic handle for further manipulations towards the production of a fluorescently tagged D-fructose derivative. As the C6 position of **78** is deoxygenated this route will require additional steps to return that functionality and will be longer than the route proposed in Chapter 2 utilizing the corresponding aldehyde. As this research project was entirely product driven, no route with reasonable potential could be overlooked.

Simultaneously with the attempts to oxidize the C6 iodide **78** to the aldehyde, we investigated the use of the potential umplong reactivity of alkyl halides whereby the C6 carbon becomes nucleophilic rather than electrophilic.<sup>1-3</sup> Alkyl halides are the starting materials for many processes using transition metals. These include metal-halide bond insertions including the formation of Grignard type reagents<sup>4</sup>, alkyllithium reagents, organocuprate (Gilman) reagents<sup>5</sup> and others.<sup>6</sup> All of these reactions involve a low valent metal species oxidatively adding into the carbon-halide bond making a new, high energy, carbon metal-bond. Depending on the metal of choice, temperature, solvent, and other

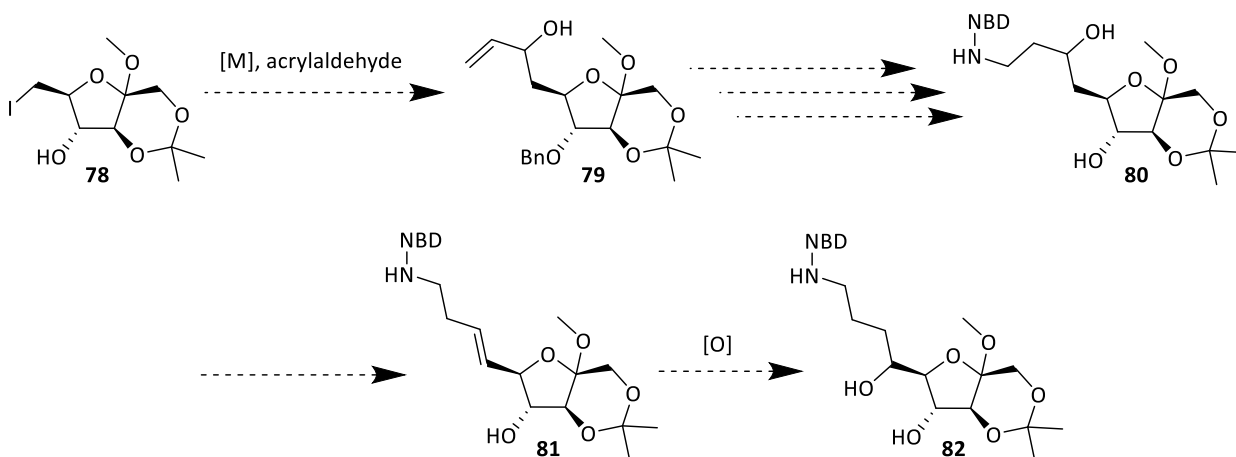
reaction conditions the reactivity of these alkyl metal reagents and their formation can be, to some extent, mediated. In fact, these highly reactive, often pyrophoric reagents have found a place in pharmaceutical and other large scale chemical operations in some instances.<sup>7</sup>

In the specific case of the iodinated intermediate **78** these methodologies should allow for the creation of new carbon-carbon bonds in the nucleophilic manifold rather than the electrophilic one which proved to be unsuccessful as described in Chapter 2. Using **78** as a nucleophile gives many more opportunities for functionalization of the C6 position and the single step introduction of linker chains at this site. A competent alkyl-metal species arising from this alkyl iodide could be subjected to an array of reactions, rapidly increasing molecular complexity and moving the synthesis towards the desired products. The non-trivial task of re-oxygenating the C6 position after these synthetic manipulations would still need to be accomplished.

### 3.2: Attempted Metal-Halogen Exchange

Having encountered significant difficulty when attempting to oxidize partially protected D-fructose derivatives, we hypothesized using the iodinated derivative **78** as a nucleophile to form a new carbon-carbon bond could be a successful pathway to our desired product (Scheme 3.1). Further manipulation of intermediate **79** could yield a D-fructose derivative **80** labelled with the 4-chloro-7-nitrobenofurazan (NBD) attached through the C6 position **80**. Notably, compound **80** possesses a hydroxyl group on the side-chain that is displaced by one carbon from the normal C6 position, raising interesting questions about its recognition by GLUT5 and hexokinase. Alternately, intermediate **80** could be dehydrated to

give an alkene **81** which could then be oxidized to give a compound with a hydroxyl at C6 such as **82**. Either **80** or **82** could be quickly deprotected to reveal the NBD labeled hexose.



**Scheme 3.1: Proposed route from 78 to 82 via an alkyl metal mediated C-C bond formation at the C6 position of 78 and further manipulations.**

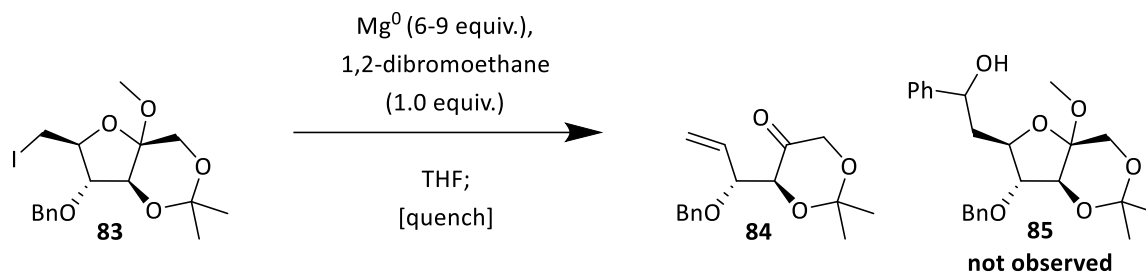
This route could require re-optimization depending on the tolerance of the NBD moiety to dehydration, oxidation, or other reaction conditions employed. The suite of relevant dehydration and oxidations conditions available in the common chemical tool box should be more than sufficient to carry out the desired transformations.

### 3.2: Attempts to Generate a Grignard Reagent from the Corresponding Alkyl Iodide Derived From D-Fructose

Formation of the Grignard reagent originating from alkyl iodide **83** was initially attempted using magnesium metal in THF at room temperature. Compound **83** was produced by benzylation of the precursor **78** which was prepared as per Scheme 2.12. This derivative was chosen as it is a fully protected D-fructose derivative with the C6 iodide which could be

conveniently purified rapidly. THF was chosen as a solvent as it is compatible with the Grignard reaction conditions and was able to dissolve compound **83**. Diethyl ether is also a common solvent in Grignard reagent preparation but iodide **83** was very poorly soluble in diethyl ether. Manual scratching of the magnesium metal and heating of the solution failed to initiate the reaction. In further attempts for initiation of the reaction, a full equivalent of 1,2-dibromoethane was co-added with **83** via a two barrel syringe pump over 1 hour to a flask containing a large excess of magnesium turnings in THF. The reaction initiated quickly as indicated by bubbling on the metal surface and heat being generated, boiling the solvent. The solution was quenched with a large excess of either water or benzaldehyde to determine if the alkyl magnesium was being formed in solution. <sup>1</sup>H-NMR analysis revealed the same product from both quenches, alkene **84** (Table 3.1).

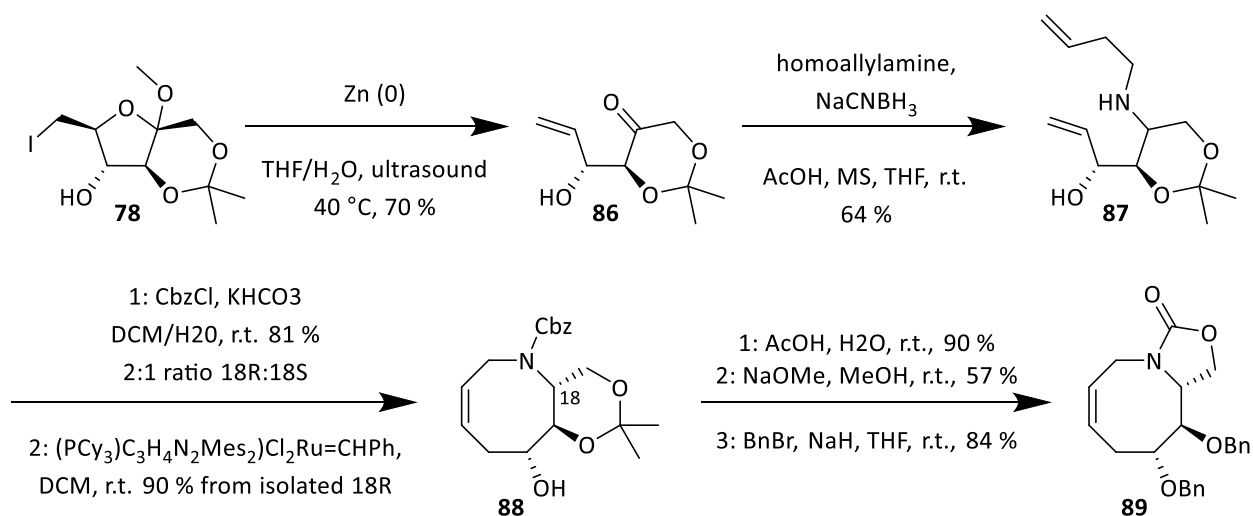
**Table 3.1: Attempted formation and trapping of a Grignard-type reagent from iodo-fructose derivative **83**.<sup>a</sup>**



Entry	Temperature ( °C)	Quench <sup>b</sup>	Conversion (%) <sup>c</sup>	<b>84</b> (%)
1	22 → 66	H <sub>2</sub> O	100	83
2	-10	H <sub>2</sub> O	100	81
3	-41	H <sub>2</sub> O	100	84
4	-78	H <sub>2</sub> O	0	0
5	-78 → -41	H <sub>2</sub> O	100	73
6	22 → 66	Benzaldehyde	100	78
7	-10	Benzaldehyde	100	77
8	-41	Benzaldehyde	100	83
9	-78	Benzaldehyde	0	0
10	-78 → -41	Benzaldehyde	100	71

a: All reactions carried out in 15 mL of THF with 5-7 equivalents of solid magnesium. Starting material was added in 1 mL of THF via syringe pump. 1 equivalent of 1,2-dibromoethane in 1 mL of THF was co-added with starting material from a separate syringe. b: 5-8 equivalents of water or benzaldehyde added in one portion as a solution in 3 mL THF c: Based on recovered starting material

This elimination product arises from furanoside ring opening and the ejection of the anomeric methoxide. This process had previously been observed by Madsen and Lauritsen in their work towards the production of naturally occurring iminosugars (Scheme 3.2).<sup>8</sup> They utilized the presence of the ketone and terminal alkene in **86** to create medium ring iminosugars via a reductive elimination to give **87** followed by ring-closing-metathesis to give **88**. Three short steps furnished, in good yield, the advanced intermediate **89**. Compound **89** intercepts an intermediate three steps from the end of the total synthesis of Australine as published by White and Hrniciar in 2000.<sup>8,9</sup>



**Scheme 3.2: The route of Madsen and Lauritsen in their formal synthesis of the naturally occurring iminosugar australine.<sup>8,9</sup>**

The observed formation of the alkene **84** is promising considering that it most likely arises from the insertion of magnesium into the carbon-iodine bond. The high reactivity of this Grignard reagent manifested itself poorly in the intramolecular decomposition pathway which leads to this alkene. In order to circumvent the elimination pathway, decreasing the reaction temperature was evaluated. The reaction was first attempted at -10 °C (Table 3.1 entry 2), then at -41 °C (entry 3), and lastly at -78 °C (entry 4). At -10 °C and -41 °C the elimination product was the only species observed after quenching the reaction with water. At -78 °C unreacted starting material was obtained when the quench was performed at -78 °C and **84** was obtained when the reaction was started at -78 °C and subsequently warmed to -41 °C before quenching with water (entry 5). The reactions were repeated whereupon an excess of benzaldehyde was added in the place of water. At all of the temperatures used only the elimination product was formed and no adduct incorporating benzaldehyde, **85**, could be observed in the crude <sup>1</sup>H-NMR spectrum (entries 6-10). These results suggest that the

elimination process to form **84** could be extremely fast and the desired Grignard reagent does not persist long enough to be utilized before the unwanted intramolecular ring opening occurred..

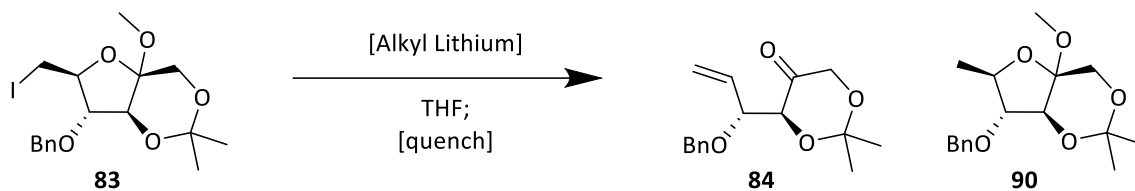
### 3.3: Attempts to Generate an Alkylolithium Reagent from the Corresponding Iodo-D-Fructose Derivative.

Given the difficulty encountered while attempting to harness the reactivity of the D-fructose Grignard derivative, attention was turned to forming the corresponding alkylolithium species. Alkylolithium formation via lithium-halogen exchange can be carried out extremely low temperatures and it was hoped that this would circumvent the unwanted decomposition of the alkyl-metal species which was observed with Grignard type reactions. We hypothesised that the alkylolithium species could be formed and used in place of the Grignard reagent to yield compound **79** through an analogous route as outlined above. The formation of alkylolithium occurs through an exchange of the carbon-halogen bond for a carbon-lithium bond which can occur at cryogenically low temperatures, and is extremely fast, often faster than competing proton exchange or nucleophilic additions.<sup>10-15</sup>

Lithium-halogen exchange was attempted with *n*-butyllithium (*n*-BuLi), *sec*-butyllithium (*s*-BuLi) and tertiary butyllithium (*t*-BuLi) at -41 °C, -78 °C and -100 °C (Table 3.2). At -41 °C rapid decomposition was observed yielding a mixture of the elimination product **84** and a number of non-isolable compounds (entries 1, 3, 5). At -78 °C only **84** was observed after quenching the *n*-BuLi reaction with water (entry 2). When *s*-BuLi was used to initiate the lithium-halogen exchange only decomposition was observed (entry 4). The use of

*t*-BuLi at -78 °C gave a mixture of the reduction and elimination products in low yields (entry 6) while quenching with benzaldehyde gave only the elimination product (entry 7). Warming the reactions to -41 °C after being quenched with either a water or benzaldehyde solution gave similar results to those observed previously (entry 8-11). The lithium-halogen exchange was then attempted at -100 °C with *t*-BuLi in hopes of avoiding the unimolecular decomposition.<sup>10,14,16</sup> Bailey and co-workers worked diligently to show that at -100 °C the alkyl lithium species should not undergo any other processes allowing the alkyl lithium to persist until it could react with an electrophile of some kind.<sup>14,15</sup> When a water:THF solution was used to quench the lithium halogen exchange (entries 10 and 11) the reduced compound **90** was recovered from a mixture of mainly decomposition products. By visual observation the reaction mixture had no change upon initial addition of *t*-BuLi at -100 °C. The solution then turned grey after a few minutes and turned dark grey/black immediately upon warming or quenching with water or benzaldehyde. It appears that the lithium halogen exchange may be occurring at -100 °C but decomposition occurs more rapidly than any other process including protonation of the alkyl lithium. The expedient decomposition precluded forming more stable organometallics via transmetallation and therefore further study was abandoned.

**Table 3.2: Investigation of the formation of an alkyllithium reagent from 83 and the resulting products observed.<sup>a</sup>**



Entry	Li Source	Temperature ( °C)	Quench <sup>b</sup>	Conversion (%) <sup>c</sup>	84 (%)	90 (%)
1	<i>n</i> -BuLi	-41	H <sub>2</sub> O	100	0	0
2	<i>n</i> -BuLi	-78	H <sub>2</sub> O	100	24	0
3	<i>sec</i> -BuLi	-41	H <sub>2</sub> O	100	0	0
4	<i>sec</i> -BuLi	-78	H <sub>2</sub> O	100	0	0
5	<i>t</i> -BuLi	-41	H <sub>2</sub> O	100	0	0
6	<i>t</i> -BuLi	-78	H <sub>2</sub> O	100	37	17
7	<i>t</i> -BuLi	-78	Benzaldehyde	100	28	0
8	<i>t</i> -BuLi	-78 → -41	H <sub>2</sub> O	100	46	25
9	<i>t</i> -BuLi	-78 → -41	Benzaldehyde	100	0	0
10	<i>t</i> -BuLi	-100 → -41	H <sub>2</sub> O	100	0	16
11	<i>t</i> -BuLi	-100 → -41	Benzaldehyde	100	0	0

a: Reactions carried out in 15 mL of THF. 1.0 or 2.5 equivalents of alkyl lithium was added as a solution in THF from titrated stock bottles of reagent. Yields given are from experiments with 1.0 equivalents, no significant change in outcome was observed with 2.5 equivalents. b: 5-7 equivalents of water or benzaldehyde were added as a solution in 3 mL THF in one portion. c: Based on recovered starting material.

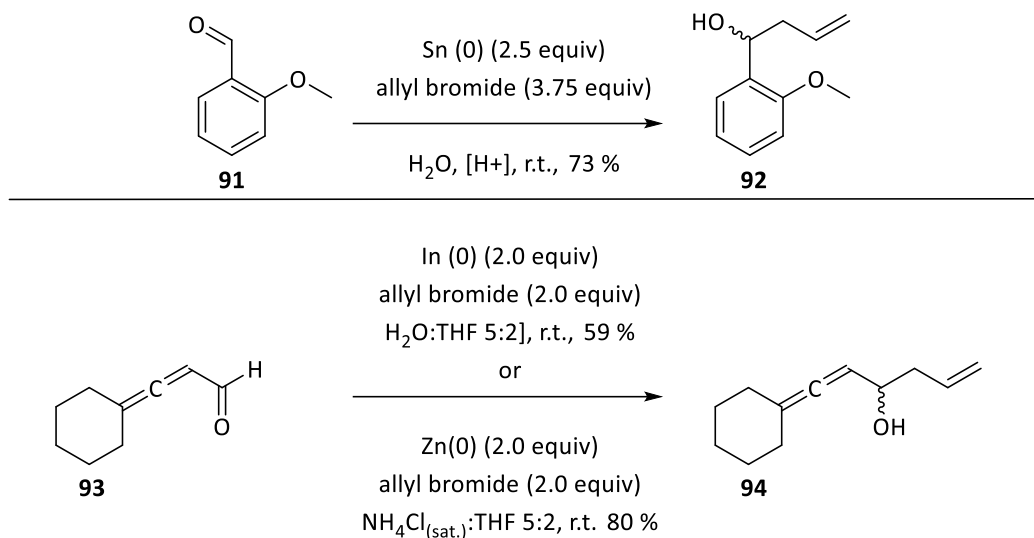
### 3.4: Attempts to Generate a Grignard Reagent Under Barbier-Type Conditions From a Iodo-D-Fructose Derivative.

After its introduction to the literature in the early 1900's the scope of reactions classified as Barbier reactions has grown significantly. Barbier is considered the pioneer of the extremely well known and utilized field of organomagnesium reagents,<sup>6</sup> although his student Dr. Victor Grignard would later expand upon this field of reagents and become synonymous with their usage. The Barbier reaction is not limited to magnesium mediated reactions as currently the use of tin<sup>17,18</sup>, copper<sup>19</sup>, zinc<sup>8,20-22</sup>, samarium<sup>23,24</sup>, and indium<sup>25</sup> are

all classified as Barbier reactions so long as they adhere to these further guidelines. Barbier reactions are one-pot and involve the generation of the alkyl metal species from an alkyl halide and a reactive metal. The alkyl metal species reacts with the electrophile that is already present in solution to form a new bond. The metal halogen exchange can occur via a single electron or a two electron process depending on both the metal employed and the reaction conditions.<sup>26–28</sup> The most common electrophiles employed in Barbier reactions are carbonyl compounds, (mainly aldehydes and ketones) as these types of electrophiles allow for coordination of the alkyl metal species to the carbonyl oxygen, facilitating a closed mechanism with an ordered transition state.<sup>18,29,30</sup> A wide array of alkyl halides, electrophiles, metals, and ligands have been demonstrated in the literature highlighting the functional group tolerance, and a large array of scaffolds is available by this simple reaction. Of particular importance to this research is the report of the Barbier reaction done in aqueous solvents, mixed solvent systems, and with carbohydrate substrates.<sup>19,23–25,31–33</sup> Recent publications utilizing the Barbier reaction have shown a wide substrate scope including advanced intermediates in the synthesis of natural products<sup>34</sup> and other complex substrates.<sup>23,33,35,36</sup> The use of non-traditional solvents for alkyl-metal chemistry, including water, and surfactant additives has been shown to increase the rate of Barbier type additions.<sup>37–44</sup> At the center of these micelles is a small, hydrophobic core where the local concentration of alkyl halide is greatly increased driven by hydrophobic effects. This leads to an increase in the rate of oxidative addition inside the micelles and the overall rate of the Barbier reaction. Once the Barbier reagent is formed it can escape the micelle and encounter the electrophile in the bulk solution or the electrophile can enter the micelle and the C-C bond formation can occur there.

The exact location of the C-C bond forming event depends on the hydrophobic/hydrophilic character of the two materials.<sup>37-39</sup>

Previously, during the use of iodo-fructose derivative **78** as a starting material for an alkyl metal reaction it was observed that metal/halogen exchange occurred in the presence of magnesium or lithium as described above. Unfortunately the highly polarized metal-carbon bonds led to rapid elimination or decomposition by uncharacterized pathways. We hypothesized that the Barbier reagents would form under mild conditions and react with an *in situ* electrophile without decomposing owing to the less reactive nature of the variety of metal-carbon bonds that could be employed. Significant precedence for the use of Barbier type conditions to afford the desired carbon-carbon bond formation exists in the literature. Malvestiti and co-workers found that tin would act as a reducing agent in the presence of allyl bromide to give the Barbier type addition product on simple aldehydes, such as **91** giving **92** (Scheme 3.3). They also observed that the presence of an adjacent oxygen, in an ether functional group, would increase the rate of the reaction by coordinating the tin center in proximity to the aldehyde functionality (Scheme 3.3, top).<sup>17</sup> Ma and co-workers demonstrated that the use of indium or zinc metal in mixed solvent systems would lead to the desired Barbier reaction on aldehydes such as **93** and give selectivity for the coordinating aldehyde group over an adjacent allene to give products including **94** (Scheme 3.3, bottom).<sup>42</sup> Similar successes have been published using zinc-copper couple,<sup>20</sup> samarium<sup>23</sup> and other metal salts.<sup>21,45,46</sup>



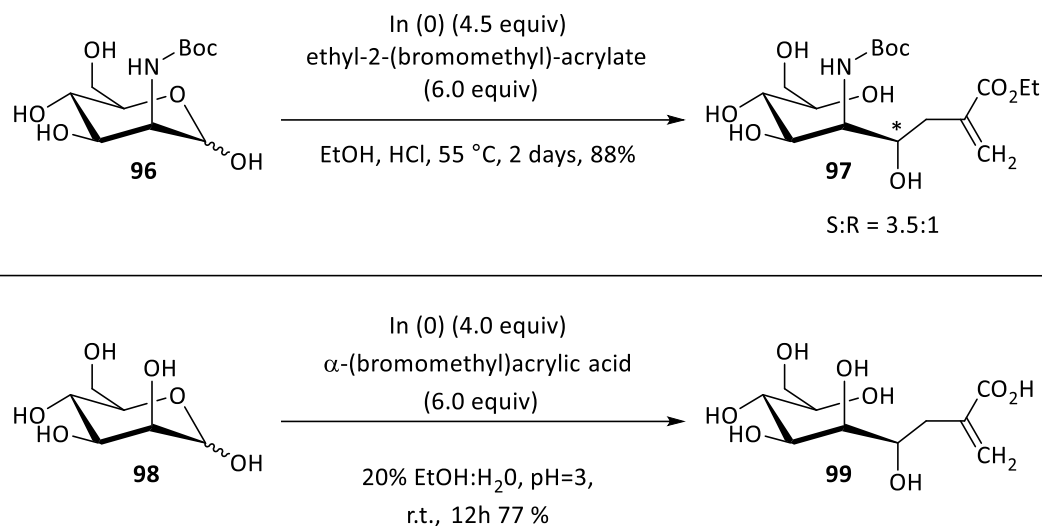
**Scheme 3.3:** The Barbier type reactions carried out by Malvestiti and co-workers (top)<sup>17</sup> and Ma and co-workers (bottom)<sup>42</sup> utilizing low valent metals to carry out the nucleophilic addition of an allyl unit into an aldehyde.

To determine if the iodo-fructose derivative **78** could be a competent partner in a Barbier reaction a series of test reactions was carried out in an attempt to produce **94** (Table 3.3). The goal of these experiments was to determine what conditions would lead to a metal inserting into the carbon-iodine bond and if the resulting reagent would be able to add into a reactive aldehyde. Towards this end, benzaldehyde was chosen as the test electrophile (Table 3.3). Benzaldehyde, and closely related aromatic aldehydes, had been used by Malvestiti and co-workers to screen their reaction conditions.<sup>17</sup> This reagent was also readily available and could be purified quickly by distillation when needed. Once suitable conditions had been found to carry out the carbon-carbon bond formation to benzaldehyde the reaction could be elaborated to a more useful substrate such as acrolein which would provide a convenient handle for further manipulations.

Initially tin was used as the reducing agent in hopes it would add into the carbon-iodine bond and add into the carbonyl of benzaldehyde similarly to the example of Malvestiti

and co-workers (Table 3.3 entry 1).<sup>17</sup> This was not successful so HCl was added to the solution, but again no reaction was observed even after heating to reflux (entry 2). In a mixture of water and THF with NH<sub>4</sub>Cl, HCl, or SDS as an additive no change was found in the outcome of the reaction (entries 3-5). Using tin as a reducing agent failed to consume any of the starting iodo-fructose derivative therefore attention was turned to zinc as the active metal in these reactions. The use of zinc (0) in THF, or in a water-THF mixture with NH<sub>4</sub>Cl failed to show any consumption of the alkyl iodide (entries 6, 7). ZnCl<sub>2</sub> and freshly prepared zinc-copper couple also failed to consume the starting material (entries 8, 9). Next a 1:1 mixture of ZnCl<sub>2</sub> and CuCl was then used in THF or in THF with SDS added but to no avail; the starting material remained untouched by these conditions (entries 10, 11).

Indium has been used as the active metal in many Barbier reactions, as described above, and on partially protected carbohydrates as demonstrated by Whitesides and co-workers<sup>46</sup> as well as Lee and Chan (Scheme 3.4).<sup>47</sup> These reactions were carried out in highly polar solvent mixtures and on poly-ol-substrates without the need for global protection. Further, the carbonyl center onto which the Barbier reagent added was, in both cases (**96** and **98**), an anomeric center which would not exist in the open chain form exclusively, adding to the difficulty of the reactions giving **97** and **99** respectively. Whitesides and co-workers as well as Lee and Chan report excellent yields for these reactions, and therefore the use of indium was the next logical choice for this reaction.

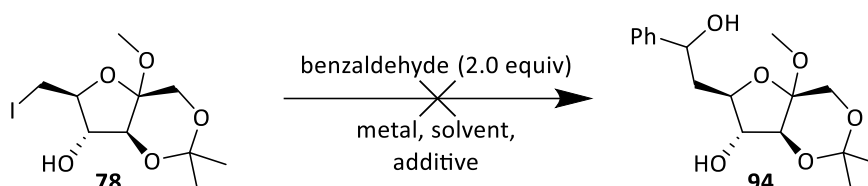


**Scheme 3.4: The work of Whitesides and co-workers (top) and Lee and Chan (bottom) utilizing indium mediated Barbier reactions to alkylate carbohydrate scaffolds at the anomeric position.**<sup>46,47</sup>

Indium (0) was used in THF, or in a water-THF mixture to help dissolve all components of the reaction. Addition of SDS, HCl, or HBr failed to give any change in the outcome of the reaction: no consumption of the starting material (Table 3.3 entries 12, 13, 16, 17). Indium (III) were then used as the metal source in the reactions. Though indium (III) is at too high an oxidation state to oxidatively add into the carbon-iodine bond, a small amount of indium (I) is known to exist in equilibrium within commercially available indium (III) salts.<sup>48-50</sup> We hypothesized that the low valence indium could insert into the carbon-iodine bond in the presence of indium (III) which could activate the carbonyl of benzaldehyde would aide in the reaction. However we found that changing the indium source from indium (0) to  $\text{InCl}_3$  or  $\text{In(OTf)}_3$  failed to give any product (entries 14, 15). Finally samarium (0) was used to attempt and initiate the Barbier reaction in THF with or without NaI or in water but no signs of the desired reaction progressing were observed (entries 18-20).

Variation in solvents, metals, temperature, and additives failed to give any reaction. Although there is significant literature precedent for primary halides smoothly reacting under several of the conditions screened, **78** failed to give any product.<sup>26,42,44</sup>

**Table 3.3: Investigation of the formation of a Barbier reagent from **78**.**<sup>a</sup>

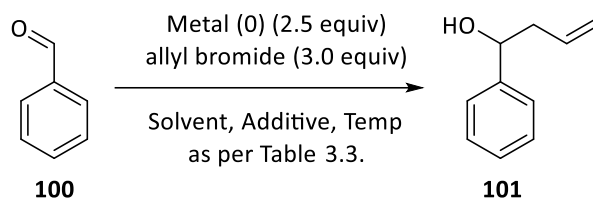


Entry	Metal	Solvent	Temperature ( °C)	Additive (mol %)	Time (hours)
1	Sn	THF	22 → 66	-	48
2	Sn	THF	22 → 66	HCl	48
3	Sn	H <sub>2</sub> O / THF <sup>b</sup>	22	NH <sub>4</sub> Cl (100)	72 <sup>c</sup>
4	Sn	H <sub>2</sub> O / THF <sup>b</sup>	22	HCl (50)	48
5	Sn	H <sub>2</sub> O	22	SDS (125)	47
6	Zn	THF	22 → 66	-	72 <sup>c</sup>
7	Zn	H <sub>2</sub> O / THF <sup>b</sup>	22	NH <sub>4</sub> Cl (100)	48
8	ZnCl <sub>2</sub>	THF	22 → 66	-	72 <sup>c</sup>
9	Zn[Cu]	THF	22 → 66	-	72 <sup>c</sup>
10	ZnCl <sub>2</sub> / CuCl	THF	22 → 66	-	72 <sup>c</sup>
11	ZnCl <sub>2</sub> / CuCl	H <sub>2</sub> O	22	SDS (125)	48
12	In	H <sub>2</sub> O / THF <sup>b</sup>	22	-	48
13	In	H <sub>2</sub> O	22	SDS (125)	48
14	InCl <sub>3</sub>	THF	22 → 66	-	72 <sup>c</sup>
15	In(OTf) <sub>3</sub>	H <sub>2</sub> O / THF <sup>b</sup>	22	-	48
16	In	H <sub>2</sub> O / THF <sup>b</sup>	22	HCl (10)	48
17	In	H <sub>2</sub> O / THF <sup>b</sup>	22	HBr (10)	48
18	Sm	THF	22 → 66	-	72 <sup>c</sup>
19	Sm	THF	22 → 66	NaI (10)	72 <sup>c</sup>
20	Sm	H <sub>2</sub> O	22	-	48

a: Test reactions run on 0.5 mmol of **78** at a 0.1 M concentration in the presence of 2.0 equivalents of allyl bromide. b: a 1:3 ratio of H<sub>2</sub>O:THF was used c: Reactions stirred at 22 °C for 24 hours and then heated to 66 °C for 48 hours.

Given that the starting material was nearly quantitatively recovered from the reaction mixtures in all cases even after prolonged heating it is unlikely metal insertion into the carbon-iodide bond was occurring. Test reactions using simple alkyl halides and aldehyde **100** confirmed that the metals being used were competent in a Barbier reaction giving compound

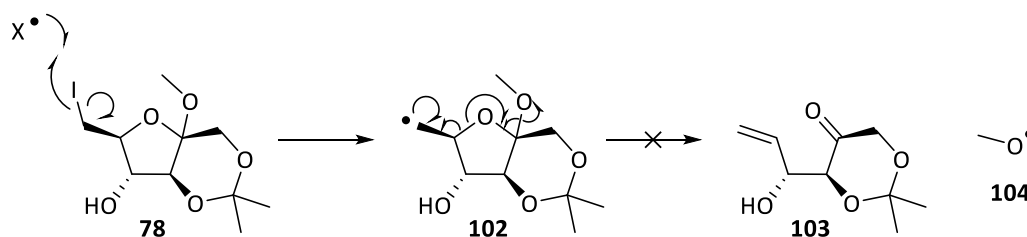
**101** (Scheme 3.5).. At this point it became apparent that **78** would not be a competent substrate for this reaction



**Scheme 3.5:** Test reactions using benzaldehyde and allyl bromide were carried out using each of the conditions listed in Table 3.3 All reaction gave the desired product **101** as determined by crude  $^1\text{H-NMR}$ .

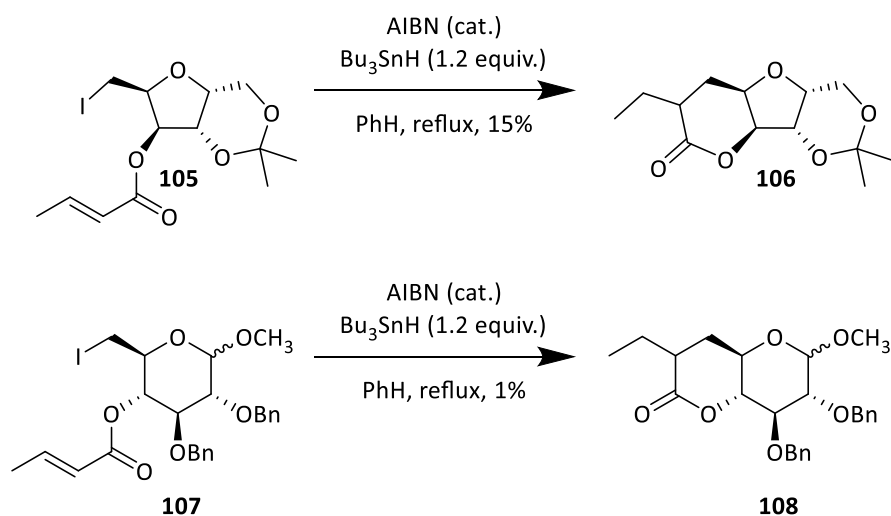
### 3.5: Attempts to Create a New C-C Bond at C6 of D-Fructose via a Radical Cyclization Reaction

With the only successful transformation on **78** found to be the removal of the iodide to produce the elimination product **84** we theorized that a radical based reaction would be more amenable to getting the desired product. The generation of the elimination product **103** from radical species **102** similar to those observed in the magnesium and lithium mediated reaction described earlier would require the ejection of methoxyl radical **104** (Scheme 3.6). This process is unlikely as the formation of methoxyl is typically only observed under highly specific conditions in the gas phase or when it is made from a peroxy starting material.<sup>51-56</sup>



**Scheme 3.6:** Mechanism of the release of methoxyl radical **103** arising from iodine radical abstraction from the C6 position of **78**.

The work of Alves and co-workers has shown that C6 iodides such as **105** or **107** derived from xylose or glucose could be cyclized to generate the fused tricyclic structures **106** and **108** through the use of a radical mediated reaction (Scheme 3.7).<sup>57</sup> In their work the authors used this reaction to study the ring closing reaction in both regio- and stereochemical aspects. They found that the cis ring fusion of their D-xylose derivative and the trans fusion of their D-glucose derivative could be formed, though the yield was lower in the case of the trans ring fusion in their D-glucose derivative.<sup>57,58</sup> We envisioned that these cyclized intermediates could be further derivatized to give the fluorophore-tagged sugar derivatives.

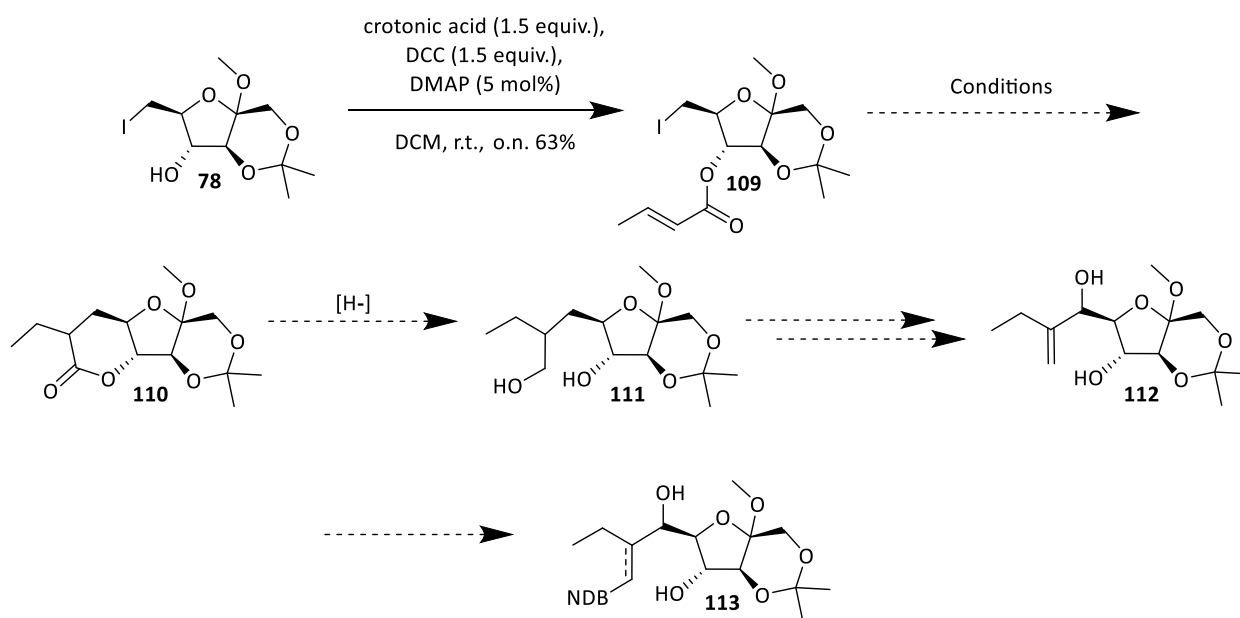


**Scheme 3.7: Production of cyclized intermediates via a radical cyclization derived from D-xylose or D-glucose as prepared by Alves and co-workers.<sup>57</sup>**

From the cyclized intermediate **109**, generated from **108** via radical cyclization, reduction would yield the diol **110** which could be selectively protected. Elimination of hydroxyl group on the pendent chain would give alkene **111** which could be allylically

oxidized to give diol **112**. The alkene could then be used as a synthetic handle to which the NBD moiety could be appended (Scheme 3.8).

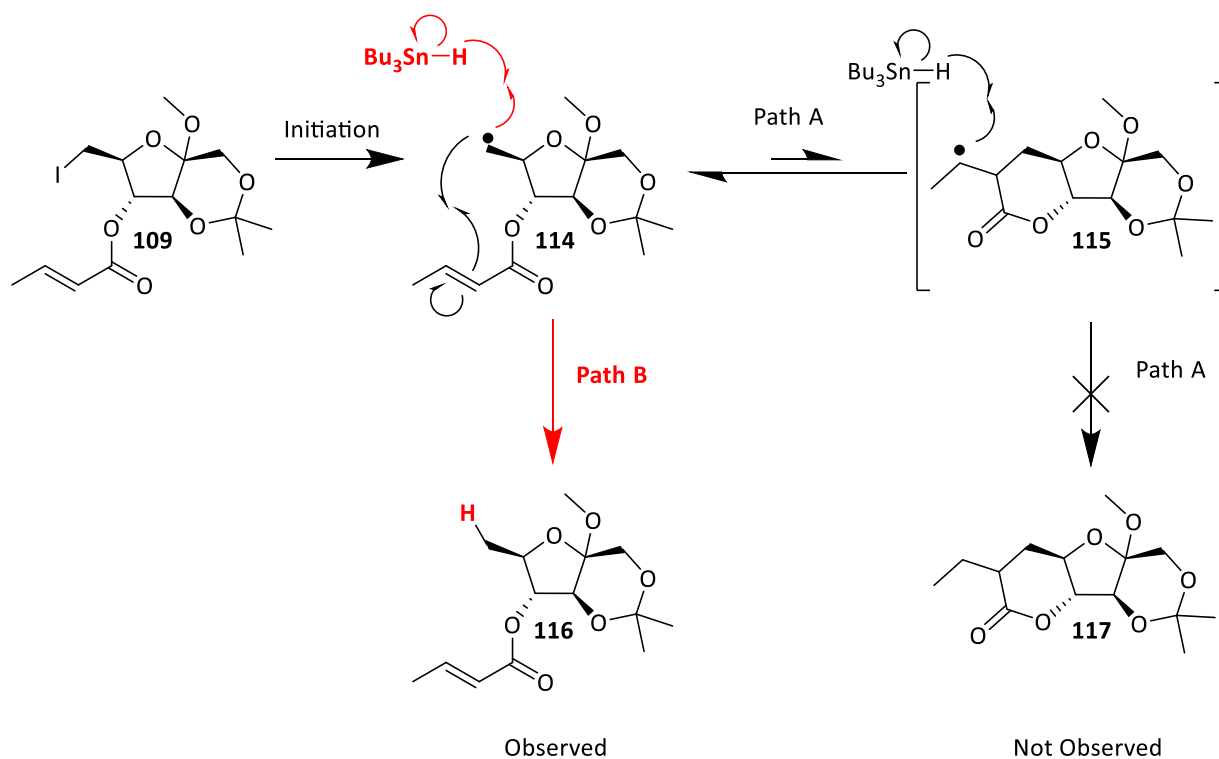
. This route would produce a branch point along the linker chain between the D-fructose core and the dye moiety which was not thought to be optimal for transport through the GLUT5 pore. It could however be a potential substrate as the two carbon branch is relatively small compared to the large NBD dye which is known to be transported. The two-carbon branch could also act as the first in a family of compounds with branched linker chains which could be used to investigate the steric tolerance of the GLUT5 pore. Alves and co-workers have already published on the radical cyclization onto the cinnamic acid derivative analogous to **78** which, if carried through the proposed synthetic scheme, would have a phenyl ring terminating the branch of the linker chain.<sup>57-59</sup>



**Scheme 3.8: Proposed route from 78 to 113 via a radical cyclization and reductive ring opening to afford the desired C-C bond formation from C6 to the  $\beta$ -carbon on crotonic acid.**

Following similar procedures to those used by Alves and co-workers, crotyl ester-fructose derivative **109** was constructed via Steglich esterification of **78** with crotonic acid and EDCI (Scheme 3.8).<sup>57,60</sup> Formation of trans-fused 6,5 ring systems from a radical cyclization are preceded in the literature including those arriving from an ester, regardless of the unfavorable geometry of the cyclization.<sup>57-59,61-66</sup>

The radical cyclization was attempted under several different conditions known to initiate radical chain reactions, including those which Alves and co-workers used on their D-xylose derivative (Scheme 3.7).<sup>59</sup> Under no conditions was any amount of cyclization product detected by TLC or crude <sup>1</sup>H-NMR. Reduction of iodo-fructose **109** to protected deoxyfructose **116** was the major product in all cases and often in near quantitative yield. It is likely that the barrier to form the trans-6-5 ring system **115** is too great and the reaction of the radical **114** is dominant (Path B Scheme 3.9). If the ring closing event to form **115** were occurring it would be a reversible process. Compound **115**, if formed in any amount, appears to be too short-lived to reaction with Bu<sub>3</sub>SnH to produce the desired **117** (Path A Scheme 3.9).



**Scheme 3.9: Proposed mechanism of the radical reduction of 109 which prevents the capture of cyclized product 117 because of the low stability or short lifetime of radical intermediate 115.**

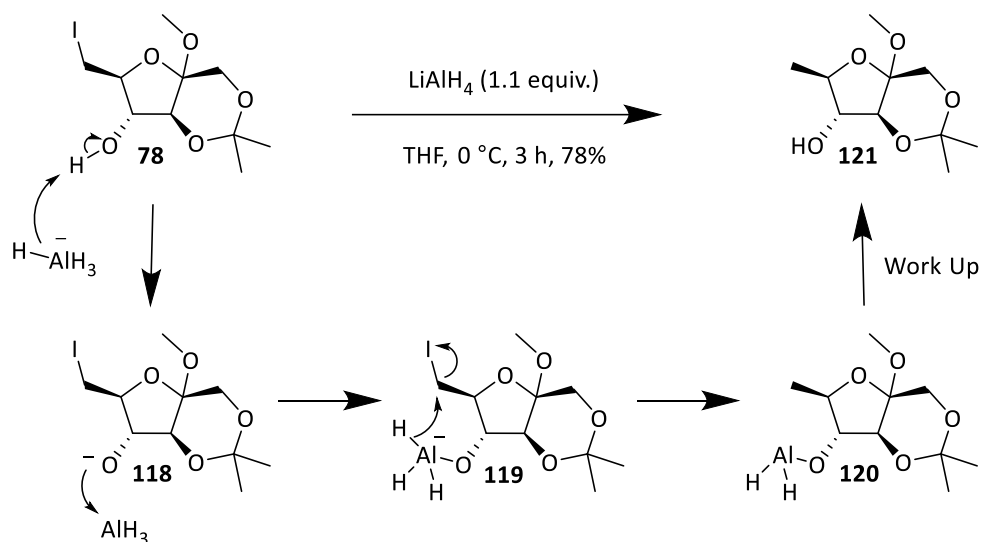
In all attempts the only observed product resulted from hydrogen atom abstraction from  $\text{Bu}_3\text{SnH}$  by the C6 radical to give **115** (Path B in Scheme 3.9). In a series of five reactions the concentration of the reaction was diluted sequentially from 0.01 M to 0.001 M and rate of addition was halved in all of these reactions. The purpose of these reactions was to allow sufficient time for the cyclization to occur before the radical chain was quenched by  $\text{Bu}_3\text{SnH}$ . In a separate series of five reactions the concentration was increased to 0.1 M and the rate of addition was doubled in hopes of intercepting the cyclized product in the brief period it existed. In all cases more than 90 % of starting material was consumed and 95 % of the mass balance could be accounted for. Unfortunately no signals that could be attributed to the cyclized product were observed in the crude  $^1\text{H-NMR}$  spectrum.

### 3.6 Reduction of the C6 Iodide Via Nucleophilic Hydride or Radical Mediated Reactions

The reduced hexoses **90** or **116**, as produced from lithium halogen exchange or from radical reduction, are protected derivatives of 6-deoxy-D-fructose, a known natural product.<sup>67</sup> This product has been reported to be formed through the use of enzymatically catalysed reactions in the past.<sup>31,68-70</sup> Published synthetic routes to 6-deoxy-D-fructose are lengthy and require the use of enzyme catalyzed steps to control the regiochemistry and absolute stereochemistry of the product.

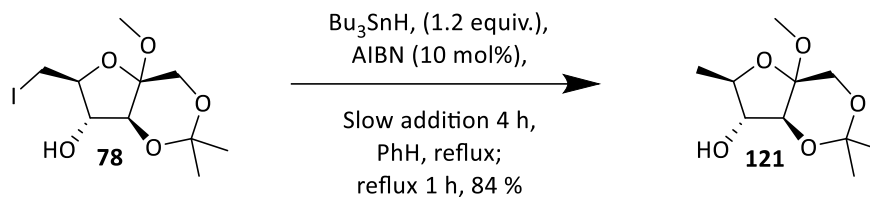
6-Deoxy-D-fructose has been used as an intermediate to Furaneol (4-hydroxy-2,5-dimethyl-3-furanone) and related analogues which are used as flavouring agents.<sup>31</sup> Considering the time and expense devoted to synthesizing deoxyfructose previously, we went about optimizing our proposed short synthesis. Optimization of the route from D-fructose to 6-deoxy-D-fructose was performed. The steps to make the key alkyl iodide **78** had previously been optimized therefore we went about further investigating the dehalogenation and deprotection to give 6-deoxy-D-fructose.

Iodide **78** was reacted with LiAlH<sub>4</sub> in THF which produced **121** in good yield quite rapidly (Scheme 3.10). Presumably the first step of this reaction is deprotonation of the C4 hydroxyl to give **118** which would complex to [AlH<sub>3</sub>] to form species **119**. From this point internal delivery of hydride in a S<sub>N</sub>2 fashion to the C6 position would produce **120** which formed **121** after acidic aqueous workup.



**Scheme 3.10: Reduction of 78 to 121 via lithium aluminum hydride.**

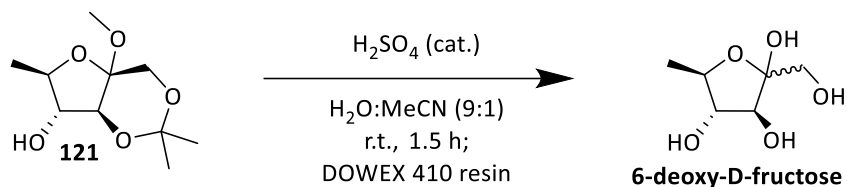
As discussed previously, crotyl ester **109** was efficiently dehalogenated using the  $\text{Bu}_3\text{SnH/AIBN}$  reduction system to give protected deoxyfructose **116** in good yield. We hypothesized that the non-crotylated compound **78** could undergo the same process under the same conditions (Scheme 3.11).<sup>71</sup> Isolation of **121** from the reaction mixture was more operationally complex due to the need to remove the alkyl tin by-products but the overall yield of this route was superior to that of the  $\text{LiAlH}_4$  route. Both reactions proved to be scalable though each had significant drawbacks. Large-scale radical reduction worked well; however, the large amount of tin waste and greater quantities of the sensitive AIBN were problematic. The  $\text{LiAlH}_4$  route could also be performed on larger scale without a detrimental effect to the yield although the addition of  $\text{LiAlH}_4$  had to be done portion-wise and carefully to prevent thermal runaway and boiling over due to the large amounts of hydrogen gas produced.



**Scheme 3.11: Reduction of 78 to 121 via the radical reduction utilizing  $\text{Bu}_3\text{SnH}$  and AIBN.**

Deprotection of **121** proved to be a non-trivial task and extensive screening of conditions was performed. Eventually the use of a small amount of sulfuric acid in a 9:1 mixture of water and acetonitrile proved to efficiently and completely remove the protecting groups from **121** (Scheme 3.12). Isolation of 6-deoxy-D-fructose required the use of an anion exchange resin to remove the large amounts of sulfuric acid from the reaction mixture DOWEX 410, a quaternary ammonium resin which has a chloride counter ion in its commercially available form was pre-washed with KOH solution to exchange the chloride for a hydroxide ion. This procedure allowed for the sulfuric acid in the reaction mixture to be quenched and for small amounts of 6-deoxy-D-fructose to be isolated in a state suitable for characterization. Extraction of the water soluble sugar derivative **120** was fruitless and no suitable crystallization technique could be found to separate **120** from 6-deoxy-D-fructose. Passage through the ion exchange resin and evaporation from the water/acetonitrile mixture proved to be the most efficient way to isolate 6-deoxy-D-fructose. Due to the high expense of DOWEX 410 resin this deprotection was not carried out on large scale. It was found that as the scale of the reaction increased a greater amount of resin was required to remove all of the sulfuric acid from the reaction mixture. Refreshing the resin by washing with a 1 M solution of KOH allowed for the resin to be reused six times before signs of resin decomposition were

observed to be washed into the product. These impurities could not be removed from the highly water soluble **121** through any methodology attempted.



**Scheme 3.12: Deprotection of 121 to give 6-deoxy-D-fructose.**

The developed methodology to produce 6-deoxy-D-fructose from D-fructose via iodo fructose derivative **78**, stands as the shortest route to 6-deoxy-D-fructose and is the only route known that does not utilize an enzymatic processes in any way.

6-Deoxy-D-fructose exists in solution as an equilibrating mixture of the  $\alpha$  and  $\beta$  anomers as well as in the open-chain form. As observed by Fessner and co-workers, and described in their publication, the  $\beta$  anomer is the predominant form in solution over the open chain and the  $\alpha$  anomer, though all are detectable.<sup>68</sup> This mixture makes analysis of the <sup>1</sup>H-NMR spectrum difficult; however, there is a diagnostic methyl doublet signal, indicative of the deoxygenated C6 position. This characteristic peak allows for rapid identification of the deoxygenated compound and discrimination from the C6 iodide or the C6 hydroxyl compounds. In contrast to the 6-NBD labelled hexoses or several other related compounds reviewed in Chapter 1, 6-deoxy-D-fructose is not locked in a furanose or pyranose conformation. Those compounds are locked in one ring conformation allowing for more straightforward analysis of the <sup>1</sup>H NMR spectrum.

The constant flux between conformations as observed with 6-deoxy-D-fructose would lead to complex results if this compound were to be used in an inhibition study for hexose

transport via a GLUT transporter. The concentration of 6-deoxy-D-fructose added to the solution would not be directly proportional to the amount of  $\alpha$  or  $\beta$  anomer that actually encountered the GLUT binding site. Further, the relative ratio of  $\alpha$ ,  $\beta$  or open chain 6-deoxy-D-fructose would be different than observed in an  $^1\text{H-NMR}$  study as the complex mixture of salts and biomolecules in the cell medium would alter the ratio of these three conformations. A comparison of the GLUT binding characteristics of 6-deoxy-D-fructose to any of the known fluorescently labelled D-fructose analogs would not give correlatable results as these compounds are locked in one ring conformation. As noted by Holman and co-workers, discussed in Chapter 1, the different anomers of simple hexoses have different binding affinities for the GLUT transporters.<sup>72,73</sup> For these reasons the interaction of 6-deoxy-D-fructose was not screened as an inhibitor for GLUT transporter function. In the future this evaluation could be carried out to evaluate the ability of 6-deoxy-D-fructose to inhibit the uptake of a fluorescently labelled hexose mimic once a rapid and repeatable test for these interactions can be established.

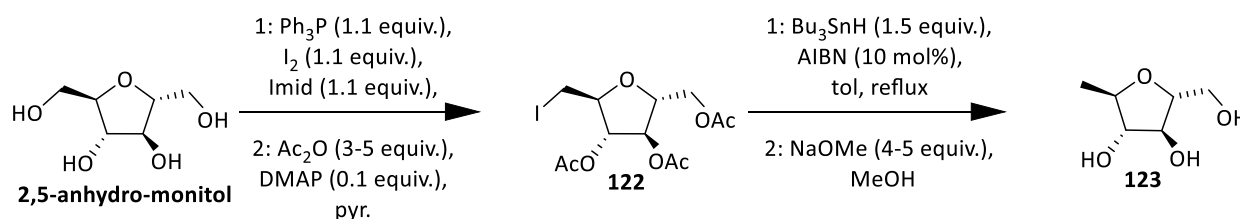
### 3.7: Summary

Despite a thorough survey of conditions for metal-halogen exchange, a useable organometallic derivative of 6-iodo-D-fructose was not realized. The alkyl-metal species that were investigated only led to unimolecular decomposition, too quickly to observe any nucleophilic behavior of the carbanion. The products **84** and 6-deoxy-D-fructose have previously been reported and only 6-deoxy-D-fructose has commercial value. This compound could be used as an intermediate towards further GLUT probes or inhibitors to help gain further knowledge about the function of these transporters. The synthesis of 6-deoxy-D-

fructose reported here is the shortest synthetic route known to date and could be adopted for commercial use at a later date should the need arise.

### 3.8: Future Directions:

The success found with the synthesis of 6-deoxy-D-fructose lends itself to the idea that a similar compound, locked in the furanose ring form, could be produced. A derivative of 2,5-anhydromanitol would be an excellent candidate for this research as it is a known substrate of GLUT5.<sup>74</sup> As shown in Scheme 3.13 an analogous route as was used to produce 6-deoxy-6-D-fructose could be applied to the synthesis of **123**.



Scheme 3.13: Route from 2,5-anhydro-manitol to the deoxygenated derivative **123**

Standard Appel reaction conditions would afford the primary iodide which could be globally acetylated to aid in the purification of **122**. This intermediate could then be reduced using AIBN and Bu<sub>3</sub>SnH which, after deprotection would give the desired product **123**. Compound **123** could then be tested for its ability to be recognized and/or transported by GLUT5.

### 3.9: Experimental:

All reactions were carried out in oven-dried glassware sealed with a rubber septa and vented to room air unless otherwise stated. Transfer of anhydrous solvents and reagents was

accomplished with oven-dried syringes or via cannula transfer. The following solvents when used in reactions were purified using a solvent purification system manufactured by LC Technology Solutions Inc. and operated according to the manufactures specifications before use: dichloromethane (DCM), diethyl ether (Et<sub>2</sub>O), tetrahydrofuran (THF), acetonitrile (MeCN). Toluene (PhMe) was distilled before use from sodium metal under a positive nitrogen atmosphere. Pyridine was dried over solid KOH for a minimum of 24 hours before use. All other commercially available solvents and reagents were used without additional purification and were purchased from the Sigma-Aldrich company. Thin layer chromatography was carried out on glass plates coated with 0.25 mm silica gel produced by the SiliCycle Company. Visualization of spots on the TLC plates was achieved via UV light or treatment with 2.5% *p*-anisaldehyde in AcOH: H<sub>2</sub>SO<sub>4</sub>: EtOH in a 1:3:38 ratio and heated to give colour development. Flash chromatography columns were packed with 230-400 mesh silica gel produced by the Silicycle Company with the specified solvent system. Proton nuclear magnetic resonance spectra (<sup>1</sup>H-NMR) were recorded at 400 MHz or 500 MHz in the indicated solvents. Chemical shifts were reported in ppm using the solvent peak as the internal standard. The reported coupling constants were reported in hertz (Hz) and standard notation was used to describe the multiplicity of each of the signals observed: singlet (s), doublet (d), triplet (t), broad (br), multiplet (m), etc. Carbon nuclear magnetic resonance spectra (<sup>13</sup>C-NMR) were recorded at 100 MHz or 125 MHz in the indicated solvents. The solvent peaks were reported in ppm and the solvent peaks were used as the internal standard. Infrared spectra (IR) were measured with a Nic-Plan FTIR Microscope instrument. IR spectra were reported in cm<sup>-1</sup> from neat samples as recorded using a Mattson Galaxy Series FT-IR 3000 spectrometer. Mass spectra were determined on a Kratos MS50 high-resolution

electrospray instrument recording in positive ion mode. Optical rotations were recorded on a Perkin Elmer 241 Polarimeter using the D line of sodium (589 nm).

### **Synthesis of methyl 1,3,-*O*-isopropylidene-4-*O*-benzyl 6-deoxy-6-iodo-D-fructofuranoside (83)**

To a solution of **78** (0.458 g, 1.33 mmol) in THF (15 mL) was added benzyl bromide (0.296 g, 1.73 mmol) and sodium hydride (0.069 g, 60% dispersed in mineral oil, 1.73 mmol) in a single portion. The reaction mixture was stirred at room temperature overnight before water (10 mL) was added. The reaction mixture was extracted with DCM (3 x 10 mL) and the organic portions were combined, washed with brine (10 mL), and dried over MgSO<sub>4</sub> before the solvent was removed under reduced pressure. The crude yellow oil was purified through a silica gel column using 40% EtOAc:Hex to afford a pale yellow oil (0.364 g, 0.84 mmol, 63%) Rf 0.68 (40% EtOAc:Hex). <sup>1</sup>H-NMR, and <sup>13</sup>C-NMR were consistent with those published by Ye and co-workers.<sup>75</sup>

### **Typical procedure for Grignard reagent preparation:**

Magnesium turnings (0.102 g, 4.23 mmol) which had been dried for at least 24 h in a glassware oven were added to a flask containing THF (15 mL) and a stir bar under a positive nitrogen pressure and the flask was cooled to the specified temperature (See Table 3.1). Separately a solution of **83** (0.182 g, 0.529 mmol) in THF (1 mL) and a solution of 1,2-dibromoethane (0.099 g, 0.530 mmol) in THF (1 mL) were loaded into 1 mL plastic syringes in a double barrel syringe pump. The solutions of **83** and 1,2-dibromoethane were co-added over 60 min to the flask containing magnesium metal. After the addition was complete the solution was stirred for 60 min before being transferred by cannula to a fresh flask under a positive nitrogen pressure held at the required temperature. To this solution was added either water (0.08 mL, 4.37 mmol) in THF (3 mL)) or benzaldehyde (0.461 g, 4.36 mmol in THF (3

mL)) in a single portion and allowed to stir for 15 min. The reaction was diluted with water (20 mL) and extracted with DCM (3 x 10 mL) and the organic fractions were combined, washed with brine (10 mL), and dried over MgSO<sub>4</sub> before the solvent was removed under reduced pressure. Crude <sup>1</sup>H-NMR and TLC of the resulting residue was performed to determine reaction success.

**Synthesis of (1'R, 4S)-2,2-dimethyl-4-(1'-benzyloxyallyl)-1,3-dioxan-5-one (84):**

Compound **83** (0.207g, 0.612 mmol) was subjected to the general procedure for Grignard reagent procedures in THF at 22 °C and quenched with water. After workup a clear oil was purified through a silica gel column using 25 % EtOAc:Hex to afford a clear oil (0.077 g, 0.41 mmol 37%). R<sub>f</sub> 0.21 (25% EtOAc:Hex) <sup>1</sup>H-NMR, <sup>13</sup>C-NMR, and HRMS were consistent with the data published by Madsen and co-workers.<sup>8</sup>

**General procedure for lithium halogen exchange reactions:**

To a solution of **83** (0.174 g, 0.506 mmol) in THF (15 mL) held at the indicated temperature was added the alkyl lithium (solution in hexane, titrated before use, 1 or 2.5 mmol) which were allowed to stir for 15 minutes before being quenched with either water (0.045 mL, 2.5 mmol in THF (3 mL) or benzaldehyde (0.265 g, 2.5 mmol in THF (3 mL)). In cases when the quench was performed at a different temperature than the initial addition of alkyl lithium the flask was moved from the first cooling bath to the second after stirring for 15 min at the initial temperature. The solution was then stirred at the second temperature for 15 min before the reaction was quenched. The reaction mixture was then warmed to room temperature before being diluted with water (10 mL) and extracted with DCM (3 x 15 mL), the organic fractions

were combined, washed with brine (10 mL) and dried over MgSO<sub>4</sub> before the solvent was removed under reduced vacuum.

#### **General procedure for Barbier reactions:**

To a flask containing compound **78** (0.173 g, 0.501 mmol) dissolved in the indicated solvent (5 mL) at room temperature was added allyl bromide (0.061 g, 1.0 mmol) and the indicated metal (1.5 mmol), and additive (see Table 3.3 for stoichiometry). The reaction was stirred at room temperature for 24 h and followed by TLC. Some reactions were then heated to reflux for a further 24 h as indicated in Table 3.3. Workup of reactions was performed by diluting the reaction mixture with water (10 mL) and extracting with DCM (3 x 15 mL). The organic fractions were combined and washed with brine (10 mL) before being dried over MgSO<sub>4</sub> and the solvent was removed under reduced pressure. <sup>1</sup>H-NMR and TLC were performed on the resulting residue to determine reaction outcome.

#### **Synthesis of methyl 1,3-*O*-isopropylidene-4-*O*-crotonyl-6-deoxy-6-iodo- $\alpha$ -D-fructofuranoside (**109**):**

To a solution of **78** (0.388 g, 1.13 mmol) in DCM (45 mL) at room temperature was added DMAP (0.014 g, 0.11 mmol), DCC (0.291 g, 1.41 mmol), and crotonic acid (0.980 g, 1.14 mmol) which was stirred for 24 h before being diluted with water (25 mL). The reaction mixture was extracted with DCM (3 x 15 mL) and the organic fractions were combined, washed with brine (10 mL) and dried over MgSO<sub>4</sub> before the solvent was removed under reduced pressure. The resulting residue was purified through a silica gel column using 20 % EtOAc:Hex affording a clear oil (0.073 g, 0.178 mmol, 63%). R<sub>f</sub> 0.72 (35% EtOAc:Hex); [ $\alpha$ ]<sub>D</sub><sup>20</sup> +23.06 (*c* 1.20, DCM); IR: 2990, 2940, 2834, 1724, 1655, 1525, 1444, 1414, 1373,

1316, 1294, 1264, 1222, 1175, 1151, 1105, 1082, 1054, 1028, 970, 941, 894, 857, 766, 705, 689; HRMS Expected: 412.22 Observed M+Na 435.03; <sup>1</sup>H NMR (400 MHz, CDCl<sub>3</sub>) δ 7.02 (dq, *J* = 15.6, 6.9 Hz, 1H), 5.88 (dq, *J* = 15.5, 1.7 Hz, 1H), 4.89 (dd, *J* = 4.1, 0.9 Hz, 1H), 4.15 – 4.06 (m, 2H), 3.98 – 3.79 (m, 2H), 3.56 – 3.39 (m, 2H), 3.29 (s, 3H), 1.89 (dd, *J* = 6.9, 1.8 Hz, 3H), 1.41 (d, *J* = 0.7 Hz, 3H), 1.38 (d, *J* = 0.7 Hz, 3H); <sup>13</sup>C NMR (126 MHz, CDCl<sub>3</sub>) δ 171.67, 147.41, 122.20, 121.90, 102.50, 98.75, 87.66, 80.22, 79.60, 77.29, 77.04, 76.79, 61.89, 48.85, 27.81, 19.45, 18.12, 5.36.

#### **General procedure for radical ring closing reactions:**

To a refluxing solution of **109** (0.119 g, 0.289 mmol) in benzene (40 mL) under a positive nitrogen atmosphere was added AIBN (0.005 g, 0.03 mmol in benzene (1 mL)) and Bu<sub>3</sub>SnH (0.066 g, 0.29 mmol in benzene (1 mL)) via two barrel syringe pump over 3 h. Once addition had been completed the reaction was allowed to stir at reflux for an additional 1 h before being cooled to room temperature. The solvent was removed under reduced pressure through rotary evaporation inside a fume hood and the resulting residue was dissolved in MeCN (20 mL) and washed with hexane (4 x 15 mL) before the MeCN layer was dried over MgSO<sub>4</sub> and the solvent being removed under reduced pressure. The resulting residue was analysed by TLC and <sup>1</sup>H-NMR to determine reaction outcome. NOTE: The hexane fractions were combined and disposed as per University of Alberta standards for alkyl tin containing waste.

#### **Synthesis of methyl 1,3-O-isopropylidene-6-deoxy- $\alpha$ -D-fructofuranoside (121):**

##### **Via radical reduction:**

A solution of compound **78** (0.128 g, 0.37 mmol) in benzene (20 mL) was heated to reflux under a positive nitrogen atmosphere AIBN (0.006 g, 0.04 mmol in benzene (1 mL)) and

Bu<sub>3</sub>SnH (0.085 g, 0.37 mmol in benzene 1 mL)) were added via a two barrel syringe pump over 3 h. Once addition had been completed the reaction was allowed to stir at reflux for an additional 1 h before being cooled to room temperature. The solvent was removed under reduced pressure through rotary evaporation inside a fume hood and the resulting residue was dissolved in MeCN (15 mL) and washed with hexane (4 x 15 mL) before the MeCN layer was dried over MgSO<sub>4</sub> and the solvent being removed under reduced pressure. The resulting residue was purified through a silica gel column using 20% EtOAc:Hex affording a clear oil (0.067 g, 0.31 mmol, 84%) NOTE: The hexane fractions were combined and disposed as per University of Alberta standards for alkyl tin containing waste.

#### **Via LiAlH<sub>4</sub> reduction:**

To a solution of **78** (0.135 g, 0.39 mmol) in THF at 0 °C was added LiAlH<sub>4</sub> (0.007 g, 0.39 mmol) in 2 portions over 20 min. The reaction was allowed to stir at 0 °C for 3 h before water (15 mL) and HCl (10 mL, 10% w/v) were sequentially added in a drop wise fashion. The reaction mixture was concentrated under reduced pressure and diluted with water (10 mL) before being extracted with DCM (3 x 15 mL). The organic fractions were combined, washed with brine (10 mL) and dried over MgSO<sub>4</sub> before the solvent was removed under reduced pressure. The resulting residue was purified through a silica gel column using 20% EtOAc:Hex to afford a clear oil (0.066 g, 0.30 mmol, 78%). R<sub>f</sub> 0.43 (50% EtOAc:Hex); [ $\alpha$ ]<sub>D</sub><sup>20</sup> +20.74 (c 2.36, MeOH); IR: 3459, 1987, 2834, 1455, 1376, 1326, 1294, 1265, 1221, 1169, 1150, 1105, 1088, 1050, 1027, 989, 955, 929, 896, 878, 853, 761, 721; HRMS: Expected 218.25 Observed M+Na 241.10; <sup>1</sup>H NMR (498 MHz, CDCl<sub>3</sub>)  $\delta$  4.13 (qd, J = 6.5, 2.7 Hz, 1H), 4.02 (d, J = 1.0 Hz, 1H), 3.93 (s, 2H), 3.78 – 3.71 (m, 1H), 3.31 (s, 3H), 2.52 (d, J = 10.5

Hz, 1H), 1.50 – 1.45 (m, 3H), 1.42 (d, J = 6.6 Hz, 3H), 1.41 (q, J = 0.7 Hz, 3H); <sup>13</sup>C NMR (126 MHz, D<sub>2</sub>O) δ 102.77, 101.14, 82.37, 82.19, 81.89, 62.43, 49.17, 27.28, 20.52, 19.13.

### Synthesis of 6-deoxy-D-fructose

5 drops of concentrated H<sub>2</sub>SO<sub>4</sub> were added to a solution of **121** (0.087 g, 0.40 mmol) in water:MeCN (9:1, 3 mL) at room temperature and stirred for 1.5 h. The reaction mixture was directly applied to a column of DOWEX 410 ion exchange resin (3 cm diameter, 7 cm tall which had been pre-washed with an aqueous KOH solution (10% w/v)) and then washed with water (3x 25 mL). The column was washed repeatedly with water and the collected solution was concentrated to dryness under reduced pressure. This afforded a clear oil which partially solidified upon prolonged standing in an open vessel (0.017 g, 0.11 mmol). <sup>1</sup>H-NMR, <sup>13</sup>C-NMR, and HRMS of this oil was consistent with the published data of Fessner of co-workers.<sup>68</sup>

### 3.10: References:

- (1) Harutyunyan, S. R.; López, F.; Browne, W. R.; Correa, A.; Peña, D.; Badorrey, R.; Meetsma, A.; Minnaard, A. J.; Feringa, B. L. *J. Am. Chem. Soc.* **2006**, *128* (28), 9103–9118.
- (2) Normant, J. F. *Synthesis* **1972**, *1972* (2), 63–80.
- (3) Lai, Y.-H. *Synthesis* **1981**, *1981* (8), 585–604.
- (4) Grignard, V. *Compt Rend* **1900**, *130*, 1322.
- (5) Gilman, H.; Jones, R. G.; Woods, L. A. *J. Org. Chem.* **1952**, *17* (12), 1630–1634.
- (6) Barbier, P. *Compt Rend* **1899**, *128*, 110.
- (7) Wu, G.; Huang, M. *Chem. Rev.* **2006**, *106* (7), 2596–2616.
- (8) Lauritsen, A.; Madsen, R. *Org. Biomol. Chem.* **2006**, *4* (15), 2898.
- (9) White, J. D.; Hrnčiar, P. *J. Org. Chem.* **2000**, *65* (26), 9129–9142.
- (10) Bailey, W. F.; Patricia, J. J.; Nurmi, T. T.; Wang, W. *Tetrahedron Lett.* **1986**, *27* (17), 1861–1864.
- (11) Rogers, H. R.; Houk, J. *J. Am. Chem. Soc.* **1982**, *104* (2), 522–525.

- (12) Farnham, W. B.; Calabrese, J. C. *J. Am. Chem. Soc.* **1986**, *108* (9), 2449–2451.
- (13) Bailey, W. F.; Patricia, J. J. *J. Organomet. Chem.* **1988**, *352* (1), 1–46.
- (14) Ovaska, T. V.; Snieckus, V.; Nolte, B. In *Encyclopedia of Reagents for Organic Synthesis*; John Wiley & Sons, Ltd, 2001.
- (15) Bailey, W. F.; Wachter-Jurcsak, N. In *Encyclopedia of Reagents for Organic Synthesis*; John Wiley & Sons, Ltd, 2001.
- (16) Aidhen, I. S.; Ahuja, J. R. *Tetrahedron Lett.* **1992**, *33* (37), 5431–5432.
- (17) Guimarães, R. L.; Lima, D. J.; Barros, M. E. S.; Cavalcanti, L. N.; Hallwass, F.; Navarro, M.; Bieber, L. W.; Malvestiti, I. *Molecules* **2007**, *12* (9), 2089–2105.
- (18) Majumdar, K. K. *Tetrahedron Asymmetry* **1997**, *8* (13), 2079–2082.
- (19) Costello, D. P.; Geraghty, N. W. A. *Synth. Commun.* **1999**, *29* (18), 3083–3096.
- (20) Tuanjie, M.; Xianqiang, H.; Jin-Xian, W.; Li, X. *Chin. J. Org. Chem.* **2014**, *35* (3), 712–718.
- (21) Jögi, A.; Mäeorg, U. *Molecules* **2001**, *6* (12), 964–968.
- (22) Breton, G. W.; Shugart, J. H.; Hughey, C. A.; Conrad, B. P.; Perala, S. M. *Molecules* **2001**, *6* (8), 655–662.
- (23) Basu, M. K.; Banik, B. K. *Tetrahedron Lett.* **2001**, *42* (2), 187–189.
- (24) Curran, D. P.; Xin, G.; Zhang, W.; Dowd, P. *Tetrahedron* **1997**, *53* (27), 9023–9042.
- (25) Haddad, T. D.; Hirayama, L. C.; Singaram, B. *J. Org. Chem.* **2010**, *75* (3), 642–649.
- (26) Wang, Z. In *Comprehensive Organic Name Reactions and Reagents*; John Wiley & Sons, Inc., 2010.
- (27) Blomberg, P. D. C. In *The Barbier Reaction and Related One-Step Processes; Reactivity and Structure: Concepts in Organic Chemistry*; Springer Berlin Heidelberg, 1993; pp 137–165.
- (28) Moyano, A.; Perica's, M. A.; Riera, A.; Luche, J.-L. *Tetrahedron Lett.* **1990**, *31* (52), 7619–7622.
- (29) Chérest, M.; Felkin, H. *Tetrahedron Lett.* **1968**, *9* (18), 2205–2208.
- (30) Keinicke, L.; Fristrup, P.; Norrby, P.-O.; Madsen, R. *J. Am. Chem. Soc.* **2005**, *127* (45), 15756–15761.
- (31) Wong, C. H.; Mazonod, F. P.; Whitesides, G. M. *J. Org. Chem.* **1983**, *48* (20), 3493–3497.
- (32) Partibha Choudhary; , Varun Sharma; , Hari Om; , Poonam Devi. *Am. J. Chem.* **2013**, *3* (5), 115–125.
- (33) Wu, S.; Li, Y.; Zhang, S. *J. Org. Chem.* **2016**, *81* (17), 8070–8076.
- (34) Takahashi, K.; Komine, K.; Yokoi, Y.; Ishihara, J.; Hatakeyama, S. *J. Org. Chem.* **2012**, *77* (17), 7364–7370.
- (35) Wilson, S. R.; Guazzaroni, M. E. *J. Org. Chem.* **1989**, *54* (13), 3087–3091.
- (36) Li, C. *J. Chem. Rev.* **1993**, *93* (6), 2023–2035.
- (37) Kobayashi, S. *Chem. Commun.* **1998**, No. 1, 19–20.
- (38) Kobayashi, S.; Wakabayashi, T.; Oyamada, H. *Chem. Lett.* **1997**, *26* (8), 831–832.
- (39) Manabe, K.; Mori, Y.; Wakabayashi, T.; Nagayama, S.; Kobayashi, S. *J. Am. Chem. Soc.* **2000**, *122* (30), 7202–7207.
- (40) Kobayashi, S.; Wakabayashi, T.; Nagayama, S.; Oyamada, H. *Tetrahedron Lett.* **1997**, *38* (26), 4559–4562.
- (41) Firouzabadi, H.; Iranpoor, N.; Jafari, A. A. *Adv. Synth. Catal.* **2005**, *347* (5), 655–661.
- (42) Kong, W.; Fu, C.; Ma, S. *Org. Biomol. Chem.* **2008**, *6* (24), 4587–4592.

- (43) Sun, X.-W.; Xu, M.-H.; Lin, G.-Q. *Org. Lett.* **2006**, *8* (21), 4979–4982.
- (44) Li, C.-J. *Tetrahedron* **1996**, *52* (16), 5643–5668.
- (45) Augé, J.; Lubin-Germain, N.; Marque, S.; Seghrouchni, L. *ResearchGate* **2003**, *679* (1), 79–83.
- (46) Choi, S.-K.; Lee, S.; Whitesides, G. M. *J. Org. Chem.* **1996**, *61* (25), 8739–8745.
- (47) Chan, T.-H.; Lee, M.-C. *J. Org. Chem.* **1995**, *60* (13), 4228–4232.
- (48) Pardoe, J. A. J.; Downs, A. J. *Chem. Rev.* **2007**, *107* (1), 2–45.
- (49) Hepler, L. G.; Hugus, Z. Z.; Latimer, W. M. *J. Am. Chem. Soc.* **1953**, *75* (22), 5652–5654.
- (50) Gynane, M. J. S.; Worrall, I. J. *J. Organomet. Chem.* **1974**, *81* (3), 329–334.
- (51) Paul B. McCay; Edward K. Lai; J. Lee Poyer; Coit M. DuBose; Edward G. Janzen. *J. Biol. Chem.* **1994**, *259* (4), 2135–2143.
- (52) Wright, J. S.; Shadnia, H.; Chepelev, L. L. *J. Comput. Chem.* **2009**, *30* (7), 1016–1026.
- (53) McBay, H. C.; Tucker, O. *J. Org. Chem.* **1954**, *19* (6), 869–883.
- (54) Gray, P.; Williams, A. *Chem. Rev.* **1959**, *59* (2), 239–328.
- (55) Benson, S. W. *J. Am. Chem. Soc.* **1964**, *86* (19), 3922–3924.
- (56) Svein Saebø; Leo Radom. *J. Chem. Phys.* **1983**, *78* (2), 845–853.
- (57) Oliveira, R. B. de; Alves, R. J.; Souza Filho, J. D. de; Prado, M. A. F. *J. Braz. Chem. Soc.* **2003**, *14* (3), 442–448.
- (58) de Oliveira, M. T.; Cesar, A.; Leal, D. H. S.; Prado, M. A. F.; da Silva, T. H. Á.; Alves, R. J. *Org. Biomol. Chem.* **2010**, *8* (7), 1619.
- (59) de Oliveira, R. B.; de Souza Filho, J. D.; Prado, M. A. F.; Eberlin, M. N.; Meurer, E. C.; Santos, L. S.; Alves, R. J. *Tetrahedron* **2004**, *60* (44), 9901–9908.
- (60) Neises, B.; Steglich, W. *Angew. Chem. Int. Ed. Engl.* **1978**, *17* (7), 522–524.
- (61) Barth, F.; O-Yang, C. *Tetrahedron Lett.* **1990**, *31* (8), 1121–1124.
- (62) Baldwin, J. E.; Adlington, R. M.; Mitchell, M. B.; Robertson, J. *J. Chem. Soc. Chem. Commun.* **1990**, No. 22, 1574–1575.
- (63) Ishizaki, M.; Ozaki, K.; Kanematsu, A.; Isoda, T.; Hoshino, O. *J. Org. Chem.* **1993**, *58* (15), 3877–3885.
- (64) Bowman, W. R.; Mann, E.; Parr, J. *J. Chem. Soc. [Perkin I]* **2000**, No. 17, 2991–2999.
- (65) Porter, N. A.; Chang, V. H. T.; Magnin, D. R.; Wright, B. T. *J. Am. Chem. Soc.* **1988**, *110* (11), 3554–3560.
- (66) Baldwin, J. E. *J. Chem. Soc., Chem. Commun.* **1976**, No. 18, 734–736.
- (67) Zemek, J.; Kučár, Š. *Collect. Czechoslov. Chem. Commun.* **1988**, *53* (1), 173–180.
- (68) Rale, M.; Schneider, S.; Sprenger, G. A.; Samland, A. K.; Fessner, W.-D. *Chem. - Eur. J.* **2011**, *17* (9), 2623–2632.
- (69) Kakinuma, H.; Yuasa, H.; Hashimoto, H. *Carbohydr. Res.* **1998**, *312* (3), 103–115.
- (70) Hecquet, L.; Bolte, J.; Demuynck, C. *Tetrahedron* **1994**, *50* (29), 8677–8684.
- (71) Corey, E. J.; Suggs, J. W. *J. Org. Chem.* **1975**, *40* (17), 2554–2555.
- (72) Arnaud Tatibouet, Jing Yang, Christophe Morin and Geogrey D. Holman. *Bioorg. Med. Chem.* **2000**, *8*, 1825–1833.
- (73) Girniene, J.; Tatibouët, A.; Sackus, A.; Yang, J.; Holman, G. D.; Rollin, P. *Carbohydr. Res.* **2003**, *338* (8), 711–719.
- (74) Tanasova, M.; Plutschack, M.; Muroski, M. E.; Sturla, S. J.; Strouse, G. F.; McQuade, D. T. *ChemBioChem* **2013**, *14* (10), 1263–1270
- (75) Wang, G.-N.; Yang, L.; Zhang, L.-H.; Ye, Z.-S. *J. Org. Chem.* **2011**, *76*, 2001–2009



## **Chapter 4: Evaluation of 6-NBD-Hexose Derivatives by Flow Cytometry**

### **4.1: A Brief Introduction to Flow Cytometry**

With the compounds 6NBDF, 6NBDP, 6NBBDT, and 6NBDS in hand we required a methodology to determine if these compounds were being taken into cells and if so, via what transport pathway they were utilizing. It was theorized that flow cytometry would be a suitable method to determine if these compounds were being taken into cells and through the use of various inhibitors we would be able to obtain evidence for which transport pathway they were taking. The information about uptake would help us move on and produce a new group of fluorescent compounds which could be better substrates for the GLUT5 pathway.

Flow cytometry was originally designed to allow for the rapid screening of large cell populations based on optical density, fluorescence, or other characteristics, which allowed researchers to monitor cellular events in real time.<sup>1-5</sup> Flow cytometry functions by drawing a stream of buffer fluid containing a free-floating population of single cells through the beam path of a laser. Through hydrodynamic focusing the cells are drawn into a single fine line and are moved through the beam path of a laser. The light of the laser is scattered by the cells as they pass (Figure 4.1). Two types of light scattering are detected by the flow cytometer, allowing for important information about the cells to be obtained. Light that is scattered around the surface of the cell strikes a detector located opposite to the laser and gives information about the size and surface characteristics of the cell. Larger cells—containing membranes more densely decorated with proteins and polysaccharides—show increased

scattering, which is referred to as forward scatter. Light that is scattered by interacting with organelles within the cell, a measure called side scatter, is quantified by a second detector located at a right angle to the laser beam path. The more complex and populous the organelles within the cell, the greater the degree of side scatter.<sup>6</sup> These two metrics are most commonly displayed on the X and Y axes of a graph to show the absolute and relative amounts of each type of scatter.

The absolute and relative magnitude of front and side scatter allows for the identification of cell types within a mixture. In a mixture of two cell species, each with a distinct size and internal composition, the two populations can be identified and measured without a physical separation of the mixture before it passes through the cytometer. As the mixture of cells passes through the detector, each cell is individually measured by the cytometer, resulting in two clusters of data points corresponding to the two cell populations. Together, these data points provide a metric for determining cell morphology. Data points falling outside these populations are often the result of cell fragments, clusters of cells, dead cells, or impurities in the sample, and can be selectively ignored in the analysis. Once the two cell populations have been distinguished in flow, they can be analysed separately within the cytometer.

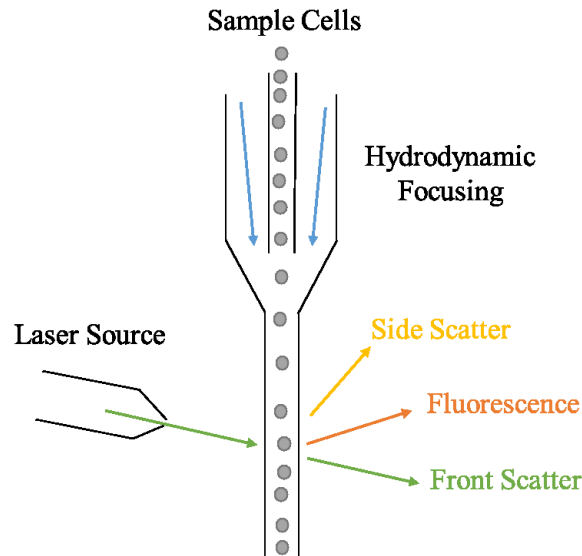


**Figure 4.1: A general overview of a flow cytometer.**

The utility of flow cytometry is expanded when another laser/detector is added to the system, allowing for additional metrics to be determined, along with cell morphology. Commonly, this is achieved by the addition of a fluorescence laser and detector, so that the activity of one or more fluorophores can be investigated along with cell morphology. By the mid-1980s, this had been extended to include multiple fluorescence lasers and detectors operating at differing wavelengths simultaneously, to target multiple fluorophores. Each cell can be measured for front scatter, side scatter, and a third characteristic simultaneously and all the data can be analysed.<sup>7,8</sup> This methodology can be applied to a single population of cells to isolate only healthy cells, and discard data from clumped, dead, or otherwise damaged cells that may be present in the solution.<sup>9-11</sup>

One disadvantage of flow cytometry is that cells are required to be free floating in solution before they can be analysed. This is of little consequence for cells that naturally exist in a suspended state; however, adherent cells such as HeLa, EMT6, or MCF7 cells must first

be prepared prior analysis by flow cytometry.<sup>12-14</sup> Sample preparation generally involves the cleavage of cell adhesion proteins and resuspension of the cells in a buffer solution. Though not labour intensive or difficult, this step is time consuming, preventing rapid, high throughput analysis.<sup>15,16</sup>

## **4.2: The use of Flow Cytometry to Investigate the Transport of NBD Labelled Compounds**

Flow cytometry has been used over the past several decades to monitor the uptake of glucose in several cell lines using, among others, the fluorescence probes described in Chapter 1. In 2005, Dimitriadis and co-workers used 6NBDG (Figure 4.2) as a tracer to monitor uptake of D-glucose in monocytes extracted from human blood.<sup>17</sup> The authors used a suspension of monocytes incubated with 6NBDG to follow the uptake of the tracer over time and observed a linear increase in the observed fluorescent signal associated with 6NBDG uptake. This increase in fluorescence was used as a measure of D-glucose uptake as D-glucose could not be measured directly. A dose-dependent response was observed between 6NBDG uptake and insulin, Wortmannin (an insulin signaling pathway inhibitor), and anti-insulin receptor antibody exposure. Therefore the authors concluded that D-glucose uptake was insulin dependent.<sup>17</sup> The authors also attempted to block the efflux of 6NBDG in their cell samples by fixing the cell membranes with a paraformaldehyde based cell fixation buffer added at the end of the incubation period. Measurement of samples which had been treated with the fixation buffer were compared to samples lacking fixation buffer. This comparison revealed that 6NBDG efflux resisted fixation. It appeared that the fixation process did not block the GLUTs and other pores through which 6NBDG could exit the cell. This was

indicated by the observation that the measured fluorescence between the two sample preparation conditions did not change.<sup>17</sup>

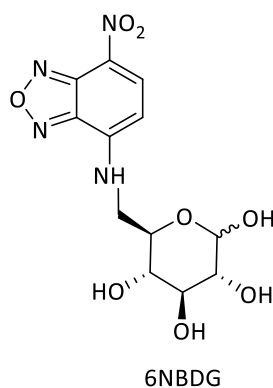


**Figure 4.2: The structure of 6NBDG.**

Snyder and co-workers used flow cytometry and 6NBDG to monitor D-glucose uptake in rat neurons and astrocytes. They found that the amount of 6NBDG uptake was directly correlated to the amount of D-glucose uptake.<sup>18</sup> Snyder's group used co-incubation with increasing concentrations of D or L-glucose to inhibit the uptake of 6NBDG. They found that the uptake of 6NBDG was reduced by co-incubation of D-glucose but not by L-glucose. They also confirmed that the known class I GLUT inhibitor, cytochalasin B, inhibited the transport of 6NBDG. The authors showed that a suitable method for inhibiting the uptake of an NBD-labelled D-glucose analog was to use an excess of the natural substrate for the transporter being studied, in this case D-glucose. This inhibition method was shown to be just as effective as the use of cytochalasin B, while no effect was observed when L-glucose was used.

2NBDG has been used to monitor the effect of several pharmaceutical agents on GLUTs, in order to give insights on how these agents influence the activity of the GLUT transporters. Shen and co-workers monitored the effect of several anti-diabetic drugs and drug candidates on GLUTs using 2NBDG as a tracer molecule for D-glucose uptake.<sup>19</sup> The

authors found that D-glucose uptake was temperature dependent. The response to a select set of anti-diabetic drugs was monitored and compared to uptake under standard conditions. 2NBDG was shown to be a suitable tracer for measuring D-glucose uptake in all cases explored by the authors with the exception of those when the drug tested showed auto-fluorescence in the same wavelength as 2NBDG. The authors note that an increase in observed fluorescence caused by the drug compound must be considered in this methodology as this complication could lead to a false positive when screening new compounds by this method.<sup>19</sup>

### **4.3: Determination of the Appropriate Cell Lines for the Evaluation of New Compounds**

With the established precedent outlined above, and that by Gambhir and co-workers described in Chapter 1,<sup>20</sup> flow cytometry was selected to measure the uptake of newly synthesized fluorescent NBD labelled hexoses, produced by Dr. Olivier Soueidan in the West group (Figure 4.3). These compounds all maintain the furanose ring system varying in stereochemistry at the C3, C4, and C5 positions respectively. Investigating how these stereochemical changes affected the binding and selectivity in GLUT transport would give more insight into binding site interactions. The synthesis of these compounds as well as their biological evaluation has been published<sup>21</sup> and was briefly discussed in Chapter 1. Before the publishing of the article in ACS Chemical Biology, flow cytometry was employed to measure uptake of these compounds in various cell lines, and explore the pathway through which they were taken up.

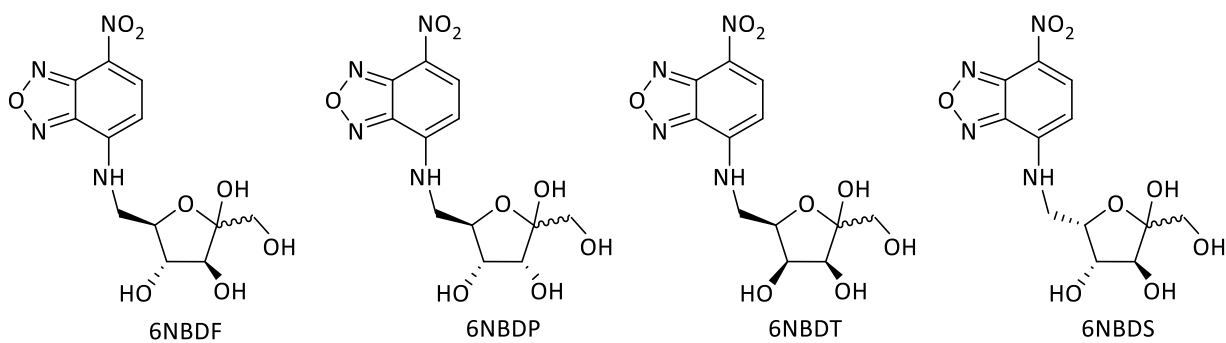


**Figure 4.3: The structure of 6NBDF, 6NBDP, 6NBDT, and 6NBDS.<sup>21</sup>**

Two cell lines were selected for this study, EMT6 and MCF7. EMT6 cells is a mouse breast cancer cell line first isolated and cultured by Fajardo and co-workers in 1972.<sup>22</sup> Since their introduction to the field, EMT6 cells have been used as a model cell line for several purposes including measuring macrophage induced cytotoxicity,<sup>10</sup> membrane permeability,<sup>23</sup> enzyme reaction kinetics<sup>24</sup> and cellular metabolism.<sup>13</sup> This breast cancer cell line has also been previously used in the radiopharmaceutical evaluation of the closely related PET imaging probe 6FDF.<sup>25</sup>

The second cell line selected was MCF7, a human breast cancer cell line first cultured in 1973.<sup>14</sup> This cell line is known to express GLUT1, GLUT2, and GLUT5 as well as other members of the GLUT family to varying levels.<sup>26</sup> The metabolic pathways present in MCF7 cells have been investigated by Diamandis and co-workers in 2012 using a quantitative proteomic technique known as selective reaction monitoring as well as mass spectrometry based analysis.<sup>27</sup> The authors found that these cell lines adapted quickly to stresses including starvation, hypoxia, and treatment with growth hormones. GLUT1 was found to be up-regulated under high-galactose, no-glucose, and hypoxic conditions. Under standard growth

conditions GLUT expression levels by the MCF7 cells were similar to those observed by Vera and co-workers.<sup>26</sup> These results show that GLUT1 is expressed as the primary D-glucose transporter and GLUT5 is present on the cell membrane along with GLUT2.

#### **4.4: Evaluation of 6NBDF as a GLUT Substrate Through Flow Cytometry**

The mean fluorescent intensity (MFI), as calculated by geometric mean, was recorded and is presented along the y-axis of cytometry plots. This value was used as the data from the cell populations gave a normal bell-shaped distribution and the cell population had a high degree of homogeneity. These factors allow for MFI to be a rapid and convenient comparison method for these probes.

Negative controls and results from some flow cytometry optimization have been included in Appendix II. Several other control studies were carried out with 6NBDF, 6NBDFP, 6NBDFDT, and 6NBDFDS. These studies include: the effects of temperature on the transport of these compounds; comparison of transport in cells which do and cells which do not overexpress GLUT5; Western blotting to establish the presence of GLUT1, GLUT2, and GLUT5 on the cell membranes; the use of a non-sugar NBD labelled compound; transfection of CHO cells with GLUT5 mRNA and the resulting change in compound transport; inhibition studies challenging the uptake of NBD labelled derivatives using [<sup>14</sup>C] labelled D-fructose and D-glucose. All of these studies can be found in the 2017 ACS Chemical Biology publication and the accompanying SI.<sup>21</sup> These studies were carried out by other members of the West group and are thus not included in this document.

The uptake of 6NBDF was measured in EMT6 cells by incubating them with 250  $\mu\text{M}$  6NBDF in phosphate buffer solution (PBS). The uptake of 6NBDF was observed to increase over 2 hours with a slightly greater rate of uptake observed in the initial 60 minutes (Figure 4.4). Linear regression analysis was performed and the slope of the trend line is listed in the legend of Figure 4.4.

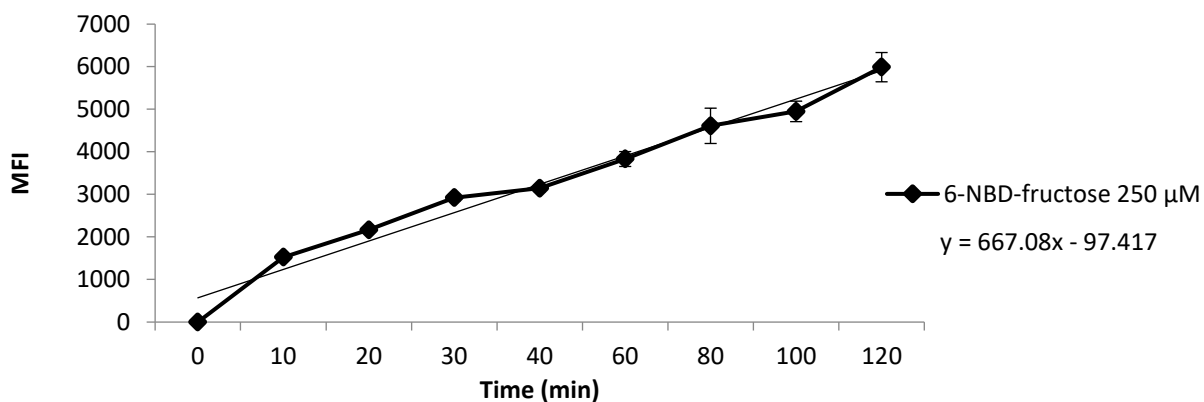


**Figure 4.4: Observed uptake of 6NBDF (250  $\mu\text{M}$ ) in EMT6 cells.**

Co-incubation of 6-NBDF with 10  $\mu\text{M}$  D-fructose in EMT6 cells resulted in a decrease in fluorescence as determined by a change in the slope of the linear regression trend line (Figure 4.5). Criteria for change in uptake were set so that at a given time point the difference between an inhibition experiment and the control must be greater than the sum of the error of the data in each time course. When 250  $\mu\text{M}$  of D-fructose was used the observed fluorescence was greater than the control throughout the time course except at the 120 min point at which the two uptakes are within error of each other. This suggests that D-fructose acts to inhibit the transport of 6NBDF into the cell by competing for binding with GLUT5 at low concentration while at high concentration, cis stimulation appears to negate some of the inhibitory effect of D-fructose.<sup>28</sup> Cis-stimulation is the observed effect wherein the observed

amount of substrate uptake is increased due the presence of a substrate which increases the rate limiting step in the transport cycle; turnover of the GLUT from inward-open to the outward-open conformation.<sup>28,29</sup> High concentrations of various hexoses have been shown to dramatically affect the rate and direction of net transport of glucose in human erythrocytes, which have long been used as model cells for GLUT1 transport studies.<sup>30-37</sup> Depending on the concentration and type of hexose used in transport kinetics experiments, both inhibition and stimulation effects are known to occur.<sup>30-37</sup>

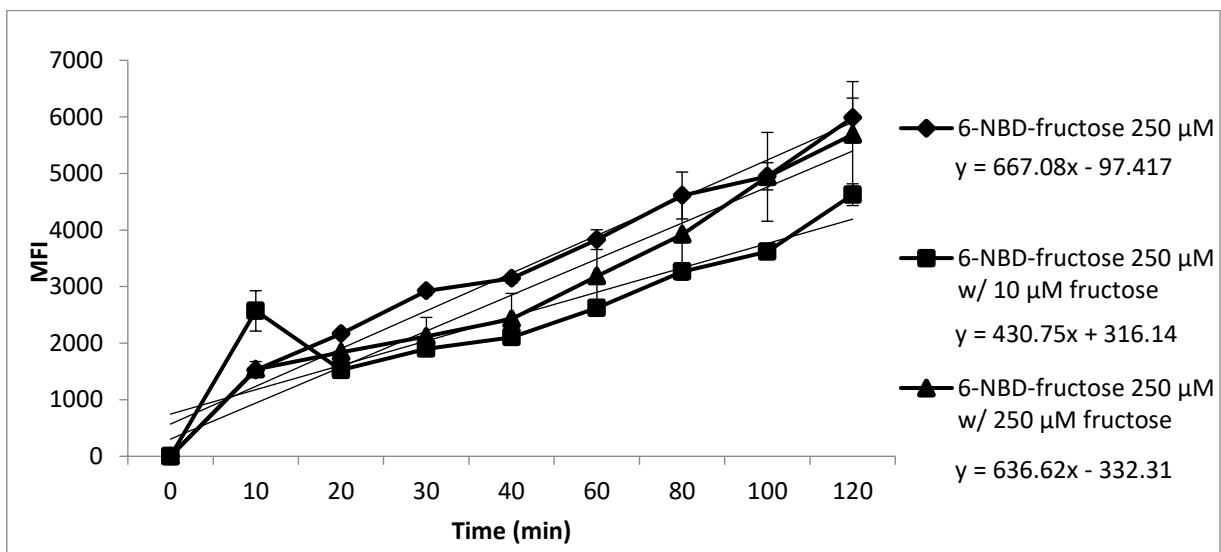


**Figure 4.5: Inhibition of 6NBDF (250 μM) with varying concentrations of extracellular D-fructose in EMT6 cells.**

To determine if cis-stimulation was occurring, the concentration of extracellular D-fructose was increased to 1 and 2 mM. These experiments revealed an increase in observed fluorescence to a level that was greater than the original uptake experiment, indicating that the increased concentration of extracellular D-fructose is indeed stimulating uptake when 2 mM D-fructose was used (Figure 4.6). 1 mM D-fructose showed a slight increase in uptake but was within error ranges of the standard uptake. These changes in transport kinetics are only

observed in cases when the substrate being monitored and the hexose being added to the system are transported by the same transporter.<sup>30-37</sup>

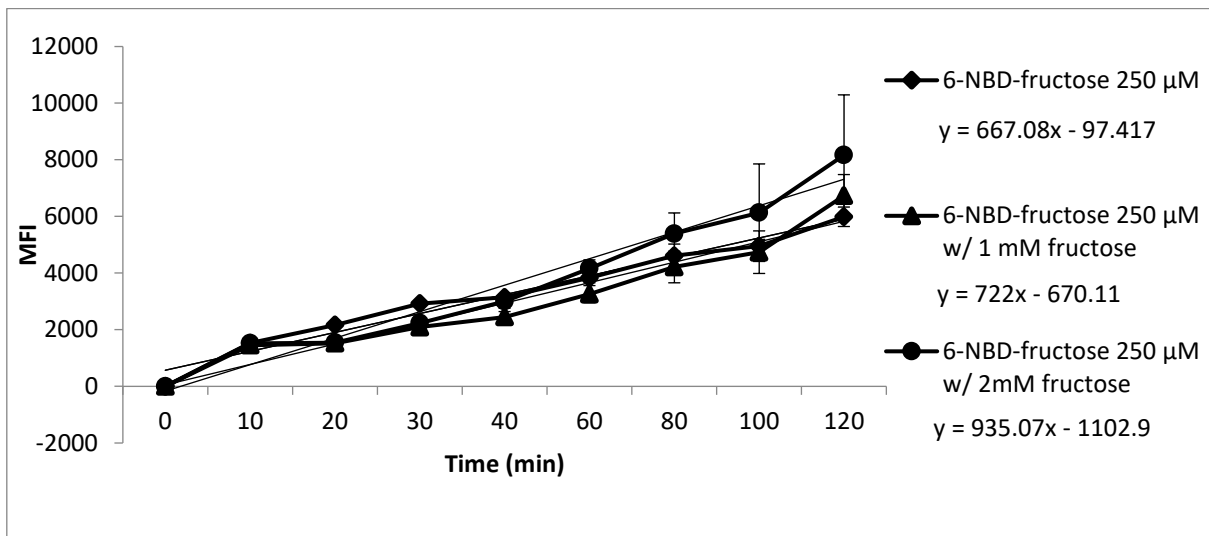


**Figure 4.6: Uptake of 6NBDF (250 μM) with varying, high concentrations of extracellular D-fructose in EMT6 cells.**

Co-incubation with 10, 25, or 250 μM of D-glucose resulted a decrease in the observed fluorescence at all concentrations, as shown in Figure 4.7. The use of the known class I GLUT inhibitors quercetin<sup>38,39</sup> (100 or 250 μM, Figure 4.8) or cytochalasin B<sup>40,41</sup> (50 μM, Figure 4.9) showed similar inhibition to co-incubation with D-glucose. No cis-stimulation is observed when the concentration of D-glucose was increased, which indicates that GLUT1 or GLUT2 are not transporting a significant amount of 6NBDF. The small decrease in uptake observed does seem to show that a portion of 6NBDF is being transported by a transport protein which is sensitive to D-glucose, quercetin, and cytochalasin B. D-glucose would act as a competitive inhibitor of a D-glucose transporter while quercetin and cytochalasin B are allosteric inhibitors of the Class I GLUT transporters. Quercetin binds to the exofacial side of the GLUT while cytochalasin B binds the endofacial side of the transporter. The most likely

candidate for this transporter is GLUT2, which is known to transport both D-fructose and D-glucose, and is sensitive to the inhibitors. The bulk of 6NBDF transport is associated with a transporter that is sensitive to D-fructose and not D-glucose, quercetin, or cytochalasin B. Given these observations, the most likely candidate for 6NBDF transport is the GLUT5 pathway, while the GLUT2 pathway plays a minor role.

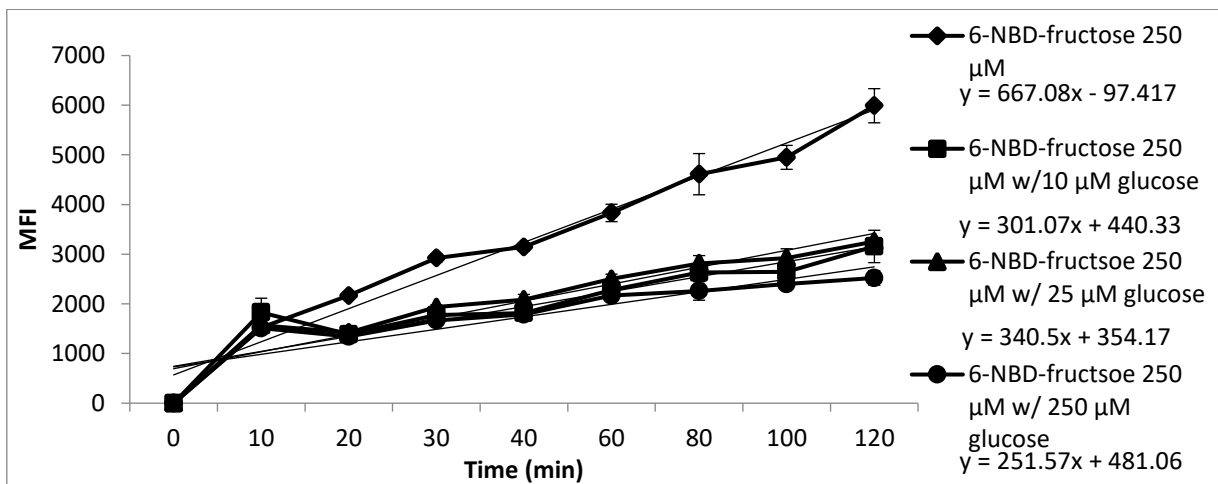


Figure 4.7: Uptake of 6NBDF (250 μM) with varying concentrations of extracellular D-glucose in EMT6 cells.

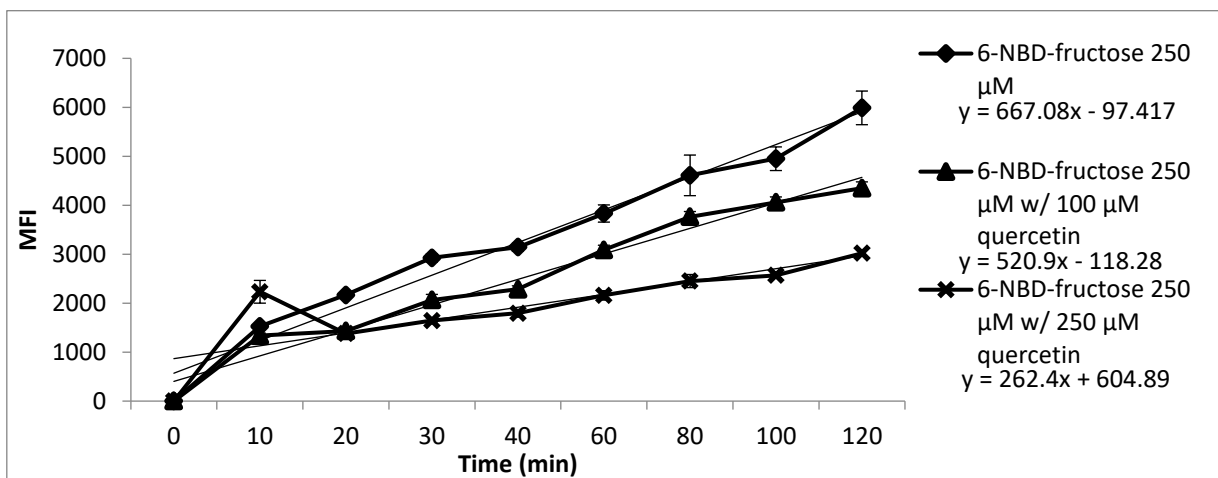
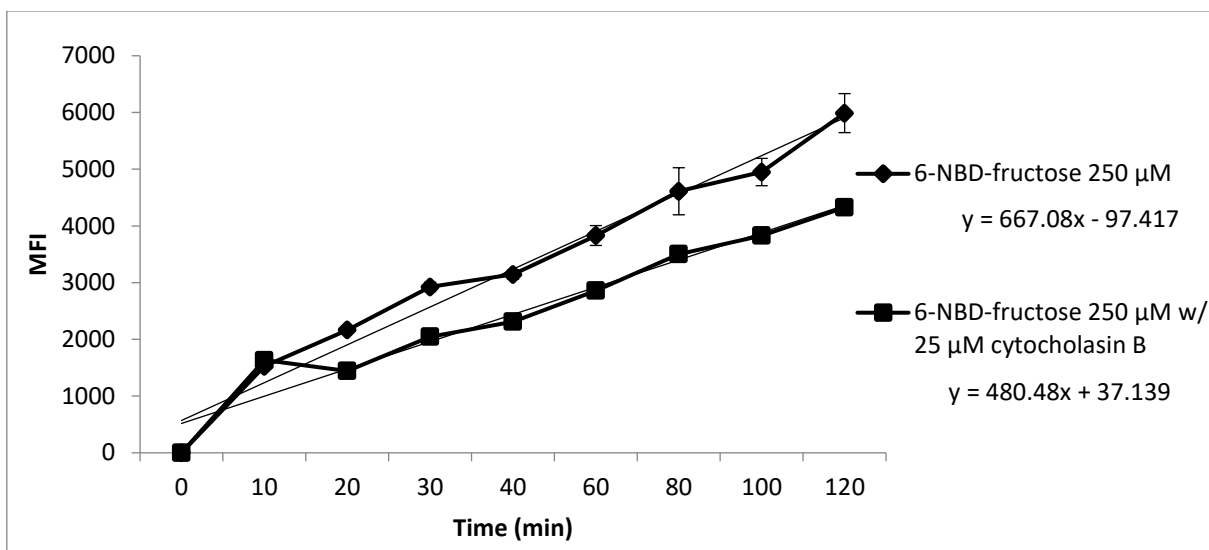
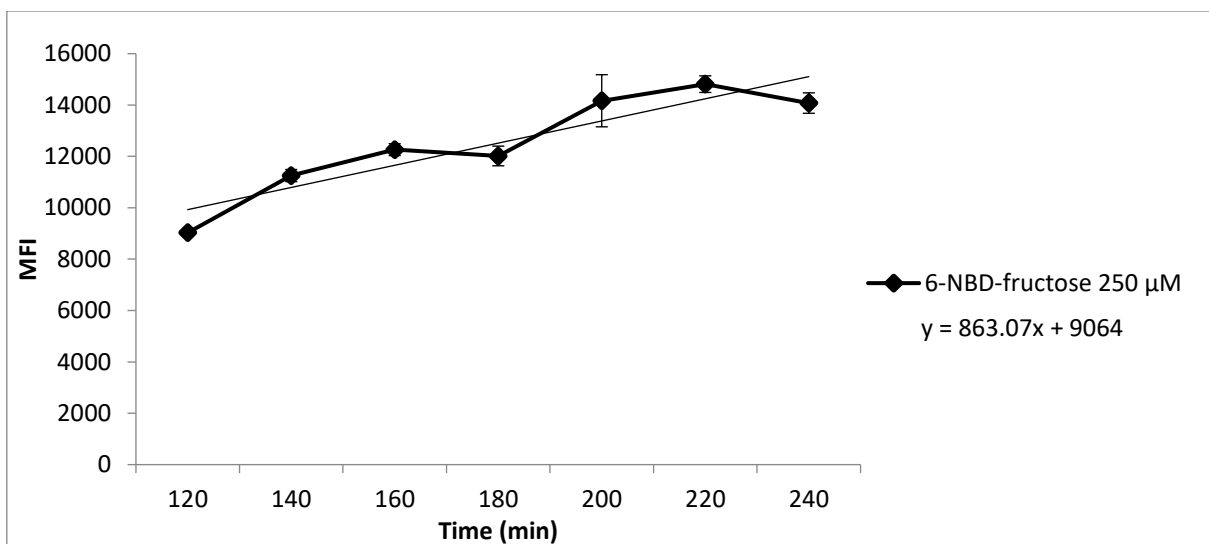


Figure 4.8: Uptake of 6-NBDF (250 μM) with varying concentrations of extracellular quercetin in EMT6 cells.



**Figure 4.9: Uptake of 6NBDF (250 μM) with cytochalasin B (250 μM) in EMT6 cells.**

To investigate if 6NBDF uptake would continue beyond 2 hours, the uptake experiment was repeated and allowed to run for 4 hours. For the first 2 hours of the experiment the sample plate was incubated, and from the 2 hours until the end of the experiment, the standard sample preparation and wash was applied (See Experimental Section Below). The fluorescence data showed that the uptake took place for approximately 3.5 hours before uptake stopped increasing (Figure 4.10). The uptake at 2 hours was slightly higher in the experiments designed to run 4 hours than those run for 2 hours. This is most likely due to the 2 hour experiments having plates removed from the incubator at each time point between 10 minutes and 2 hours, allowing for washing of some wells or addition of 6NBDF containing buffer to other wells of the plate. Though the periodic decrease in temperature and manipulation of the plates would lead to changes in the amount of 6NBDF transported into the cell, the general trend of uptake did not change.



**Figure 4.10: Uptake of 6NBDF (250  $\mu$ M) in EMT6 cells over a 4 hour time course.**

Efflux of 6NBDF was found to be rapid and difficult to measure using flow cytometry. EMT6 cells were incubated for 60 minutes in PBS buffer containing 250  $\mu$ M 6NBDF and then washed quickly with clean PBS buffer. PBS buffer was added and the cells were allowed to sit in the incubator for 10 to 120 min, allowing for efflux of 6NBDF. At the end of the efflux period, the cells were cleaved from the incubation plate using trypsin and a cell preparation was prepared for flow cytometry. The trypsination, preparation of the cell solution, and transport to the flow cytometry lab took 48 minutes on average. Efflux was found to be rapid and dropped to near or below the threshold for measurement of the cytometer after 50 minutes. Therefore the bulk of 6NBDF leaves the cell in approximately 100 minutes after the cells were first washed. This rapid time frame indicates that 6NBDF is not being trapped inside the cells to a significant extent.

When trying to measure the uptake of 6NBDF in MCF7 cells, it was found that the fluorescence reading was very low when using the same conditions as with EMT6 cells. Upon doubling the concentration of 6NBDF to 500  $\mu$ M, the measured fluorescence signal in

MCF7 was approximately half that observed in EMT6 cells (Figure 4.11). Uptake was found to vary between replicates on MCF7 cell preparations as compared to EMT6 experiments, which provided more consistent fluorescence readings. When the concentration of 6NBDF was increased to 750  $\mu\text{M}$ , the observed fluorescence was increased as compared to uptake at 500  $\mu\text{M}$ , but the cell morphology, as determined by the flow cytometer or by visual microscopy, was significantly altered indicating that the cells were no longer healthy at higher concentrations.

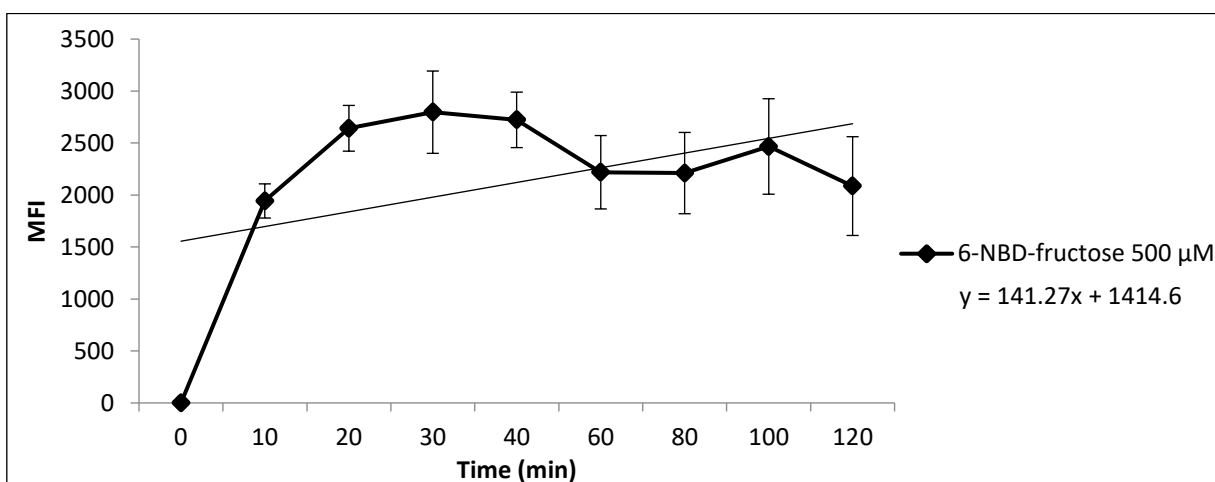


**Figure 4.11: Uptake of 6NBDF (500  $\mu\text{M}$ ) in MCF7 cells.**

To obtain consistent data between replicates of MCF7 cell preparations, a paraformaldehyde containing cell fixation buffer was added to the cells after the incubation period, immediately before preparation for analysis by the flow cytometer. The role of the paraformaldehyde in the fixation buffer is to cross-link amino acid residues in the transporter pores, preventing 6NBDF from exiting the cell. No change was observed in the number of cells observed to have a significant fluorescence signal when measured by the flow cytometer. Without a sufficient number of cells displaying fluorescence the measured values cannot be

used with confidence. This result is consistent with the results of Dimitriadis and co-workers, who in 2005 found that 6NBDG efflux resisted fixation.<sup>17</sup>

Inhibition experiments, attempted with D-glucose, D-fructose, quercetin or cytochalasin B gave no data that met the requirements for reliability and reproducibility as described in the experimental section below. The addition of any inhibitory compounds to the uptake experiments resulted in observed fluorescence levels near or below the detection limit of the cytometer. No relevant conclusions could be drawn from the results of these experiments.

#### **4.5: Evaluation of 6NBDP as a GLUT Substrate Through Flow Cytometry**

Using similar conditions to those evaluating 6NBDF in MCF7 cells, 6NBDP uptake was monitored. At a 250  $\mu\text{M}$  concentration of 6NBDP no measurable uptake could be detected by flow cytometry. The concentration of compound was subsequently increased until repeatable fluorescence measurements were obtained. A concentration of 750  $\mu\text{M}$  was required to obtain data that met the pre-set standards for reproducibility as outlined in the experimental section below, and an increase to 2 mM 6NBDP gave the most consistent data over multiple replicates (Figure 4.12). At lower concentrations measurements were highly variable due to the low number of cells having fluorescence intensity greater than background.

Upon co-incubation with D-fructose, D-glucose, quercetin, or cytochalasin B, the observed fluorescence was found to be very low, and data suitable for comparison to the uninhibited uptake could not be obtained. The number of cells with observed fluorescence above background was found to be extremely low, zero in some experiments.

The same concentrations, 250  $\mu$ M up to 2 mM, of 6NBDP was used with cultures of EMT6 cells and no measurable fluorescence was observed. There was an increase in the total fluorescence measured by the cytometer but the observed fluorescence did not exceed the minimum threshold required. The fluorescence observed was greater than in the control samples, but was not high enough to be considered significant in the study. A small number of cells were observed to have a significant increase in fluorescence, but due to the limited number, repeatable data could not be obtained.

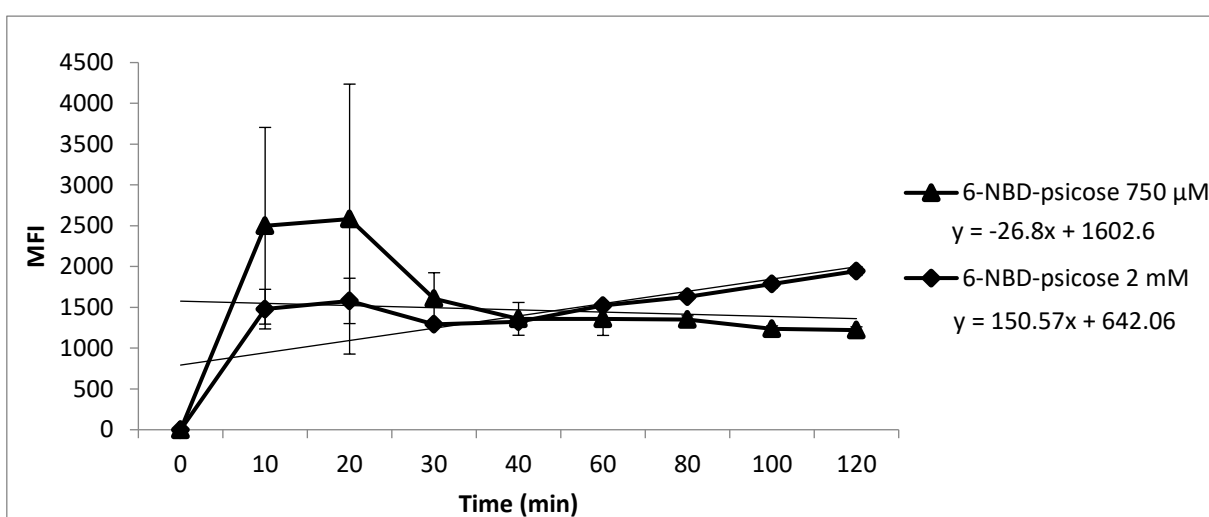


Figure 4.12: Uptake of 6NBDP at 750  $\mu$ M or 2 mM in MCF7 cells.

The initial spike observed in the uptake curves of 6NBDP may be a result transport stimulation arising from a rapid exchange of 6NBDP through the GLUT transporters. 6NBDP may be transported rapidly in both directions across the cell membrane at the start of the time course but reaches an equilibrium after 40 min. Without a method for analysis of initial kinetics this can not be proven conclusively. As no further data could be obtained using 6NBDP, no conclusions can be drawn about the 6NBDP transport pathway. Inhibition studies

failed to give conclusive data, thus discussion of the mechanism of transport for 6NBDP cannot be elaborated.

#### **4.6: Evaluation of 6NBDS as a GLUT Substrate Through Flow Cytometry**

6NBDS was evaluated using the same methodology as used with 6NBDF. In EMT6 cells a 500  $\mu\text{M}$  concentration of 6NBDS was needed to obtain consistent fluorescence data. These uptake data are shown Figure 4.13. The observed uptake was found to increase rapidly at the start of the experiment and plateau almost immediately. A very similar result was found in the MCF7 cell line though a 750  $\mu\text{M}$  concentration of 6NBDS was needed to obtain consistent data in this cell line as shown in Figure 4.14. As in the EMT6 cell line the initial uptake was rapid and plateaued very quickly.

All inhibition studies failed to show any significant fluorescence. Co-incubation with even a low concentration of D-glucose, D-fructose, quercetin, or Cytochalasin B resulted in a drop in fluorescence to levels below the measurable limit of the cytometer.

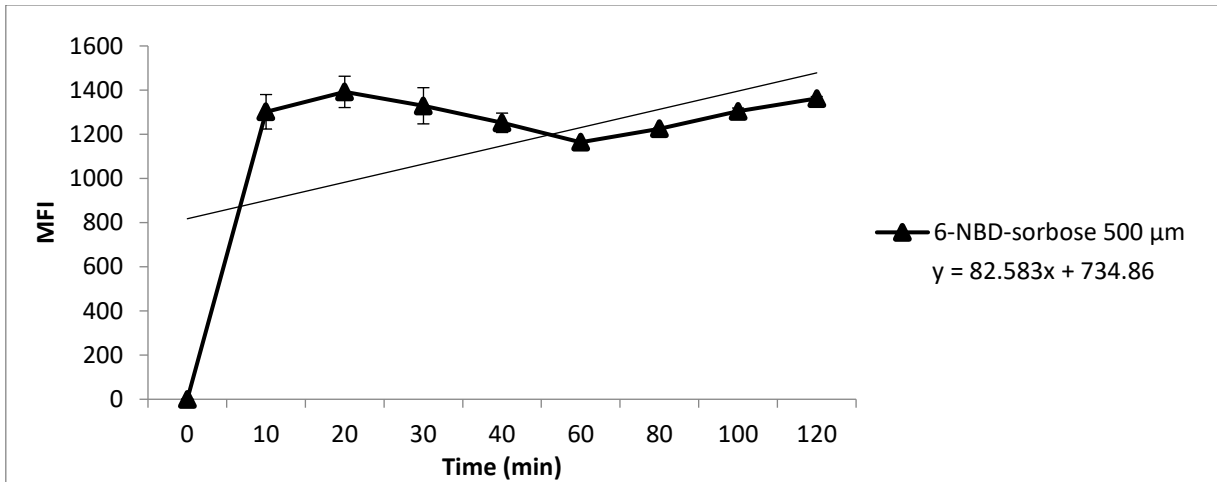


Figure 4.13: Uptake of 6NBDs (500 μM) in EMT6 cells.

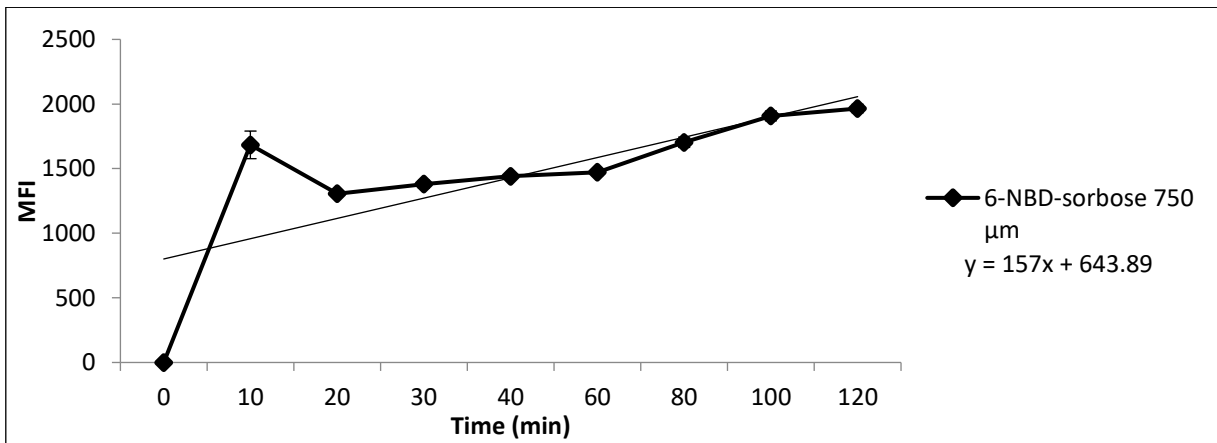
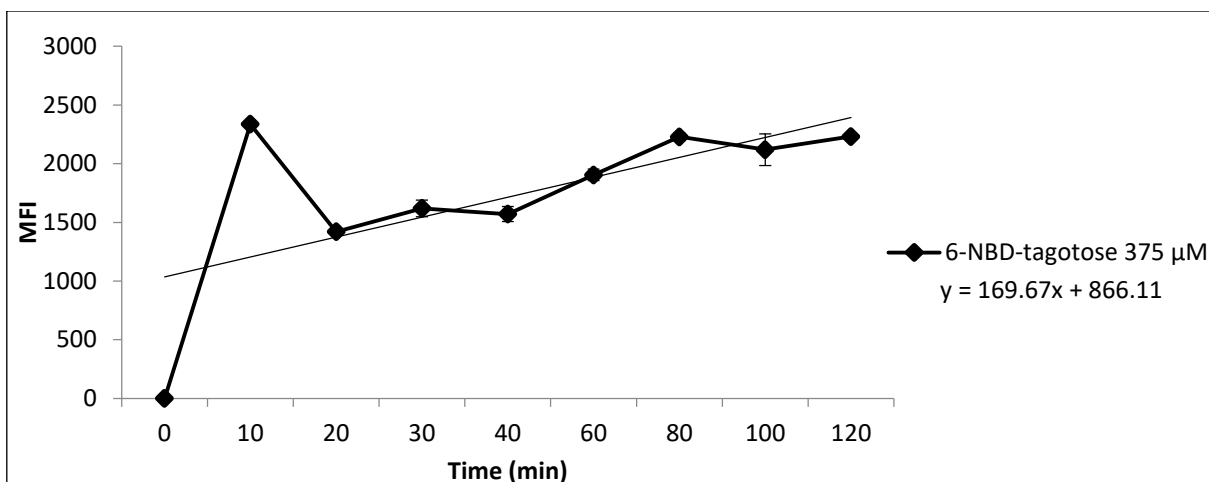


Figure 4.14: Uptake of 6NBDP (750 μM) in MCF7 cells.

## 4.7: Evaluation of 6NBDT as a GLUT Substrate Through Flow Cytometry

A 375 μM concentration of 6NBDT was sufficient to obtain good data in EMT6 cell. The uptake was found to spike at the 10 minute time point and then decrease between 20 and 40 minutes before returning to a value near the initial spike after approximately 80 minutes as shown in Figure 4.15.



**Figure 4.15: Uptake of 6NBDT (375  $\mu$ M) in EMT6 cells.**

Co-incubation with 50  $\mu$ M D-glucose was found to cause a slight inhibition of 6NBDT uptake while co-incubation with 100  $\mu$ M D-glucose resulted in close to 60% inhibition of uptake as determined by comparison of the MFI at 120 minutes. Interestingly the uptake of 6NBDT plateaued after 30 minutes when 100  $\mu$ M D-glucose was used to inhibit uptake though a strong initial spike in uptake was still observed at the 10 minute time point. The initial spike was not observed when 50  $\mu$ M of D-glucose was used. These results seem to indicate that D-glucose is effecting the uptake of 6NBDT. There is not a clear relationship between the concentration of D-glucose and the observed fluorescence through this experiment. Further, the initial spike in fluorescence observed in the parent experiment and in the 100  $\mu$ M D-glucose experiment is not observed with a lower concentration of D-glucose. These data are presented in Figure 4.16.

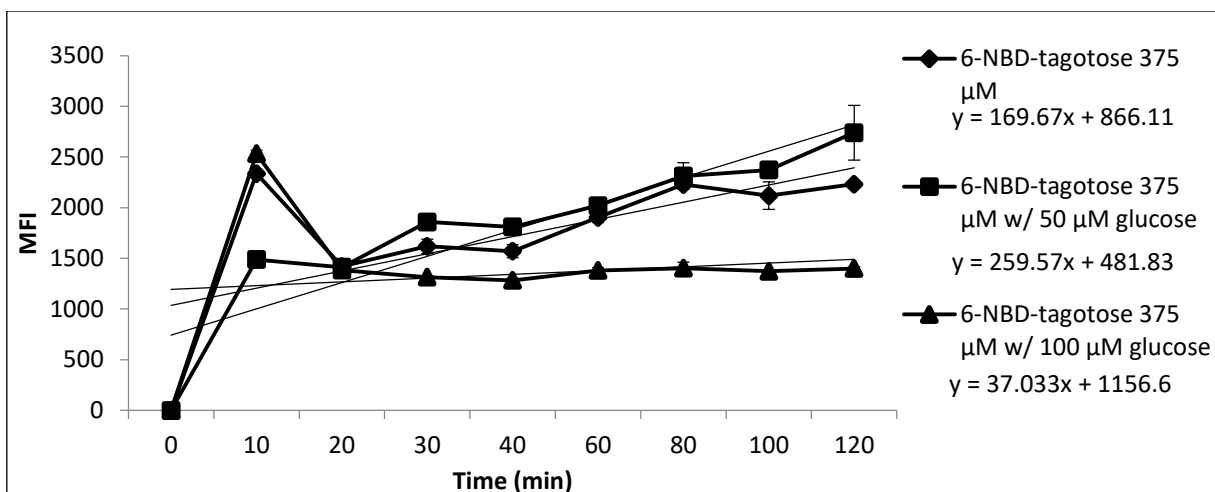


**Figure 4.16: Uptake of 6NBDT (375 μM) with varying concentrations of extracellular D-glucose in EMT6**

Inhibition with D-fructose, quercetin, or cytochalasin B resulted in fluorescence measurements were too low and highly varied to give any kind of reliable result. With the lack of a dose-dependent relationship in the D-glucose inhibition studies and no further reliable data little could be concluded about the mechanism of 6NBDT uptake in EMT6 cells.

We next turned our attention to the uptake of 6NBDT in the MCF7 cell line. Starting with a 250 μM, the concentration of 6NBDT was increased until consistent data were obtained in uptake experiments. This was found at a 350 μM as shown in Figure 4.17. When the concentration was increased to 500 μM, the data obtained were highly varied at the 10 to 20 minute mark of the uptake experiment. Data at these time points was not found to repeatable despite several additional replicates of the uptake studies being performed. Consistent data points for replicates were obtained at later time points, though the MFI did not increase as expected with the increase in concentration.

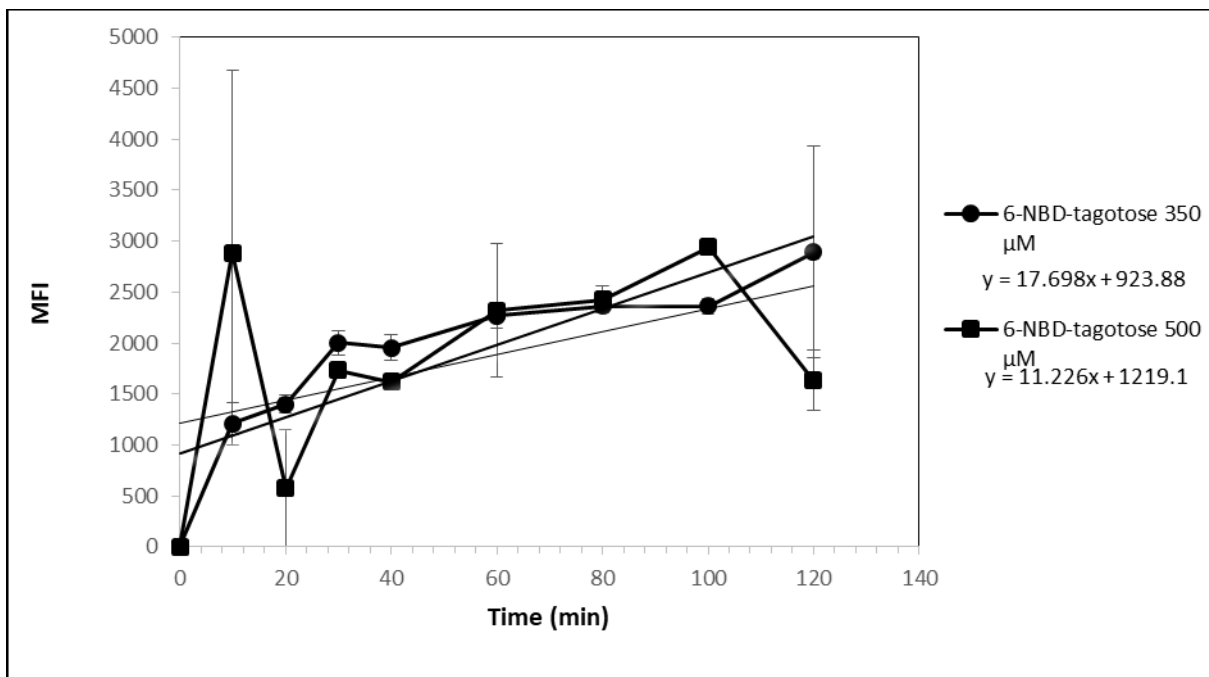
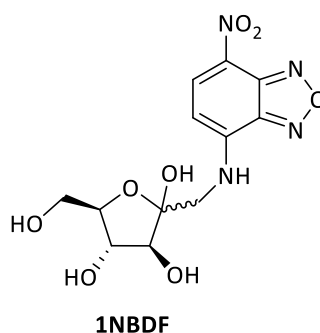


Figure 4.17: Uptake of 6NBDT at 375  $\mu$ M or 500  $\mu$ M in MCF7 cells.

## 4.8: Evaluation of 1NBDF as a GLUT Substrate Through Flow Cytometry

As described in Chapter 1, Gambhir and coworkers have developed and published on the fluorescent D-fructose analog 1NBDF (Figure 4.18).<sup>20</sup> In this publication the authors describe the synthesis of 1NBDF, and evaluation of its uptake in human breast cancer cell lines by confocal microscopy. The authors also comment that the results of their confocal microscopy experiments are mirrored by complimentary experiments monitored by flow cytometry. In brief, the authors conclude that 1NBDF is taken into the cell lines via GLUT5, and see inhibition of this uptake with both D-fructose and D-glucose.<sup>20</sup> To evaluate our methodology for monitoring the uptake of our compounds, we set out to replicate the results published by Gambhir and co-workers. We also hoped that we could repeat the inhibition

experiments done by Gambhir and co-workers to validate the use of D-fructose, D-glucose, and other inhibitors in our system. The 1NBDF we used was produced in-house by Dr. Soueidan following the published methods of Gambhir and co-workers<sup>20</sup> as reported in the supplementary information of our publication.<sup>21</sup>



**Figure 4.18: The structure of 1NBDF.**

In the murine cell line EMT6, uptake of 1NBDF was observed over a 2 hour time course with a plateau appearing after approximately 40 minutes. The longer the cells were allowed to incubate with 1NBDF the more variable the measured fluorescence (Figure 4.19).

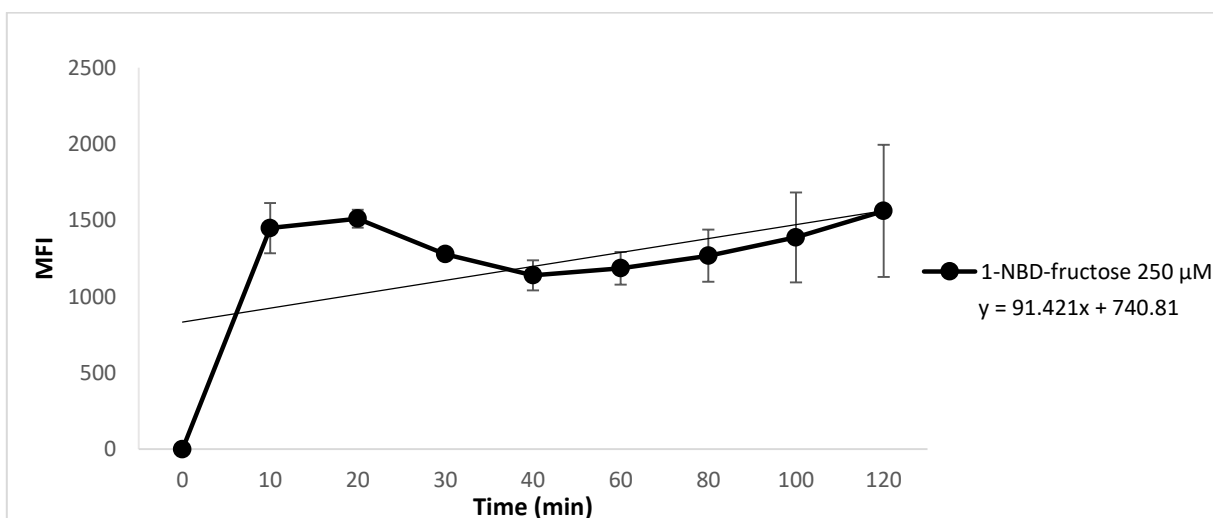


**Figure 4.19: Uptake of 1NBDF (250 μM) in EMT6 cells.**

When inhibition experiments were performed using D-fructose or D-glucose, the measurable uptake dropped below the limit of the cytometer at all time points. Interestingly, an increase in the concentration of 1NBDF did not lead to an increased level of observed fluorescence. Presumably the pathway through which 1NBDF is being transported reaches saturation quickly and accumulation of 1NBDF in the cell does continue. This could be due to a rapid efflux through one or more GLUT pathways. No measurable fluorescence signal was observed with 1NBDF upon co-incubation with D-glucose or D-fructose at concentrations from 10  $\mu$ M to 2 mM.

The uptake of 1NBDF was found to increase linearly over the 2 hour time course in MCF7 cells (Figure 4.20). Co-incubation with 250  $\mu$ M D-fructose, 50  $\mu$ M D-glucose, or 100  $\mu$ M D-glucose resulted in a partial inhibition of the observed uptake of 1NBDF (Figure 4.21 and 4.22). D-Fructose (250  $\mu$ M), reduced the observed fluorescence by approximately 50%, while D-glucose reduced observed fluorescence by 10 and 20% at 50 and 100  $\mu$ M respectively. Concentrations of D-fructose under 250  $\mu$ M did not show an effect on the uptake of 1NBDF. Increasing the concentration of D-fructose above 250  $\mu$ M resulted in inconsistent data, as well as evidence for significant changes in the cell morphology as determined by front and side scatter measurements in the flow cytometer and by direct observation by microscopy. These results, that both D-fructose and D-glucose inhibit 1NBDF uptake and mirror the results published by Gambhir and co-workers.<sup>20</sup>

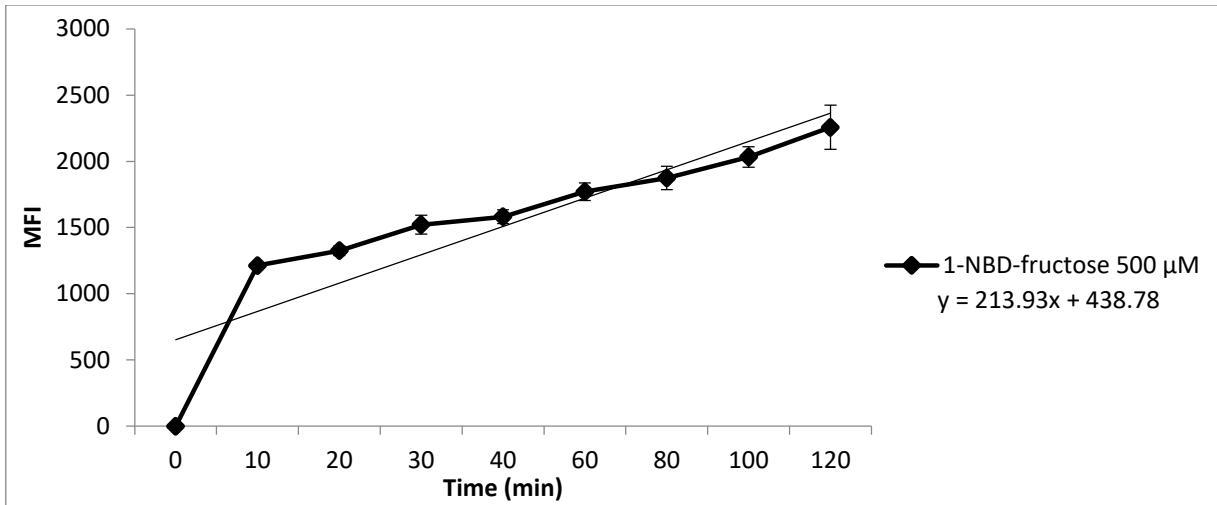


Figure 4.20: Uptake of 1NBDF (500 μM) in MCF7 cells.

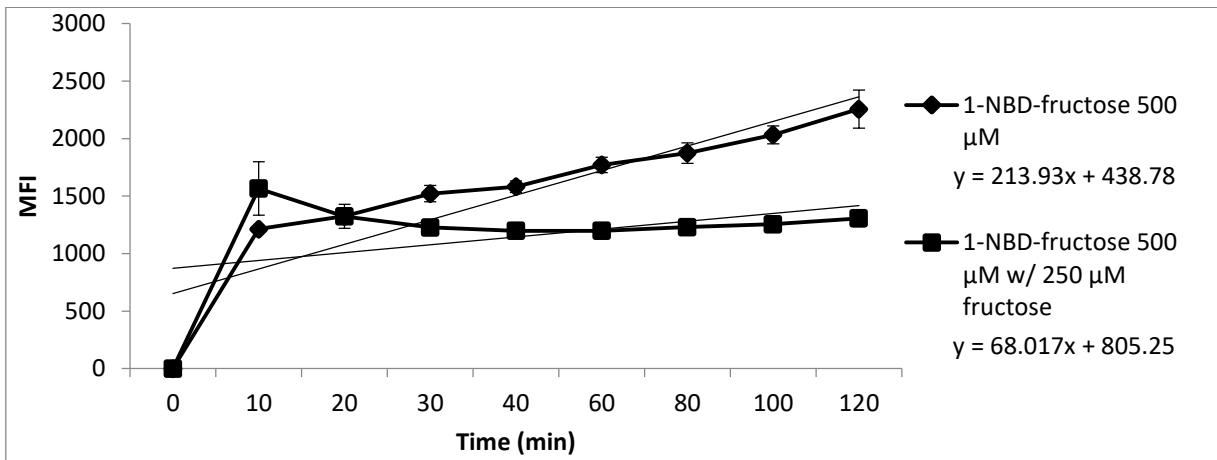
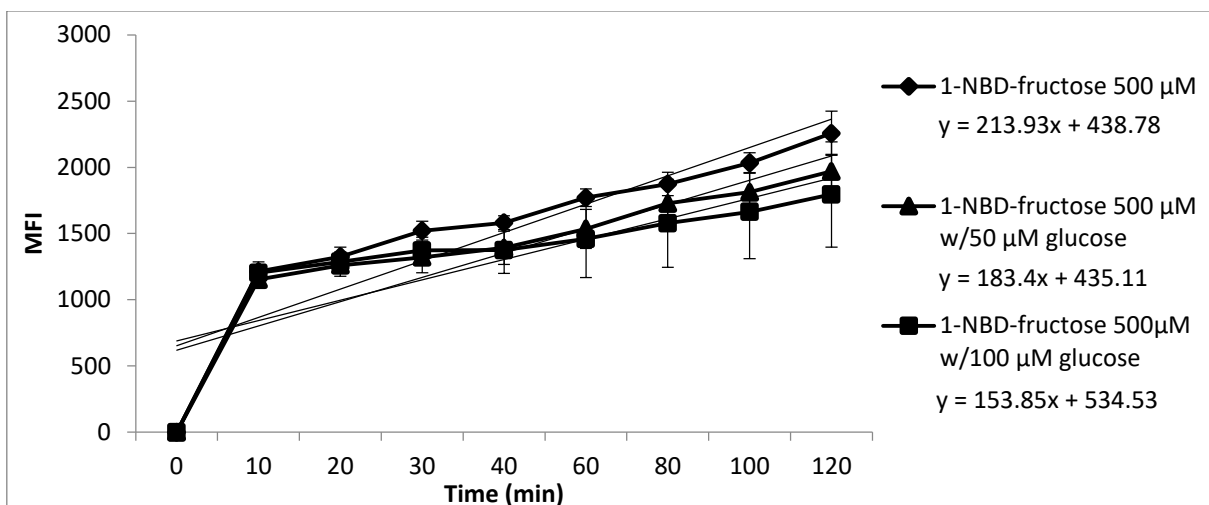


Figure 4.21: Uptake of 1NBDF (500 μM) and the effect of co-incubation with extracellular D-fructose (250 μM) in MCF7 cells.



**Figure 4.22: Uptake of 1NBDF (500 μM) and the effect of co-incubation with extracellular D-glucose (50 or 100 μM) in MCF7 cells.**

When the results of these experiments and the original data published by Gambhir and co-workers are compared to those found with 6NBDF, 6NBDP, 6NBDT, and 6NBDS, we cannot conclude that the uptake of 1NBDF is being handled by GLUT5 alone, as Gambhir states.<sup>20</sup> The inhibition by both D-fructose and D-glucose points towards a combination of GLUT transporters handling the transport of 1NBDF. If GLUT5 were the only transporter carrying 1NBDF, as proposed by Gambhir and co-workers, then D-glucose should not inhibit uptake, as D-glucose is not a substrate of GLUT5. Since our results and those of Gambhir and co-workers show that both D-fructose and D-glucose inhibit the uptake of 1NBDF, 1NBDF is most likely transported by more than one transporter, likely a combination of GLUT1, 2 and 5. As flow cytometry was not able to accurately measure the uptake of 1NBDF in EMT6 cell lines with co-incubation of D-glucose or D-fructose, it is difficult to conclude which of these transporters is responsible for the uptake of 1NBDF and to what extent each is involved, as we were unable to measure cis-stimulation and inhibition. Further elucidation of the transport of 1NBDF was carried out in West group, and is described in our

2017 publication.<sup>21</sup> The additional experiments carried out by other researchers in the West group have shown that 1NBDF appears to be a GLUT1/GLUT2 substrate and that GLUT5 is minimally involved in its transport.

#### **4.9: Conclusion:**

Flow cytometry has proven to be a valuable tool for screening the uptake of fluorescent fructose derivatives. Significant limitations were observed in regard to signal intensity and sample preparation, which prevented the full screening up the uptake properties of all the compounds. Removing these adherent cell lines from the plate on which they grew was a time consuming process. Consequently, the delay between the end of the incubation period and analysis of the cells in the cytometer resulted in significant loss of signal intensity. Despite these limitations, some conclusions on the pathways of transport can be drawn from the results obtained.

6NBDF was found to be the best substrate for uptake into EMT6 cells and could be fully evaluated through several inhibition studies. The uptake of 6NBDF in this cell line was found to be highly responsive to the presence of extracellular D-fructose and weakly responsive to the presence of extracellular D-glucose. The inhibitory agents quercetin and cytochalasin B also inhibited the uptake of 6NBDF. The observed, dose-dependent responses to these compounds show both inhibition and cis-stimulation effects which are indicative of a transported-mediated pathway. These results further indicate that GLUT5 is the primary transporter, which carries 6NBDF across the cell membrane and into EMT6 cells. The small reduction in observed uptake caused by D-glucose, quercetin, and cytochalasin B indicate that GLUT2 may be involved in the transport of 6NBDF to some extent. The magnitude of

inhibition observed is small and thus, the involvement of GLUT2 is likely much less than the involvement of GLUT5. Future work to determine the binding coefficients of 6NBDF to GLUT1, 2, or 5, by expression of a single transporter on cell which lacks other hexose transporters such as *Xenopus* oocytes, would provide valuable insights.<sup>42,43</sup>

A dose-dependent inhibitory response to extracellular D-glucose was observed when monitoring the uptake of 6NBDT. This indicates that 6NBDT may be transported by GLUT1 and/or GLUT2, but the lack of comparative results using D-fructose, quercetin, and cytochalasin B makes a conclusive identification of the transporter handling 6NBDT uptake impossible.

Evaluation of the other fluorescently labelled hexoses, 6NBDP and 6NBDS, failed to give consistent and repeatable data by flow cytometry. This could be due to the long work-up time between incubation and analysis, or by a lack of transport into the cells. Experiments performed using other techniques, which do not have the long workup times associated with flow cytometry, have shown that 6NBDF, 6NBDP, 6NBDT and 6NBDS were all taken up into both EMT6 and MCF7 cells in a dose-dependent manner, and were affected by inhibitors including D-fructose, D-glucose, and cytochalasin B.<sup>21,44</sup> Use of the fluorescent plate reader allowed for the rapid sampling of adherent cells incubated with 6NBDF, 6NBDP, 6NBDT, or 6NBDS. These results were reproducible, allowing for minimization of the standard deviation between replicates. This technique does not require the cells to be removed from the plate or manipulated before measuring their fluorescence, allowing the sample preparation time to be reduced to less than 5 minutes from 48 minutes in flow cytometry. These data, along with other investigations into the transport of 6NBDF, 6NBDP, 6NBDT, and 6NBDS, along with their synthesis, was produced in collaboration with Dr. Olivier Soueidan in the West group

and was published in 2017 in ACS Chemical Biology. The results presented in this chapter were the initial findings that inspired our subsequent investigation of the uptake of fluorescent D-fructose analogs by hexose transporter proteins using other methods of detection. Due to the multiple problems encountered in this work, flow cytometry is no longer used in uptake studies of new compounds produced in this research stream. Instead, fluorescent plate reader experiments are now favoured.

## **4.10: Experimental:**

### **General:**

Media and other solutions were purchased from Fisher Scientific and used without additional modification unless otherwise noted. Glucose-free Krebs-Ringer solution and PBS buffer were made by dissolving solid chemicals purchased from the Fisher Scientific or Sigma Aldrich fine chemical companies in distilled water which had been passed through a Milli-Q purification cartridge. Buffer solutions were autoclaved after preparation and used for no more than 14 days after preparation.

### **Cell culture:**

EMT-6 and MCF-7 cells were grown in a 5% CO<sub>2</sub> incubator at 37 °C in Gibco DMEM/F12 media supplemented with 15 mM HEPES, L-glutamine, 10% fetal bovine serum and 1% penicillin/streptomycin with media renewed every 2 days.

### **Uptake Experiments:**

Uptake studies were performed after allowing cells to reach confluence in 12 well plates (~200,000 cells/well for EMT-6 and ~300,000 cells/well for MCF-7 cells). Growth media was removed by aspiration and 750  $\mu$ M of glucose free Krebs-Ringer solution was added. The cells were incubated at 37 °C for 90 min before the Krebs-Ringer solution was removed and a solution of the NBD-labelled hexose at the required concentration in glucose-free Krebs-Ringer solution (120 mM NaCl, 4 mM KCl, 1.2 mM  $\text{KH}_2\text{PO}_4$ , 2.5 mM  $\text{MgSO}_4$ , 25 mM  $\text{NaHCO}_3$ , 70  $\mu$ M  $\text{CaCl}_2$ , pH 7.4) was added. These solutions were prepared by diluting concentrated stock solutions of the NBD-labelled hexose in glucose-free Krebs-Ringer solution which were stored frozen. The plate was held in the 5%  $\text{CO}_2$  incubator at 37 °C and removed for the minimum time required to add NBD-labelled hexose solution to other wells during the experimental period. All wells were utilized in an order so that all experiments ended at the same time allowing for a single workup period for the plate.

At the end of the incubation period the NBD-labelled hexose containing solution was removed by aspiration and the cells were rinsed three times with glucose-free Krebs-Ringer solution. After the third rinse 5 drops of Trypsin-EDTA solution was added to each well and held in the 5%  $\text{CO}_2$  incubator at 37 °C for 5 min. 1 mL of glucose-free Krebs-Ringer solution was then added to each well and gently pipetted in place 10 times. The cell containing solution was then transferred to a centrifuge tube and spun at 125 x g for 10 min to form a cell pellet. Supernatant was removed by aspiration and the cell pellet was resuspended in 500  $\mu$ L of ice cold glucose-free Krebs-Ringer solution or 500  $\mu$ L of ice cold BD-Scientific cell fixation buffer. The tubes were stored on ice and transported directly to the FACS Canto II flow cytometer for analysis.

**Efflux Experiments:**

Growth media was removed and 750  $\mu\text{M}$  of sugar free Krebs-Ringer solution was added. The cells were held at 37 °C for 90 min before the media was removed and a 500  $\mu\text{M}$  solution of NBD-labelled hexose in glucose-free Krebs-Ringer solution was added to each well. The cells were then incubated in the 5%  $\text{CO}_2$  at 37 °C incubator for 1 hour. These solutions were prepared by diluting concentrated stock solutions of the NBD-labelled hexose in glucose-free Krebs-Ringer solution which were stored frozen. The NBD-labelled hexose containing solution was removed by aspiration and the cells were rinsed 3 times with glucose-free Krebs-Ringer solution. The cell plates were held in the 5%  $\text{CO}_2$  incubator at 37 °C at all times when not being handled. Time points were arranged to allow for all experiments to end at the same time allowing for one workup period for the plate. At the end of the experimental period the glucose-free Krebs-Ringer solution in the wells was removed by aspiration and the cells were rinsed three times with glucose-free Krebs-Ringer solution. The procedure to remove the cells from the plate which was used in uptake experiments was repeated and the cells were analysed by the FACS Canto II flow cytometer.

**Inhibition Experiments:**

The procedure for the uptake experiments was repeated except that the NBD-labelled hexose containing solution also contained the inhibitor at the specified concentration. These solutions were prepared by diluting concentrated stock solutions of the NBD-labelled hexose in glucose-free Krebs-Ringer solution which were stored frozen. Inhibitors were incorporated

from stock solutions prepared in glucose-free Krebs-Ringer solution which were stored frozen.

### **Control Studies:**

Cell cultures prepared as stated above were subjected to PBS buffer containing D-glucose or D-fructose at 0.5 mM, 1 mM, 2 mM, and 5 mM separately. These cells were incubated at 37 °C for 1 hour before being removed from the well as described above and analysed by flow cytometry. No change in the relative size or health was observed as measured by comparison of the FSC and SSC under standard flow cytometry conditions.

### **Data Analysis:**

Experiments were carried out in triplicate on sequential days using cells from a single bulk culture for all replicates. The average MFI at each time point was calculated along with the standard error. Error bars on graphs represent one unit of standard error in both the positive and negative direction from each time point. Comparison of uptake curves was done by determining if the difference between data at the same time point in different experiments was greater than the sum of one unit of standard error from each curve. In cases where uptake curves crossed each other at more than point, the time points between 40 min and 100 min were used to compare the graphs. To further aide in the determination of change between inhibited and control uptake studies linear regression was performed on each data set. The slopes of the trend lines were analysed via a t-test to determine if change was significant with a p value of 0.5. The formula for the trend line resulting from linear regression is listed in the legend of each figure under the label for each uptake line.

## 4.11: References:

- (1) Fulwyler, M. J., U. *Science* **1965**, *150*, 910–911.
- (2) Virgo, P. F.; Gibbs, G. J. *Ann. Clin. Biochem.* **2012**, *49* (1), 17–28.
- (3) Brown, M.; Wittwer, C. *Clin. Chem.* **2000**, *46* (8), 1221–1229.
- (4) Martin, J. C.; Swartzendruber, D. E. *Science* **1980**, *207* (4427), 199–201.
- (5) Laerum, O. D.; Farsund, T. *Cytometry* **1981**, *2* (1), 1–13.
- (6) Bakke, A. C. *Lab. Med.* **2001**, *32* (4), 207–211.
- (7) Otten, G. R.; Loken, M. R. *Cytometry* **1982**, *3* (3), 182–187.
- (8) Watt, S. M.; Burgess, A. W.; Metcalf, D.; Batty, F. L. *J. Histochem. Cytochem. Off. J. Histochem. Soc.* **1980**, *28* (9), 934–946.
- (9) Berney, M. *Microbiology* **2006**, *152* (6), 1719–1729.
- (10) Stevenson, A. P.; Martin, J. C.; Stewart, C. C. *Cancer Res.* **1986**, *46* (1), 99–105.
- (11) Basiji, D. A.; Orty, W. E.; Liang, L.; Venkatachalam, V.; Morrissey, P. *Clin. Lab. Med.* **2007**, *27* (3), 653–670.
- (12) Ohl, C.-D.; Wolfrum, B. *Biochim. Biophys. Acta BBA - Gen. Subj.* **2003**, *1624* (1–3), 131–138.
- (13) Wehrle, J. P.; Ng, C. E.; McGovern, K. A.; Aiken, N. R.; Shungu, D. C.; Chance, E. M.; Glickson, J. D. *NMR Biomed.* **2000**, *13* (6), 349–360.
- (14) Soule, H. D.; Maloney, T. M.; Wolman, S. R.; Peterson, W. D.; Brenz, R.; McGrath, C. M.; Russo, J.; Pauley, R. J.; Jones, R. F.; Brooks, S. C. *Cancer Res.* **1990**, *50* (18), 6075–6086.
- (15) Perez, O. D.; Nolan, G. P. *Nat. Biotechnol.* **2002**, *20* (2), 155–162.
- (16) BioTechniques - Two-step protocol for preparing adherent cells for high-throughput flow cytometry  
<http://www.biotechniques.com/BiotechniquesJournal/2015/September/Two-step-protocol-for-preparing-adherent-cells-for-high-throughput-flow-cytometry/biotechniques-360318.html> (accessed Jan 27, 2017).
- (17) Dimitriadis, G.; Maratou, E.; Boutati, E.; Psarra, K.; Papasteriades, C.; Raptis, S. A. *Cytometry A* **2005**, *64A* (1), 27–33.
- (18) Aller, C. B.; Ehmann, S.; Gilman-Sachs, A.; Snyder, A. K. *Cytometry* **1997**, *27* (3), 262–268.
- (19) Zou, C.; Wang, Y.; Shen, Z. *J. Biochem. Biophys. Methods* **2005**, *64* (3), 207–215.
- (20) Levi, J.; Cheng, Z.; Gheysens, O.; Patel, M.; Chan, C. T.; Wang, Y.; Namavari, M.; Gambhir, S. S. *Bioconjug. Chem.* **2007**, *18* (3), 628–634.
- (21) Soueidan, O.-M.; Scully, T. W.; Kaur, J.; Panigrahi, R.; Belovodskiy, A.; Do, V.; Matier, C. D.; Lemieux, M. J.; Wuest, F.; Cheeseman, C.; West, F. G. *ACS Chem. Biol.* **2017**, *12* (4), 1087–1094.
- (22) Rockwell, S. C.; Kallman, R. F.; Fajardo, L. F. *J. Natl. Cancer Inst.* **1972**, *49* (3), 735–749.
- (23) Dive, C.; Watson, J. V.; Workman, P. *Cancer Res.* **1991**, *51* (3), 799–806.
- (24) Dive, C.; Workman, P.; Watson, J. V. *Cytometry* **1987**, *8* (6), 552–561.
- (25) Wuest, M.; Trayner, B. J.; Grant, T. N.; Jans, H.-S.; Mercer, J. R.; Murray, D.; West, F. G.; McEwan, A. J. B.; Wuest, F.; Cheeseman, C. I. *Nucl. Med. Biol.* **2011**, *38* (4), 461–475.

- (26) Zamora-León, S. P.; Golde, D. W.; Concha, I. I.; Rivas, C. I.; Delgado-López, F.; Baselga, J.; Nualart, F.; Vera, J. C. *Proc. Natl. Acad. Sci.* **1996**, *93* (5), 1847–1852.
- (27) Drabovich, A. P.; Pavlou, M. P.; Dimitromanolakis, A.; Diamandis, E. P. *Mol. Cell. Proteomics* **2012**, *11* (8), 422–434.
- (28) Felix Bronner; Arnost Kleinzeller; Paul G. LeFevre. *Current Topics in Membranes and Transport*; Academic Press, 1975.
- (29) Rappoport, D. A.; Fritz, R. R.; Yamagami, S.; Herrmann, R. L.; Palladin, A. V.; Poljakova, N. M.; Schenkein, I.; Sokoloff, L.; Lajtha, A.; Marks, N.; Smythies, J. R.; Brodsky, W. A.; Shamoo, A. E.; Schwartz, I. L.; Wyssbrod, H. R.; Scott, W. N.; Brodsky, W. A.; Schwartz, I. L. *Metabolic Turnover in the Nervous System*; Springer Science & Business Media, 2013.
- (30) Naftalin, R. J. *Biochim. Biophys. Acta BBA - Biomembr.* **1997**, *1328* (1), 13–29.
- (31) Naftalin, R. J.; Rist, R. J. *Biochim. Biophys. Acta BBA - Biomembr.* **1994**, *1191* (1), 65–78.
- (32) Levine, K. B.; Robichaud, T. K.; Hamill, S.; Sultzman, L. A.; Carruthers, A. *Biochemistry (Mosc.)* **2005**, *44* (15), 5606–5616.
- (33) LeFevre, P. G. *Am. J. Physiol. Content* **1962**, *203* (2), 286–290.
- (34) Geck, P. *Biochim. Biophys. Acta BBA - Biomembr.* **1971**, *241* (2), 462–472.
- (35) Baker, G. F.; Widdas, W. F. *J. Physiol.* **1973**, *231* (1), 143–165.
- (36) May, J. M.; Beechem, J. M. *Biochemistry (Mosc.)* **1993**, *32* (11), 2907–2915.
- (37) Appleman, J. R.; Lienhard, G. E. *Biochemistry (Mosc.)* **1989**, *28* (20), 8221–8227.
- (38) Cunningham, P.; Afzal-Ahmed, I.; Naftalin, R. J. *J. Biol. Chem.* **2006**, *281* (9), 5797–5803.
- (39) Strobel, P.; Allard, C.; Perez-Acle, T.; Calderon, R.; Aldunate, R.; Leighton, F. *Biochem. J.* **2005**, *386* (3), 471–478.
- (40) Carruthers, A.; Helgerson, A. L. *Biochemistry (Mosc.)* **1991**, *30* (16), 3907–3915.
- (41) Walmsley, A. R.; Lowe, A. G.; Henderson, P. J. F. *Eur. J. Biochem.* **1994**, *221* (1), 513–522.
- (42) Manolescu, A.; Salas-Burgos, A. M.; Fischbarg, J.; Cheeseman, C. I. *J. Biol. Chem.* **2005**, *280* (52), 42978–42983.
- (43) Manolescu, A. R.; Augustin, R.; Moley, K.; Cheeseman, C. *Mol. Membr. Biol.* **2007**, *24* (5–6), 455–463.
- (44) *Physiol Res* **1999**, No. Lloyd, P. G., Hardin, C. D., Sturek, M., 401–410.

## Chapter 5: Conclusions and Future Directions

### 5.1: Conclusions

At the end of this research project several conclusions can be made about the D-fructose derivatives that have been produced and their reactivity. It is now clear that the oxidation of the C6 position of D-fructose to an aldehyde cannot be carried out in a worthwhile yield or scale. Though a small amount of the desired aldehyde was produced and isolated, as described in Chapter 2, this reaction proved to be non-scalable and has very poor reproducibility. A great deal of time was invested into this key reaction and the poor results obtained were a great disappointment. Based on observations of the isolated product is highly likely that the aldehyde was formed in these reactions but was unstable once formed, or decomposed during isolation and purification.

The C6 iodinated compounds produced and used extensively in Chapter 3 were found to be of fair synthetic utility allowing for the production of 6-deoxy-D-fructose in a short sequence. The radical ring closing reactions attempted failed to produce the desired product showing that the trans-fused six member ring system could not be formed in this case. These iodinated derivatives could act as intermediates towards other reactions in the future as a primary halogen is a versatile reactive handle.

Analysis by flow cytometry showed that 6NBDF was the best substrate for uptake into tumor cell lines. The C3, C4, and C5 epimers of this compound gave mixed results and little insight could be gained from these studies. A combination of the efflux properties of these compounds and the lag time between incubation and analysis by flow cytometry contributed heavily to the issues encountered. More rapid methods for analysis of these cell culture

studies, including the use of a fluorescent plate reader, have now replaced flow cytometry in this research stream. Both the ease of use and the quality of data derived from the fluorescent plate reader are superior to the flow cytometer for this application.<sup>1</sup>

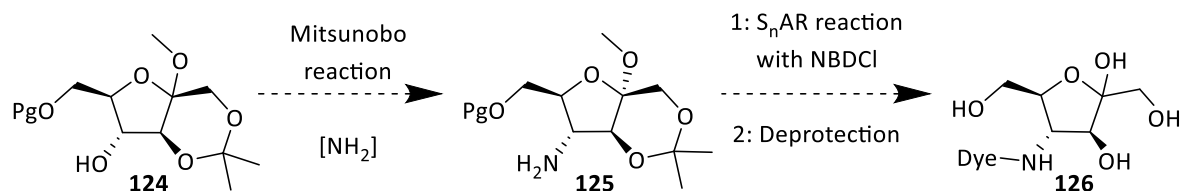
## 5.2: Future Directions

As the C6 position of D-fructose has proven to be a poor target for synthetic manipulation, other avenues in this research program must be considered. With modification of D-fructose at the C1 position having been explored by Gambhir and co-workers, the other functionalizable sites on D-fructose are left to be explored.<sup>2</sup> The recently published work by West and co-workers shows that the stereochemistry at C3, C4, and C5 must be maintained in order to favour recognition by GLUT5.<sup>1</sup>

In a recent publication from the West Group it was demonstrated that the replacement of the C3 hydroxyl of 2,5-anhydro-D-manitol with an amine capable of participating as a hydrogen bond donor maintained the hexoses ability to be transported by GLUT5. When the amine was functionalized to act only as a hydrogen bond acceptor the transport by GLUT5 was abolished and the hexose was found to be a GLUT1 substrate.<sup>3</sup> These findings suggest that the next step in this project should be to modify one or more of the C2, C3, and C4 positions while retaining the stereochemistry of these positions and their hydrogen bond properties.

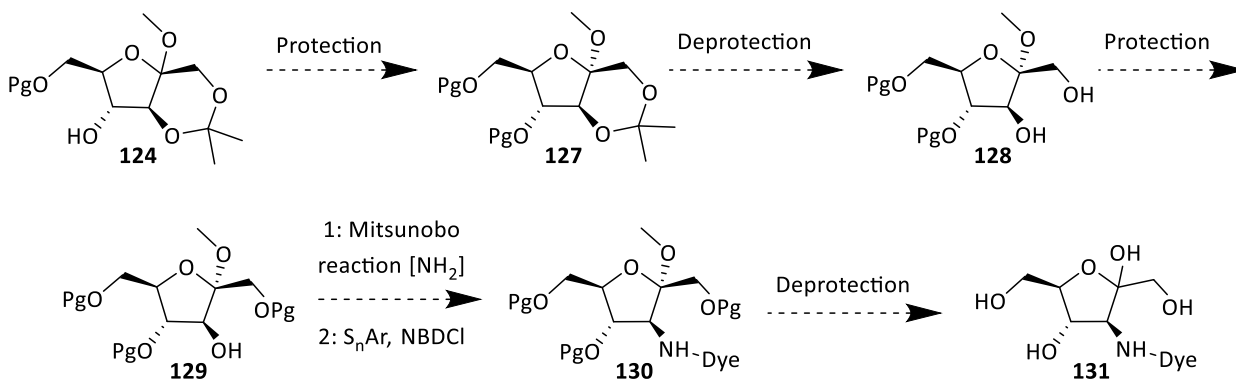
Selective protection/deprotection strategies could be employed to access these intermediates as shown in Scheme 5.1. The intermediate **124** leaves the C4 hydroxyl group open for functionalization to create a free amine **125**. This could be accomplished using a Mitsunobo reaction with a nitrogen source such as azide as used previously.<sup>4</sup> This

nucleophilic nitrogen atom could be used in a  $S_NAr$  type reaction with NBDCl and finally deprotected to form **126**. The protecting groups used in this process could be modified as required so that the coupling to the dye moiety and final deprotection are high yielding.



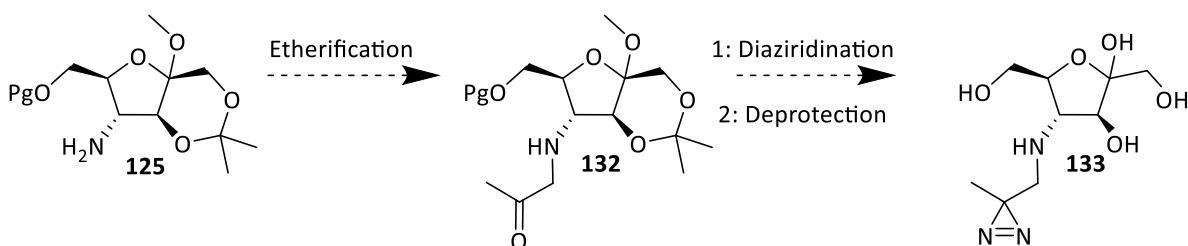
**Scheme 5.1: Approach to a D-fructose derivative modified at the C4 position.**

Accessing an intermediate that is vulnerable to modification at C2 is a more complex task but could be accomplished as shown in Scheme 5.2. Intermediate **124** could be fully protected to give **127** before the acetal protecting the C1 and C3 positions is removed leaving **128**. The primary and secondary hydroxyl groups at C1 and C3 respectively are chemically distinct which should allow for the C3 hydroxyl to be functionalized selectively giving **129**. An analogous method as described in Scheme 5.1 using Mitsunobo chemistry to introduce an amine followed by a  $S_NAr$  reaction to couple NBD to the hexose could be employed to produce **130**. Full deprotection to reveal **131** should be rapid and high yielding. This route requires several steps, nearly all of which are protecting group modifications, though most of these should be high yielding.



**Scheme 5.2: Approach to a D-fructose derivative modified at the C3 hydroxyl through a protection/deprotection strategy.**

The exact orientation of the hexose during the binding to GLUT5 is not fully known. Experimentally determining which amino acid residues are involved in the binding interaction would greatly aid in the development of new GLUT5 targeted probes. To help elucidate the exact binding interactions of GLUT5 and a D-fructose derived probe molecule a physical linking study could be carried out (Scheme 5.3). Following the example of Kohler and Tanaka<sup>5</sup> a diazirine containing D-fructose could be synthesised and incubated with GLUT5 expressing cells. Amine **125** could be alkylated with an alpha halo ketone to give **132** using the copper mediated methodology published by MacMillan and co-workers.<sup>6</sup> Subsequent diaziridination and deprotection would give **133**.



**Scheme 5.3: A possible route to produce 133, which could be used for photo cross linking to GLUT5.**

Upon exposure to light the diazirine would generate a reactive carbene that will link to the nearest amino acid residue. Digestion and analysis of GLUT5 after the photo cross linking would reveal which residues were cross linked to the D-fructose moiety. These results would

help identify the exact residues which interact during the binding event. This information, combined with the published crystal structure of GLUT5 should allow for a more rapid and targeted synthesis of GLUT5 probes.<sup>7</sup> With a map of which residues line the binding site derived from cross coupling results a more accurate map of the GLUT5 binding site could be modelled utilizing molecular modeling techniques. These types of models have been used to help explain the selectivity of GLUTS for varying hexoses and with more information about the binding site, could be used to help model a new, ideal substrate for GLUT5.<sup>1</sup>

### 5.3: References:

- (1) Soueidan, O.-M.; Scully, T. W.; Kaur, J.; Panigrahi, R.; Belovodskiy, A.; Do, V.; Matier, C. D.; Lemieux, M. J.; Wuest, F.; Cheeseman, C.; West, F. G. *ACS Chem. Biol.* **2017**, *12* (4), 1087–1094.
- (2) Levi, J.; Cheng, Z.; Gheysens, O.; Patel, M.; Chan, C. T.; Wang, Y.; Namavari, M.; Gambhir, S. S. *Bioconjug. Chem.* **2007**, *18* (3), 628–634.
- (3) Kumar Kondapi, V. P.; Soueidan, O.-M.; Cheeseman, C. I.; West, F. G. *Chem. – Eur. J.* **2017**, *23* (33), 8073–8081.
- (4) Kondapi, K.; Pavan, V.; Soueidan, O.-M.; Hosseini, S. N.; Jabari, N.; West, F. G. *Eur. J. Org. Chem.* **2016**, *2016* (7), 1367–1379.
- (5) Tanaka, Y.; Kohler, J. J. *J. Am. Chem. Soc.* **2008**, *130* (11), 3278–3279.
- (6) Evans, R. W.; Zbieg, J. R.; Zhu, S.; Li, W.; MacMillan, D. W. C. *J. Am. Chem. Soc.* **2013**, *135* (43), 16074–16077.
- (7) Nomura, N.; Verdon, G.; Kang, H. J.; Shimamura, T.; Nomura, Y.; Sonoda, Y.; Hussien, S. A.; Qureshi, A. A.; Coincon, M.; Sato, Y.; Abe, H.; Nakada-Nakura, Y.; Hino, T.; Arakawa, T.; Kusano-Arai, O.; Iwanari, H.; Murata, T.; Kobayashi, T.; Hamakubo, T.; Kasahara, M.; Iwata, S.; Drew, D. *Nature* **2015**, *526* (7573), 397–401.

## Bibliography:

### Chapter 1:

- (1) Kayano, T.; Burant, C. F.; Fukumoto, H.; Gould, G. W.; Fan, Y. S.; Eddy, R. L.; Byers, M. G.; Shows, T. B.; Seino, S.; Bell, G. I. *J. Biol. Chem.* **1990**, *265* (22), 13276–13282.
- (2) Marger, M. D.; Saier, M. H. *Trends Biochem. Sci.* **1993**, *18* (1), 13–20.
- (3) Joost, H.-G.; Bell, G. I.; Best, J. D.; Birnbaum, M. J.; Charron, M. J.; Chen, Y. T.; Doege, H.; James, D. E.; Lodish, H. F.; Moley, K. H.; Moley, J. F.; Mueckler, M.; Rogers, S.; Schürmann, A.; Seino, S.; Thorens, B. *Am. J. Physiol. - Endocrinol. Metab.* **2002**, *282* (4), E974–E976.
- (4) Uldry, M.; Thorens, B. *Pflüg. Arch.* **2003**, *447* (5), 480–489.
- (5) Sogin, D. C.; Hinkle, P. C. *J. Supramol. Struct.* **1978**, *8* (4), 447–453.
- (6) Micihiro Kashahara; Peter, C. Hinkle. *J Biol Chem* **1977**, *252* (20), 7384–7390.
- (7) Mueckler, M.; Caruso, C.; Baldwin, S. A.; Panico, M.; Blench, I.; Morris, H. R.; Allard, W. J.; Lienhard, G. E.; Lodish, H. F. *Science* **1985**, *229* (4717), 941–945.
- (8) Burant, C. F.; Takeda, J.; Brot-Laroche, E.; Bell, G. I.; Davidson, N. O. *J. Biol. Chem.* **1992**, *267* (21), 14523–14526.
- (9) Colville, C. A.; Seatter, M. J.; Gould, G. W. *Biochem. J.* **1993**, *294* (Pt 3), 753–760.
- (10) Colville, C. A.; Seatter, M. J.; Jess, T. J.; Gould, G. W.; Thomas, H. M. *Biochem. J.* **1993**, *290* (3), 701–706.
- (11) Uldry, M.; Ibberson, M.; Horisberger, J.-D.; Chatton, J.-Y.; Riederer, B. M.; Thorens, B. *EMBO J.* **2001**, *20* (16), 4467–4477.
- (12) Abramson, J.; Smirnova, I.; Kasho, V.; Verner, G.; Kaback, H. R.; Iwata, S. *Science* **2003**, *301* (5633), 610–615.
- (13) Chen, L.-Q.; Hou, B.-H.; Lalonde, S.; Takanaga, H.; Hartung, M. L.; Qu, X.-Q.; Guo, W.-J.; Kim, J.-G.; Underwood, W.; Chaudhuri, B.; Chermak, D.; Antony, G.; White, F. F.; Somerville, S. C.; Mudgett, M. B.; Frommer, W. B. *Nature* **2010**, *468* (7323), 527–532.
- (14) Tao, Y.; Cheung, L. S.; Li, S.; Eom, J.-S.; Chen, L.-Q.; Xu, Y.; Perry, K.; Frommer, W. B.; Feng, L. *Nature* **2015**, *527* (7577), 259–263.
- (15) Deng, D.; Xu, C.; Sun, P.; Wu, J.; Yan, C.; Hu, M.; Yan, N. *Nature* **2014**, *510* (7503), 121–125.
- (16) Nomura, N.; Verdon, G.; Kang, H. J.; Shimamura, T.; Nomura, Y.; Sonoda, Y.; Hussien, S. A.; Qureshi, A. A.; Coincon, M.; Sato, Y.; Abe, H.; Nakada-Nakura, Y.; Hino, T.; Arakawa, T.; Kusano-Arai, O.; Iwanari, H.; Murata, T.; Kobayashi, T.; Hamakubo, T.; Kasahara, M.; Iwata, S.; Drew, D. *Nature* **2015**, *526* (7573), 397–401.
- (17) Carruthers, A.; DeZutter, J.; Ganguly, A.; Devaskar, S. U. *Am. J. Physiol. - Endocrinol. Metab.* **2009**, *297* (4), E836–E848.
- (18) Manolescu, A. R.; Witkowska, K.; Kinnaird, A.; Cessford, T.; Cheeseman, C. *Physiology* **2007**, *22* (4), 234–240.
- (19) Mueckler, M. *Eur. J. Biochem.* **1994**, *219* (3), 713–725.
- (20) Zhao, F.-Q.; Keating, A. F. *Curr. Genomics* **2007**, *8* (2), 113–128.
- (21) Davies, A.; Ciardelli, T. L.; Lienhard, G. E.; Boyle, J. M.; Whetton, A. D.; Baldwin, S. A. *Biochem. J.* **1990**, *266* (3), 799–808.

- (22) Zuniga, F. A.; Shi, G.; Haller, J. F.; Rubashkin, A.; Flynn, D. R.; Iserovich, P.; Fischbarg, J. *J. Biol. Chem.* **2001**, *276* (48), 44970–44975.
- (23) Lachaal, M.; Rampal, A. L.; Lee, W.; Shi, Y.; Jung, C. Y. *J. Biol. Chem.* **1996**, *271* (9), 5225–5230.
- (24) Mueckler, M.; Makepeace, C. *J. Biol. Chem.* **2006**, *281* (48), 36993–36998.
- (25) Ibberson, M.; Uldry, M.; Thorens, B. *J. Biol. Chem.* **2000**, *275* (7), 4607–4612.
- (26) Sun, L.; Zeng, X.; Yan, C.; Sun, X.; Gong, X.; Rao, Y.; Yan, N. *Nature* **2012**, *490* (7420), 361–366.
- (27) Salas-Burgos, A.; Iserovich, P.; Zuniga, F.; Vera, J. C.; Fischbarg, J. *Biophys. J.* **2004**, *87* (5), 2990–2999.
- (28) Barnett, J. E.; Holman, G. D.; Chalkley, R. A.; Munday, K. A. *Biochem. J.* **1975**, *145* (3), 417–429.
- (29) Oleg Jardetzky. *Nature* **1966**, *211*, 969–970.
- (30) Anandkrishnan, R.; Zuckerman, D. M. *PLOS ONE* **2017**, *12* (3), e0173500.
- (31) Hoare, D. G. *Biochem. J.* **1972**, *127* (3), 62P.
- (32) Hernández, J. A. *J. Membr. Biol.* **1998**, *165* (3), 235–242.
- (33) Stein, W. D. *Ann. N. Y. Acad. Sci.* **1972**, *195* (1), 412–428.
- (34) Deng, D.; Sun, P.; Yan, C.; Ke, M.; Jiang, X.; Xiong, L.; Ren, W.; Hirata, K.; Yamamoto, M.; Fan, S.; Yan, N. *Nature* **2015**, *526* (7573), 391–396.
- (35) Madej, M. G.; Sun, L.; Yan, N.; Kaback, H. R. *Proc. Natl. Acad. Sci. U. S. A.* **2014**, *111* (7), E719–E727.
- (36) Madej, M. G.; Kaback, H. R. *Proc. Natl. Acad. Sci. U. S. A.* **2013**, *110* (50), E4831–E4838.
- (37) Madej, M. G.; Dang, S.; Yan, N.; Kaback, H. R. *Proc. Natl. Acad. Sci.* **2013**, *110* (15), 5870–5874.
- (38) Dimitriadis, G.; Maratou, E.; Boutati, E.; Psarra, K.; Papasteriades, C.; Raptis, S. A. *Cytometry A* **2005**, *64A* (1), 27–33.
- (39) Girniene, J.; Tatibouët, A.; Sackus, A.; Yang, J.; Holman, G. D.; Rollin, P. *Carbohydr. Res.* **2003**, *338* (8), 711–719.
- (40) Gould, G. W.; Holman, G. D. *Biochem. J.* **1993**, *295* (Pt 2), 329.
- (41) Carruthers, A.; Helgerson, A. L. *Biochemistry (Mosc.)* **1991**, *30* (16), 3907–3915.
- (42) Carruthers, A. *Physiol. Rev.* **1990**, *70* (4), 1135–1176.
- (43) Manolescu, A.; Salas-Burgos, A. M.; Fischbarg, J.; Cheeseman, C. I. *J. Biol. Chem.* **2005**, *280* (52), 42978–42983.
- (44) Manolescu, A. R.; Augustin, R.; Moley, K.; Cheeseman, C. *Mol. Membr. Biol.* **2007**, *24* (5–6), 455–463.
- (45) De Giorgis, V.; Veggiotti, P. *Seizure* **2013**, *22* (10), 803–811.
- (46) Brockmann, K. *Brain Dev.* **2009**, *31* (7), 545–552.
- (47) Wang, D.; Pascual, J. M.; De Vivo, D. In *GeneReviews*(®); Pagon, R. A., Adam, M. P., Ardinger, H. H., Wallace, S. E., Amemiya, A., Bean, L. J., Bird, T. D., Fong, C.-T., Mefford, H. C., Smith, R. J., Stephens, K., Eds.; University of Washington, Seattle: Seattle (WA), 1993.
- (48) Klepper, J. *Epilepsia* **2008**, *49*, 46–49.
- (49) Breast cancer statistics - Canadian Cancer Society <http://www.cancer.ca/en/cancer-information/cancer-type/breast/statistics/?region=bc> (accessed Dec 14, 2016).

- (50) Autier, P.; Boniol, M.; Smans, M.; Sullivan, R.; Boyle, P. *PLOS ONE* **2016**, *11* (4), e0154113.
- (51) Franklin D. Gaylis; Jae Choi; A. Karim Kader; Peter R. Eby; Tamer M. Fouad; H. Gilbert Welch; David H. Gorski; Peter C. Albertsen. *N. Engl. J. Med.* **2016**, *374* (6), 594–596.
- (52) Berry, D. A.; Cronin, K. A.; Plevritis, S. K.; Fryback, D. G.; Clarke, L.; Zelen, M.; Mandelblatt, J. S.; Yakovlev, A. Y.; Habbema, J. D. F.; Feuer, E. J. *N. Engl. J. Med.* **2005**, *353* (17), 1784–1792.
- (53) Warburg, O.; Wind, F.; Negelein, E. *J. Gen. Physiol.* **1927**, *8* (6), 519–530.
- (54) Koppenol, W. H.; Bounds, P. L.; Dang, C. V. *Nat. Rev. Cancer* **2011**, *11* (5), 325–337.
- (55) Kim, J.; Dang, C. V. *Cancer Res.* **2006**, *66* (18), 8927–8930.
- (56) Chan, D. A.; Sutphin, P. D.; Nguyen, P.; Turcotte, S.; Lai, E. W.; Banh, A.; Reynolds, G. E.; Chi, J.-T.; Wu, J.; Solow-Cordero, D. E.; Bonnet, M.; Flanagan, J. U.; Bouley, D. M.; Graves, E. E.; Denny, W. A.; Hay, M. P.; Giaccia, A. J. *Sci. Transl. Med.* **2011**, *3* (94), 94ra70–94ra70.
- (57) Gottlieb, E.; Tomlinson, I. P. M. *Nat. Rev. Cancer* **2005**, *5* (11), 857–866.
- (58) Elstrom, R. L.; Bauer, D. E.; Buzzai, M.; Karnauskas, R.; Harris, M. H.; Plas, D. R.; Zhuang, H.; Cinalli, R. M.; Alavi, A.; Rudin, C. M.; Thompson, C. B. *Cancer Res.* **2004**, *64* (11), 3892–3899.
- (59) Kim, J.; Dang, C. V. *Trends Biochem. Sci.* **2005**, *30* (3), 142–150.
- (60) Buchs, A. E.; Sasson, S.; Joost, H. G.; Cerasi, E. *Endocrinology* **1998**, *139* (3), 827–831.
- (61) Blakemore, S. J.; Aledo, J. C.; James, J.; Campbell, F. C.; Lucocq, J. M.; Hundal, H. S. *Biochem. J.* **1995**, *309* (Pt 1), 7–12.
- (62) Thorens, B.; Cheng, Z. Q.; Brown, D.; Lodish, H. F. *Am. J. Physiol.-Cell Physiol.* **1990**, *259* (2), C279–C285.
- (63) Wardzzala, L.J., Cushman, S.W., Salans, L.B. Mechanism of insulin action on glucose transport in the isolated rat adipose cell.8002.full.pdf  
<http://www.jbc.org/content/253/22/8002.full.pdf?sid=6037dd77-9afd-4b06-9d95-9bdfc30bda8f> (accessed Sep 29, 2016).
- (64) Zamora-León, S. P.; Golde, D. W.; Concha, I. I.; Rivas, C. I.; Delgado-López, F.; Baselga, J.; Nualart, F.; Vera, J. C. *Proc. Natl. Acad. Sci.* **1996**, *93* (5), 1847–1852.
- (65) Godoy, A.; Ulloa, V.; Rodríguez, F.; Reinicke, K.; Yañez, A. J.; García, M. de los A.; Medina, R. A.; Carrasco, M.; Barberis, S.; Castro, T.; Martínez, F.; Koch, X.; Vera, J. C.; Poblete, M. T.; Figueroa, C. D.; Peruzzo, B.; Pérez, F.; Nualart, F. *J. Cell. Physiol.* **2006**, *207* (3), 614–627.
- (66) Chan, K. k.; Chan, J. Y. W.; Chung, K. K. W.; Fung, K.-P. *J. Cell. Biochem.* **2004**, *93* (6), 1134–1142.
- (67) Gowrishankar, G.; Zitzmann-Kolbe, S.; Junutula, A.; Reeves, R.; Levi, J.; Srinivasan, A.; Bruus-Jensen, K.; Cyr, J.; Dinkelborg, L.; Gambhir, S. S. *PLoS ONE* **2011**, *6* (11), e26902.
- (68) Soule, H. D.; Maloney, T. M.; Wolman, S. R.; Peterson, W. D.; Brenz, R.; McGrath, C. M.; Russo, J.; Pauley, R. J.; Jones, R. F.; Brooks, S. C. *Cancer Res.* **1990**, *50* (18), 6075–6086.
- (69) Sreekumar, A.; Poisson, L. M.; Rajendiran, T. M.; Khan, A. P.; Cao, Q.; Yu, J.; Laxman, B.; Mehra, R.; Lonigro, R. J.; Li, Y.; Nyati, M. K.; Ahsan, A.; Kalyana-

- Sundaram, S.; Han, B.; Cao, X.; Byun, J.; Omenn, G. S.; Ghosh, D.; Pennathur, S.; Alexander, D. C.; Berger, A.; Shuster, J. R.; Wei, J. T.; Varambally, S.; Beecher, C.; Chinnaiyan, A. M. *Nature* **2009**, *457* (7231), 910–914.
- (70) Levi, J.; Cheng, Z.; Gheysens, O.; Patel, M.; Chan, C. T.; Wang, Y.; Namavari, M.; Gambhir, S. S. *Bioconjug. Chem.* **2007**, *18* (3), 628–634.
- (71) Crick, F. *Nature* **1970**, *227* (5258), 561–563.
- (72) James, M. L.; Gambhir, S. S. *Physiol. Rev.* **2012**, *92* (2), 897–965.
- (73) Wang, D. S.; Dake, M. D.; Park, J. M.; Kuo, M. D. *J. Vasc. Interv. Radiol.* **2006**, *17* (9), 1405–1423.
- (74) Nolting, D. D.; Nickels, M. L.; Guo, N.; Pham, W. *Am. J. Nucl. Med. Mol. Imaging* **2012**, *2* (3), 273–306.
- (75) Maschauer, S.; Prante, O. *BioMed Res. Int.* **2014**, *2014*, e214748.
- (76) Imam, S. K. *Cancer Biother. Radiopharm.* **2010**, *25* (3), 365–374.
- (77) Ntziachristos, V. *Nat. Methods* **2010**, *7* (8), 603–614.
- (78) Couturier, O.; Luxen, A.; Chatal, J.-F.; Vuillez, J.-P.; Rigo, P.; Hustinx, R. *Eur. J. Nucl. Med. Mol. Imaging* **2004**, *31* (8), 1182–1206.
- (79) Cox, B. L.; Mackie, T. R.; Eliceiri, K. W. *Am. J. Nucl. Med. Mol. Imaging* **2014**, *5* (1), 1–13.
- (80) Tu, Z.; Mach, R. H. *Curr. Top. Med. Chem.* **2010**, *10* (11), 1060–1095.
- (81) Lee, E. S.; Kim, T. S.; Kim, S.-K. *Korean J. Radiol.* **2015**, *16* (1), 21–31.
- (82) Fernández-Suárez, M.; Ting, A. Y. *Nat. Rev. Mol. Cell Biol.* **2008**, *9* (12), 929–943.
- (83) Fei, X.; Gu, Y. *Prog. Nat. Sci.* **2009**, *19* (1), 1–7.
- (84) Hayashi-Takanaka, Y.; Stasevich, T. J.; Kurumizaka, H.; Nozaki, N.; Kimura, H. *PLOS ONE* **2014**, *9* (9), e106271.
- (85) Fass, L. *Mol. Oncol.* **2008**, *2* (2), 115–152.
- (86) Frangioni, J. *Curr. Opin. Chem. Biol.* **2003**, *7* (5), 626–634.
- (87) Burdette, J. E. *J. Mol. Endocrinol.* **2008**, *40* (6), 253.
- (88) Pacák, J.; Točík, Z.; Černý, M. *J. Chem. Soc. Chem. Commun.* **1969**, No. 2, 77–77.
- (89) Nasim Khan; Noboru Oriuchi; Tetsuya Higuchi; Keigo Endo. *Cancer Control* **2005**, *12* (4), 254–260.
- (90) Surasi, D. S.; Bhambhvani, P.; Baldwin, J. A.; Almodovar, S. E.; O'Malley, J. P. *J. Nucl. Med. Technol.* **2014**, *42* (1), 5–13.
- (91) Tse, N. Y.; Hoh, C. K.; Hawkins, R. A.; Zinner, M. J.; Dahlbom, M.; Choi, Y.; Maddahi, J.; Brunicardi, F. C.; Phelps, M. E.; Glaspy, J. A. *Ann. Surg.* **1992**, *216* (1), 27–34.
- (92) Krivokapich, J.; Barrio, J. R.; Huang, S.-C.; Schelbert, H. R. *J. Am. Coll. Cardiol.* **1990**, *16* (5), 1158–1167.
- (93) Boellaard, R.; O'Doherty, M. J.; Weber, W. A.; Mottaghy, F. M.; Lonsdale, M. N.; Stroobants, S. G.; Oyen, W. J. G.; Kotzerke, J.; Hoekstra, O. S.; Pruim, J.; Marsden, P. K.; Tatsch, K.; Hoekstra, C. J.; Visser, E. P.; Arends, B.; Verzijlbergen, F. J.; Zijlstra, J. M.; Comans, E. F. I.; Lammertsma, A. A.; Paans, A. M.; Willemsen, A. T.; Beyer, T.; Bockisch, A.; Schaefer-Prokop, C.; Delbeke, D.; Baum, R. P.; Chiti, A.; Krause, B. *J. Eur. J. Nucl. Med. Mol. Imaging* **2010**, *37* (1), 181–200.
- (94) Brown, R. S.; Wahl, R. L. *Cancer* **1993**, *72* (10), 2979–2985.
- (95) Jr, B.; Ns, M.; Jr, R. G.; A, N.; Js, C.; De, K. *J. Nucl. Med. Off. Publ. Soc. Nucl. Med.* **1981**, *22* (4), 372–375.

- (96) Kiselev, M. Y.; Lai, D. Process and apparatus for production of F-18 fluoride. US6567492 B2, May 20, 2003.
- (97) Carlson, C. H.; Singer, L.; Service, D. H.; Armstrong, W. D. *Int. J. Appl. Radiat. Isot.* **1959**, *4* (3), 210–213.
- (98) Tahiri, M.; Doppelt, P.; Fischer, J.; Weiss, R. *ResearchGate* **1987**, *127* (1), L1–L3.
- (99) Lee, C.-C.; Sui, G.; Elizarov, A.; Shu, C. J.; Shin, Y.-S.; Dooley, A. N.; Huang, J.; Daridon, A.; Wyatt, P.; Stout, D.; Kolb, H. C.; Witte, O. N.; Satyamurthy, N.; Heath, J. R.; Phelps, M. E.; Quake, S. R.; Tseng, H.-R. *Science* **2005**, *310* (5755), 1793–1796.
- (100) Yeung, H. W. D.; Grewal, R. K.; Gonen, M.; Schöder, H.; Larson, S. M. *J. Nucl. Med.* **2003**, *44* (11), 1789–1796.
- (101) Cohade, C.; Osman, M.; Leal, J.; Wahl, R. L. *J. Nucl. Med.* **2003**, *44* (11), 1797–1803.
- (102) Chang, J. M.; Lee, H. J.; Goo, J. M.; Lee, H.-Y.; Lee, J. J.; Chung, J.-K.; Im, J.-G. *Korean J. Radiol.* **2006**, *7* (1), 57.
- (103) Rosenbaum, S. J.; Lind, T.; Antoch, G.; Bockisch, A. *Eur. Radiol.* **2005**, *16* (5), 1054–1065.
- (104) Speizer, L.; Haugland, R.; Kutchai, H. *Biochim. Biophys. Acta BBA - Biomembr.* **1985**, *815* (1), 75–84.
- (105) Aller, C. B.; Ehmann, S.; Gilman-Sachs, A.; Snyder, A. K. *Cytometry* **1997**, *27* (3), 262–268.
- (106) Barros, L. F.; Bittner, C. X.; Loaiza, A.; Ruminot, I.; Larenas, V.; Moldenhauer, H.; Oyarzún, C.; Alvarez, M. *J. Neurochem.* **2009**, *109*, 94–100.
- (107) DiNuzzo, M.; Giove, F.; Maraviglia, B.; Mangia, S. *J. Neurochem.* **2013**, *125* (2), 236–246.
- (108) Chen, Y.; Zhang, J.; Zhang, X. *J. Mol. Neurosci.* **2015**, *55* (1), 126–130.
- (109) Raesi, E.; Mir, L. M. *J. Membr. Biol.* **2012**, *245* (10), 633–642.
- (110) Yamamoto, T.; Tanaka, S.; Suga, S.; Watanabe, S.; Nagatomo, K.; Sasaki, A.; Nishiuchi, Y.; Teshima, T.; Yamada, K. *Bioorg. Med. Chem. Lett.* **2011**, *21* (13), 4088–4096.
- (111) Zou, C.; Wang, Y.; Shen, Z. *J. Biochem. Biophys. Methods* **2005**, *64* (3), 207–215.
- (112) Nitin, N.; Carlson, A. L.; Muldoon, T.; El-Naggar, A. K.; Gillenwater, A.; Richards-Kortum, R. *Int. J. Cancer* **2009**, *124* (11), 2634–2642.
- (113) Tao, J.; Diaz, R. K.; Teixeira, C. R. V.; Hackmann, T. J. *Biochemistry (Mosc.)* **2016**, *55* (18), 2578–2589.
- (114) Yoshioka, K.; Saito, M.; Oh, K.-B.; Nemoto, Y.; Matsuoka, H.; Natsume, M.; Abe, H. *Biosci. Biotechnol. Biochem.* **1996**, *60* (11), 1899–1901.
- (115) Zou, C.; Wang, Y.; Shen, Z. *J. Biochem. Biophys. Methods* **2005**, *64* (3), 207–215.
- (116) DiNuzzo, M.; Giove, F.; Maraviglia, B.; Mangia, S. *J. Neurochem.* **2013**, *125* (2), 236–246.
- (117) Tatibouët, A.; Yang, J.; Morin, C.; Holman, G. D. *Bioorg. Med. Chem.* **2000**, *8* (7), 1825–1833.
- (118) Jing, Y.; Dowden, J.; Tatibouët, A.; Hatanaka, Y.; Holman, G. D. *Biochem. J.* **2002**, *367* (2), 533–539.
- (119) Inukai, K.; Katagiri, H.; Takata, K.; Asano, T.; Anai, M.; Ishihara, H.; Nakazaki, M.; Kikuchi, M.; Yazaki, Y.; Oka, Y. *Endocrinology* **1995**, *136* (11), 4850–4857.
- (120) Tanasova, M.; Plutschack, M.; Muroski, M. E.; Sturla, S. J.; Strouse, G. F.; McQuade, D. T. *ChemBioChem* **2013**, *14* (10), 1263–1270.

- (121) Trayner, B. J.; Grant, T. N.; West, F. G.; Cheeseman, C. I. *Bioorg. Med. Chem.* **2009**, *17* (15), 5488–5495.
- (122) Soueidan, O.-M.; Scully, T. W.; Kaur, J.; Panigrahi, R.; Belovodskiy, A.; Do, V.; Matier, C. D.; Lemieux, M. J.; Wuest, F.; Cheeseman, C.; West, F. G. *ACS Chem. Biol.* **2017**, *12* (4), 1087–1094.
- (123) Wuest, M.; Trayner, B. J.; Grant, T. N.; Jans, H.-S.; Mercer, J. R.; Murray, D.; West, F. G.; McEwan, A. J. B.; Wuest, F.; Cheeseman, C. I. *Nucl. Med. Biol.* **2011**, *38* (4), 461–475.
- (124) Niu, B.; Wen, X.; Jia, Z.; Wu, X.; Guo, W.; Sun, H. *Chin. J. Chem.* **2013**, *31* (9), 1159–1163.
- (125) Padgett, H. C.; Schmidt, D. G.; Luxen, A.; Bida, G. T.; Satyamurthy, N.; Barrio, J. R. *Int. J. Rad. Appl. Instrum. [A]* **1989**, *40* (5), 433–445.
- (126) Soueidan, O.-M.; Trayner, B. J.; Grant, T. N.; Henderson, J. R.; Wuest, F.; West, F. G.; Cheeseman, C. I. *Org. Biomol. Chem.* **2015**, *13* (23), 6511–6521.
- (127) Banhegyi, G.; Csala, M.; Benedetti, A. *J. Mol. Endocrinol.* **2008**, *42* (4), 283–289.
- (128) Mulukutla, B. C.; Khan, S.; Lange, A.; Hu, W.-S. *Trends Biotechnol.* **2010**, *28* (9), 476–484.
- (129) Akram, M.; Hamid, A. *Obes. Res. Clin. Pract.* **2013**, *7* (2), e89–e94.
- (130) Malaisse, W.J., et al. *Int J Biochem* **1991**, *23* (12), 1471–1481.
- (131) Malaisse, W.J., et al. *Diabetes Res* **1991**, *16* (1), 19–24.
- (132) Raushel, F. M.; Cleland, W. W. *J. Biol. Chem.* **1973**, *248* (23), 8174–8177.
- (133) Bais, R.; James, H. M.; Rofe, A. M.; Conyers, R. A. *Biochem. J.* **1985**, *230* (1), 53–60.

## Chapter 2:

- (1) Litjens, R. E. J. N.; van den Bos, L. J.; Codée, J. D. C.; Overkleeft, H. S.; van der Marel, G. A. *Carbohydr. Res.* **2007**, *342* (3–4), 419–429.
- (2) Angyal, S. J.; Bethell, G. S. *Aust. J. Chem.* **1976**, *29* (6), 1249–1265.
- (3) Pétursson, S. *J. Chem. Educ.* **1997**, *74* (11), 1297.
- (4) Yu, K.; Zhao, X.; Wu, W.; Hong, Z. *Tetrahedron Lett.* **2013**, *54* (22), 2788–2790.
- (5) Hanaya, T.; Sato, N.; Yamamoto, H. *Carbohydr. Res.* **2005**, *340* (16), 2494–2501.
- (6) Lewandowska, E.; Neschadimenko, V.; Wnuk, S. F.; Robins, M. J. *Tetrahedron* **1997**, *53* (18), 6295–6302.
- (7) Helferich, B. In *Advances in Carbohydrate Chemistry*; W.W. Pigman, M. L. W. and S. P., Ed.; Academic Press, 1948; Vol. 3, pp 79–111.
- (8) Lu, R. J.; Liu, D.; Giese, R. W. *Tetrahedron Lett.* **2000**, *41* (16), 2817–2819.
- (9) Bowden, K.; Heilbron, I. M.; Jones, E. R. H.; Weedon, B. C. L. *J. Chem. Soc.* **1946**, No. 0, 39–45.
- (10) Jefford, C. W.; Wang, Y. *J. Chem. Soc., Chem. Commun.* **1988**, No. 10, 634–635.
- (11) Omura, K.; Sharma, A. K.; Swern, D. *J. Org. Chem.* **1976**, *41* (6), 957–962.
- (12) Tojo, G.; Fernandez, M. I. *Oxidation of Alcohols to Aldehydes and Ketones: A Guide to Current Common Practice*; Springer Science & Business Media, 2006.
- (13) Jeong, T. S.; Choi, C. H.; Lee, J. Y.; Oh, K. K. *Bioresour. Technol.* **2012**, *116*, 435–440.
- (14) Omura, K.; Swern, D. *Tetrahedron* **1978**, *34* (11), 1651–1660.
- (15) Pfitzner, K. E.; Moffatt, J. G. *J. Am. Chem. Soc.* **1963**, *85* (19), 3027–3028.

- (16) Parikh, J. R.; Doering, W. v. E. *J. Am. Chem. Soc.* **1967**, *89* (21), 5505–5507.
- (17) Golubev, V. A.; Voronina, G. N.; Rozantsev, E. G. *Bull. Acad. Sci. USSR Div. Chem. Sci.* **1970**, *19* (11), 2449–2451.
- (18) Cella, J. A.; Kelley, J. A.; Kenahan, E. F. *J. Org. Chem.* **1975**, *40* (12), 1860–1862.
- (19) Lucio Anelli, P.; Biffi, C.; Montanari, F.; Quici, S. *J. Org. Chem.* **1987**, *52* (12), 2559–2562.
- (20) Zhao, M.; Li, J.; Mano, E.; Song, Z.; Tschaen, D. M.; Grabowski, E. J. J.; Reider, P. J. *J. Org. Chem.* **1999**, *64* (7), 2564–2566.
- (21) Sen, V. D.; Golubev, V. A. *J. Phys. Org. Chem.* **2009**, *22* (2), 138–143.
- (22) Bobbitt, J. M. *ChemInform* **2011**, *42* (21), 1–10.
- (23) Ma, Y.; Loyns, C.; Price, P.; Chechik, V. *Org. Biomol. Chem.* **2011**, *9* (15), 5573–5578.
- (24) Sheldon, R. A.; Arends, I. W. C. E.; ten Brink, G.-J.; Dijkman, A. *Acc. Chem. Res.* **2002**, *35* (9), 774–781.
- (25) Angelin, M.; Hermansson, M.; Dong, H.; Ramström, O. *Eur. J. Org. Chem.* **2006**, *2006* (19), 4323–4326.
- (26) Hamada, S.; Wada, Y.; Sasamori, T.; Tokitoh, N.; Furura, T.; Kawabata, T. *Tetrahedron Lett.* **2014**, *55* (11), 1943–1945.
- (27) Zhdankin, V. V. *Arkivoc* **2009**, *1*, 1–62.
- (28) Reddy, S. R.; Stella, S.; Chadha, A. *Synth. Commun.* **2012**, *42* (23), 3493–3503.
- (29) Liu, J.; Ma, S. *Tetrahedron* **2013**, *69* (47), 10161–10167.
- (30) Liu, J.; Ma, S. *Org. Biomol. Chem.* **2013**, *11* (25), 4186–4193.
- (31) Dess, D. B.; Martin, J. C. *J. Org. Chem.* **1983**, *48* (22), 4155–4156.
- (32) Meyer, S. D.; Schreiber, S. L. *J. Org. Chem.* **1994**, *59* (24), 7549–7552.
- (33) Yadav, J. S.; Reddy, B. V. S.; Basak, A. K.; Venkat Narsaiah, A. *Tetrahedron* **2004**, *60* (9), 2131–2135.
- (34) More, J. D.; Finney, N. S. *Org. Lett.* **2002**, *4* (17), 3001–3003.
- (35) Marco Frigerio, Marco Santagostino, Simona Sputore, and Giovanni Palmisano. *J. Org. Chem.* **1995**, *60*, 7272–7276.
- (36) Guérin, C.; Bellosta, V.; Guillamot, G.; Cossy, J. *Org. Lett.* **2011**, *13* (13), 3534–3537.
- (37) Uyanik, M.; Ishihara, K. *Chem. Commun.* **2009**, No. 16, 2086.
- (38) Tohma, H.; Kita, Y. *Adv. Synth. Catal.* **2004**, *346* (23), 111–124.
- (39) Thottumkara, A. P.; Bowsher, M. S.; Vinod, T. K. *Org. Lett.* **2005**, *7* (14), 2933–2936.
- (40) Nicolaou, K. C.; Mathison, C. J. N.; Montagnon, T. *J. Am. Chem. Soc.* **2004**, *126* (16), 5192–5201.
- (41) Piccialli, V.; Zaccaria, S.; Oliviero, G.; D’Errico, S.; D’Atri, V.; Borbone, N. *Eur. J. Org. Chem.* **2012**, *2012* (23), 4293–4305.
- (42) Minkyung Lim,; Seungchan Oh,; and Hakjune Rhee. *Bull Korean Chem Soc* **2011**, *32* (8), 3179–3182.
- (43) Hoover, J. M.; Stahl, S. S. *J. Am. Chem. Soc.* **2011**, *133* (42), 16901–16910.
- (44) Markó, I. E.; Gautier, A.; Dumeunier, R.; Doda, K.; Philippart, F.; Brown, S. M.; Urch, C. J. *Angew. Chem. Int. Ed.* **2004**, *43* (12), 1588–1591.
- (45) Xu, B.; Lumb, J.-P.; Arndtsen, B. A. *Angew. Chem. Int. Ed.* **2015**, *54* (14), 4208–4211.
- (46) Allen, S. E.; Walvoord, R. R.; Padilla-Salinas, R.; Kozlowski, M. C. *Chem. Rev.* **2013**, *113* (8), 6234–6458.
- (47) Hoover, J. M.; Ryland, B. L.; Stahl, S. S. *J. Am. Chem. Soc.* **2013**, *135* (6).
- (48) Hoover, J. M.; Steves, J. E.; Stahl, S. S. *Nat. Protoc.* **2012**, *7* (6), 1161–1166.

- (49) Esguerra, K. V. N.; Fall, Y.; Petitjean, L.; Lumb, J.-P. *J. Am. Chem. Soc.* **2014**, *136* (21), 7662–7668.
- (50) Ley, S. V.; Norman, J.; Griffith, W. P.; Marsden, S. P. *Synthesis* **1994**, *1994* (7), 639–666.
- (51) Griffith, W. P.; Ley, S. V.; Whitcombe, G. P.; White, A. D. *J. Chem. Soc., Chem. Commun.* **1987**, No. 21, 1625–1627.
- (52) Schmidt, A.-K. C.; Stark, C. B. W. *Org. Lett.* **2011**, *13* (16), 4164–4167.
- (53) J. Zerk, T.; W. Moore, P.; M. Williams, C.; V. Bernhardt, P. *Chem. Commun.* **2016**, *52* (67), 10301–10304.
- (54) Read, C. D. G.; Moore, P. W.; Williams, C. M. *Green Chem* **2015**, *17* (9), 4537–4540.
- (55) Moore, P. W.; Mirzayans, P. M.; Williams, C. M. *Chem. – Eur. J.* **2015**, *21* (9), 3567–3571.
- (56) Appel, R. *Angew. Chem. Int. Ed. Engl.* **1975**, *14* (12), 801–811.
- (57) Skaanderup, P. R.; Poulsen, C. S.; Hyldtoft, L.; Jørgensen, M. R.; Madsen, R. *Synthesis* **2002**, *2002* (12), 1721–1727.
- (58) Kornblum, N.; Powers, J. W.; Anderson, G. J.; Jones, W. J.; Larson, H. O.; Levand, O.; Weaver, W. M. *J. Am. Chem. Soc.* **1957**, *79* (24), 6562–6562.
- (59) Kwon, H. B.; von Itzstein, M.; Jung, K.-Y. *Tetrahedron Lett.* **2009**, *50*, 2543–2544
- (60) Wang, G.-N.; Yang, L.; Zhang, Li-H.; Ye, X.-S. *J. Org. Chem.* **2011** *76*, 2001–2009

### Chapter 3:

- (1) Harutyunyan, S. R.; López, F.; Browne, W. R.; Correa, A.; Peña, D.; Badorrey, R.; Meetsma, A.; Minnaard, A. J.; Feringa, B. L. *J. Am. Chem. Soc.* **2006**, *128* (28), 9103–9118.
- (2) Normant, J. F. *Synthesis* **1972**, *1972* (2), 63–80.
- (3) Lai, Y.-H. *Synthesis* **1981**, *1981* (8), 585–604.
- (4) Grignard, V. *Compt Rend* **1900**, *130*, 1322.
- (5) Gilman, H.; Jones, R. G.; Woods, L. A. *J. Org. Chem.* **1952**, *17* (12), 1630–1634.
- (6) Barbier, P. *Compt Rend* **1899**, *128*, 110.
- (7) Wu, G.; Huang, M. *Chem. Rev.* **2006**, *106* (7), 2596–2616.
- (8) Lauritsen, A.; Madsen, R. *Org. Biomol. Chem.* **2006**, *4* (15), 2898.
- (9) White, J. D.; Hrcnciar, P. *J. Org. Chem.* **2000**, *65* (26), 9129–9142.
- (10) Bailey, W. F.; Patricia, J. J.; Nurmi, T. T.; Wang, W. *Tetrahedron Lett.* **1986**, *27* (17), 1861–1864.
- (11) Rogers, H. R.; Houk, J. *J. Am. Chem. Soc.* **1982**, *104* (2), 522–525.
- (12) Farnham, W. B.; Calabrese, J. C. *J. Am. Chem. Soc.* **1986**, *108* (9), 2449–2451.
- (13) Bailey, W. F.; Patricia, J. J. *J. Organomet. Chem.* **1988**, *352* (1), 1–46.
- (14) Ovaska, T. V.; Snieckus, V.; Nolte, B. In *Encyclopedia of Reagents for Organic Synthesis*; John Wiley & Sons, Ltd, 2001.
- (15) Bailey, W. F.; Wachter-Jurcsak, N. In *Encyclopedia of Reagents for Organic Synthesis*; John Wiley & Sons, Ltd, 2001.
- (16) Aidhen, I. S.; Ahuja, J. R. *Tetrahedron Lett.* **1992**, *33* (37), 5431–5432.
- (17) Guimarães, R. L.; Lima, D. J.; Barros, M. E. S.; Cavalcanti, L. N.; Hallwass, F.; Navarro, M.; Bieber, L. W.; Malvestiti, I. *Molecules* **2007**, *12* (9), 2089–2105.
- (18) Majumdar, K. K. *Tetrahedron Asymmetry* **1997**, *8* (13), 2079–2082.

- (19) Costello, D. P.; Geraghty, N. W. A. *Synth. Commun.* **1999**, *29* (18), 3083–3096.
- (20) Tuanjie, M.; Xianqiang, H.; Jin-Xian, W.; Li, X. *Chin. J. Org. Chem.* **2014**, *35* (3), 712–718.
- (21) Jõgi, A.; Mäeorg, U. *Molecules* **2001**, *6* (12), 964–968.
- (22) Breton, G. W.; Shugart, J. H.; Hughey, C. A.; Conrad, B. P.; Perala, S. M. *Molecules* **2001**, *6* (8), 655–662.
- (23) Basu, M. K.; Banik, B. K. *Tetrahedron Lett.* **2001**, *42* (2), 187–189.
- (24) Curran, D. P.; Xin, G.; Zhang, W.; Dowd, P. *Tetrahedron* **1997**, *53* (27), 9023–9042.
- (25) Haddad, T. D.; Hirayama, L. C.; Singaram, B. *J. Org. Chem.* **2010**, *75* (3), 642–649.
- (26) Wang, Z. In *Comprehensive Organic Name Reactions and Reagents*; John Wiley & Sons, Inc., 2010.
- (27) Blomberg, P. D. C. In *The Barbier Reaction and Related One-Step Processes; Reactivity and Structure: Concepts in Organic Chemistry*; Springer Berlin Heidelberg, 1993; pp 137–165.
- (28) Moyano, A.; Perica's, M. A.; Riera, A.; Luche, J.-L. *Tetrahedron Lett.* **1990**, *31* (52), 7619–7622.
- (29) Chérest, M.; Felkin, H. *Tetrahedron Lett.* **1968**, *9* (18), 2205–2208.
- (30) Keinicke, L.; Fristrup, P.; Norrby, P.-O.; Madsen, R. *J. Am. Chem. Soc.* **2005**, *127* (45), 15756–15761.
- (31) Wong, C. H.; Mazenod, F. P.; Whitesides, G. M. *J. Org. Chem.* **1983**, *48* (20), 3493–3497.
- (32) Partibha Choudhary; , Varun Sharma; , Hari Om; , Poonam Devi. *Am. J. Chem.* **2013**, *3* (5), 115–125.
- (33) Wu, S.; Li, Y.; Zhang, S. *J. Org. Chem.* **2016**, *81* (17), 8070–8076.
- (34) Takahashi, K.; Komine, K.; Yokoi, Y.; Ishihara, J.; Hatakeyama, S. *J. Org. Chem.* **2012**, *77* (17), 7364–7370.
- (35) Wilson, S. R.; Guazzaroni, M. E. *J. Org. Chem.* **1989**, *54* (13), 3087–3091.
- (36) Li, C. *J. Chem. Rev.* **1993**, *93* (6), 2023–2035.
- (37) Kobayashi, S. *Chem. Commun.* **1998**, No. 1, 19–20.
- (38) Kobayashi, S.; Wakabayashi, T.; Oyamada, H. *Chem. Lett.* **1997**, *26* (8), 831–832.
- (39) Manabe, K.; Mori, Y.; Wakabayashi, T.; Nagayama, S.; Kobayashi, S. *J. Am. Chem. Soc.* **2000**, *122* (30), 7202–7207.
- (40) Kobayashi, S.; Wakabayashi, T.; Nagayama, S.; Oyamada, H. *Tetrahedron Lett.* **1997**, *38* (26), 4559–4562.
- (41) Firouzabadi, H.; Iranpoor, N.; Jafari, A. A. *Adv. Synth. Catal.* **2005**, *347* (5), 655–661.
- (42) Kong, W.; Fu, C.; Ma, S. *Org. Biomol. Chem.* **2008**, *6* (24), 4587–4592.
- (43) Sun, X.-W.; Xu, M.-H.; Lin, G.-Q. *Org. Lett.* **2006**, *8* (21), 4979–4982.
- (44) Li, C.-J. *Tetrahedron* **1996**, *52* (16), 5643–5668.
- (45) Augé, J.; Lubin-Germain, N.; Marque, S.; Seghrouchni, L. *ResearchGate* **2003**, *679* (1), 79–83.
- (46) Choi, S.-K.; Lee, S.; Whitesides, G. M. *J. Org. Chem.* **1996**, *61* (25), 8739–8745.
- (47) Chan, T.-H.; Lee, M.-C. *J. Org. Chem.* **1995**, *60* (13), 4228–4232.
- (48) Pardoe, J. A. J.; Downs, A. J. *Chem. Rev.* **2007**, *107* (1), 2–45.
- (49) Hepler, L. G.; Hugus, Z. Z.; Latimer, W. M. *J. Am. Chem. Soc.* **1953**, *75* (22), 5652–5654.
- (50) Gynane, M. J. S.; Worrall, I. J. *J. Organomet. Chem.* **1974**, *81* (3), 329–334.

- (51) Paul B. McCay; Edward K. Lai; J. Lee Poyer; Coit M. DuBose; Edward G. Janzen. *J. Biol. Chem.* **1994**, 259 (4), 2135–2143.
- (52) Wright, J. S.; Shadnia, H.; Chepelev, L. L. *J. Comput. Chem.* **2009**, 30 (7), 1016–1026.
- (53) McBay, H. C.; Tucker, O. *J. Org. Chem.* **1954**, 19 (6), 869–883.
- (54) Gray, P.; Williams, A. *Chem. Rev.* **1959**, 59 (2), 239–328.
- (55) Benson, S. W. *J. Am. Chem. Soc.* **1964**, 86 (19), 3922–3924.
- (56) Svein Saebo; Leo Radom. *J. Chem. Phys.* **1983**, 78 (2), 845–853.
- (57) Oliveira, R. B. de; Alves, R. J.; Souza Filho, J. D. de; Prado, M. A. F. *J. Braz. Chem. Soc.* **2003**, 14 (3), 442–448.
- (58) de Oliveira, M. T.; Cesar, A.; Leal, D. H. S.; Prado, M. A. F.; da Silva, T. H. Á.; Alves, R. J. *Org. Biomol. Chem.* **2010**, 8 (7), 1619.
- (59) de Oliveira, R. B.; de Souza Filho, J. D.; Prado, M. A. F.; Eberlin, M. N.; Meurer, E. C.; Santos, L. S.; Alves, R. J. *Tetrahedron* **2004**, 60 (44), 9901–9908.
- (60) Neises, B.; Steglich, W. *Angew. Chem. Int. Ed. Engl.* **1978**, 17 (7), 522–524.
- (61) Barth, F.; O-Yang, C. *Tetrahedron Lett.* **1990**, 31 (8), 1121–1124.
- (62) Baldwin, J. E.; Adlington, R. M.; Mitchell, M. B.; Robertson, J. *J. Chem. Soc. Chem. Commun.* **1990**, No. 22, 1574–1575.
- (63) Ishizaki, M.; Ozaki, K.; Kanematsu, A.; Isoda, T.; Hoshino, O. *J. Org. Chem.* **1993**, 58 (15), 3877–3885.
- (64) Bowman, W. R.; Mann, E.; Parr, J. *J. Chem. Soc. [Perkin I]* **2000**, No. 17, 2991–2999.
- (65) Porter, N. A.; Chang, V. H. T.; Magnin, D. R.; Wright, B. T. *J. Am. Chem. Soc.* **1988**, 110 (11), 3554–3560.
- (66) Baldwin, J. E. *J. Chem. Soc., Chem. Commun.* **1976**, No. 18, 734–736.
- (67) Zemek, J.; Kučár, Š. *Collect. Czechoslov. Chem. Commun.* **1988**, 53 (1), 173–180.
- (68) Rale, M.; Schneider, S.; Sprenger, G. A.; Samland, A. K.; Fessner, W.-D. *Chem. - Eur. J.* **2011**, 17 (9), 2623–2632.
- (69) Kakinuma, H.; Yuasa, H.; Hashimoto, H. *Carbohydr. Res.* **1998**, 312 (3), 103–115.
- (70) Hecquet, L.; Bolte, J.; Demuynck, C. *Tetrahedron* **1994**, 50 (29), 8677–8684.
- (71) Corey, E. J.; Suggs, J. W. *J. Org. Chem.* **1975**, 40 (17), 2554–2555.
- (72) Arnaud Tatibouet, Jing Yang, Christophe Morin and Geoffrey D. Holman. *Bioorg. Med. Chem.* **2000**, 8, 1825–1833.
- (73) Girniene, J.; Tatibouët, A.; Sackus, A.; Yang, J.; Holman, G. D.; Rollin, P. *Carbohydr. Res.* **2003**, 338 (8), 711–719.
- (74) Tanasova, M.; Plutschack, M.; Muroski, M. E.; Sturla, S. J.; Strouse, G. F.; McQuade, D. T. *ChemBioChem* **2013**, 14 (10), 1263–1270
- (75) Wang, G-N.; Yang, L.; Zhang, L-H.; Ye, Z-S. *J. Org. Chem.* **2011**, 76, 2001–2009

#### Chapter 4:

- (1) Fulwyler, M. J., U. *Science* **1965**, 150, 910–911.
- (2) Virgo, P. F.; Gibbs, G. J. *Ann. Clin. Biochem.* **2012**, 49 (1), 17–28.
- (3) Brown, M.; Wittwer, C. *Clin. Chem.* **2000**, 46 (8), 1221–1229.
- (4) Martin, J. C.; Swartzendruber, D. E. *Science* **1980**, 207 (4427), 199–201.
- (5) Laerum, O. D.; Farsund, T. *Cytometry* **1981**, 2 (1), 1–13.
- (6) Bakke, A. C. *Lab. Med.* **2001**, 32 (4), 207–211.

- (7) Otten, G. R.; Loken, M. R. *Cytometry* **1982**, *3* (3), 182–187.
- (8) Watt, S. M.; Burgess, A. W.; Metcalf, D.; Battye, F. L. *J. Histochem. Cytochem. Off. J. Histochem. Soc.* **1980**, *28* (9), 934–946.
- (9) Berney, M. *Microbiology* **2006**, *152* (6), 1719–1729.
- (10) Stevenson, A. P.; Martin, J. C.; Stewart, C. C. *Cancer Res.* **1986**, *46* (1), 99–105.
- (11) Basiji, D. A.; Ortyn, W. E.; Liang, L.; Venkatachalam, V.; Morrissey, P. *Clin. Lab. Med.* **2007**, *27* (3), 653–670.
- (12) Ohl, C.-D.; Wolfrum, B. *Biochim. Biophys. Acta BBA - Gen. Subj.* **2003**, *1624* (1–3), 131–138.
- (13) Wehrle, J. P.; Ng, C. E.; McGovern, K. A.; Aiken, N. R.; Shungu, D. C.; Chance, E. M.; Glickson, J. D. *NMR Biomed.* **2000**, *13* (6), 349–360.
- (14) Soule, H. D.; Maloney, T. M.; Wolman, S. R.; Peterson, W. D.; Brenz, R.; McGrath, C. M.; Russo, J.; Pauley, R. J.; Jones, R. F.; Brooks, S. C. *Cancer Res.* **1990**, *50* (18), 6075–6086.
- (15) Perez, O. D.; Nolan, G. P. *Nat. Biotechnol.* **2002**, *20* (2), 155–162.
- (16) BioTechniques - Two-step protocol for preparing adherent cells for high-throughput flow cytometry  
<http://www.biotechniques.com/BiotechniquesJournal/2015/September/Two-step-protocol-for-preparing-adherent-cells-for-high-throughput-flow-cytometry/biotechniques-360318.html> (accessed Jan 27, 2017).
- (17) Dimitriadis, G.; Maratou, E.; Boutati, E.; Psarra, K.; Papasteriades, C.; Raptis, S. A. *Cytometry A* **2005**, *64A* (1), 27–33.
- (18) Aller, C. B.; Ehmann, S.; Gilman-Sachs, A.; Snyder, A. K. *Cytometry* **1997**, *27* (3), 262–268.
- (19) Zou, C.; Wang, Y.; Shen, Z. *J. Biochem. Biophys. Methods* **2005**, *64* (3), 207–215.
- (20) Levi, J.; Cheng, Z.; Gheysens, O.; Patel, M.; Chan, C. T.; Wang, Y.; Namavari, M.; Gambhir, S. S. *Bioconjug. Chem.* **2007**, *18* (3), 628–634.
- (21) Soueidan, O.-M.; Scully, T. W.; Kaur, J.; Panigrahi, R.; Belovodskiy, A.; Do, V.; Matier, C. D.; Lemieux, M. J.; Wuest, F.; Cheeseman, C.; West, F. G. *ACS Chem. Biol.* **2017**, *12* (4), 1087–1094.
- (22) Rockwell, S. C.; Kallman, R. F.; Fajardo, L. F. *J. Natl. Cancer Inst.* **1972**, *49* (3), 735–749.
- (23) Dive, C.; Watson, J. V.; Workman, P. *Cancer Res.* **1991**, *51* (3), 799–806.
- (24) Dive, C.; Workman, P.; Watson, J. V. *Cytometry* **1987**, *8* (6), 552–561.
- (25) Wuest, M.; Trayner, B. J.; Grant, T. N.; Jans, H.-S.; Mercer, J. R.; Murray, D.; West, F. G.; McEwan, A. J. B.; Wuest, F.; Cheeseman, C. I. *Nucl. Med. Biol.* **2011**, *38* (4), 461–475.
- (26) Zamora-León, S. P.; Golde, D. W.; Concha, I. I.; Rivas, C. I.; Delgado-López, F.; Baselga, J.; Nualart, F.; Vera, J. C. *Proc. Natl. Acad. Sci.* **1996**, *93* (5), 1847–1852.
- (27) Drabovich, A. P.; Pavlou, M. P.; Dimitromanolakis, A.; Diamandis, E. P. *Mol. Cell. Proteomics* **2012**, *11* (8), 422–434.
- (28) Felix Bronner; Arnost Kleinzeller; Paul G. LeFevre. *Current Topics in Membranes and Transport*; Academic Press, 1975.
- (29) Rappoport, D. A.; Fritz, R. R.; Yamagami, S.; Herrmann, R. L.; Palladin, A. V.; Poljakova, N. M.; Schenkein, I.; Sokoloff, L.; Lajtha, A.; Marks, N.; Smythies, J. R.; Brodsky, W. A.; Shamoo, A. E.; Schwartz, I. L.; Wyssbrod, H. R.; Scott, W. N.;

Brodsky, W. A.; Schwartz, I. L. *Metabolic Turnover in the Nervous System*; Springer Science & Business Media, 2013.

- (30) Naftalin, R. J. *Biochim. Biophys. Acta BBA - Biomembr.* **1997**, *1328* (1), 13–29.
- (31) Naftalin, R. J.; Rist, R. J. *Biochim. Biophys. Acta BBA - Biomembr.* **1994**, *1191* (1), 65–78.
- (32) Levine, K. B.; Robichaud, T. K.; Hamill, S.; Sultzman, L. A.; Carruthers, A. *Biochemistry (Mosc.)* **2005**, *44* (15), 5606–5616.
- (33) LeFevre, P. G. *Am. J. Physiol. Content* **1962**, *203* (2), 286–290.
- (34) Geck, P. *Biochim. Biophys. Acta BBA - Biomembr.* **1971**, *241* (2), 462–472.
- (35) Baker, G. F.; Widdas, W. F. *J. Physiol.* **1973**, *231* (1), 143–165.
- (36) May, J. M.; Beechem, J. M. *Biochemistry (Mosc.)* **1993**, *32* (11), 2907–2915.
- (37) Appleman, J. R.; Lienhard, G. E. *Biochemistry (Mosc.)* **1989**, *28* (20), 8221–8227.
- (38) Cunningham, P.; Afzal-Ahmed, I.; Naftalin, R. J. *J. Biol. Chem.* **2006**, *281* (9), 5797–5803.
- (39) Strobel, P.; Allard, C.; Perez-Acle, T.; Calderon, R.; Aldunate, R.; Leighton, F. *Biochem. J.* **2005**, *386* (3), 471–478.
- (40) Carruthers, A.; Helgerson, A. L. *Biochemistry (Mosc.)* **1991**, *30* (16), 3907–3915.
- (41) Walmsley, A. R.; Lowe, A. G.; Henderson, P. J. F. *Eur. J. Biochem.* **1994**, *221* (1), 513–522.
- (42) Manolescu, A.; Salas-Burgos, A. M.; Fischbarg, J.; Cheeseman, C. I. *J. Biol. Chem.* **2005**, *280* (52), 42978–42983.
- (43) Manolescu, A. R.; Augustin, R.; Moley, K.; Cheeseman, C. *Mol. Membr. Biol.* **2007**, *24* (5–6), 455–463.
- (44) *Physiol Res* **1999**, No. Lloyd, P. G., Hardin, C. D., Sturek, M., 401–410.

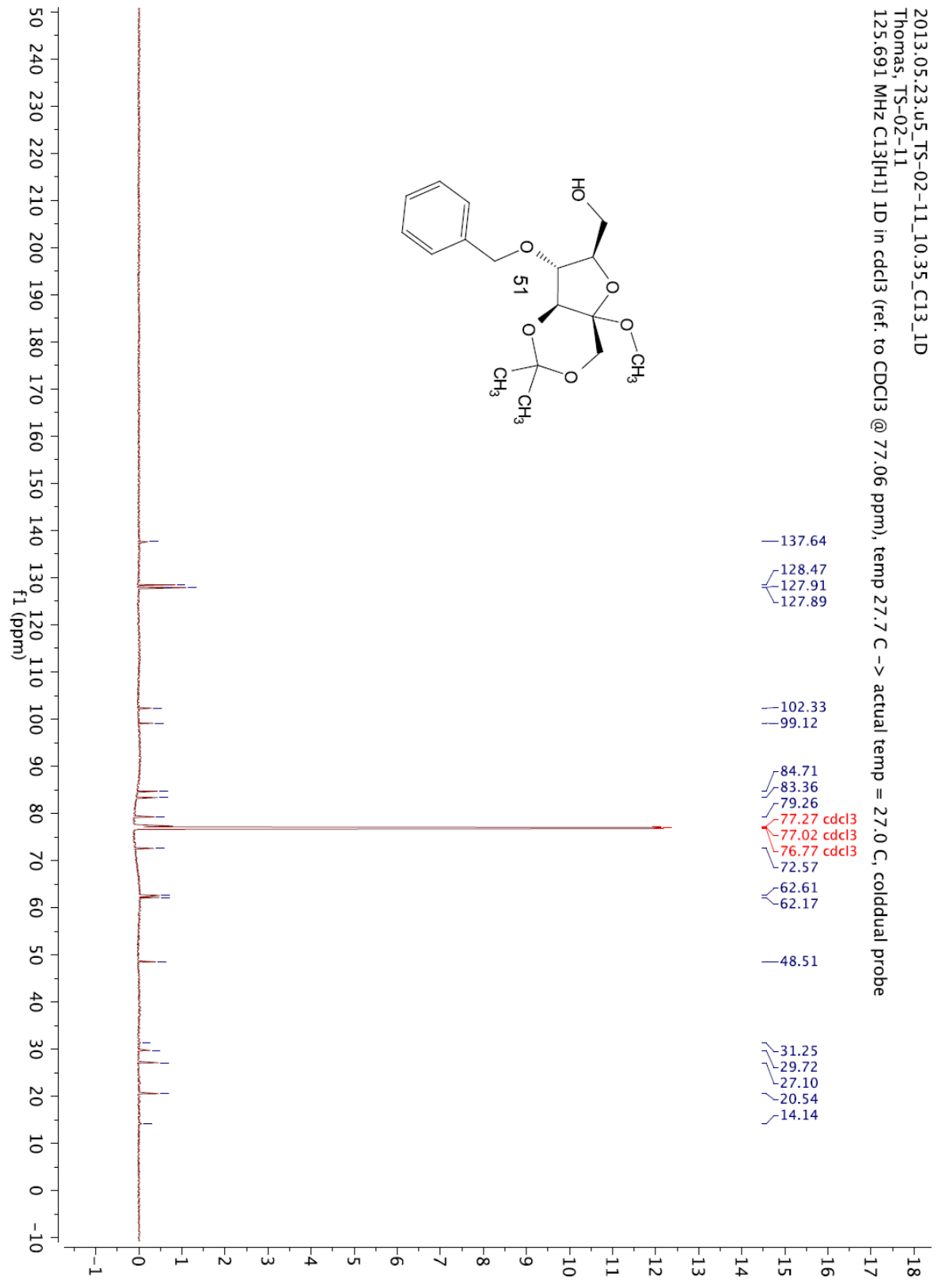
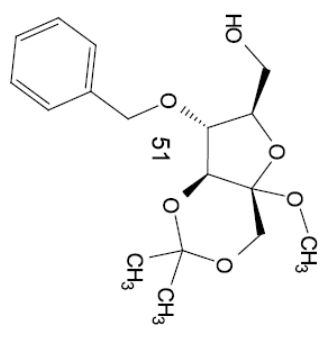
## Chapter 5:

- (1) Soueidan, O.-M.; Scully, T. W.; Kaur, J.; Panigrahi, R.; Belovodskiy, A.; Do, V.; Matier, C. D.; Lemieux, M. J.; Wuest, F.; Cheeseman, C.; West, F. G. *ACS Chem. Biol.* **2017**, *12* (4), 1087–1094.
- (2) Levi, J.; Cheng, Z.; Gheysens, O.; Patel, M.; Chan, C. T.; Wang, Y.; Namavari, M.; Gambhir, S. S. *Bioconjug. Chem.* **2007**, *18* (3), 628–634.
- (3) Kumar Kondapi, V. P.; Soueidan, O.-M.; Cheeseman, C. I.; West, F. G. *Chem. – Eur. J.* **2017**, *23* (33), 8073–8081.
- (4) Kondapi, K.; Pavan, V.; Soueidan, O.-M.; Hosseini, S. N.; Jabari, N.; West, F. G. *Eur. J. Org. Chem.* **2016**, *2016* (7), 1367–1379.
- (5) Tanaka, Y.; Kohler, J. J. *J. Am. Chem. Soc.* **2008**, *130* (11), 3278–3279.
- (6) Evans, R. W.; Zbieg, J. R.; Zhu, S.; Li, W.; MacMillan, D. W. C. *J. Am. Chem. Soc.* **2013**, *135* (43), 16074–16077.
- (7) Nomura, N.; Verdon, G.; Kang, H. J.; Shimamura, T.; Nomura, Y.; Sonoda, Y.; Hussien, S. A.; Qureshi, A. A.; Coincon, M.; Sato, Y.; Abe, H.; Nakada-Nakura, Y.; Hino, T.; Arakawa, T.; Kusano-Arai, O.; Iwanari, H.; Murata, T.; Kobayashi, T.; Hamakubo, T.; Kasahara, M.; Iwata, S.; Drew, D. *Nature* **2015**, *526* (7573), 397–401.

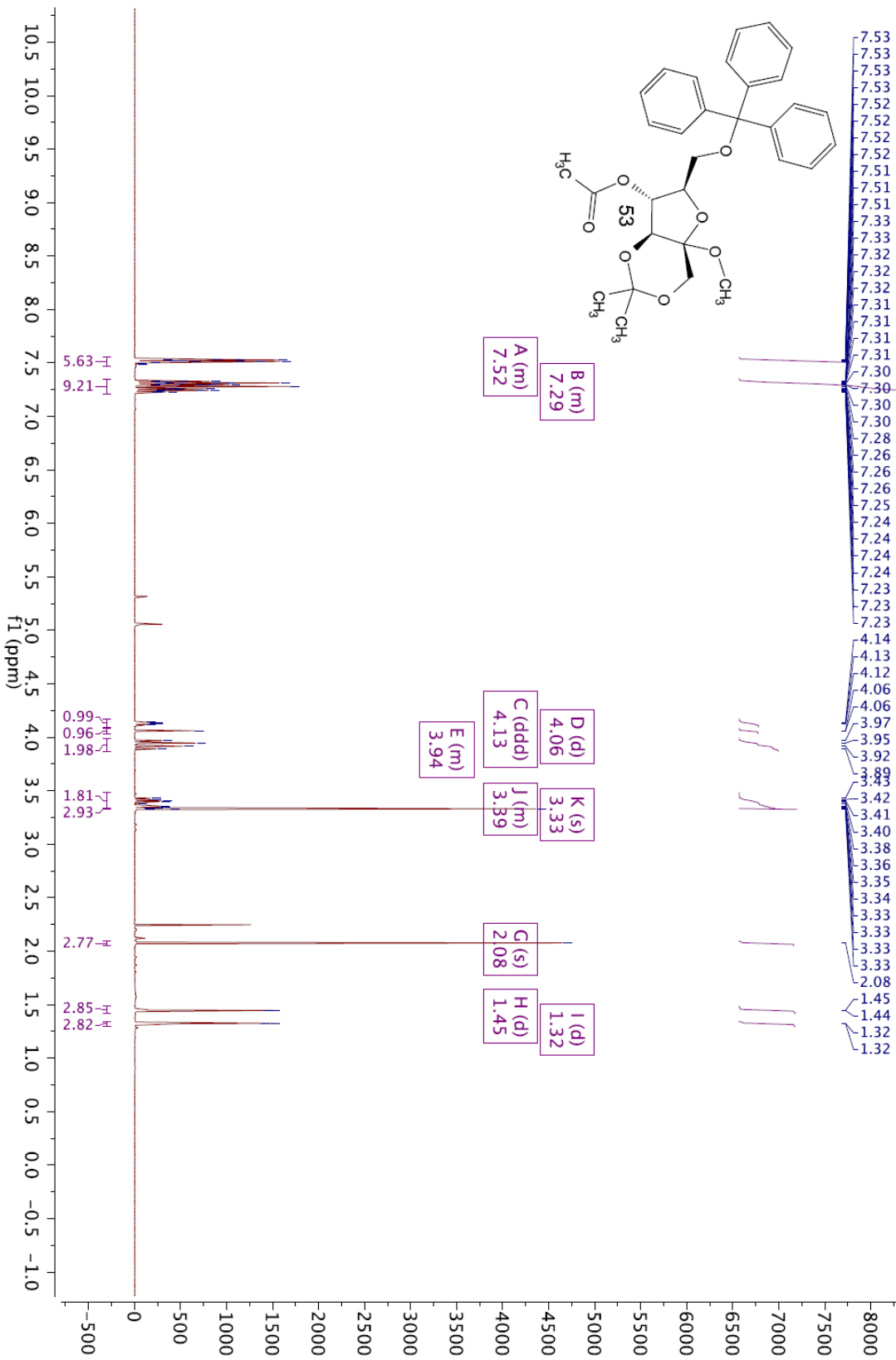
## **Appendix I: Selected NMR Spectra**



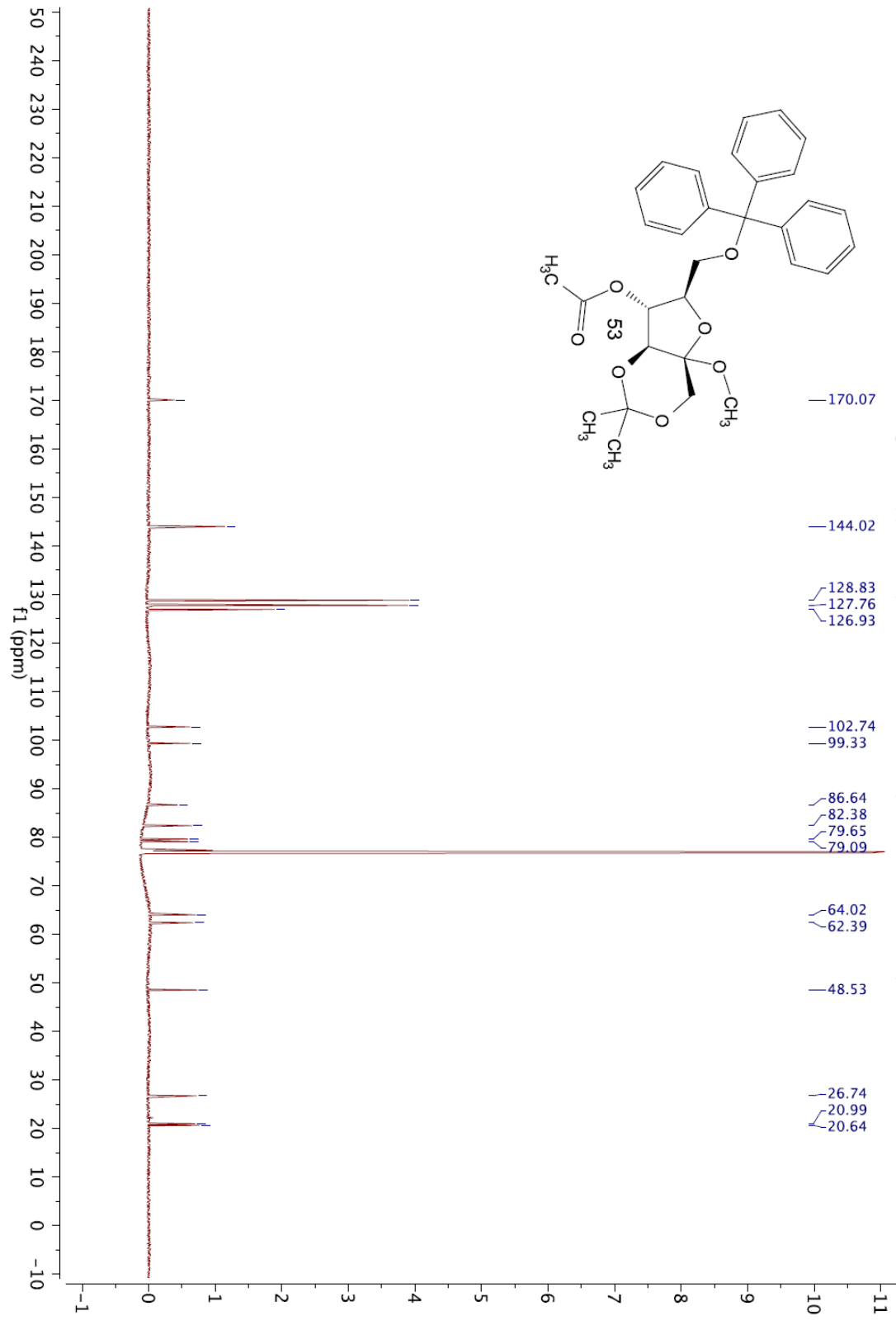
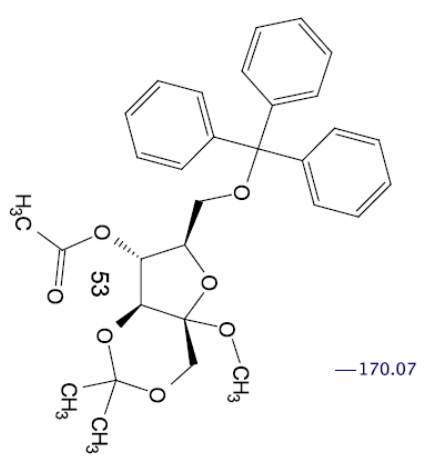
2013.05.23.u5\_TS-02-11\_10.35\_C13\_1D  
Thomas, TS-02-11  
125.691 MHz C13[H1] 1D in cddcl3 (ref. to CDCl3 @ 77.06 ppm), temp 27.7 C -> actual temp = 27.0 C, cold dual probe



498.118 MHz H1 ID in cdcl3 (ref. to CDCl3 @ 7.26 ppm), temp 26.4 C -> actual temp = 27.0 C, autotxdb probe

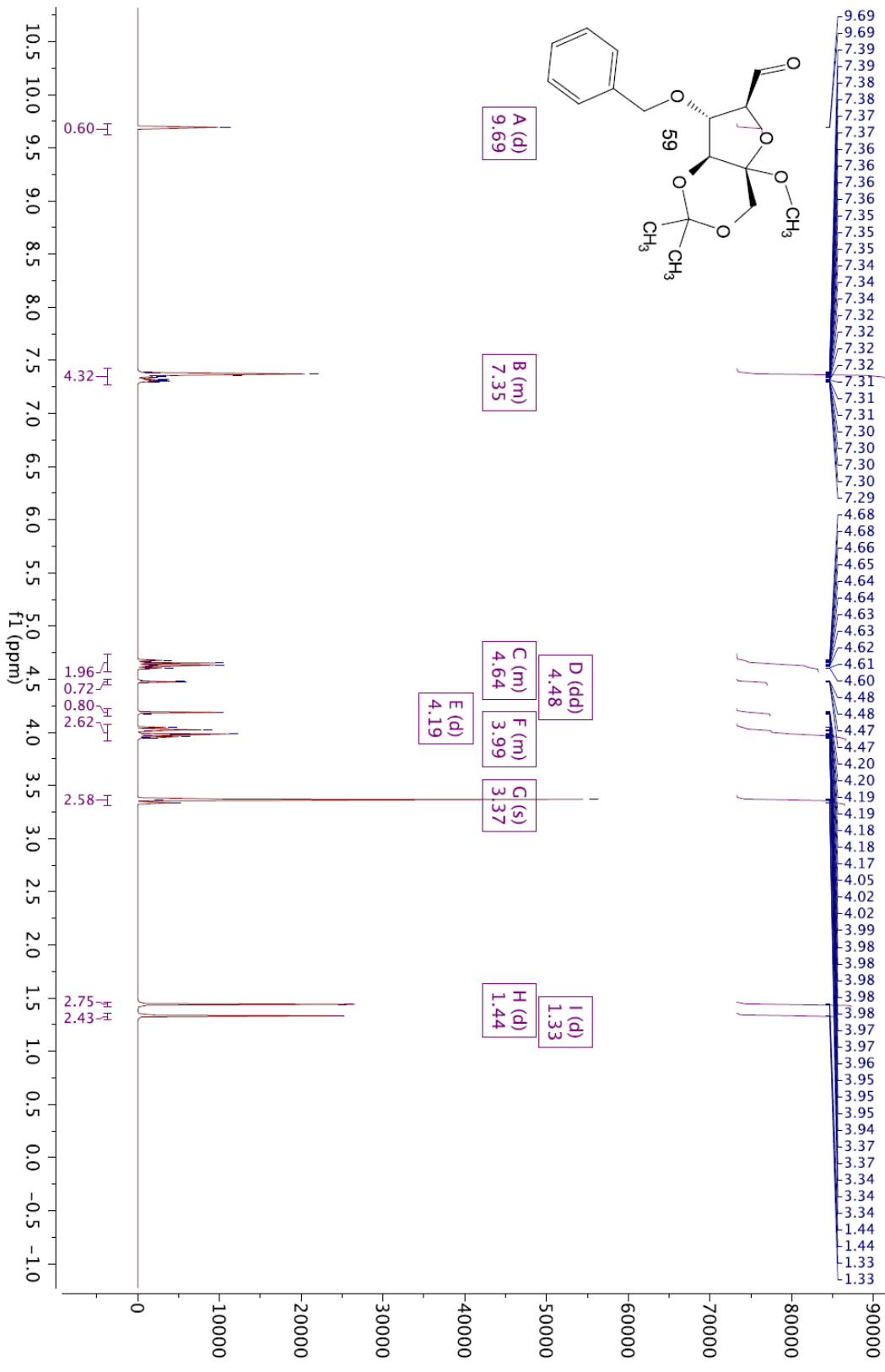


2014.11.10.u5\_TS-02-62\_loc9\_09.39\_C13\_1D  
Thomas, TS-02-62  
125.691 MHz C13[H1] 1D in cdcl3 (ref. to CDCl3 @ 77.06 ppm), temp 27.7 C -> actual temp = 27.0 C, coldual probe

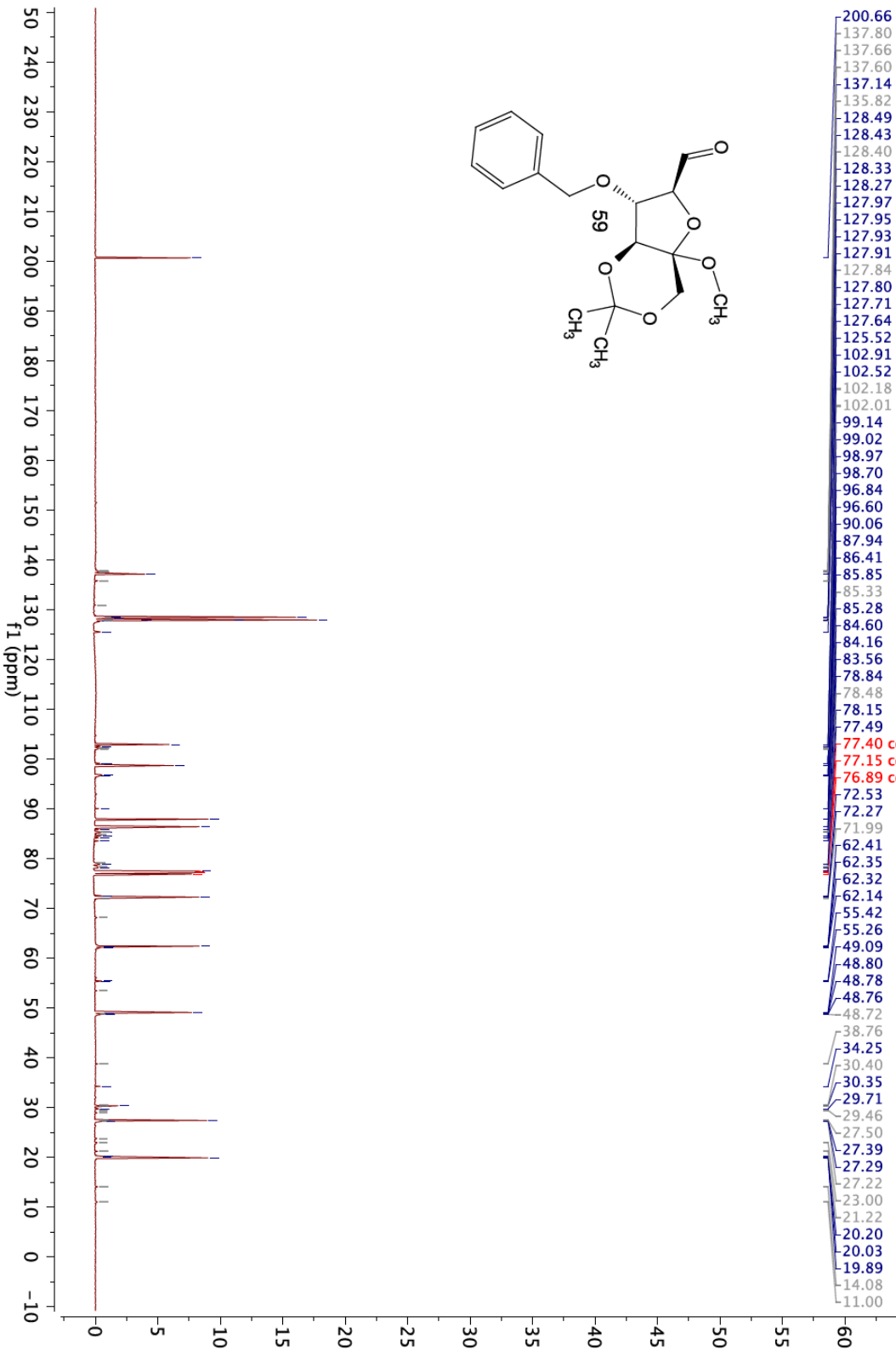
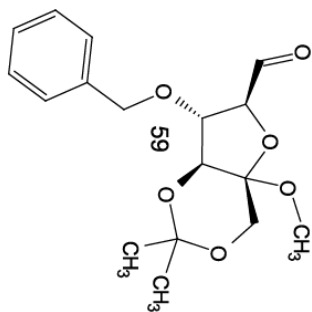


TS-02-20-ether\_pentane\_column\_bottom\_spot

498.118 MHz H1 ID in cdd13 (ref. to CDCl3 @ 7.26 ppm), temp 26.4 C -> actual temp = 27.0 C, autotxodb probe

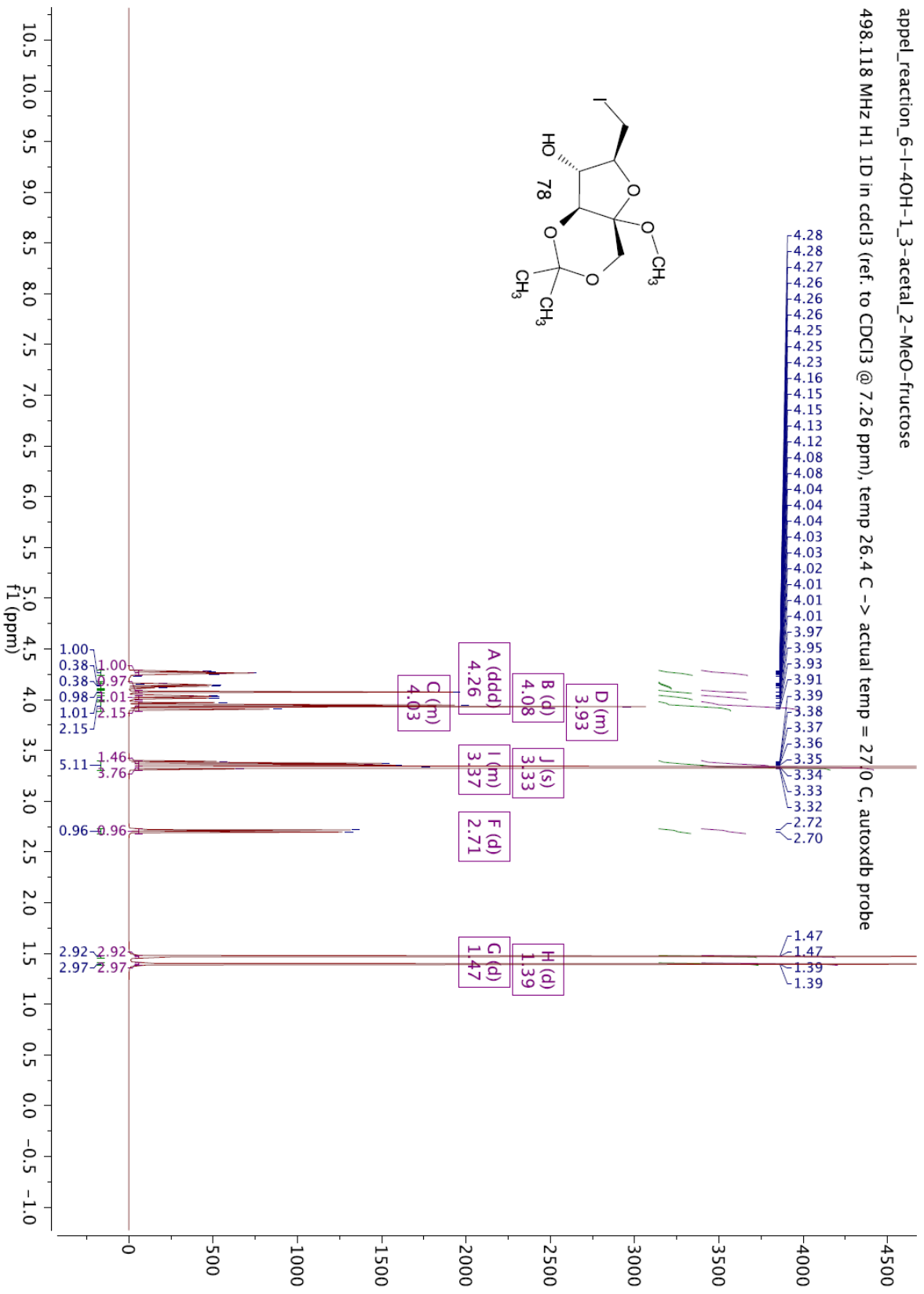
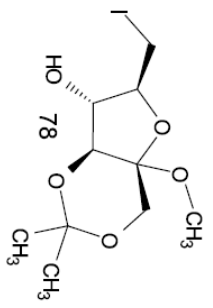


2013.07.5.u5\_TS-02-20-ether\_pentane\_column\_bottom\_spot  
 Thomas, TS-02-20-ether\_pentane\_column\_bottom\_spot  
 125.691 MHz C13[H1] ID in cdcl3 (ref: to CDCl3 @ 77.06 ppm), temp 27.7 C -> actual temp = 27.0 C, cold dual probe



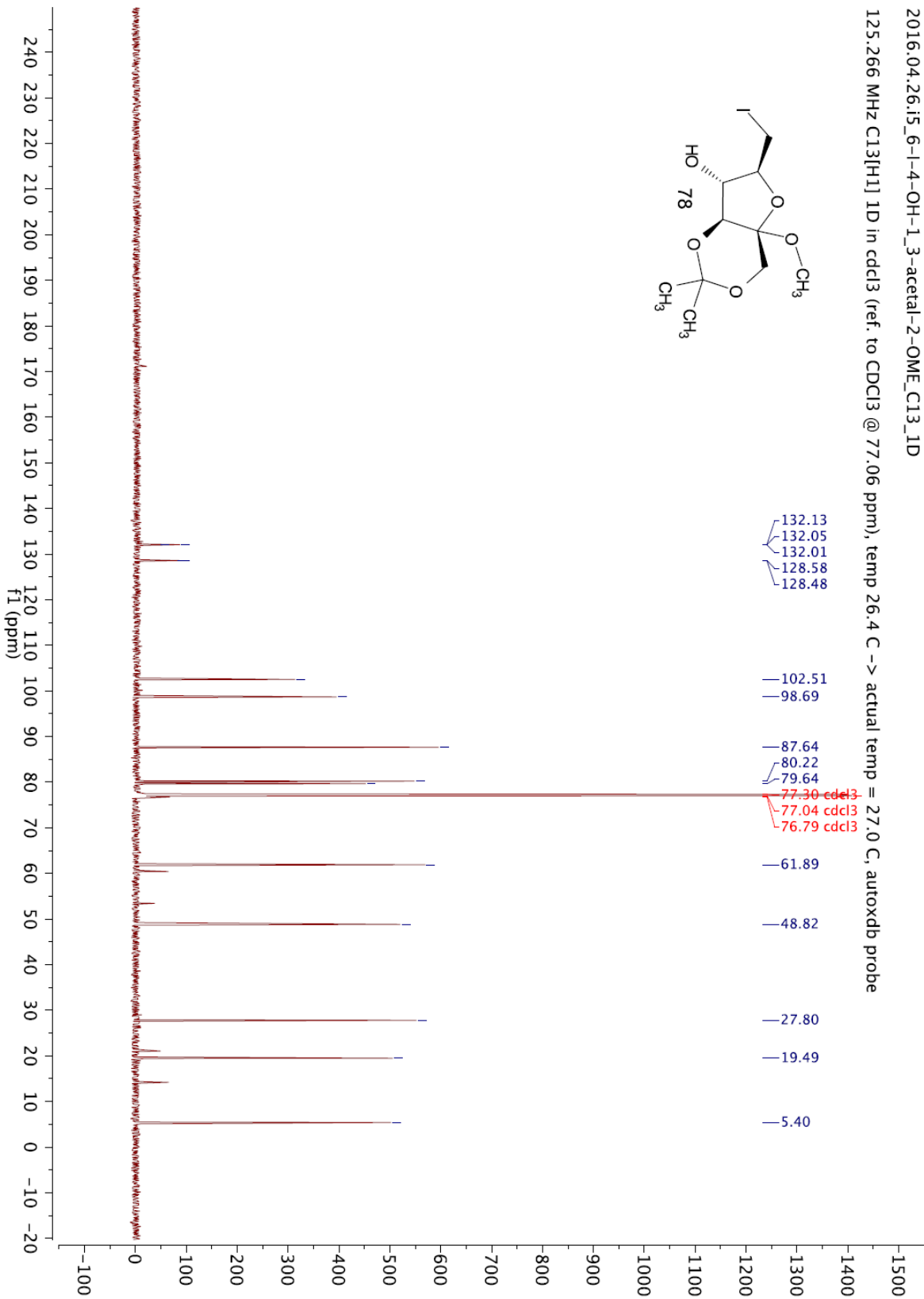
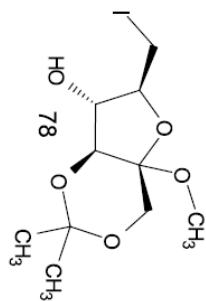
appel\_reaction\_6-1-4OH-1\_3-acetal\_2-MeO-fructose

498.118 MHz H1 ID in cdcl3 (ref. to CDCl3 @ 7.26 ppm), temp 26.4 C -> actual temp = 27.0 C, autoudb probe



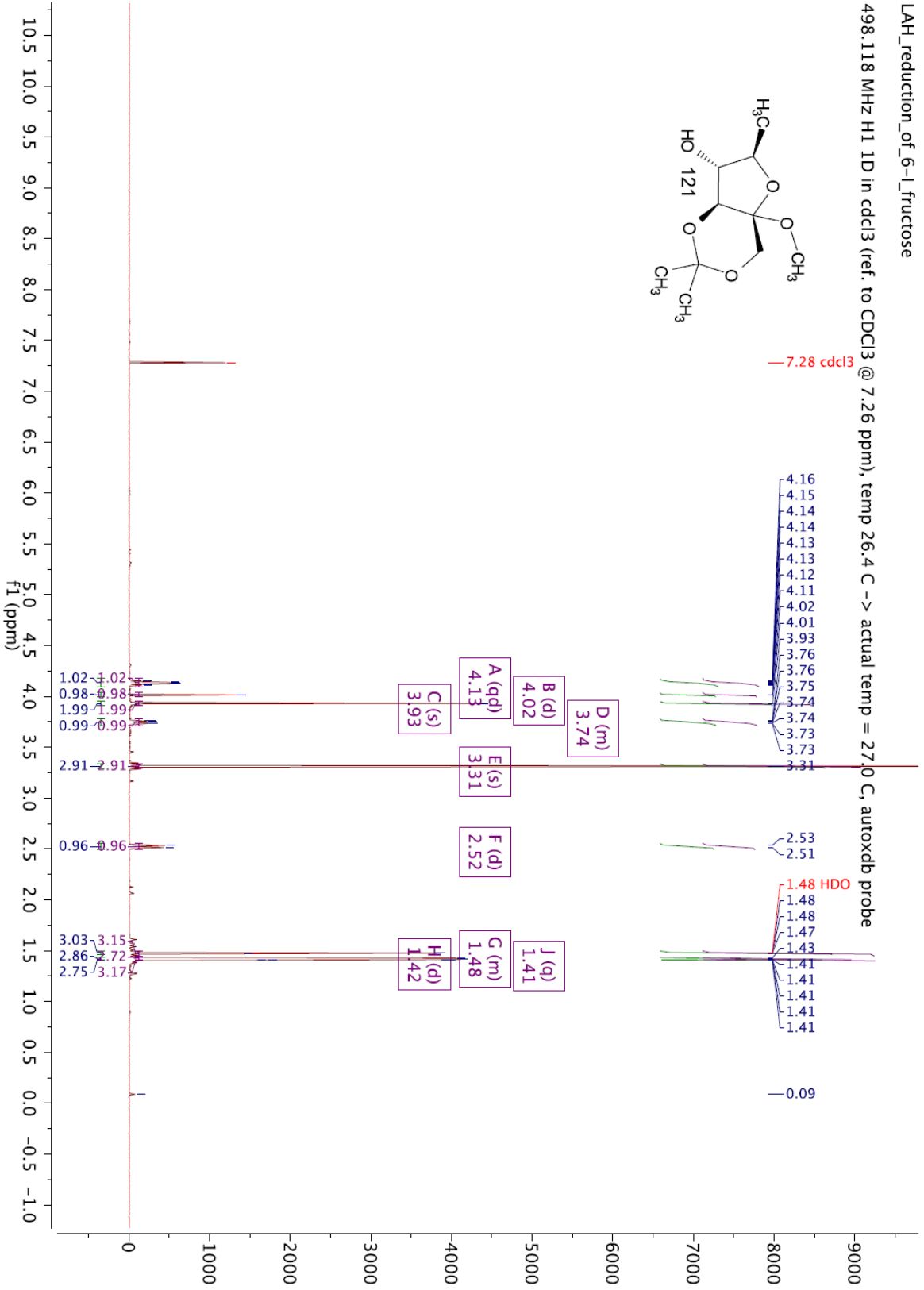
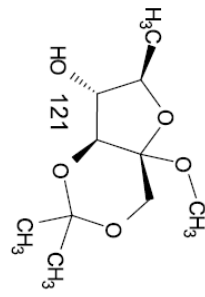
2016.04.26;15\_6-l-4-OH-1\_3-acetal-2-OME\_C13\_ID

125.266 MHz C13[H1] ID in cdcl3 (ref. to CDCl3 @ 77.06 ppm), temp 26.4 C -> actual temp = 27.0 C, autoxtdb probe

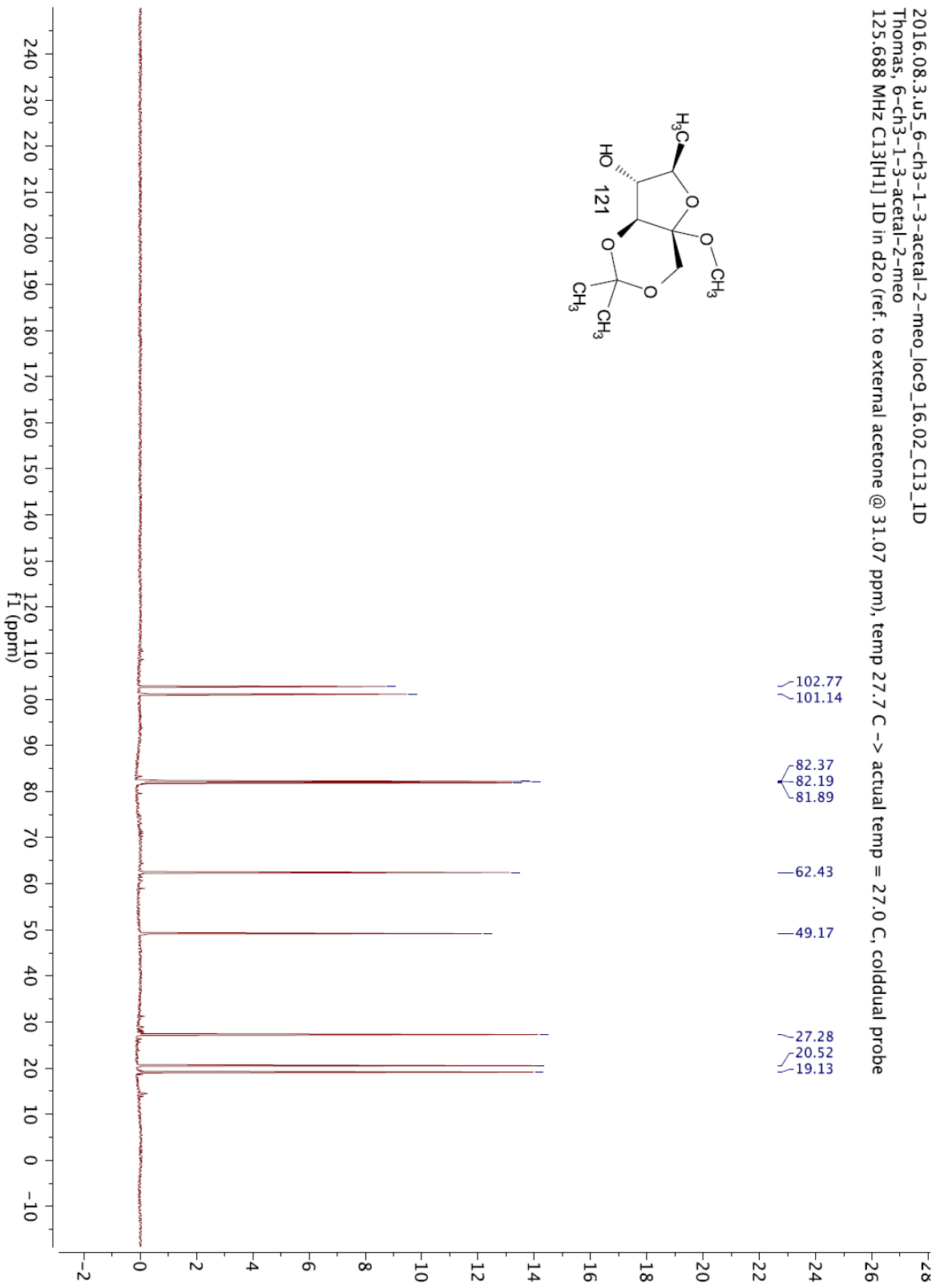
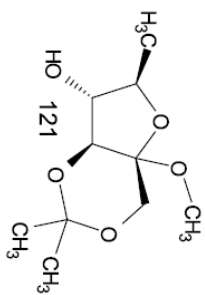


LAH\_reduction\_of\_6-l\_fructose

498.118 MHz H1 ID in cdcl3 (ref. to CDCl3 @ 7.26 ppm), temp 26.4 C -> actual temp = 27.0 C, autotx2db probe



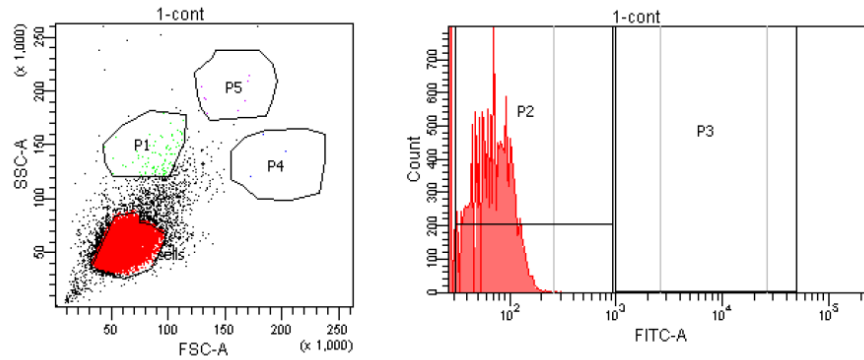
2016.08.3.u5\_6-ch3-1-3-acetal-2-meo\_loc9\_16.02\_C13\_ID  
-Thomas, 6-ch3-1-3-acetal-2-meo  
125.688 MHz C13[H1] ID in d2o (ref. to external acetone @ 31.07 ppm), temp 27.7 C -> actual temp = 27.0 C, cold dual probe



# Appendix II: Selected Flow Cytometry Raw Data

Negative control of EMT6 cells.

FACSDiva Version 6.1.3



Tube: cont

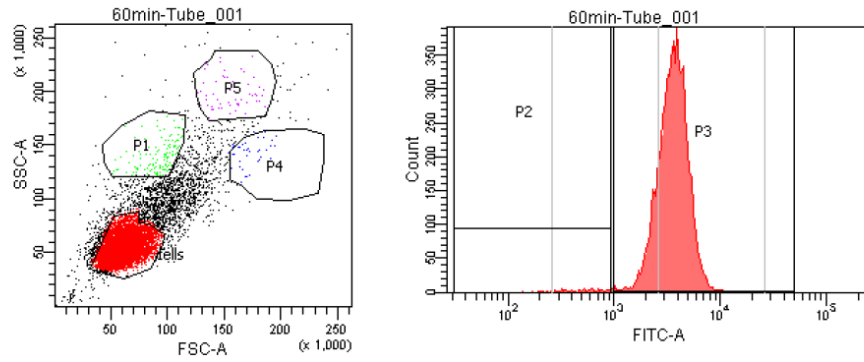
Population	%Parent
All Events	####
cells	90.1
P2	78.4
P3	0.0
P1	0.4
P4	0.0
P5	0.0

Experiment Name: cm-0556 250um exp 3  
 Specimen Name: 1  
 Tube Name: cont  
 Record Date: Jan 22, 2013 2:18:21 PM  
 \$OP: Cheeseman  
 GUID: 89032c91-374f4cdb-b676-2aefe5b80897

Population	#Events	%Parent	FITC-A Mean
cells	18,019	90.1	60
P2	14,133	78.4	74
P3	0	0.0	####
P1	84	0.4	179
P4	3	0.0	204
P5	8	0.0	227

EMT6 cells after 60 min of incubation with 250  $\mu$ M 6-NBDF

FACSDiva Version 6.1.3



Tube: Tube\_001

Population	%Parent
All Events	###
cells	77.7
P2	1.2
P3	98.7
P1	1.3
P4	0.4
P5	0.6

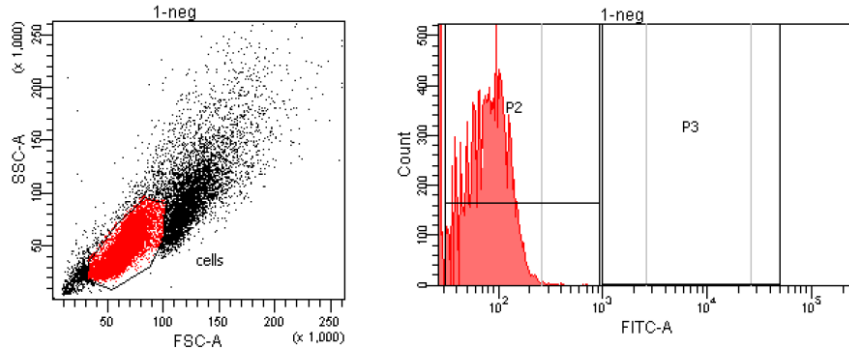
Experiment Name:	cm-0556 250um exp 3
Specimen Name:	60min
Tube Name:	Tube_001
Record Date:	Jan 22, 2013 2:25:29 PM
\$OP:	Cheeseman
GUID:	5c457bcd-9cd1-461f-83bf-8cc0793b90e9

Population	#Events	%Parent	FITC-A Mean
cells	7,771	77.7	3,746
P2	95	1.2	516
P3	7,668	98.7	3,789
P1	126	1.3	9,699
P4	44	0.4	10,082
P5	56	0.6	14,363

# Negative control of MCF7 cells

FACSDiva Version 6.1.3



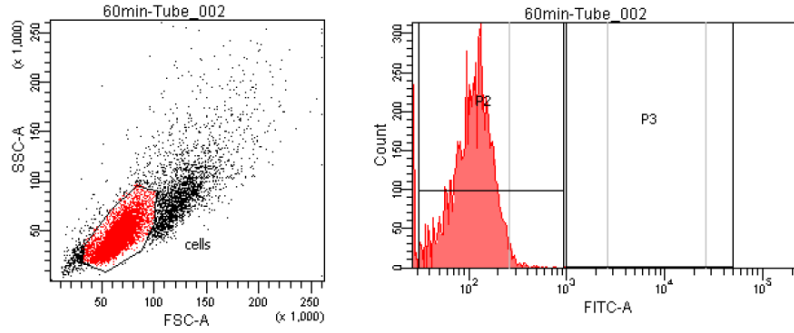
Tube: neg

Population	%Parent
■ All Events	###
■ cells	69.6
☒ P2	86.9
☒ P3	0.0

Experiment Name: EXP1 250UM 6-NBD-FRUCTOSE BD CYTO				
Specimen Name: 1				
Tube Name: neg				
Record Date: Nov 14, 2013 1:03:26 PM				
\$OP: Cheeseman				
GUID: 8c23f8fc-bca9-4ef7-b4e8-5a84544944b6				
Population	#Events	%Parent	FITC-A	
			Mean	
■ cells	13,930	69.6	78	
☒ P2	12,100	86.9	88	
☒ P3	0	0.0	###	

MCF7 cells after 60 min of incubation with 250  $\mu$ M of 6NBDF

FACSDiva Version 6.1.3



Tube: Tube\_002

Population	%Parent
All Events	###
cells	73.1
P2	96.3
P3	0.0

Experiment Name:	EXP1 250UM 6-NBD-FRUCTOSE BD CYTO		
Specimen Name:	60min		
Tube Name:	Tube_002		
Record Date:	Nov 14, 2013 1:16:01 PM		
\$OP:	Cheeseman		
GUID:	e0e6c838-72cf-4959-85de-42b14df471ef		
Population	#Events	%Parent	FITC-A Mean
cells	7,313	73.1	117
P2	7,043	96.3	121
P3	0	0.0	###